DOE/MC/29117 -- 5061
(DE96000601)

Stabilization and Reuse of Heavy Metal Contaminated Soils by Means of Quicklime Sulfate Salt Treatment

Final Report
September 1992 - February 1995

D. Dermatas

August 1995

Work Performed Under Contract No.: DE-AC21-92MC29117

For

U.S. Department of Energy
Office of Environmental Management
Office of Technology Development
Washington, DC

U.S. Department of Energy
Office of Fossil Energy
Morgantown Energy Technology Center
Morgantown, West Virginia

By
Center for Environmental Engineering
Hoboken, New Jersey

DISCLAIMER

DOE/MC/29117 -- 5061
(DE96000601)

Stabilization and Reuse of Heavy Metal Contaminated Soils by Means of Quicklime Sulfate Salt Treatment

Final Report
September 1992 - February 1995

D. Dermatas

Work Performed Under Contract No.: DE-AC21-92MC29117

For

U.S. Department of Energy
Office of Environmental Management
Office of Technology Development
1000 Independence Avenue
Washington, DC 20585

U.S. Department of Energy
Office of Fossil Energy
Morgantown Energy Technology Center
P.O. Box 880
Morgantown, West Virginia 26507-0880

By
Center for Environmental Engineering
Stevens Institute of Technology
Castle Point
Hoboken, New Jersey 07030

August 1995

ABSTRACT

Capillary and hydraulic flows of water in porous media contaminated by heavy metal species often result in severe aquifer contamination. In the present study a chemical admixture stabilization approach is proposed, where heavy metal stabilization/immobilization is achieved by means of quicklime-based treatment. Both in-situ treatment by injection and on-site stabilization by excavation, mixing, and compaction will be investigated. In addition, the potential to reuse the resulting stabilized material as readily available construction material will also be investigated. The heavy metals under study include: arsenic, chromium, lead, and mercury. The proposed technical approach consists of three separate phases. During phase A, both artificial and naturally occurring contaminated soil mixes were treated, and then tested for stress-strain properties, leachability, micromorphology, mineralogical composition, permeability, setting time, and durability. In such a way, the effectiveness of the proposed remediation technology was verified, the treatment approach was optimized, and the underlying mechanisms responsible for stabilization were established. During phase B, the proposed technology will be tested for two DOE-site subscale systems, involving naturally occurring contaminated soil, using the same testing methodology as the one outlined for phase A. Provided that the proposed technology is proven effective for the sub-scale systems, a field application will be demonstrated. Again process quality monitoring will be performed by testing undisturbed samples collected from the treated sites, in the same fashion as for the previous phases. Following completion of the proposed study, a set of comprehensive guidelines for field applications will be developed.

ACKNOWLEDGMENTS

This work was made possible with United States Department of Energy, funding, under contract No. DE-AC21-92MC291117, under the supervision of Morgantown Energy Technology Center (METC).

I acknowledge and appreciate the interest and constructive support throughout the project of the DOE contracting office representative and project manager Mr. Steven J. Bossart, as well as Mr. Robert C. Bedick who was the director of the Environmental and Waste Management Division at METC. I would also like to extend our appreciation for the help and support in dealing with some of the administrative issues, of Mark L. Estel and Mary Beth Ashbaugh from DOE-METC and Peter Guzanick from Energetics, Inc. Furthermore, I wish to express my gratitude for those who have intellectually and physically have contributed to this work. First and foremost, I would like to acknowledge the continuous and substantive input in all facets of the project of Dr. Xiaoguang Meng, our Research Engineer here at the Center for Environmental Engineering, at Stevens Institute of Technology. I would like to also acknowledge the work of the numerous students that worked under this project with the hope that I didn't forget any of them: Nick Gargoulas, Sunilla Goyal, Ajay Patwari, Scott Durski, Rajiv Sinha, Hooman Heravi, Steven Lin, Jaideep Nair, Wengui Xin, Deok Moon and Leslie Brunnel. Finally, I would like to extend my gratitude to Keith Axsom, director of the sponsored projects office here at Stevens and his staff for keeping my administrative problems to an absolute minimum.

TABLE OF CONTENTS

LIST OF FIGURES

LIST OF TABLES

NOMENCLATURE

Al	aluminum
a	activity of metal ion.
ANC	acid neutralization capacity.
ANS	American Nuclear Society.
ANS 16.1	American Nuclear Society test 16.1, a leaching test.
As	arsenic
ASTM	American Society for Testing and Materials
C	concentration
CERCLA	Comprehensive Environmental Response, Compensation, and Liability Act.
CAH	calcium (CaO) aluminum (Al_2O_3) hydrate (H_2O)
Cr	chromium
CSH	calcium silicate (SiO_2) hydrate
D	diffusion coefficient
DFGD	dry flue gas desulfurization
DOE	U.S. Department of Energy
EDX	energy dispersive x-ray
EPA	U.S. Environmental Protection Agency
FGD	flue gas desulfurization
Hg	mercury
i	hydraulic gradient
k	hydraulic conductivity
P	rainfall intensity
Pb	lead
R	chemical retardation factor
RCRA	Resource Conservation and Recovery Act.
RH	relative humidity
S	geometric surface area of specimen
S/S	stabilization and solidification
SEM	scanning electron microscope
t	time
TCLP	toxicity characteristic leaching procedure
U	flow rate
V	volume of specimen
x	distance
XRD	x-ray diffraction
γ	soil unit weight
τ	physical retardation factor

GLOSSARY

adsorption — attraction of solid, liquid, or gas molecules, ions, or atoms to particle surfaces by physiochemical forces. The adsorbed material may have different properties from those of the material in the pore space at the same temperature and pressure due to altered molecular arrangement.

additives — materials included in the binder to improve the S/S process. Examples of some types of additives are: (1) silicates or other materials that alter the rate of hardening, (2) clays or other sorbents to improve retention of water or contaminants, or (3) emulsifiers and surfactants that improve the incorporation of organic compounds.

alkalinity — the quantitative capacity of aqueous media to react with hydrogen ions.

binder — a cement, cement like material, or resin (possibly in conjunction with water, extender, or other additives) used to hold particles together.

capillarity — the movement of water, due to effects other than gravity, through very small void spaces that exist in a soil mass. Water movement occurs in very small channels such as capillary-sized openings because of the affinity between soil and water, which acts to increase the boundary of contact between the two materials, and the surface tension property developed by water in contact with air. Capillary flow can occur in a direction opposite to that of the pull of gravity.

clay — fine-grained soil or the fine-grained portion of soil that can be made to exhibit plasticity (putty-like properties) within a range of water contents and that exhibits considerable strength when air-dry.

compressive strength (unconfined or uniaxial compressive strength) — the load per unit area at which an unconfined cylindrical specimen of soil or rock will fail in a simple compression test. Commonly the failure load is the maximum that the specimen can withstand in the test.

contaminant — typically an undesirable minor constituent that renders another substance impure.

diffusion — movement of molecules towards an equilibrium driven by heat or concentration gradients (mass transfer without bulk fluid flow).

disposal — the activities associated with the long-term handling of (1) solid wastes that are collected and of no further use and (2) the residual matter after solid wastes have been processed and the recovery of conversion products of energy has been accomplished. Normally, disposal is accomplished by means of sanitary landfill.

durability — the ability of solidified/stabilized wastes to resist physical wear and chemical attack over time.

ettringite — a mineral composed of hydrous basic calcium and aluminum sulfate. The formula for ettringite is $Ca_6Al_2(SO_4)_3(OH)_{12}{\cdot}26H_2O$.

fly ash — small solid particles of ash and soot generated when coal, oil, or solid wastes are burned. With proper equipment, fly ash is collected before it enters the atmosphere. Fly ash residue can be used for building materials (bricks) or in a sanitary landfill.

freeze/thaw cycle — alternation of a sample temperature to allow determination of swell and visual observation of sample disintegration resulting from phase change from water to ice

heavy metals metals such as cadmium, lead and mercury which may be found in MSW in discarded items such as batteries, lighting fixtures, colorants, and inks.

immobilization the reduction in the ability of contaminants to move through or escape from S/S-treated waste.

kaolinite a common clay mineral having the general formula $Al_2(Si_2O_5)(OH_4)$.

leachability a measure of release of constituents from a waste of solidified/stabilized waste. Leachability is one measure of the mobility of a constituent. High leachability means high constituent mobility.

leachant liquid that comes in contact with a material either from natural exposure (e.g., water in a disposal site) or in a planned test of leachability. The typically used leachants are pure distilled water or water containing salts, acids, or both.

leachate liquid that has percolated through solid waste or another medium. Leachate from landfill usually contains extracted, dissolved, and suspended materials, some of which may be harmful.

lime specifically, calcium oxide, also loosely, a general term for the various chemical and physical forms of quicklime, hydrated lime, and hydraulic hydrated lime.

long-term stability the ability of solidified/stabilized wastes to maintain their properties over time while exposed to the environment.

monolith a free standing solid consisting of one piece.

montmorillonite a group of clay minerals characterized by a weakly bonded sheet-like internal molecular structure; consisting of extremely finely divided hydrous aluminum of magnesium silicates that swell on wetting, shrink on drying, and have ion exchange capacity.

percolation movement of water under hydrostatic pressure or gravity through the smaller interstice of rock, soil, wastes, or S/S-treated wastes.

permeability a measurement of flow of a fluid through the tortuous pore structure of the waste or S/S-treated waste. It is expressed as the proportionality constant between flow velocity and the hydraulic gradient. It is a function of both media. If the permeating fluid is water, the permeability is termed as hydraulic conductivity.

pore a small cavity or void in a solid

pozzolan a siliceous or siliceous and aluminous material, which in itself possesses little or no cementitious value but will, in finely divided form and in the presence of moisture, chemically react with calcium hydroxide at ordinary temperatures to form compounds with cementitous properties. The term is divided from an early source of natural pozzolanic material, Pozzouli, Italy.

solid wastes any of a wide variety of solid materials, as well as some liquid containers, which are discarded or rejected as being spent, useless, worthless, or in excess. Does not usually include waste solids from treatment facilities.

solidification a process in which materials are added to the waste to convert it to a solid or to simply improve its handing and physical properties. The process may or may not involve a chemical bonding between the waste, its contaminants, and the binder. In solidification, the mechanical

	binding of contaminants can be on the microscale (microencapsulation, absorption, or adsorption) or the macroscale (macroencapsulation).
solubility	the maximum concentration of a substance dissolved in a solvent at a given temperature.
sorption	a general term used to encompass the processes of adsorption absorption, desorption, ion exchange, ion exclusion, ion retardation, chemisorption, and dialysis.
stabilization	a process by which a waste is converted to a more chemically stable form. The term may include solidification, but also includes chemical changes to reduce contaminant mobility.

1 EXECUTIVE SUMMARY

1.1 General Approach

Capillary and hydraulic flows of water in porous media contaminated by heavy metal species often result in severe aquifer contamination, posing an immediate threat to the stability of ecosystems and the health of humans and animals. The Center for Environmental Engineering at Stevens Institute of Technology has undertaken a multi-phase effort to develop a chemical admixture remediation technology aimed at the immobilization of heavy metals in soil environments. Application of the proposed technology entails a quicklime-based stabilization/solidification (S/S) treatment approach, resulting in immobilization of the heavy metal species in a stabilized solid matrix, which can subsequently be reused as readily available construction material. The present research effort focuses mainly on representative heavy metal species designated by the U.S. Environmental Protection Agency (EPA) as priority pollutants. More specifically, the heavy metals of interest in the present study include the transition metal Chromium (Cr), the nonmetal Arsenic (As), and the heavy metals Lead (Pb) and Mercury (Hg).

Presently, among the primary remedial options for heavy metal contaminated soils and solid waste deposits, pozzolanic-based S/S approaches, similar to the technology developed herein, are considered to be the most economical, yet effective solutions. Both in-situ and ex-situ cement or lime based S/S applications are widely demonstrated and equipment and vendors are readily available. During such applications, large volumes of waste can be effectively treated at nominal cost ($30-170 per cu yd.). However, the long-term effectiveness of S/S, especially in the presence of sulfates is not yet established. Furthermore, field applications at Superfund sites were not always successful, mainly due to the inadequacy of existing design and field implementation guidelines. This inadequacy stems from the lack of fundamental understanding of the underlying mechanisms responsible for heavy metal immobilization. Once these mechanisms are delineated and the conditions leading to long term effectiveness of cement or lime S/S remediation technologies is established, a reliable broad-based design, field implementation, and quality control monitoring scheme can be developed and put in place.

The main goal in implementing the proposed technology is to convert hazardous soil and sludge wastes, found in DOE sites, into non-hazardous solids. The resulting solid could be then safely landfilled as non-hazardous, or reused as a readily available construction material. Depending on the engineering properties of the treated solid, a wide array of reuse options exist, ranging from construction fill to waste containment and road subgrade applications. Furthermore, by implementing the proposed lime-based approach as an interim solution, the rate of release of heavy metals into the subsurface can be tightly controlled for long periods of time. Therefore, the treated material could be left in place until effective means of fully reclaiming it are developed.

Contrary to all other S/S alternatives, the proposed technology, when designed accordingly, may result in a soil material that could be revegetated following some time after treatment. Overall, the proposed technology could provide an effective solution to both contemporary waste disposal problems as well as long-term contaminated soil reclamation scenarios.

The proposed heavy metal remediation technology development program is divided into three phases, each at a higher level of maturity, and will culminate with the commercial availability of design, field application and quality control protocols. During Phase 1, which is described herein, the effectiveness and long-term reliability of the proposed lime-based S/S technology was established in the presence of sulfates, the underlying mechanisms responsible for heavy metal immobilization were elucidated and a preliminary set of guidelines for field application of the proposed technology was developed. During Phase 2, the information obtained during Phase 1 will be used to test the proposed technology under sub-scale conditions in DOE contaminated sites. In Phase 3, full-scale demonstration of the proposed technology will be pursued at previously selected DOE site(s).

During Phase 1 of the present study, the overall treatment effectiveness was verified under laboratory conditions. Treatment was found to be effective since it was successful in converting hazardous heavy metal contaminated soils to a non-hazardous soil material, that can be reused in construction applications. Moreover, special emphasis was placed in elucidating the underlying mechanisms responsible for heavy metal immobilization and the conditions leading to long-term treatment effectiveness, especially in the presence of sulfates. All this was achieved by undertaking a multi-dimensional experimental program which included macroscopic and microscopic material characterization, determination of its pertinent engineering properties and assessment of its geoenvironmental behavior.

Regulatory benchmark (toxicity characteristic leaching procedure, TCLP), flow-through and static leaching tests were performed in order to assess the amount and rate of heavy metal release prior to and following treatment. These tests were also used to assess the release mechanisms and long-term treatment effectiveness. Unconfined compressive strength and confined vertical swell tests were performed in order to establish the reusability potential of the material in construction applications. The acid neutralization capacity (ANC) test was mainly used to obtain the treatment design levels. X-ray diffraction (XRD) and scanning electron microscope (SEM) analyses along with a number other tests were undertaken in order to elucidate the treatment underlying mechanisms, and to provide supporting information needed to explain and/or confirm other experimental results. Finally, freeze/thaw and wet/dry durability testing provided the basis for assessing the long-term physical durability of the treated soils.

1.2 Objectives and Scope

The main objectives pursued during Phase 1 of this project can be summarized as follows:

- Verify the effectiveness of the proposed treatment in terms of meeting the TCLP non-hazardous leachability criteria, and in meeting both the strength (unconfined compressive strength levels should be higher than 700 KPa) and swell (vertical swell magnitudes should be less than 5%) criteria.
- Establish the optimal levels of treatment as a function of existing soil conditions.
- Investigate the long term durability of the treated material, under different environmental stresses.
- Identify the underlying mechanisms responsible for the heavy metal stabilization in the soil-quicklime matrix.
- Develop a design methodology for applying the proposed technology in the field.

Meeting these objectives entailed detailed investigations of:

a. the relative influence of amount and reactivity of the solid surface area present

b. the relative influence of the amount and form of heavy metal contaminants present

c. the compositional and micromorphological changes resulting from treatment

d. the formation and subsequent hydration of ettringite and other reaction products

e. the ability of these reaction products to entrap heavy metal species

f. the leachability characteristics of the stabilized matrix under different leaching scenarios

g. the hydraulic properties of the treated material

In order to attain the project objectives, an experimental program was designed and undertaken where compacted soil specimens were prepared and tested under a variety of testing conditions.

1.3 Experimental Methodology

Clay-sand mixes, artificially contaminated using heavy metal salts or oxides, as well as some actual field contaminated soils, were dry mixed with quicklime (CaO) and sodium sulfate in our laboratory. For the artificial soil mixes, two different types of clay were used, kaolinite and montmorillonite. These types of clay were used because they represent the two extremes of layered

aluminosilicate surface area attributes and overall behavior. In some cases, fly ash, barium hydroxide and sulfides were also added into the contaminated soils to improve their physico-chemical behavior. First, a number of batch-type tests were performed in order to optimize treatment design. The actual treatment entailed compaction of the dry-mixed soils at optimum water content, and curing of the compacted specimens. Following different curing periods, specimens were tested to determine their leaching potential and their stress-strain properties under a variety of different testing conditions.

The mechanical and physico-chemical behavior of the compacted specimens, as determined during testing, formed the basis for evaluating both the degree of immobilization of the heavy metal contaminants and the reuse potential of the treated waste form. Specifically, the effectiveness of the quicklime treatment was evaluated based on the heavy metal leachability (in terms of the Toxicity Characteristic Leaching Procedure, TCLP), unconfined compressive strength and vertical unconfined swell. In addition to these basic tests, a series of complementary experiments including static and flow-through leaching, acid neutralization capacity, durability, X-ray diffraction and scanning electron microscopy determinations, were also performed in order to evaluate the long-term effectiveness of the treatment and to understand the underlying mechanisms of heavy metal immobilization. A schematic representation of the experimental approach used during the present study is illustrated in Figure 1.

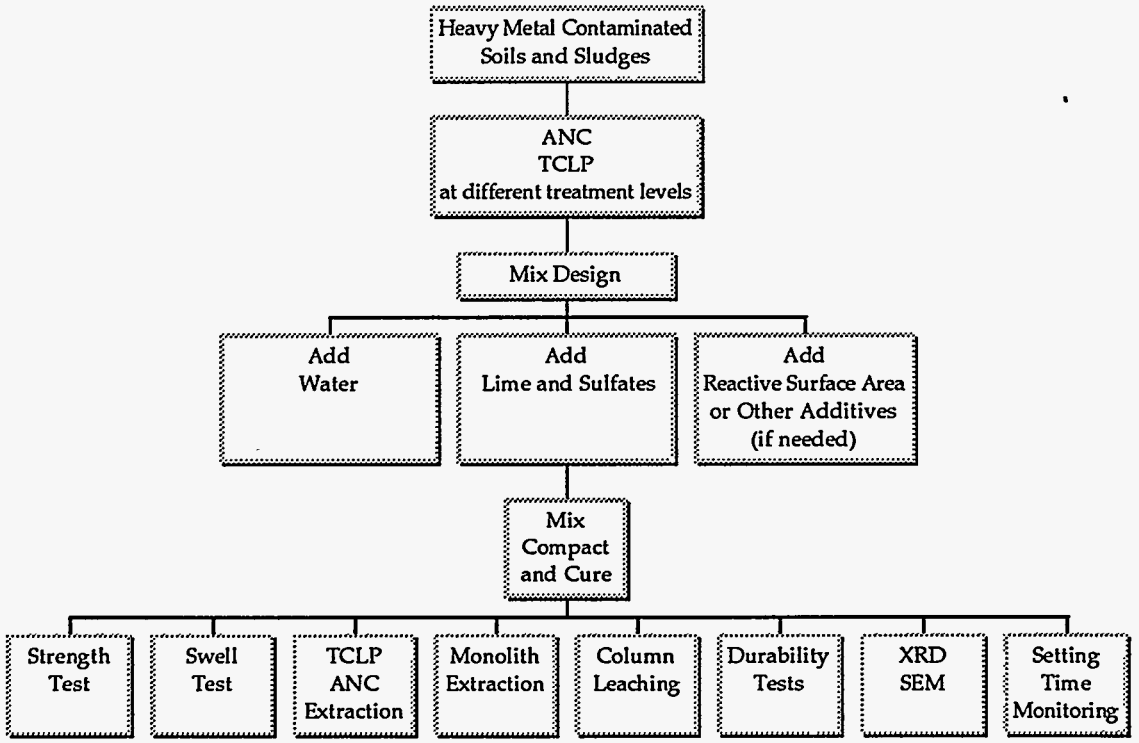

Figure 1 Experimental Methodology Outline.

1.4 Results

This report summarizes the results obtained from September 1992 to January 1995. Experimental results obtained during this study, demonstrated the following:

- The TCLP results indicated that treatment is effective in reducing the leachability of arsenic, chromium and lead to less than the TCLP criteria (5 ppm) for hazardous substances.
- Although a significant reduction was achieved for mercury leachability, treatment could not reduce mercury leachability to levels lower than the TCLP non-hazardous limit (0.2 ppm).
- For most of the clay-sand mixes tested, the optimum quicklime content was determined to be 10% by weight of the treated soil. At this treatment level both stress-strain performance and degree of heavy metal immobilization were optimized.
- The degree of lead immobilization was found to be proportionally related to the surface area amount and reactivity, and the elapsed curing time following treatment application. The heavy metal content was found to be inversely related to lead immobilization effectiveness. Lead immobilization was significantly affected by the quicklime treatment levels. Sulfate presence did not have an obvious effect.
- Chromium and arsenic immobilization were primarily influenced by the level of quicklime treatment. Surface area attributes, curing time, sulfate presence and heavy metal content did not have a significant effect on chromium and arsenic immobilization.
- Chromium immobilization due to crystal inclusion was evidenced during bentorite formation. Bentorite is a pozzolanic product isostructural to ettringite, and it only forms in the presence of chromium and sulfates.
- Treatment is increasingly effective with an increasingly soluble heavy metal contaminant source.
- Based on the flow-through leaching test results, it was estimated that the quicklime treated solids can last thousands of years in the field without significant release of the heavy metals.
- Based on static leaching test results, treatment was shown to result in a very low, matrix diffusion controlled release of the heavy metals. Conversely, heavy metal release from the untreated solids was 1 to 2 orders of magnitude higher and was identified as surface washoff or dissolution of the heavy metals as opposed to matrix diffusion.
- In addition to the immobilization of the heavy metals, the quicklime-based treatment resulted in solid forms with high strength and low swell. This means that the quicklime treated solids can be potentially reused in a variety of construction applications.

- Both surface area attributes and elapsed curing time had a major influence on strength development in the treated soils. The longer the curing time and the higher the amount and activity the surface area available for reactions, the higher the strength and the lower the swell of the treated solids.
- While in most cases the heavy metals in the solid mixes could be immobilized immediately following treatment, more than 28 days were generally needed for the compacted specimens to develop adequate levels of strength gain.
- Freeze/thaw and wet/dry durability experiments indicated that the treated solids could withstand weathering conditions encountered in temperate climates, irrespective of treatment design. If properly designed, treatment can yield materials that can withstand aggressive weathering conditions as those encountered under dessert or cold region climatic environments.
- It was also observed that when fly ash was added together with quicklime to the contaminated solids, dramatic strength increase and obvious decrease in heavy metal leachability was achieved.
- A general design methodology was developed to ensure long-term treatment effectiveness.
- Results on the treatment of contaminated natural soil and industrial sludge samples demonstrated treatment effectiveness. However, it should be noted that all field samples tested were not found to be hazardous prior to treatment.

1.5 Conclusions and Recommendations

Specific conclusions and recommendations drawn from this first phase are summarized as follows:

- The proposed technology was successful in meeting all leachability, strength and swell criteria established prior to initiation of the present work.
- The controlling mechanism for lead immobilization was found to be surface sorption to the pozzolanic reaction products. Therefore, the presence of an adequate amount of reactive surface area is of paramount importance for treatment success. A minimum of 15% by weight of clay-size active aluminosilicate surface area would ensure treatment effectiveness, for up to twice the maximum lead concentration reported in DOE sites. For coarse-grained soils, fly ash can be effectively used as a surface area substitute.
- The controlling mechanism for chromium and arsenic immobilization was found to be the precipitation of insoluble metal compounds. The presence of surface area did not have a significant effect on heavy metal release, whereas the level of quicklime treatment did. A minimum presence of 5% by weight of clay-size surface area, and a minimum of 10% by weight quicklime addition are recommended to ensure treatment effectiveness. Chromium and arsenic contamination levels need not to be taken into account for treatment design purposes.

- Among the three types of leaching behavior studied, flow-through was found to be the most critical in assessing the long-term stability of heavy metal immobilization. Under rainwater infiltration conditions, flow-through heavy metal release rates were low enough to ensure treatment effectiveness for thousands of years. When simulating acetic acid infiltration conditions, similar to those expected in landfill environments, rates of release were found to be alarmingly high in the presence of a low reactivity surface area. However, for such field conditions, it was demonstrated that incorporation of reactive surface area during treatment, would ensure long-term treatment effectiveness.
- In the presence of at least 15% by weight clay-size fraction of reactive surface area strength gain criteria were easily met within 28 days following treatment. In the presence of low reactivity surface area a curing period of six months is needed before strength criteria can be met. Addition of minimum amounts of fly ash can be used to effectively control both the rate and amount of strength development.
- Sulfate presence is of limited significance to treatment effectiveness, except when considering the swell potential and physical durability of the stabilized soil.
- In the absence of sulfates, vertical swell criteria were easily met for all the specimens tested. When sulfates were present, and only in low reactivity surface area matrices, excessive swell development was evidenced. This was attributed to the formation of the expansive mineral ettringite coupled with a low cohesive strength development in the absence of reactive surface area. However, addition of minimal amounts of barium hydroxide eliminated excessive swell development.
- Under moderate wet/dry and freeze/thaw weathering conditions, corresponding to temperate climatic conditions, the treated solids kept intact and did not show any evidence of physical degradation in the form of specimen cracking or deterioration. Similar to swell behavior, only when sulfates were present, and in low reactivity surface area mixes, physical breakdown of the treated solids was evidenced. Addition of minimal amounts of barium hydroxide eliminated physical breakdown of the treated solids.
- Under aggressive wet/dry and freeze/thaw conditions, corresponding respectively to dessert and cold region climatic conditions, the behavior of the treated solids varied considerably as a function of the corresponding surface area attributes. Generally, when increasing the amount and reactivity of the surface area present, cohesive strength development is enhanced, which in turn results to an increased physical durability of the treated solids.

Overall, as the success criteria for the first phase of this work were all satisfied, the proposed technology development program is ready to enter the sub-scale system phase.

1.6 Future work

In Phase 2 of the project, the proposed technology will be applied under sub-scale conditions. Given the technical experience acquired during Phase 1 and the apparent difficulty of shipping contaminated soils off DOE sites and to our laboratory, the original approach for Phase 2 will be modified. That is, instead of working on artificially contaminated natural soils, the sub-scale systems will consist of control instrumented areas within contaminated DOE sites. Both on-site mixing and in-situ deep injection treatment schemes will be demonstrated. Since the proposed technology does not involve any special construction requirements, up and above conventional geotechnical site improvement, the actual field work will be carried out by existing DOE site-affiliated contractors. Following such an approach we anticipate significant cost savings with respect to the original estimates of the $240,000 necessary for completion of Phase 2. Furthermore, since the work will be carried out on-site, producing the required NEPA documentation will be a faster and less involved process. Overall, the time for completion of Phase 2 is expected to be 6 months following contract award and site selection. Site selection will be performed by DOE headquarters.

1.7 Technology Relevance

Given the complexity and wide variability of field contamination scenarios within DOE facilities, it is impossible to develop a single technology to remediate all sites. Furthermore, in a global sense, the enormous cost of site remediation raises an important point about realistically meeting current cleanup goals in a timely fashion. The *"'how clean is clean"* is a hard to answer question for both regulators and environmental professionals, as well as for the general public and the owners of contaminated sites. The question is not whether contaminated sites exist; literally tens of thousands exist. What is questionable is the level of risk posed by these sites and the degree of remediation necessary to reduce these risks to acceptable levels. Currently the answer to this question is driven mostly by public perception rather than scientific consensus. This often results in establishing short-sighted, short-term remediation success criteria, that in many cases are not realistic, leading to considerable overspending of resources, without ensuring a long-term reliable solution to the problem.

In view of the above, as a first step, it is necessary to develop an innovative cost effective technology to treat heavy metal contaminated soils and sludges, that would be versatile enough as to enable its application in a broad range of DOE field conditions. In our view, there are certain elements that should be an integral part of such a technological solution:

1. Technological "know-how" and vendors should be well established and readily available within the DOE complex. The commonly accepted view that innovative technologies should only include novel technologies, often results in the development of cost prohibitive solutions that can be only applied under certain site-specific conditions.

2. The applicability of the developed technology should be as broad-based as possible. The technology should have a demonstrated effectiveness in the presence of low level radioactive and mixed contamination. Moreover, technology application should be possible in-situ or on-site.
3. The technology should be reliable for long-term immobilization. The final product should be durable to physical and chemical weathering so as to ensure long-term treatment effectiveness. Furthermore, it should attain a low permeability so physical entrapment (encapsulation) of the contaminants would further enhance their immobilization.
4. Technology application should result in a reusable material. Landfill storage space is becoming increasingly scarce, and resource recovery in contaminated sites is rarely deemed cost effective. Reusability should encompass both use in construction applications as well as reclamation by revegetation options.
5. The technology should not incorporate treatment additives or procedures that may themselves adversely affect the environment in the long run. This is the single most important uncertainty concerning field application of most innovative technologies.
6. The mechanisms responsible for treatment effectiveness should resemble natural geochemical processes. The final material treatment product should resemble the properties of materials found otherwise in natural environments, and which are not products of human activity.
7. It should allow the incorporation and/or treatment of other wastes produced in significant quantities within the DOE complex. Such wastes would include coal and incinerator fly ash, slag, wet and dry flue gas desulfurization (FGD) wastes, etc. Combining waste materials during treatment is a resourceful way to control waste volume increases.
8. The underlying mechanisms responsible for treatment effectiveness should be well established before large scale treatment application takes place.
9. Treatment effectiveness should not only be judged by current regulatory benchmarks. Instead, it should be also judged using meaningful scientific criteria based on actual behavior and not on broad-based perceptions.
10. The test and evaluation procedures developed should lead to an improved technical assessment of treatment effectiveness, which could be applied to a broad range of waste types.

The proposed technology as well as our technological development approach meets all of the above criteria. Lime is the essential ingredient in all pozzolanic-based remediation schemes and soil and sludge lime stabilization has been a standardized practice well before hazardous waste laws were introduced. Related experience from fly ash and FGD waste stabilization, equipment and vendors are readily available within the DOE complex. In addition, lime can be effectively used in a wide variety of in-situ or on-site field contamination scenarios including low-level radioactive and mixed waste conditions. Moreover, based on the results obtained during Phase 1 of this project, it can be concluded that treatment, if designed according to the methodology developed

herein, will produce a non-hazardous solid that can be reused as readily available construction material. As demonstrated, the treatment final product can effectively withstand the full spectrum of climate-induced weathering conditions and acid leaching scenarios, without jeopardizing the original treatment goals. Furthermore, treatment does not introduce questionable additives and results in the formation of otherwise naturally occurring aluminosilicate minerals and insoluble heavy metal compounds. Overall, when properly designed the quicklime-based treatment is an effective, yet simple to implement technique to immobilize heavy metals in soil environments. Application of the proposed technology would satisfy current regulatory requirements at the added benefit of significant cost savings.

2 BACKGROUND

2.1 Introduction

Heavy metal contaminants, introduced in soil environments through a wide variety of industrial, agricultural and waste disposal practices, may lead to severe pollution of both surface and ground water. As heavy metal contamination poses an immediate threat to human, animal and plant life, legislation has been introduced in both the federal and state levels, aiming at source reduction as well as remediation of already contaminated soil media. Presently, numerous sites around the country are contaminated due to the presence of high concentrations of heavy metal compounds. Heavy metal species of high priority interest include arsenic, chromium, lead, and mercury. A variety of remediation technologies have been developed to treat the contaminated solids. Among the existing remediation alternatives, it has been demonstrated that pozzolanic-based S/S methods are the most cost-effective technologies in treating high volumes of the heavy metal contaminated soils. Pushed by regulation that essentially mandates its use for many waste streams, pozzolanic-based S/S is becoming a standard unit process in hazardous waste treatment and disposal. Yet, in spite of the EPA recently published technical handbook (Cullinane and Jones, 1986), the present state of knowledge concerning the S/S treatment underlying mechanisms and long term reliability is inadequate, thus rendering the success of technology field applications uncertain.

Amongst the pozzolanic-based S/S techniques, cement-based treatment is the most commonly used. This treatment, and variations on it, were the first to be used in the nuclear waste field during the 1950s. During cement-based treatment the waste is encapsulated in an alkaline, very low permeability, monolithic medium. However, during contaminated soil applications, treatment requires the addition of large amounts of cement to the soil, which results in significant volume increase of the final waste forms and high treatment costs. Presence of very fine particles in the silt and clay size fractions, organic compounds, coal and lignite, inorganic salts, and metal compounds may prevent cement setting and render treatment ineffective. Following successful cement application, the physical properties of the soil are changed irreversibly, rendering reclamation of the concrete-like soil for vegetation purposes impossible. Moreover, cement S/S applications mainly focus in producing a material that is more amenable to past disposal practices, like ocean dumping, and do not consider the reuse potential of the stabilized materials. Finally, there is very little information available on the underlying mechanisms of contaminant immobilization since treatment effectiveness focuses mainly on the physical aspects of macroencapsulation. It is our view, that cement-based approaches, while they may well constitute the most cost-effective alternatives in the nuclear waste field, tend to be an unnecessary overtreatment of low-level radioactive and heavy metal solid wastes.

In view of the above, it is important to develop innovative and cost effective remediation techniques that provide a long term solution for heavy metal contaminated soils. It is also important to delineate the underlying mechanisms of contaminant immobilization, to ensure treatment effectiveness in a wide array of contamination scenarios. In the present study, quicklime and sulfate salt were used as the base chemical additives to stabilize/solidify heavy metal contaminated soils. Such an approach has several advantages over cement-based treatment, as outlined in the following section.

2.1.2 *Why Use Quicklime*

The introduction of the RCRA and CERCLA hazardous waste laws has spawned the development and implementation of a wide array of technologies aimed at the remediation of contaminated sites. A number of these technologies have been successful in remediating limited quantities of wastes ex-situ. However, considering the extent of sites affected by past, present and future waste disposal, economic considerations dictate the necessity of developing in-situ technologies that can treat large amounts of contaminated soils and sludges. In terms of in-situ approaches there has also been measurable success in developing successful waste-specific technologies. For instance, bioremediation or thermal treatment schemes can be effectively used to treat sites contaminated with organic pollutants only. Similarly, pozzolanic S/S can be effectively implemented to treat certain inorganics. However, the vast majority of hazardous waste contamination involves the presence of mixed organic and inorganic pollutants. To this date, only quicklime-based technologies (Payne et al., 1992) have shown promise in treating sites with mixed contamination.

In the present study the main emphasis is placed in treating heavy metal contaminated sites. As already mentioned, heavy metal contaminated media cannot be effectively treated by means of conventional thermal and biological approaches. Amongst the remaining in-situ and ex-situ options the most cost-effective alternative is pozzolanic fixation. Lime is the necessary ingredient in all pozzolanic-based S/S remediation schemes. Lime is readily soluble (the solubility of $Ca(OH)_2$ is 1,200 mg/l at 21 degrees C) and available for reactions. Soil-lime setting is a very slow process as compared to cement setting and therefore is a more flexible process regarding both its field application and the consistency of the final product. Depending on the original contaminated soil matrix and treatment levels, lime stabilized soils may resemble the structural consistency of concrete-like materials, or may forever remain as soil-like materials, amenable to reclamation through vegetation. Lime stabilized soil mortars have a high degree of permanence, while at the same time there seems to be fewer matrix restrictions in terms of treatment effectiveness. In fact, the addition of lime to portland cement has been found to counteract the retarding action experienced during cement-based S/S, and allow for a proper set to be achieved. Moreover, in the case of in-situ stabilization of deep layers by slurry injection, lime permeates the porous media much more effectively due to its relatively high solubility. Lime injection can have a much larger radius of influence than cement injection under identical injection pressures and soil conditions. Furthermore, when we are dealing with high water content wastes,

or low temperature regions, quicklime is a much more effective additive, as its heat of hydration (15.3 Kcal/g mol with water and much higher with acids) can be substantial in accelerating other on-going reactions, and reducing the time required for remediation. In addition, the subsequent drying of the surrounding ground can be a significant outcome. Finally, commercial quicklime is a much more homogeneous material and it is less expensive than cement.

Some general data available through EPA (US EPA, 1989), suggests that for heavy metal contaminated soils and sludges, lime-based S/S approaches are the most inexpensive alternatives (close to $30 per cu. yard), whereas cement-based approaches would cost close to $170 per cubic yard. In the organic waste stabilization field, a similar technology with the one proposed here, has been applied successfully. Based on information provided by Payne et al. (1992), a quicklime treatment of 20% by weight of the soil waste to be stabilized, is extremely effective in immobilizing organic contaminants, and it results in a material that generally occupies less volume than the original volume occupied by the contaminated soil. On the other hand, Suprenant et al. (1990), point out that 1 ton of cement and fly ash cementitious material will treat about 1 cubic yard of oil contaminated soil, which of course translates to approximately 95% of treatment by weight of soil waste to be stabilized, resulting in volumes of material that are much larger than the initial contaminated soil volumes involved. Overall, it is very difficult to compare actual costs or effectiveness associated with the application of the proposed technology, with other existing technologies, since the proposed technology has not been applied yet and no cost data are presently available. However, based on the EPA data and the organic waste stabilization experience, it is expected that quicklime-sulfate salt would be more effective than cement fly ash stabilization of heavy metal and/or mixed wastes, with respect to both waste minimization and cost reduction.

2.1.3 *General Treatment Principles*

Generally, when considering chemical admixture treatment of soils, a distinction may be made between two types of soil treatment:

1. *Stabilization* refers to a process during which additives are mixed with the waste to minimize the rate of contaminant migration from the waste and to reduce the toxicity of the waste. This is achieved by modifying the waste chemical and/or biological character or composition.
2. *Solidification* refers to a process during which additives are employed to alter the physical nature of the waste. This is achieved by encapsulating the contaminated soil in a monolithic solid with high structural integrity, by enhancing its engineering properties of strength, compressibility, and/or permeability.

Thus, objectives of stabilization and solidification would encompass both the reduction in waste mobility and/or toxicity as well as an improvement in the engineering properties of the stabilized material. More specifically, for solid waste scenarios, the reduction in a waste constituent mobility translates to a reduction of its leaching rate (leachability). Leaching is the process by which contaminants are transferred from a matrix to a liquid medium such as water.

Leachability control or reduction is usually achieved by limiting the waste surface area across which transfer or loss of contaminants can occur, limiting the solubility of any pollutants contained in the waste, enhancing contaminant adsorption on the solid surfaces of a waste matrix and restricting the contaminant hydraulic and/or diffusion flow path. Furthermore, reduction in waste toxicity implies a transformation of the main waste constituent(s) into a less toxic form, such as the conversion of chromium from its hexavalent to its trivalent form in the presence of reducing agents. On the other hand, improvement in the engineering properties of the stabilized waste translates to an increase in its strength and durability, and a decrease in its deformation potential and permeability.

Amongst the numerous treatment agents, some are eligible for both stabilization and solidification, depending on the amount that will be admixed to the material. One typical such double-action agent is lime. It is widely demonstrated that when mixed with lime most heavy metal contaminated wastes exhibit a reduced leachability. In addition, upon lime addition all fine-grained (clayey) soils exhibit improved plasticity, workability, and volume change characteristics. Furthermore, most clayey soils also exhibit improved strength, stress-strain, and fatigue characteristics, and develop lower values of hydraulic conductivity. Therefore, the general objectives of mixing lime with soil are to improve or control volume stability, strength and stress-strain properties, permeability and durability and to reduce the heavy metal leachability.

Volume stability (control of swelling and shrinkage processes) can be improved by replacement of high hydration cations, such as sodium (Na^{+}), by the low hydration cations such as calcium (Ca^{2+}) and/or magnesium (Mg^{2+}), and by cementation due to the formation of calcium aluminate and/or calcium silicate hydrates (CAH and CSH respectively). The development and maintenance of high strength and stiffness is achieved by elimination of large pores, by bonding particles and aggregates together, by maintenance of flocculent particle arrangements, and by prevention of swelling. Finally, permeability is altered by modification of pore size and pore size distribution. It can be increased or decreased depending upon the percentage of lime added and the final compactive effort applied. Generally, even though the data is limited, the long-term permeability of a compacted lime-soil mixture is reported to be much less than compacted soil alone (Diamond and Kinter, 1966).

The reduction of heavy metal leachability is achieved by incorporating the heavy metals in a high pH matrix. Within this high pH matrix, a significant portion of the heavy metal ions are precipitated in their least soluble forms. However, the theoretical basis for the effectiveness of lime in heavy metal contaminated soil stabilization is not well established at this point, as previous research concentrated in much more practical aspects than trying to explain the underlying mechanisms (Turco and Zenobia, 1985). There are strong indications that lime effectively reduces the hazardous potential of heavy metal contaminated soils, as it can be seen in Table 3. Even though it would be expected that preferential fixation of heavy metal species would occur during

stabilization, the results presented in Table 3 do not indicate so. It seems that lime stabilization works for all heavy metals under investigation, and that preferential immobilization would probably be significant only at extremely high heavy metal concentrations. For that reason, our experimental approach did not involve the study of a single heavy metal species. Instead mixes including all four heavy metals under study (arsenic, chromium, lead, and mercury) were only considered.

Table 1. Leachate Results Prior and Following Treatment of a Heavy Metal Contaminated Soil (modified after Turco and Zenobia, 1985).

	Prior to Treatment (ppm)			Following Treatment (ppm)					
Sample #	A	B	C	A7	B7	C7	A28	B28	C28
Arsenic	<2	<2	<2	<0.1	<0.1	<0.1	<0.1	<0.1	<0.1
Cadmium	13	<1	30	<0.01	<0.01	<0.01	<0.02	<0.07	<0.10
Chromium	500	500	6,200	0.03	0.01	0.03	0.28	0.02	0.04
Lead	1,600	1,300	370	<0.1	<0.1	<0.1	<0.1	<0.1	<0.1
Mercury	0.4	0.6	0.2	<0.1	<0.1	<0.1	<0.1	<0.1	<0.1
Selenium	<30	<40	<35	<0.1	<0.1	<0.1	<0.1	<0.1	<0.1

Overall, there seem to be three distinct mechanisms that could be responsible for the entrapment of the heavy metal species in the stabilized soil matrix. First, the formation of insoluble heavy metal hydroxides due to the stabilization-induced high pH conditions makes it difficult for heavy metal species to find their way into groundwater. However, it should be noted that some species like arsenic and chromium, remain rather soluble in alkaline solutions, and therefore their immobilization is not readily explained in terms of hydroxide complexation mechanisms. The second possible mechanism is that during stabilization heavy metal species may be incorporated into the crystal structures of the cementitious compounds formed, and consequently are not readily dissolved in water, thus not showing up into the leachate chemical composition. The third mechanism is the physical entrapment of the heavy metal species through sorption onto particle surfaces in a low permeability matrix. One of the objectives of the proposed research effort would be to establish which are the underlying mechanisms, both physical and chemical, that are responsible for heavy metal stabilization.

Finally, another main aspect of the current study was the long term performance of such stabilized waste materials under different environmental stresses, such as acidic flows as well as temperature and relative humidity fluctuations. The key to long term performance is that the treatment final product should be able

to withstand aggressive leaching and weathering conditions without a significant increase in heavy metal release or loss of its structural integrity.

2.1.4 *Lime-soil Reactions*

When a significant quantity of lime is added to a soil, the pH of the soil-lime mixture is elevated to approximately 12.4, the pH of saturated lime water. This is a very high pH compared to the pH of natural soil deposits, which typically varies in the range of 5 to 8. The solubilities of silica and alumina present in clay minerals are greatly increased at this elevated pH levels, thus making them available for reaction with the calcium from lime to form the cementitious hydrates, CAH and CSH. It is generally believed, that formation of these calcium aluminosilicate hydrates is mainly responsible for the high strength and low swell of the treated solids, as well as for heavy metal immobilization through surface sorption, inclusion and physical entrapment.

A simplified qualitative representation of some typical soil lime reactions is summarized below:

$Ca(OH)_2$ ----------> $Ca^{2+} + 2\,OH^-$

$Ca^{2+} + 2\,OH^- + SiO_2$ (Clay Silica)----------> CSH

$Ca^{2+} + 2\,OH^- + Al_2O_3$ (Clay Alumina)----------> CAH

where: C=CaO, S=SiO_2, A=Al_2O_3, and H=H_2O. A wide variety of hydrate forms can be obtained, depending on reaction conditions, e.g., quantity and type of lime, soil characteristics, curing time and temperature.

When the soil and/or groundwater contain sulfates in solution, they may combine with the alumina liberated from the clay, or possibly present in its amorphous state, to form a series of calcium-aluminate-sulfate hydrate compounds, leading ultimately to the formation of ettringite, $[Ca_3Al(OH)_6]_2(SO_4)_3 \cdot 26\,H_2O$.

The geochemical reactions involved in the growth of ettringite in natural environments, are quite complex and not adequately established for lime-treated soils. Hunter (1988) proposed a simplified geochemical mechanism for the formation of ettringite in lime stabilized soil strata, which can be summarized by the following series of stepped equilibrium reactions:

C + **H** --------> **CH**(hydration of quicklime).....(1)

CH-->Ca^{2+}+2$(OH)^-$(ionization of calcium hydroxide;pH rises to 12.4).....(2)

$\mathbf{AS_4H_n}$+2$(OH)^-$+10**H**---->$\mathbf{AH_3(OH)_2^{2-}}$+4$\mathbf{SH_2}$+n**H** (dissolution of clay mineral, at pH>10.5).....(3)

5$\mathbf{SH_2}$---->5**SH**$(OH)^-$ +5H^+ (dissociation of silicic acid).....(4)

5Ca^{2+}+5**SH**$(OH)^-$+5$(OH)^-$--->5**CSH**+5**H** (formation of tobermorite gel).....(5)

$Na_2SO_4 \cdot 10$**H**------>2Na^++SO_4^{2-} + n**H** (dissolution of sulfate minerals).....(6)

$6Ca^{2+}+AH_3(OH)_2^{2-}+4(OH)^-+3(SO_4)^{2-}+26H$------>$C_6A(SO_4)_3H_{32}$ (formation of ettringite).....(7)

where C=CaO, H=H_2O, A=Al_2O_3, S=SiO_2.

Equations 1 thru 4 are normal pozzolanic reactions resulting in cementation of lime-treated soils by the formation of tobermorite gel (CSH). Equation 3 is shown specifically for a montmorillonite clay. In fact, any clay mineral could be used in the model since the sole function of the clay is to provide a source of silica and alumina. The same holds for equation 6, where any soluble sulfate salt could have been used instead of sodium sulfate to provide the source for sulfates in solution. In the presence of excessive sulfate, the rate of the forward reaction in equilibrium pair equation 5 approaches zero, as almost all of the calcium in solution reacts with alumina sulfates and water to form ettringite (Eq. 7).

Although not investigated systematically, previous research in Japan has established the effectiveness of lime stabilization on heavy metal wastes, as well as the potential for reuse of the treated waste as a construction material (Arizumi et al., 1977; Kuroda et. al., 1980; Kujala, 1986; Shida et. al., 1987; Kamon et. al., 1988). The Japanese seem to attribute the significant strength gains of the treated waste forms as well as the immobilization of the heavy metal components to the formation of cement bacillus, commonly known as ettringite.

Ettringite, however, is known to be quite expansive when brought in contact with water, and its swelling could lead to catastrophic failures (Mitchell, 1984; Zhou and Colombo, 1987; Hunter, 1988, Mitchell and Dermatas, 1990), as well as possible releases of the previously immobilized toxic heavy metal components into adjacent water bodies. In this study we took a closer look at ettringite formation and subsequent hydration under different conditions, and came up with an explanation as to whether ettringite formation is desirable or not, and under what conditions of composition, curing, and confinement ettringite is not conducive to swelling. Furthermore, the contribution of ettringite and the other cementitious treatment products, to the resulting heavy metal immobilization and strength increases following treatment, was also investigated.

2.1.5 Heavy Metal Release

In soil environments, both the environmental impact of hazardous materials and the effectiveness of S/S treatment technologies are evaluated based on the leaching of the pollutants of concern. Leaching is the process by which contaminants are transferred from a stabilized matrix to a liquid medium such as water. Various kinds of leaching tests have been developed to evaluate the leachability of contaminants, such as the Toxicity Characteristic Leaching Procedure, TCLP (USEPA, 1985), the Acid Neutralization Capacity (ANC) test (Isenburg and Moore, 1992), the American Nuclear Society (ANS 16.1, 1986) static leaching test and the column leaching test (Bishop, 1986). The tests used to evaluate the leachability of solid wastes can be separated into batch extraction, monolith extraction, and column leaching approaches.

The TCLP test is a single step batch extraction test since during the experiment a suspension consisting of acetic acid solution and pulverized solid is mixed in a container. The pollutant concentrations in the final leachate (extract) are used by the U.S. EPA as the current regulatory benchmark to determine the hazardous potential of a waste for land disposal purposes. However, the TCLP results cannot really be used to predict the leaching behavior of pollutants in surface and subsurface environments, unless used in conjunction with other tests.

Quicklime and other alkaline binders reduce leachability by incorporating the heavy metal species in a high pH matrix. Within this high pH matrix, a significant portion of the heavy metal ions are precipitated in their least soluble forms. Suitable binders further control leachability by releasing additional hydroxides to buffer the leachant that comes in contact with the treated waste. This ability to buffer the leachant is very important since most heavy metal species become increasingly soluble as the pH drops. The ANC is a single-step batch extraction test and it is used to determine the buffering capacity of the given waste form. It involves separate extractions of several pre-dried, crushed waste samples using leaching solutions of varying levels of acidity. Generally, the higher the buffering capacity of the waste, the greater the possibility of maintaining alkaline pH conditions, thus minimizing the amount of contaminant release due to dissolution.

The monolith or tank static leaching test (ANS 16.1, 1986) is conducted by immersing the intact solid into leachant solution (Groot and van der Sloot, 1992). This test is mainly used to test solidified/stabilized wastes, such as those produced with cement and lime-based treatments. The information obtained from the monolith extraction experiment has been used to delineate the mechanisms controlling the release of pollutants from the solid phase to solution (Groot and van der Sloot, 1992). Its applicability can be limited however, as it only considers diffusion-controlled leaching.

During column leach tests, a leaching solution is passed continuously through a column packed with ground solid at controlled flow rates (Bishop, 1986). The long-term leaching behavior of the treated waste can be predicted from the pollutant breakthrough curves obtained from the column experiment. However, the physical properties of the pulverized solid, such as the hydraulic conductivity and the particle surface area available for reaction, are quite different from the monolith solid, and therefore the leachability behavior will also be different. Consequently, the results of traditional column tests should not be used for field prediction purposes. In fact, none of the tests discussed so far can be used to predict field behavior, which to a large extent, will be a function of the actual field hydraulic conductivity of the given waste form.

In the present study, a flow-through column leach test was developed to evaluate the long-term effectiveness of a proposed quicklime-based S/S technology to immobilize heavy metals in soils. During this test, leaching solutions were passed through compacted soil specimens under constant hydraulic head conditions, and the long-term leaching behavior was evaluated under different flow-through infiltration scenarios. The effect of leachate pH on the release of lead under different leaching conditions was also evaluated, since

pH is usually the most important parameter influencing the leachability of heavy metals (Welsh et al., 1981; Cote and Constable, 1982). Finally, based on TCLP, ANC, static and flow-through leaching test results, a testing protocol was developed for the design and evaluation of contaminated soil remediation technologies.

3 EXPERIMENTAL METHODOLOGY

The objective of this project is to develop a chemical admixture stabilization process for treatment of heavy metal contaminated soils, with the aim of immobilizing the existing heavy metal species, while obtaining a stabilized solid that could be reused as readily available construction material. The heavy metals under study include arsenic, chromium, lead, and mercury.

In this first phase of the study, bench-scale experiments were conducted using artificially contaminated clay-sand mixes as well as actual field contaminated soil samples. To simulate the range of texture, gradation and physicochemical soil properties expected in the field, artificial soil mixes were prepared by mixing 5 to 30% by weight of montmorillonite or kaolinite clay minerals with fine quartz sand. The choice of clay minerals, as a source of surface area and fine gradation, spans across the full spectrum of layered aluminosilicate behavior. Kaolinite is the most inactive clay in terms of its surface area and charge attributes. Conversely, montmorillonite is the most reactive clay mineral due to its high surface area and charge. In a few cases fly ash, was also used as a source of surface area, so the contribution of non-layered aluminosilicate surface area commonly found in waste by-products (fly ash, FGD wastes, slag, etc.) could also be assessed.

Heavy metals were added concurrently in the form of variable solubility commercially available reagent grade solid compounds. The solubility of the heavy metal source was purposely varied to assess its effect on treatment effectiveness. Moreover, the most soluble heavy metals were introduced in the form of nitrate and sodium salts in order to investigate the possible adverse effects of sodium and nitrate presence on treatment effectiveness. Sulfate, nitrate and sodium presence is known to lead to treatment ineffectiveness in cement-based pozzolanic S/S schemes. The information pertaining to the heavy metal levels of addition are summarized in table 1.

Table 2. Contents of Heavy Metals in the Artificial Soil Mixes

Heavy Metal	Arsenic	Chromium	Lead	Mercury
Contaminant Source (most soluble)	Sodium Arsenite	Chromium Nitrate	Lead Nitrate	Mercury Nitrate
Contaminant Source (least soluble)	Arsenic Oxide	Chromium Oxide	Lead Oxide	Mercury Oxide
mg of Speciated Metal/kg of Soil	125	4,000	7,000	2,000

The amount of quicklime added to the contaminated mixes varied from 0 to 15% in order to determine the optimum lime contents for treatment of the different kinds of solid mixes. The treatment conditions evaluated also included curing

time of the treated solids, and addition of sulfate and other additives. Sulfate was added in the form of readily soluble sodium sulfate, and its addition had a two fold purpose. First, as already mentioned, sodium as well as sulfate presence have been reported as the main causes of treatment effectiveness in cement-based S/S applications. Their adverse effect has been attributed to disruption of the pozzolanic reaction sequence in their presence. In addition, sulfate presence is responsible for ettringite formation. It is one of the objectives of the current study to investigate ettringite formation and subsequent hydration and its effect on the stress-strain behavior and heavy metal mobility within the treated solids.

Treatment can be separated into an initial batch and a final compaction step. The batch treatment was used as a preliminary step to obtain the design additive contents to be used during compaction treatment. During the batch step, the contaminated solids were mixed with additives and water at different additive contents. The final mixes were cured as loose solids for limited period of time amounting to a few days. After curing, the loose solids were tested for their TCLP leachability and acid neutralization capacity and treatment design levels were established. Generally, one to three batch treatment steps were concluded before each compaction treatment step was attempted.

Following the batch step and treatment design mix preparation, specimens were compacted in duplicates in accordance with ASTM D558-82 standards. Following compaction and specimen extrusion, weight and dimension data were recorded and specimens were placed in moisture tight plastic bags and put away in 99% relative humidity (RH) and 20°C curing chambers. Six main compaction treatments were performed during the present study, four involving artificial soil mixes and two involving actual contaminated field samples. For artificial soil mixes, the first compaction was performed to establish optimum treatment levels, the second and third to evaluate quicklime treatment effectiveness with respect to the solubility of the heavy metal source, and the fourth to repeat unsuccessful experiments and/or confirm unusual experimental results. A total of more than 750 artificial soil specimens were compacted and tested. For the actual field contaminated soils, the first compaction was performed to establish the optimum treatment levels and the second to test treatment long-term effectiveness under optimal conditions. A total of more than 200 actual field contaminated specimens were compacted and are still being tested. Overall, both artificial and actual soils were tested under the same experimental framework. Whereas all testing and evaluation is completed for the artificial soils, most tests for actual soils are still on-going.

The effectiveness of the quicklime treatment was mainly evaluated for TCLP leachability, compressive strength and vertical swell. In addition, a set of flow-through units (27 confined flexible wall chambers) were constructed to evaluate the long-term leaching behavior and hydraulic conductivity of the compacted specimens under constant hydraulic head and high hydraulic gradient conditions. A series of specimens have been tested under acetic acid or water infiltration conditions for more than one year. Heavy metal release under moderate leaching condition was evaluated using a monolith (ANS 16.1)

leaching test. In this test, the release of the heavy metals from an intact solid surface was monitored under no flow (static) conditions. Moreover, the durability of the treated specimens under accelerated weathering conditions was tested according to ASTM D560-82 freeze/thaw and D559-82 wet/dry methods. Finally, based on the data obtained from these experiments and ANC test results, a methodology was developed to predict the long-term leaching behavior of the treated solids and to design the quicklime treatment levels.

Overall, the shear volume of specimens prepared and tested and the multitude of experimental methods used resulted in the generation of large amounts of data. For the purposes of this report, only some of the data are presented as deemed appropriate for presenting all the significant results obtained. The rest of the data can be either found in the appendices section of this document or with the archives of the contractor. For the purpose of facilitating the review of this document, a specimen designation guide is outlined in Figure 2.

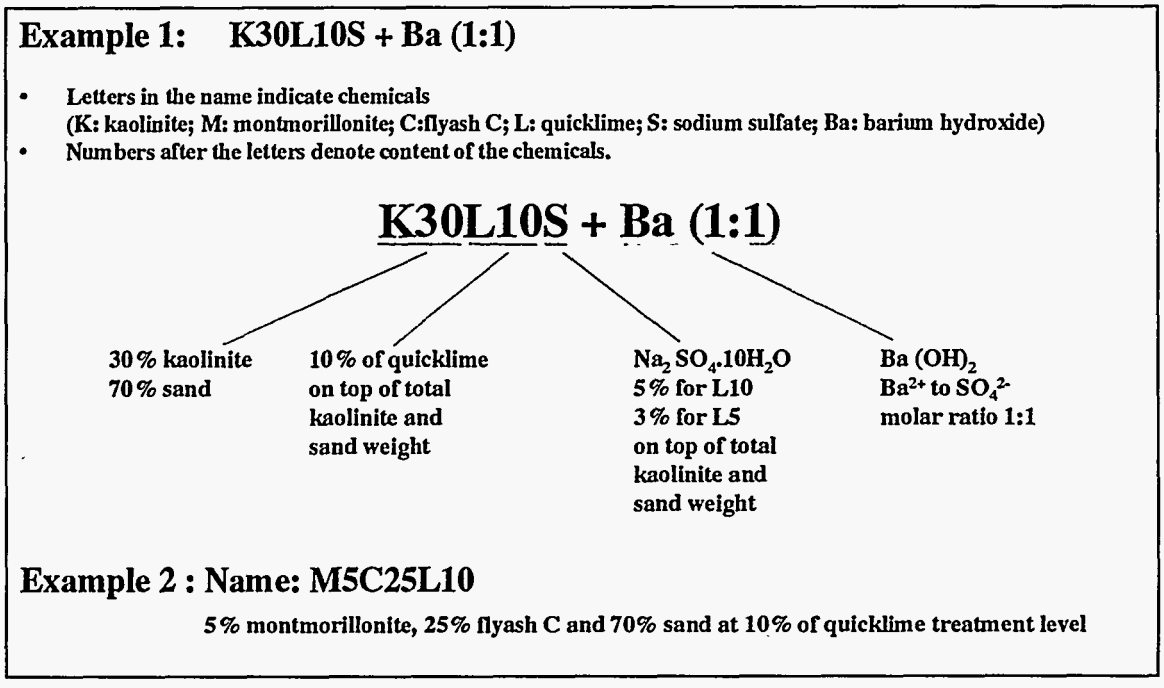

Figure 2. Specimen/Sample Designation Description.

To further facilitate the reader, we also include a comprehensive outline of all different tests used and their immediate purpose, as follows:

- Grain Size Distribution and Atterberg Limits analyses were used for general soil characterization purposes.
- The Acid Neutralization Capacity (ANC) test was performed to determine the amount of quicklime that needs to be added to the soil.

- The Toxicity Characteristic Leaching Procedure, TCLP, was performed to obtain a measure of treatment effectiveness in terms of non-hazardous regulatory compliance.
- Unconfined Compressive Strength tests were performed to obtain a measure of the strength of the treated solids.
- Unconfined Vertical Swell tests were used to evaluate the swell potential of the treated specimens in the presence of water.
- Freeze/Thaw and Wet/Dry durability tests were used to determine the long-term durability of the treated soils.
- Water content time-history tests were used to evaluate the setting of the lime-soil mixes with respect to elapsed time following treatment.
- Flow-Through column leaching tests were performed to determine the permeability and heavy metal release of the treated soils under different flow-through leaching scenarios.
- Static leaching tests were performed to evaluate heavy metal release from the treated specimens under diffusion-controlled conditions.
- X-Ray Diffraction analyses were implemented to investigate the compositional changes as a result of treatment application.
- Scanning Electron Microscopy analyses were performed to study the micromorphological changes and the particle surface compositional changes resulting from treatment.

Detailed descriptions of the experimental protocols can be found in the appendices section of this report.

4 RESULTS AND DISCUSSIONS

4.1 TCLP Leachability of Heavy Metals in the Treated Soils

The release of heavy metals from contaminated soils may create serious pollution problems to surrounding ecological systems and to groundwater resources. Unfortunately, heavy metal release cannot be assessed solely on a total content basis. The chemical form at which heavy metals are present, and the chemical composition and physical properties of both the solid and the leachant are the main factors controlling heavy metal release. When considering regulatory levels of allowable heavy metal release, the Toxicity Characteristic Leaching Procedure (TCLP) (USEPA, 1985) is currently being used by the US EPA to determine if a contaminated solid should be disposed of as a hazardous substance or not. Furthermore, when a contaminated soil layer is located at a proximity to a water resource, EPA promulgated that heavy metal release into the aqueous phase, as measured by monitoring wells, should not exceed that of drinking water standards. This latter promulgation is not always enforceable as drinking water standards are very low, some might argue unreasonably so, when applied to field contamination scenarios. Conversely, the TCLP ruling is widely applied and is also adopted by most state or other local government environmental protection agencies. According to the TCLP rule, if As, Cr and Pb concentrations are lower than 5 ppm, and Hg concentration is lower than 0.2 ppm in the TCLP leachate extracted from a solid, the solid is not considered a hazardous substance.

4.1.1 Effect of Quicklime Treatment on Heavy Metal Leachability

In view of the above, the main objective of this study is to ensure the reduction in heavy metal release below the TCLP limits, by means of a quicklime-sulfate treatment of the contaminated soils. The first step towards attaining this objective is to establish the influence of quicklime treatment levels on reducing the heavy metal release. Generally, a reduction in heavy metal release requires an increase of the contaminant geochemical attenuation capacity, since destruction or transformation to a less toxic form is a process more applicable to organic contaminants. Geochemical attenuation is a strong function of heavy metal solubility and various soil-contaminant interactions such as adsorption, isomorphous substitution, absorption processes, etc. In turn, heavy metal solubility and soil-contaminant interactions are very sensitive to pH changes. Therefore, levels of heavy metal release and the long-term durability of the treated soils should be significantly influenced by the capacity of the treated soil to withstand such pH changes and maintain the treatment target pH. Generally, treatment pH is related proportionally to the level of quicklime addition, since quicklime (CaO) is a strong alkaline reagent. Quicklime reacts spontaneously with water to form hydrated lime ($Ca(OH)_2$), thus raising the pH of the solid. The soil capacity to withstand pH changes induced by acid leaching is termed acid neutralization capacity (ANC). The level of ANC is proportional to the

level of quicklime presence, and is also affected by the acidity or alkalinity of the soil.

Overall, during the present study, a two-fold approach was implemented. On one hand, the influence of the level of quicklime treatment on the ability of the treated soil to withstand pH drops caused by acid leaching was assessed by performing ANC tests. Concurrently, while again varying the level of quicklime treatment, soil mixes were tested for their TCLP levels of heavy metal release. Based on both the ANC and TCLP results, optimum levels of quicklime treatment were then established.

4.1.1.1 ANC Results

In order to assess the capacity of the treated soil to withstand pH drops caused by acid leaching as a function of the level of treatament (i.e., amount of quicklime and sulfate presence added), the treated soils were titrated using acetic acid. Acetic acid was used to enable data comparisons with the TCLP results, as titration of the treated soil using 2 equivalents of acetic acid per kg of solid is equivalent to TCLP testing conditions for alkaline waste materials. The pH's of montmorillonite-sand mixes containing different amounts of quicklime are plotted in Figure 3 as a function of the number of equivalents of the acid used to titrate one kg of the solid. Figure 3 indicates that the untreated montmorillonite-sand mix has negligible ANC, whereas one kg of the mix at a quicklime treatment level of at least 10% can neutralize 2 equivalents of acid without a significant drop of pH. Moreover, the addition of sulfate to the sample mixes does not seem to have a major effect on ANC. Similar results were obtained for kaolinite-sand mixes.

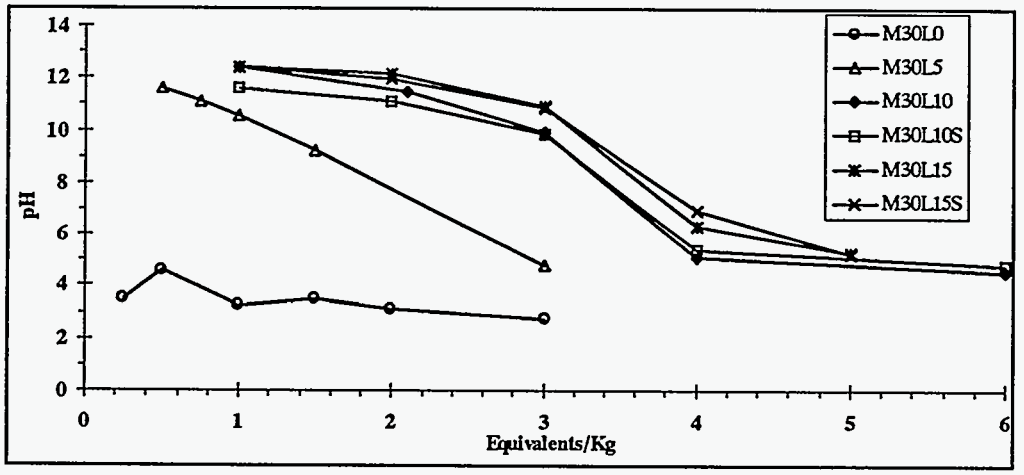

Figure 3. Effect of Quicklime-sulfate Treatment on the Acid Neutralization Capacity of Montmorillonite (30%)-sand Mixes after 28 Days of Curing.

Further experimentation suggested when quicklime treated samples were cured, the free-lime content, and hence the sample ANC, decreased with increasing curing time, more so for montmorillonite than for kaolinite-sand mixes (Figures 4 and 5). These results indicate that interactions in the montmorillonite-sand mixes consumed more free-lime than in kaolinite-sand mixes. This is expected, since montmorillonite possesses a higher surface area and cation exchange capacity, and therefore a higher degree of interaction with the calcium and hydroxyl ions available through quicklime dissolution. In addition, pozzolanic reactions that would consume alkalinity are happening faster for the more reactive montmorillonite clay (Mitchell and Dermatas, 1992). Therefore, the consumption of lime during long periods of reaction time and its corresponding effect on heavy metal release must also be considered in designing for quicklime treatment levels. Additional information on the curing time effect on heavy metal release is presented in the following section.

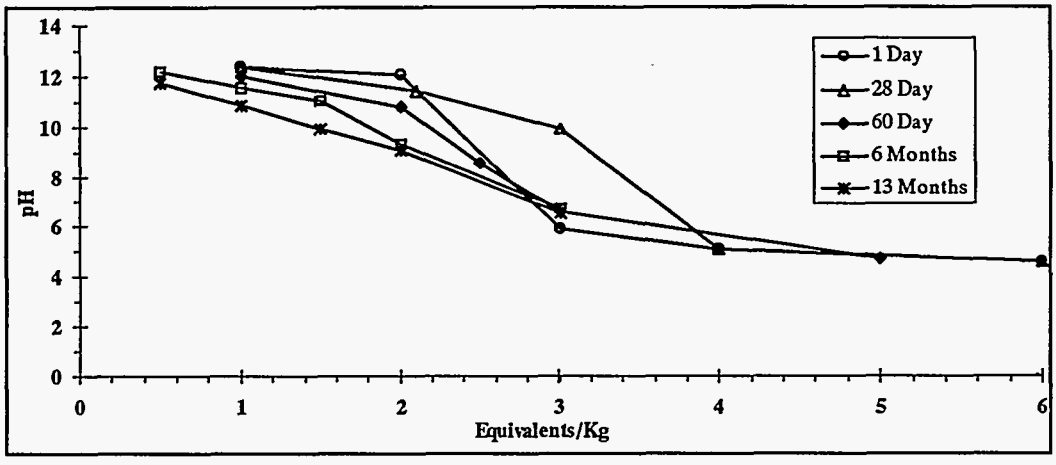

Figure 4. Effect of Curing Time on the ANC of the M30L10 Mix.

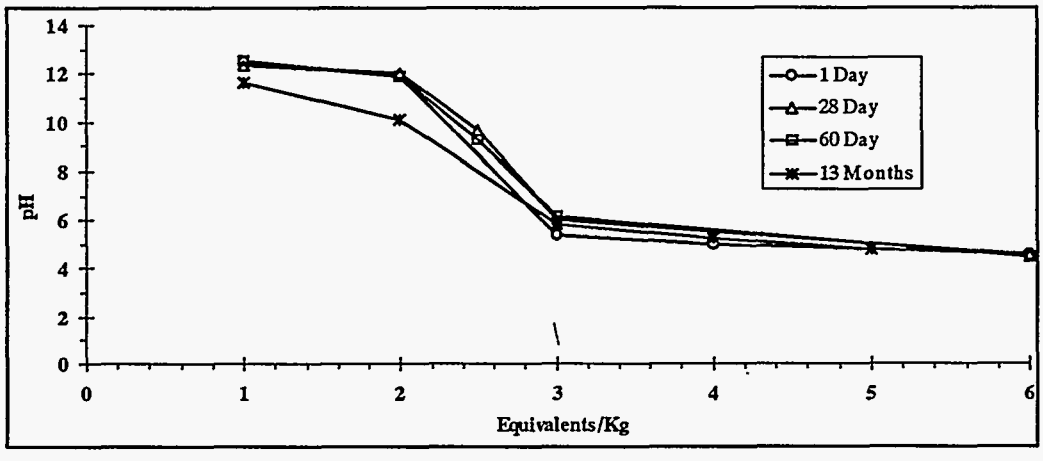

Figure 5. Effect of Curing Time on the ANC of the K30L10 Mix.

Overall, the acid titration results clearly showed that the higher the quicklime content and the lower the reactivity of the aluminosiliceous surface area (clay minerals), the higher the ANC of the solids. However, because of the amphoteric behavior of most heavy metals, their leachability may increase if the pH is too high, thus making undesirable the existence of a high level of ANC in the solid. In addition, ANC changes over time may also adversely influence heavy metal release. Therefore, heavy metal TCLP release information was also needed to establish the optimum quicklime treatment levels.

4.1.1.2 TCLP Results

ARSENIC

In this study, As_2O_3 was mainly used as the As contaminant source, except for selected samples, for which sodium arsenite, $NaAsO_2$, was added into the clay-sand mixes. The main reason for doing so was to study the effect of the solubility of the contaminant source on the overall treatment effectiveness. Sodium arsenite is more soluble than As_2O_3, and it is the most toxic and most mobile amongst commercially available arsenic salts. The TCLP arsenic release levels for kaolinite-sand mixes in the presence of sulfates are shown in Figure 6 as a function of the quicklime content.

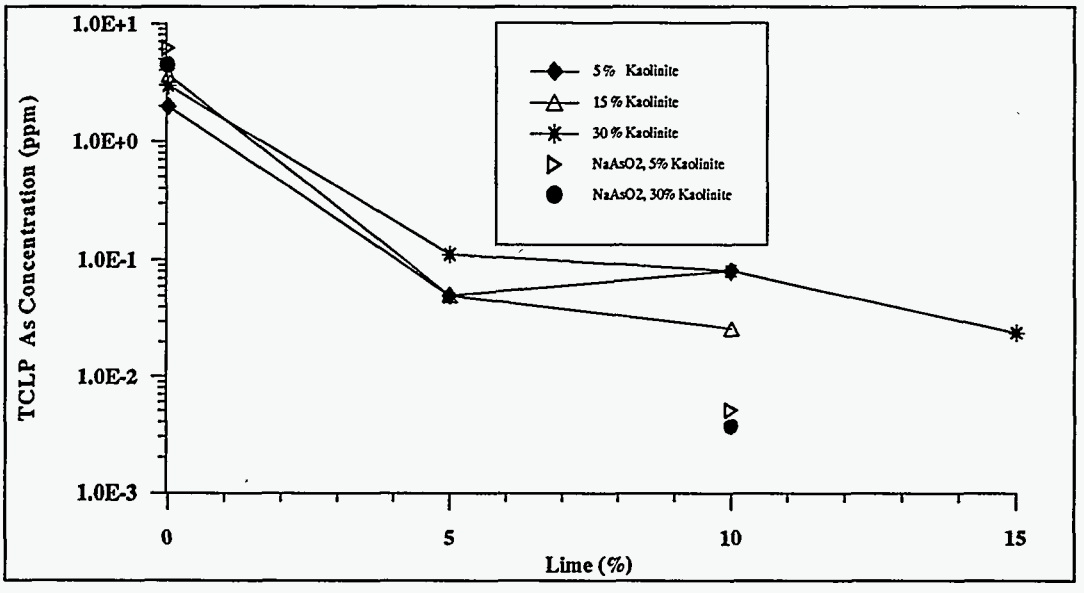

Figure 6. Effect of Quicklime Levels on As Leachability of Kaolinite-sand Mixes in the Presence of Sulfates Following 28 Days of Curing.

The results in Figure 6 indicate that for all the kaolinite-sand mixes contaminated using As_2O_3, the addition of 5% quicklime significantly reduced As leachability. No further reduction in As leachability was achieved when quicklime content increased from 5% to 15%. For the untreated samples (no

quicklime), more As was released from samples contaminated using sodium arsenite than those contaminated using As_2O_3, mainly due to the higher solubility of sodium arsenite. However, when the samples were treated with 10% quicklime, much less As was leached out from sodium arsenite contaminated samples than from arsenic oxide contaminated samples. The results suggest readily soluble $NaAsO_2$ can react more effectively in the quicklime treated clay-sand mixes than As_2O_3. In other words, the higher the solubility (mobility) of the As contaminant species, the more effective quicklime treatment is in immobilizing As. Overall, the leachability of both kinds of arsenic chemicals in kaolinite-sand mixes was reduced to 0.1 ppm or less in the TCLP leachate, which is more than 50 times lower than the TCLP limit (5 ppm).

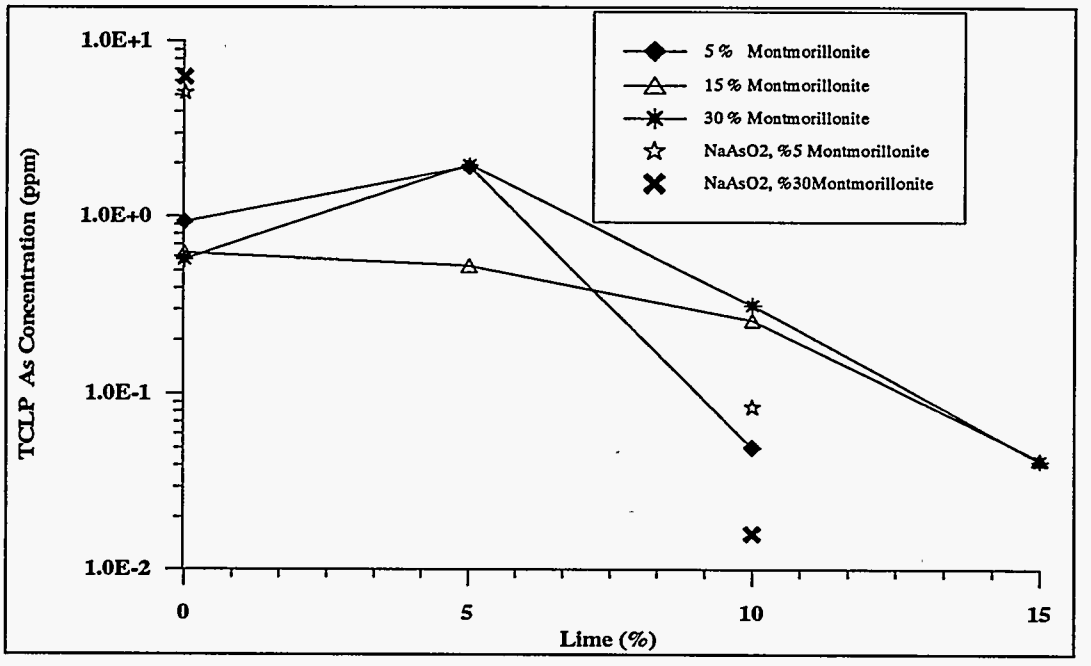

Figure 7. Effect of Quicklime Levels on As Leachability of Montmorillonite-Sand Mixes in the Presence of Sulfates Following 28 Days of Curing.

Similar to arsenic leaching behavior in kaolinite-sand samples, more arsenic was released from the untreated montmorillonite-sand samples contaminated using sodium arsenite than using the oxide (Figure 7). Contrary to kaolinite-sand mixes, the addition of 5% quicklime into montmorillonite-sand samples did not result in a significant reduction of As release, even though the 5 ppm TCLP limit was satisfied (Figure 7). Arsenic leachability was significantly reduced only when montmorillonite-sand samples were treated at 10% and 15% quicklime levels. This was expected as the ANC results had showed that more quicklime was consumed in montmorillonite-sand samples than in kaolinite-sand samples. Other than this, arsenic immobilization was not significantly affected by type and amount of clay mineral present and thus was probably solubility controlled.

CHROMIUM

Chromium (III) leaching results are shown in Figures 8 and 9 for kaolinite-sand and montmorillonite-sand samples, respectively. Approximately 100 ppm of Cr (III) was detected in the TCLP leachate for untreated samples. It is clear from Figure 9 that minimum Cr release was achieved when montmorillonite samples were treated with 10% of quicklime. Optimum quicklime content for the immobilization of Cr in kaolinite samples was also 10% (Figure 8). At optimum quicklime level, Cr concentration was reduced to approximately 0.1 ppm, which is 50 times less than the TCLP limit for Cr (5 ppm), and 1,000 times leachability reduction comparing to Cr concentration for the untreated samples.

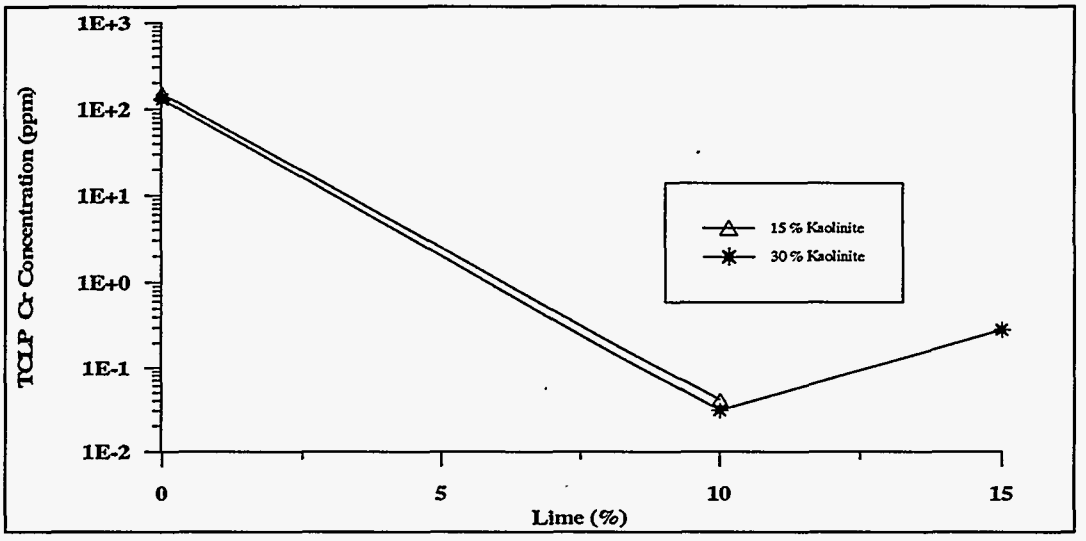

Figure 8. Effect of Quicklime Levels on Cr Leachability of Kaolinite-sand Mixes in the Presence of Sulfates Following 28 Days of Curing.

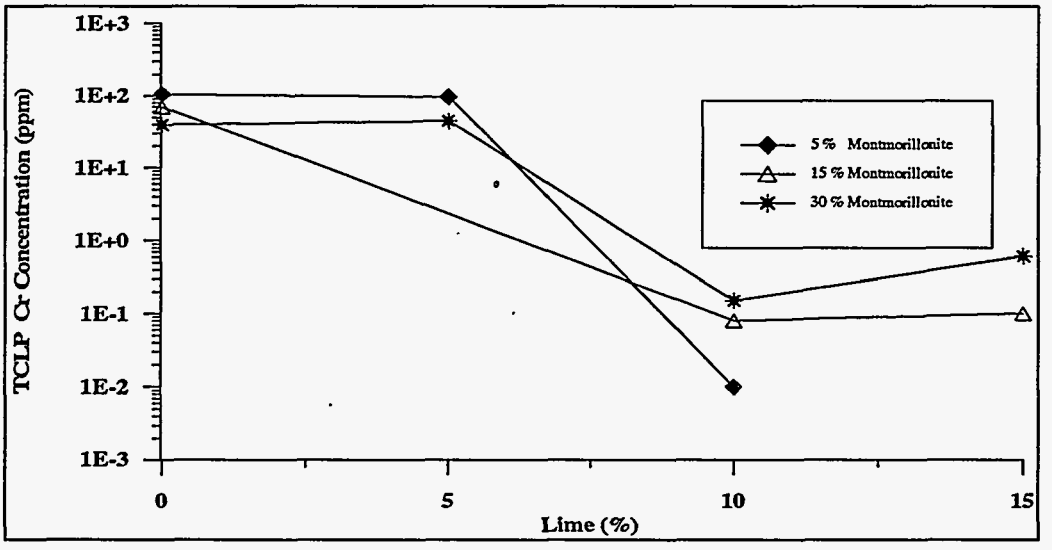

Figure 9. Effect of Quicklime Levels on Cr Leachability of Montmorillonite-sand Mixes in the Presence of Sulfates (28 Days Curing).

The results in Figures 8 and 9 show that at equivalent quicklime contents, the TCLP Cr release levels were similar for different samples irrespective of the type and amount of clay present. It seems that Cr leachability is only affected by the amount of quicklime present. This suggests that the leachability of Cr (III) is mainly controlled by the solubility of Cr hydroxides, as type and amount of fine particles did not have obvious effect on Cr (III) leachability. At 5% quicklime, there was not enough free lime to neutralize acetic acid from the TCLP leachant. On the other hand, the highest leachate pH was attained for samples treated with 15% quicklime. Under both low and high pH conditions, Cr (III) may be leached out due to its amphoteric behavior. Our results indicate that Cr (III) levels of release are maximum at lower pHs.

The leachability results discussed above were obtained for samples contaminated using trivalent chromium oxide, Cr_2O_3. It is known that hexavalent chromium, Cr(VI), is more mobile as well as more toxic than Cr(III) because of its high solubility and low adsorption tendency. Therefore, several samples were prepared using Cr(VI) and treated with quicklime/ferrous sulfate or quicklime/fly ash. This work was not included in the project proposal and it was conducted by a graduate student who took a special topic course with the principal investigator. In Figure 10 the TCLP results show when 10% quicklime was used to treat the contaminated kaolinite (5%)-sand samples, Cr(VI) leachability was only reduced from 217 ppm to 150 ppm. The addition of 15% class C fly ash reduced the leachability to 146 ppm. Only when both 15% fly ash and 10% quicklime were added together to treat the contaminated sample, Cr(VI) leachability was reduced to 4 ppm, thus meeting the TCLP criteria. Cr(VI) leachability was also successfully reduced by a quicklime-ferrous sulfate treatment approach. The complete results for this study have been reported in one of our papers (Dermatàs and Meng, 1994). Overall, our results demonstrated that both quicklime and reducing agents (ferrous ion or fly ash) had to be used together immobilize hexavalent Cr(VI) in the contaminated soils.

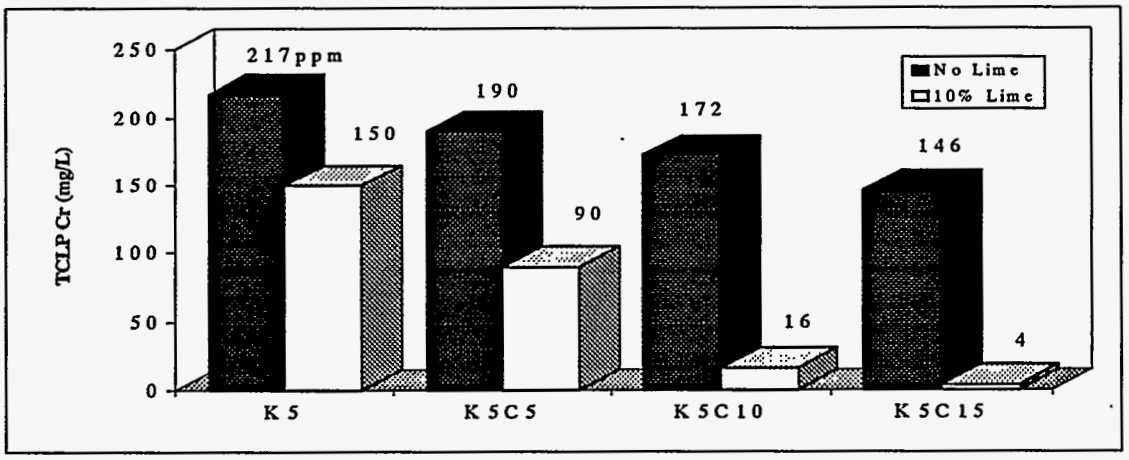

Figure 10. Chromium Leachability in the Fly Ash/Lime Treatment System; C5 - 5% Fly Ash; C10 - 10% Fly Ash; C15 - 15% Fly Ash.

MERCURY

Mercury, Hg(II), leachability was not effectively reduced by the quicklime-sulfate treatment (Figures 11 and 12). Hg concentrations in the TCLP leachate were reduced from approximately 70 ppm for the untreated samples to less than 20 ppm for samples treated using 10% quicklime. This concentration is nearly 100 times higher than the TCLP limit for Hg (0.2 ppm). The addition of at least 10% quicklime was necessary for significant reduction in Hg leachability to take place. The type and amount of clay present did not affect Hg TCLP levels, and therefore release seems to be mainly controlled by Hg solubility.

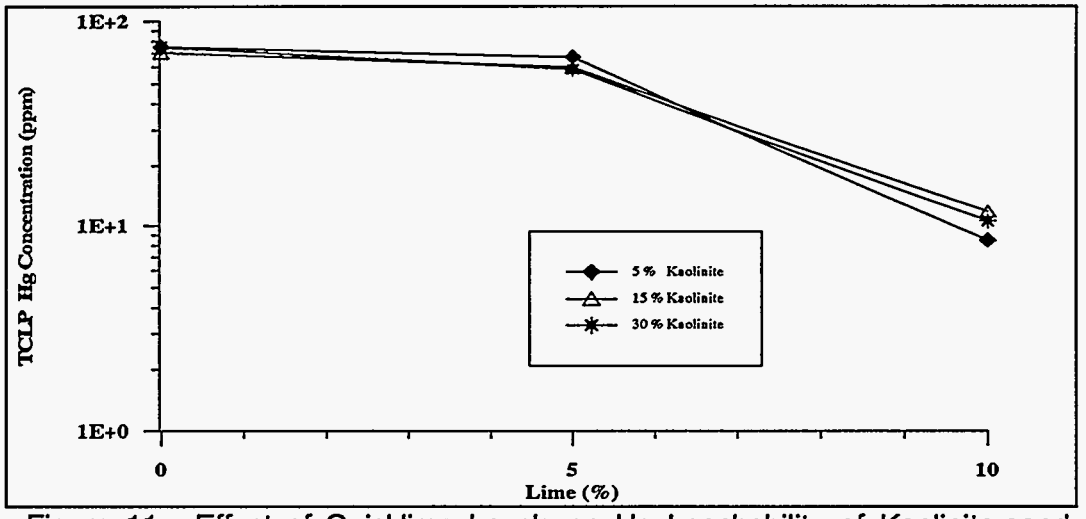

Figure 11. Effect of Quicklime Levels on Hg Leachability of Kaolinite-sand Mixes in the Presence of Sulfates Following 28 Days of Curing.

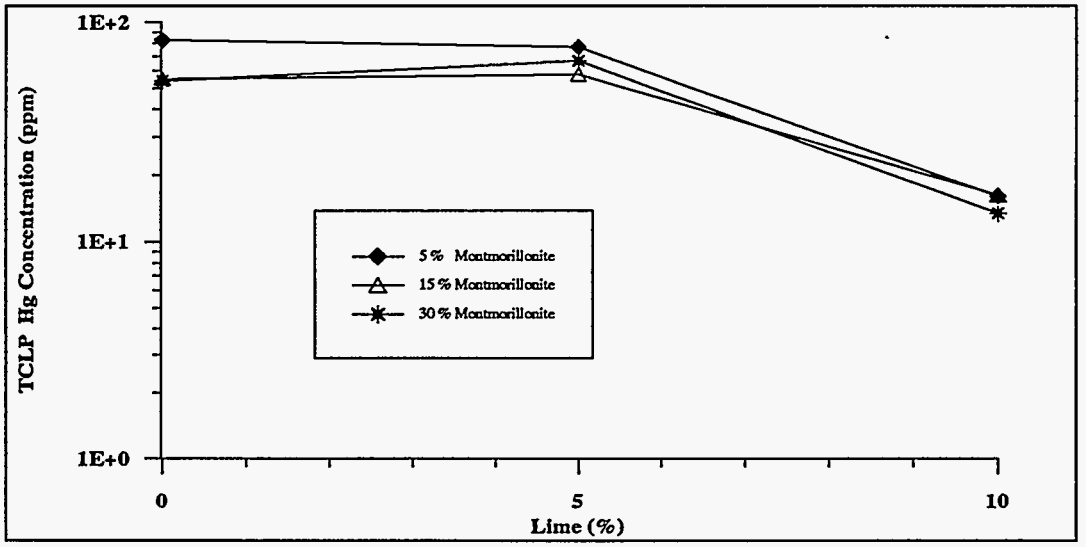

Figure 12. Effect of Quicklime Levels on Hg Leachability of Montmorillonite-sand Mixes in the Presence of Sulfates Following 28 Days of Curing.

The high TCLP leachability observed for Hg in Figures 11 and 12 was attributed to the high solubility of Hg hydroxide complexes and the low adsorption tendency of these species to clay minerals. In order to effectively reduce Hg leachability, Na_2S was added because the resulting HgS precipitate has a very low solubility. The addition of Na_2S did result in further reduction of Hg leachability (Figure 13). However, the Hg concentrations in the TCLP leachate were still higher than those predicted based on HgS solubility data. Consequently, the TCLP non-hazardous criteria could not be met. This may be due to the formation of mercury-polysulfide complexes at high Hg and S concentrations.

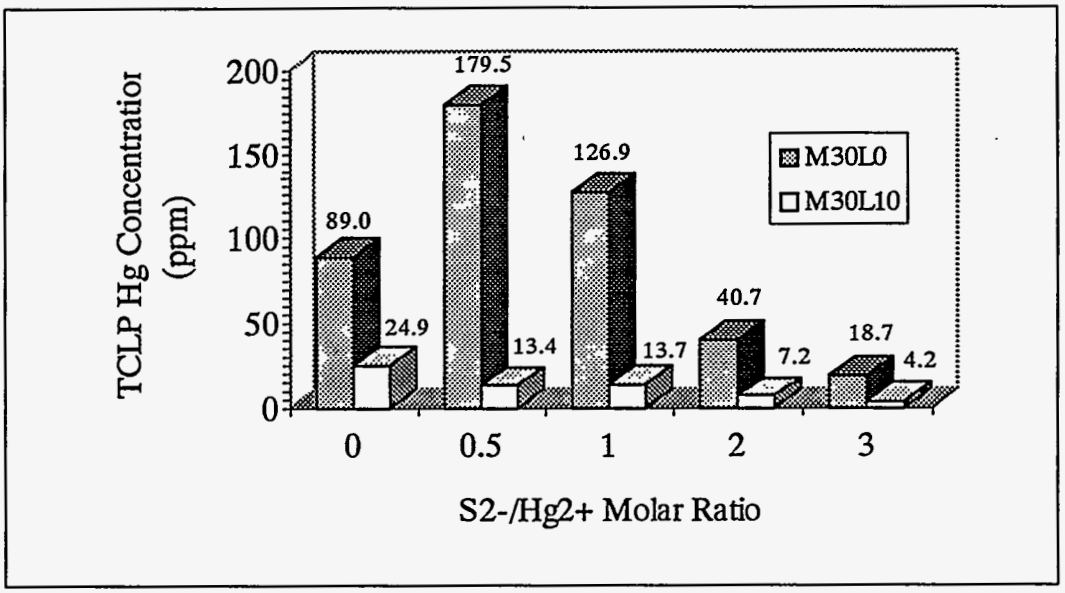

Figure 13. Effect of Sulfide to Mercury Molar Ratio on the Leaching of Mercury from Treated Versus Untreated Mmontmorillonite-sand Mixes.

LEAD

Similar to the Cr results in Figures 8 and 9, minimum Pb leachability was achieved at 10% quicklime treatment level for both kaolinite-sand and montmorillonite-sand samples (Figures 14 and 15). The fact that lead release increases when quicklime content is increased from 10% to 15% was initially attributed to the amphoteric behavior of lead. However, the leachability of Pb is not only affected by quicklime contents. The types of clays and clay content also influence Pb leachability in the quicklime treated samples. At 10% quicklime content, Pb leachability decreased as clay contents increased from 5% to 30% (Figures 14 and 15). Moreover, when the samples were treated with 10% and 15% quicklime, much less Pb was released from montmorillonite-sand samples than from kaolinite-sand samples. At optimum quicklime content, Pb concentration was reduced to less than 0.1 ppm in the 30% montmorillonite sample (Figure 15). However, when the 30% kaolinite sample was treated with

10% quicklime, Pb concentration was only reduced to 3 ppm. When the artificial soil mixes contained up to 15% kaolinite or 5% montmorillonite, Pb leachability could not be effectively reduced to meet the TCLP criteria (5 ppm). The results suggest that if a contaminated soil has a low fine particle content, quicklime treatment may not be effective in immobilizing lead. In this case, fly ash can be added together with quicklime to effectively immobilize Pb. Results pertaining to the use of fly ash will be discussed in following sections.

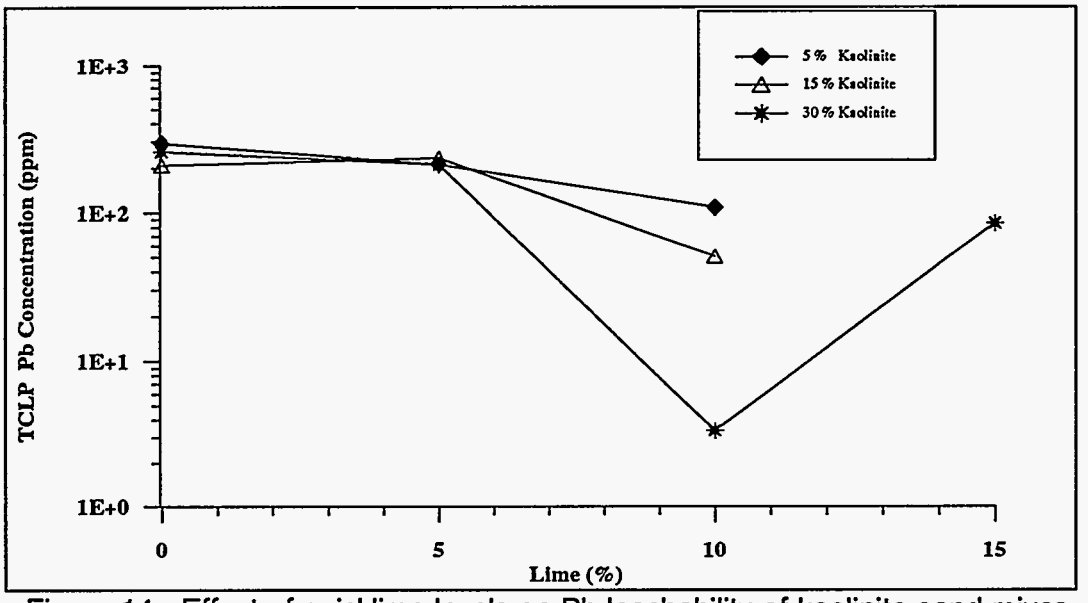

Figure 14. Effect of quicklime levels on Pb leachability of kaolinite-sand mixes in the presence of sulfates following 28 days of curing.

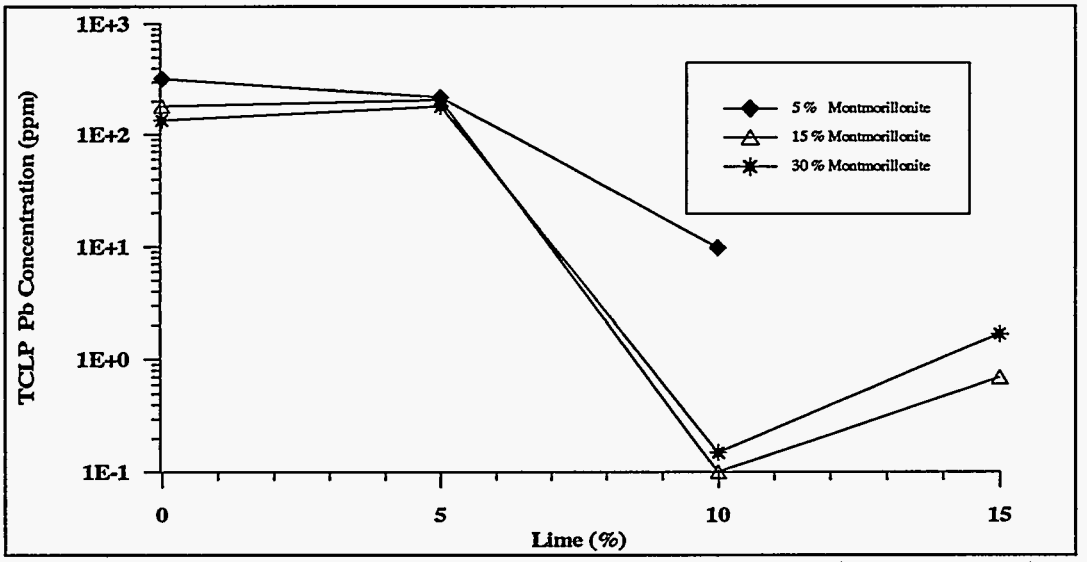

Figure 15. Effect of quicklime levels on Pb leachability of montmorillonite-sand mixes in the presence of sulfates following 28 days of curing.

adsorption. When the clay content in the artificial soils is increased, an increasingly larger surface area is available to adsorb Pb. Moreover, at the same content, montmorillonite has a much higher specific surface area than kaolinite. Consequently, less Pb was released from samples containing montmorillonite rather than kaolinite, and release was inversely proportional to the sample's clay content. However, quicklime content is also an important factor for Pb immobilization because Pb adsorption seems to be strongly pH dependent.

4.1.1.3 Summary

Overall, the TCLP results demonstrated that As, Cr(III) and Pb could be effectively immobilized by the proposed quicklime-sulfate treatment. Hexavalent Cr(VI) could be immobilized by using quicklime along with a reducing agent, such as fly ash or ferrous salts. Quicklime treatment was not effective in immobilizing Hg in terms of satisfying the TCLP criteria. Furthermore, the immobilization of As, Hg and Cr in the quicklime treated samples was precipitation controlled, and Pb leachability was mainly influenced by surface adsorption. The optimum quicklime level of treatment was determined to be 10%, based on both ANC and TCLP test results. However, ANC results demonstrated a treatment effectiveness dependency on curing time (Figures 4 and 5) which will be further discussed in the following section.

4.1.2 Effect of Curing Time on Heavy Metal Leachability

The leaching results discussed in the previous section were obtained for quicklime treated samples cured for 28 days. However, as demonstrated in Figures 4 and 5, pH is decreasing with increasing sample curing time. Changes in the pH of the treated mixes may in turn affect the levels of TCLP heavy metal release. The possibility of a curing time effect on heavy metal release is an important factor concerning the applicability of the proposed technique to real world scenarios. That is, in order to expedite a remediation field application, it is desirable that the immobilization of heavy metals by the proposed quicklime treatment is a fast process. More importantly, to ensure long term treatment effectiveness, heavy metals within the treated waste forms should remain immobile for long periods of curing time. To assess the influence of curing time on heavy metal release, samples cured from 1 day to 13 months were regularly tested for TCLP heavy metal release.

The TCLP results in Figures 16 to 19 show that As and Cr were immobilized one day after kaolinite-sand or montmorillonite-sand samples were treated using quicklime. The heavy metals were still immobilized 390 days following quicklime treatment. The fact that As and Cr were immobilized immediately following sample treatment, further demonstrates that the leachability of these metals was controlled by precipitation. That is, as long as there is enough free lime in the treated solid to neutralize the acid in the leachant, As and Cr leachability will be more than one order of magnitude lower than the TCLP limits.

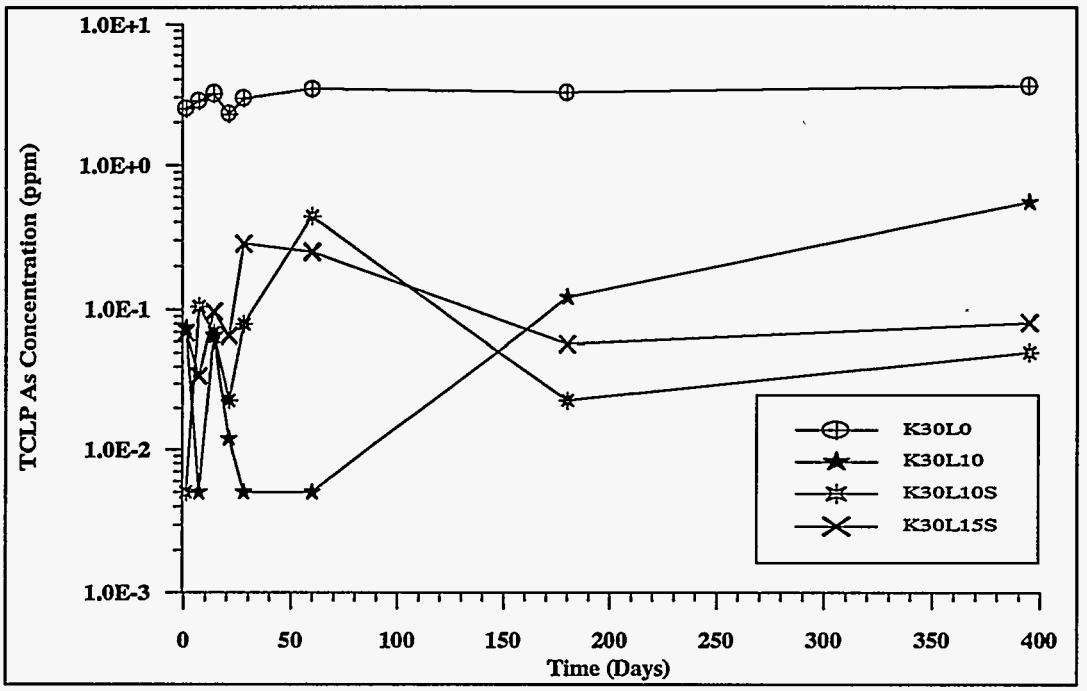

Figure 16. As Leachability as a Function of Kaolinite-sand Sample Curing Time.

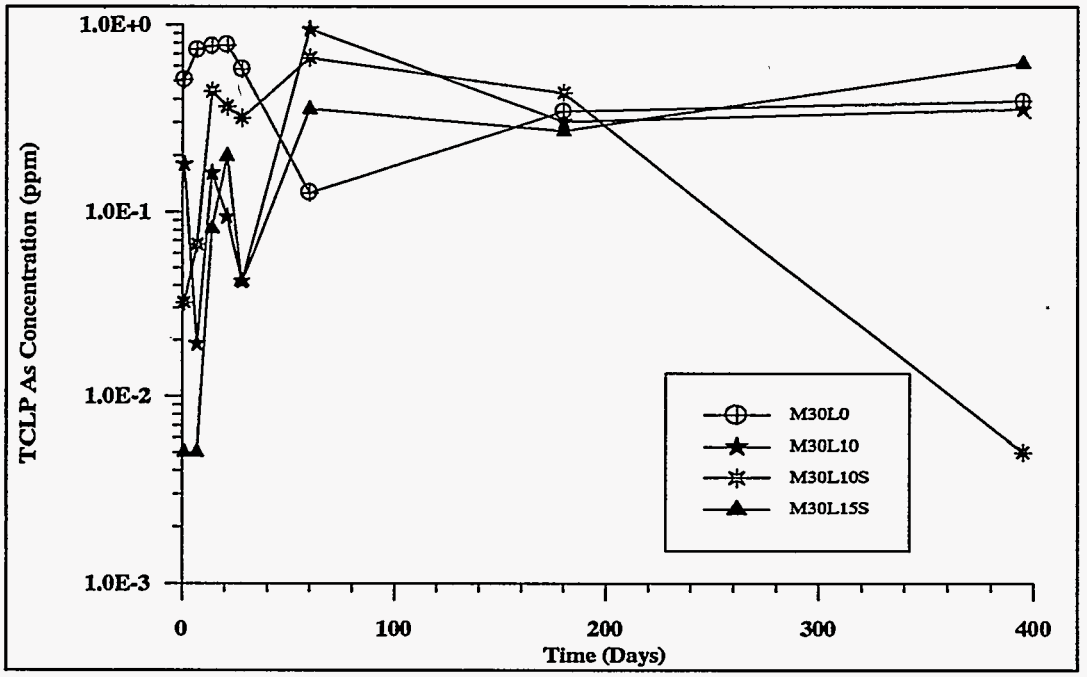

Figure 17. As Leachability as a Function of Montmorillonite-sand Sample Curing Time.

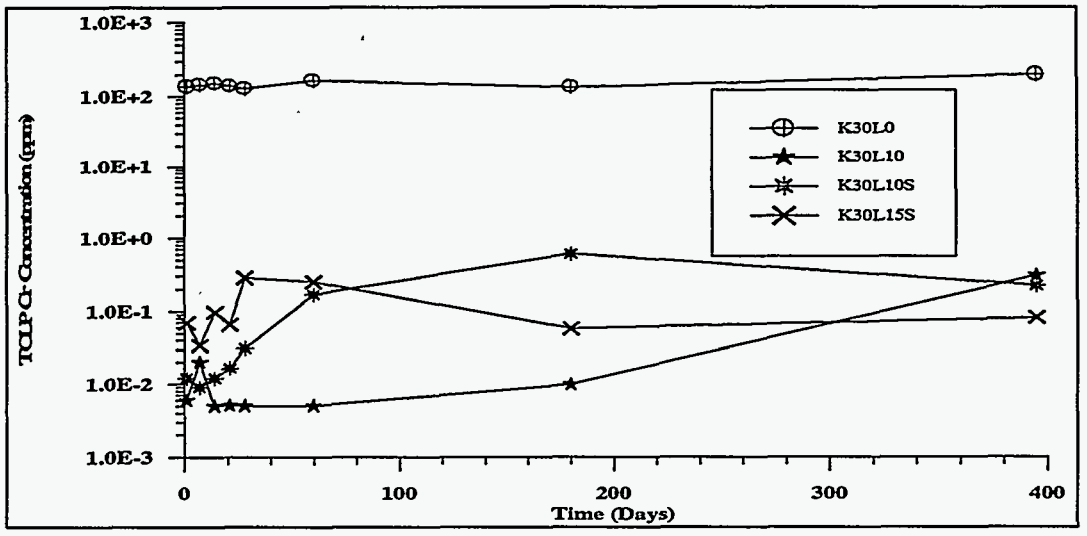

Figure 18. Cr Leachability as a Function of Kaolinite-sand Sample Curing Time.

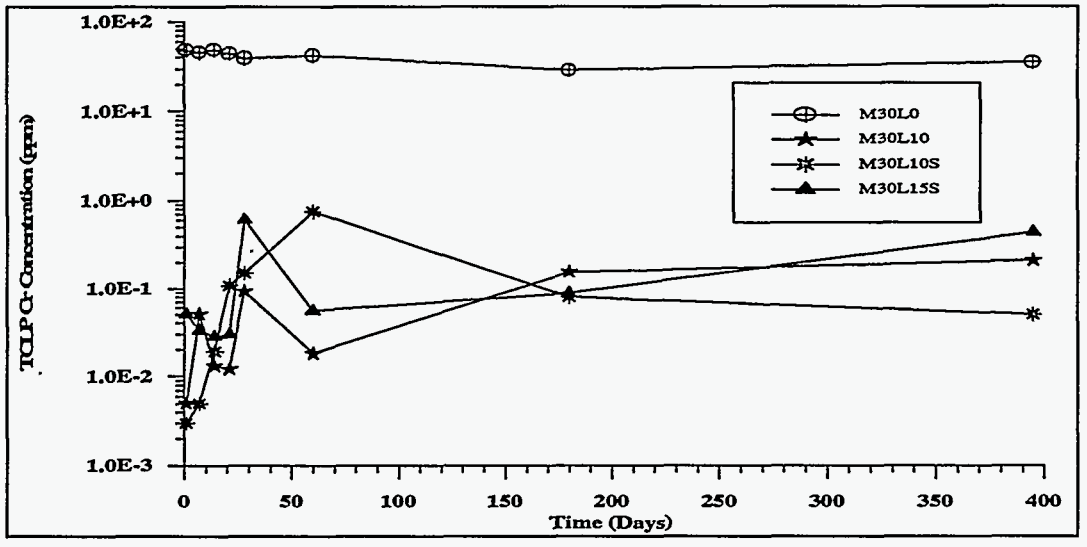

Figure 19. Cr Leachability as a Function of Montmorillonite-sand Sample Curing Time.

Contrary to the Cr and As results, curing time had a significant effect on TCLP Pb release, especially for kaolinite-sand samples (Figure 20). For samples treated with 10% quicklime, lead concentration in the TCLP leachate decreased significantly when the curing time increased from one day to 28 days, but only after 28 days of sample curing, Pb concentration in the leachate was reduced to lower than the TCLP limit of 5 ppm. When the curing time increased from 28 to 390 days, Pb leachability further decreased gradually. The leachability of Pb from the kaolinite-samples treated with 15% quicklime also decreased gradually over the 390 days of curing, being reduced to 5 ppm after the treated sample was cured for approximately 250 days.

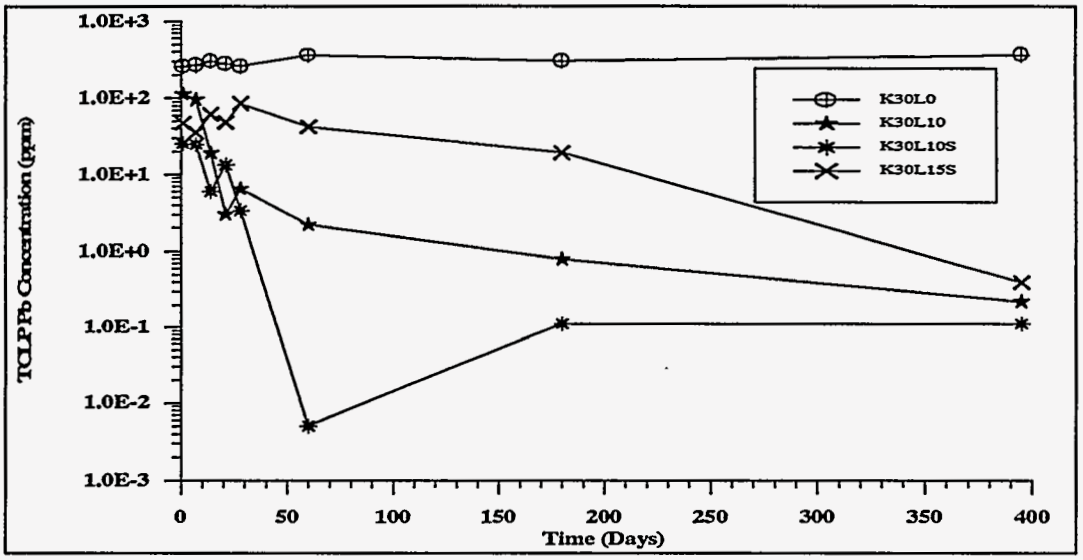

Figure 20. Pb Leachability in Kaolinite-sand Mixes as a Function of Sample Curing Time.

The immobilization of Pb in quicklime treated montmorillonite-sand samples took place faster than in kaolinite-sand mixes (Figure 21). Lead leachability was immediately reduced to less than 1 ppm in the mixes treated at 10% quicklime. For the sample treated at 15% quicklime, it took nearly 7 days to reduce Pb concentration to 3 ppm. Furthermore, Pb release continued to decrease all the way through the 13 month monitoring period.

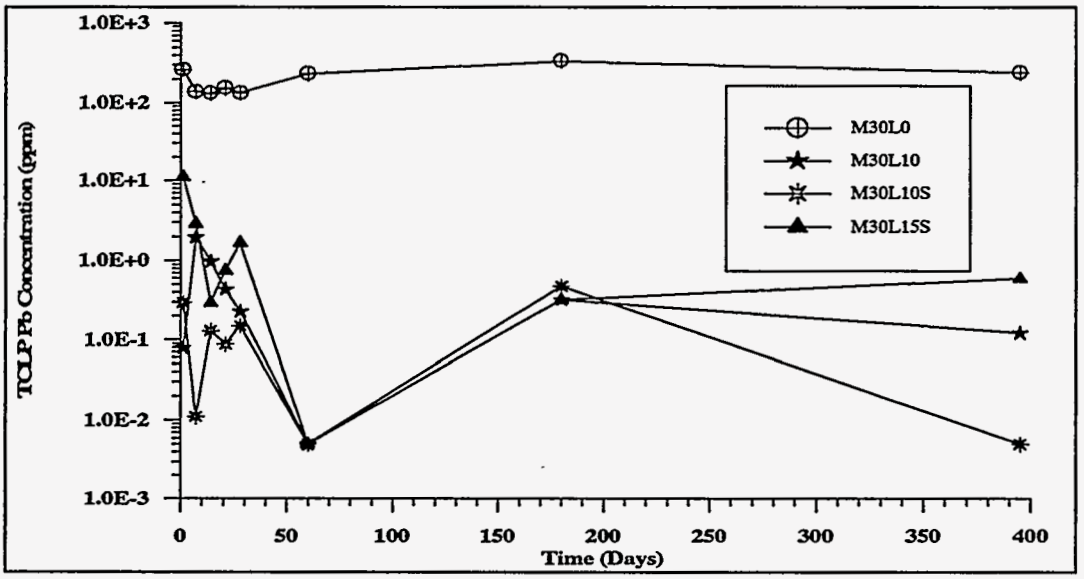

Figure 21. Pb Leachability in Kaolinite-sand Mix as a Function of Sample Curing Time.

In summary, curing time does not affect As and Cr TCLP release, in spite of pH decreases with increasing curing time. Conversely, curing time has a major effect on Pb immobilization. As free lime is consumed with elapsed curing time, sample pH is dropping and new pozzolanic products are being formed. In turn, Pb release is gradually decreasing, probably due to increased adsorption on the newly formed solid surfaces and a decreased solubility at pHs lower than 12.

4.1.3 *Effect of Sulfate Addition on Heavy Metals Leachability*

All the treatment results presented thus far, unless otherwise indicated, were obtained in the presence of both quicklime and sulfates. Sulfate ions often co-exist with heavy metals in the contaminated soils. Furthermore, sulfates are also present in industrial waste sludges and coal and incineration waste by-products such as fly ash, boiler slags and flu gas desulfurization wastes. In the presence of sulfate ions, alumina and quicklime, ettringite, $[Ca_3Al(OH)_6]_2(SO_4)_3 \cdot 26H_2O$, will be the major pozzolanic reaction mineral product. It has been reported that heavy metals can be immobilized by ettringite formation through isomorphous substitution of the ions in the mineral structure (Kamon and Nontananandh, 1991; Kumarathasan et al., 1990). In the present study, sample mixes with and without sodium sulfate were prepared in pairs to evaluate the sulfate addition and subsequent ettringite formation effect on heavy metal release.

In order to confirm that pozzolanic reactions did occur in the lime treated mixes and to identify the main treatment products, samples cured for 28 days were analyzed using x-ray diffraction and scanning electron microscopic (SEM) techniques. X-ray diffraction powder analyses can only detect crystalline mineral forms that exist in relative abundance (i.e., more than approximately 5% by weight presence of the individual mineral). Kaolinite and clean quartz sand were the only mineral forms detected in the untreated kaolinite-sand mix (Figure 22). Besides kaolinite and sand, some excess lime as well as the pozzolanic reaction products aluminum oxide, calcium silicate hydroxide, and calcium silicate hydrate, were detected in the quicklime treated kaolinite-sand sample (Figure 23). As expected, no ettringite was detected in these samples since no sulfate ions were present. Conversely, ettringite did form in the presence of sulfate ions in the quicklime treated mix (Figure 24). Along with ettringite, calcium silicate hydrate and unreacted lime were also detected in the x-ray scan. The formation of ettringite was further confirmed by SEM micrograph studies. In Figure 25, an SEM micrograph is shown, in which ettringite formation is evidenced by the presence of needle shaped ettringite crystals. Further analyses of the crystal surface by energy dispersive x-ray (EDX), indicated a surface elementary chemical composition that resembled that of pure ettringite. Overall, similar to the kaolinite-sand samples, ettringite formation was evidenced in all quicklime treated clay-sand mixes when sulfates were present. Additional information pertaining to ettringite formation will be presented in following sections. In this section, the possible ettringite contribution in heavy metal immobilization is only discussed.

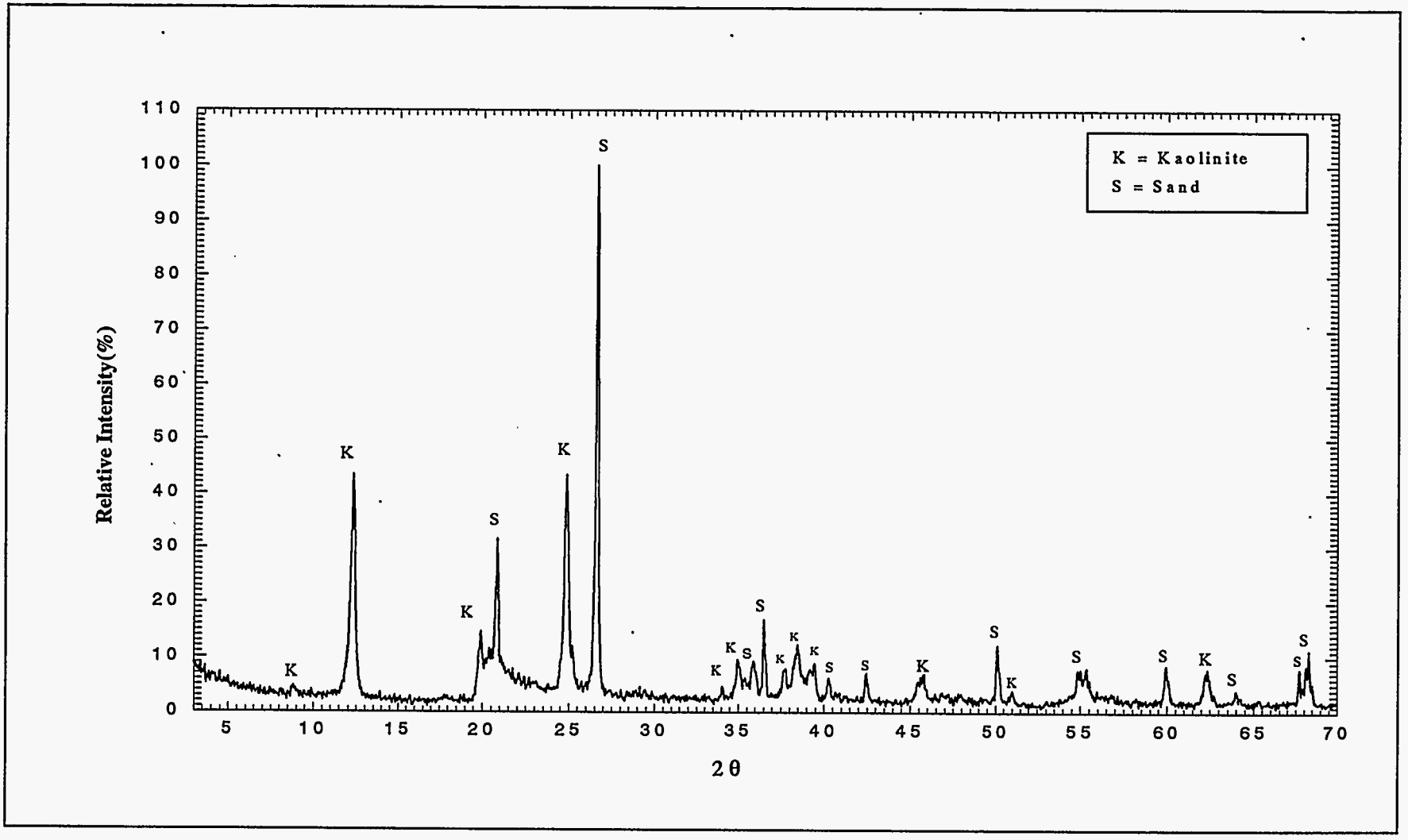

Figure 22. X - ray Scan of Untreated Sample Composed of 30% of Kaolinite and 70% of Sand (K30L0), 28 Days of Curing.

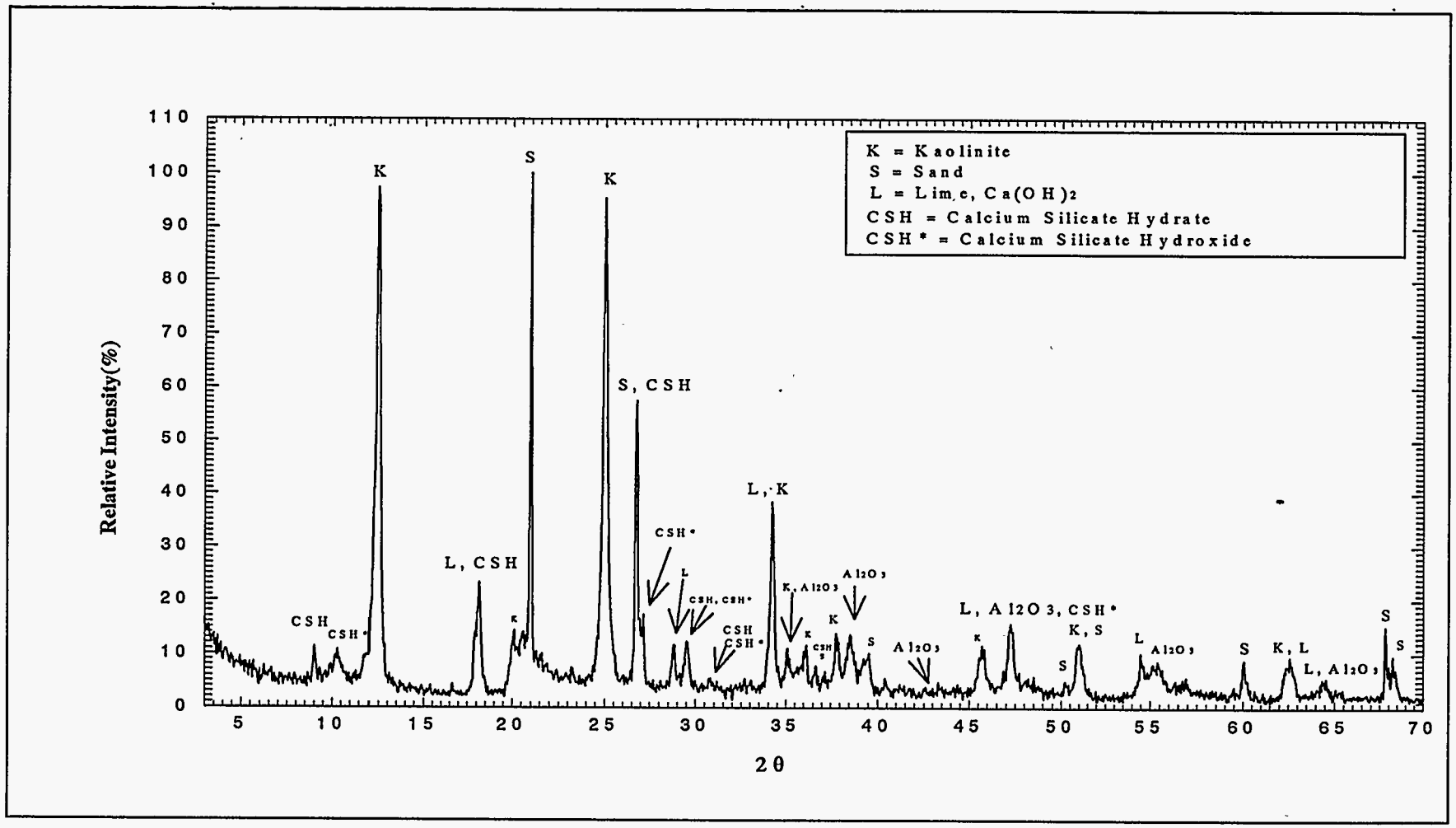

Figure 23. X - ray Scan of Treated Sample Composed of 30% of Kaolinite, 10% of Lime and 70% of Sand (K30L10), 28 Days of Curing.

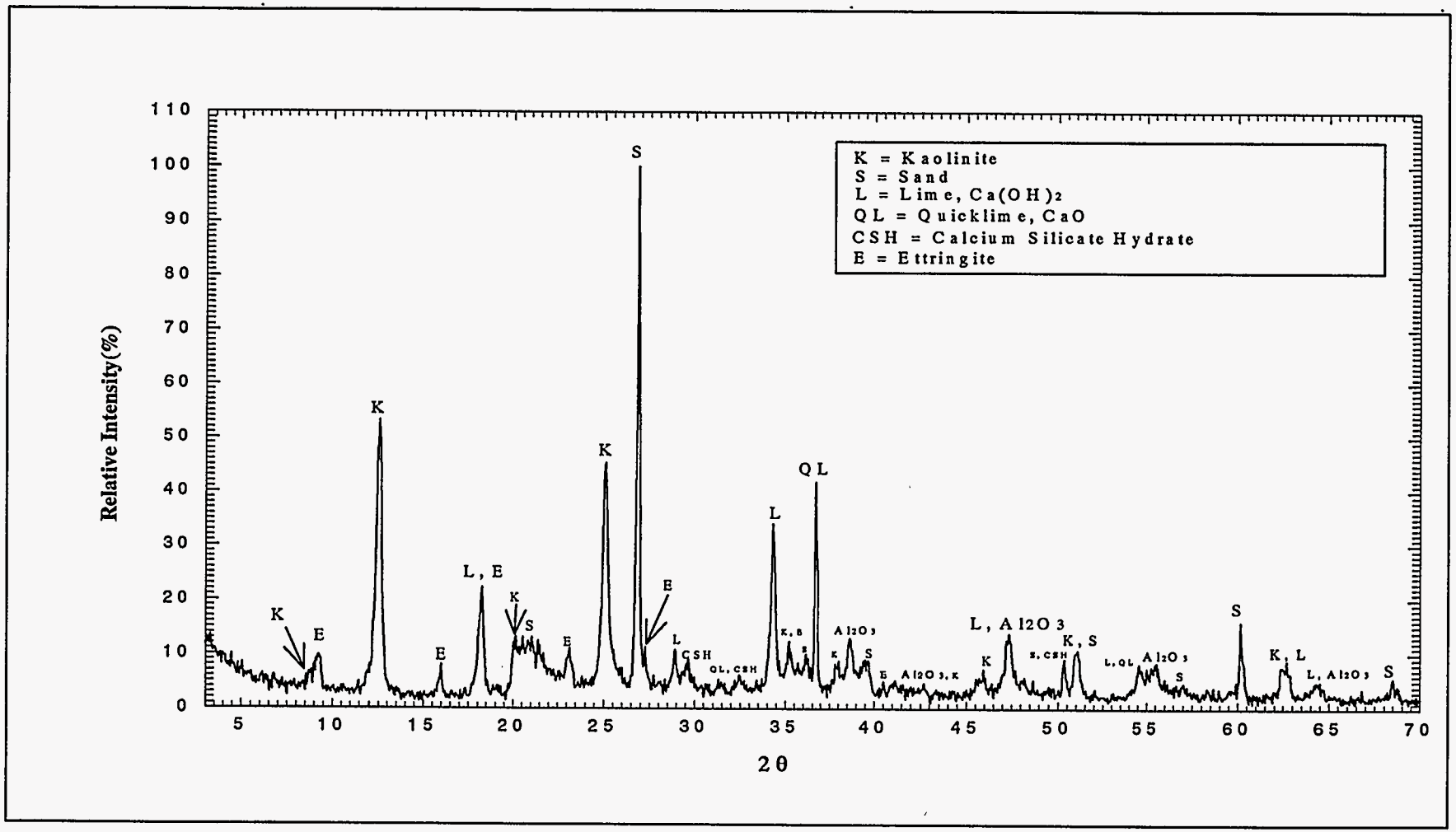

Figure 24. X - ray Scan of Treated Sample Composed of 30% of Kaolinite, 10% of Lime, 5% of Sodium Sulfates and 70% of Sand (K30L10S), 28 Days of Curing.

Figure 25. SEM Micrograph of K30L10S Sample Cured for 6 Months.

The TCLP levels of heavy metal release from quicklime treated 30% clay- 70% sand samples, prepared with and without sulfate addition, are presented in Figures 26 to 29, as a function of quicklime treatment levels. As these figures indicate, there seems to be no major effect of sulfate addition and subsequent ettringite formation, on the levels of heavy metal immobilization.

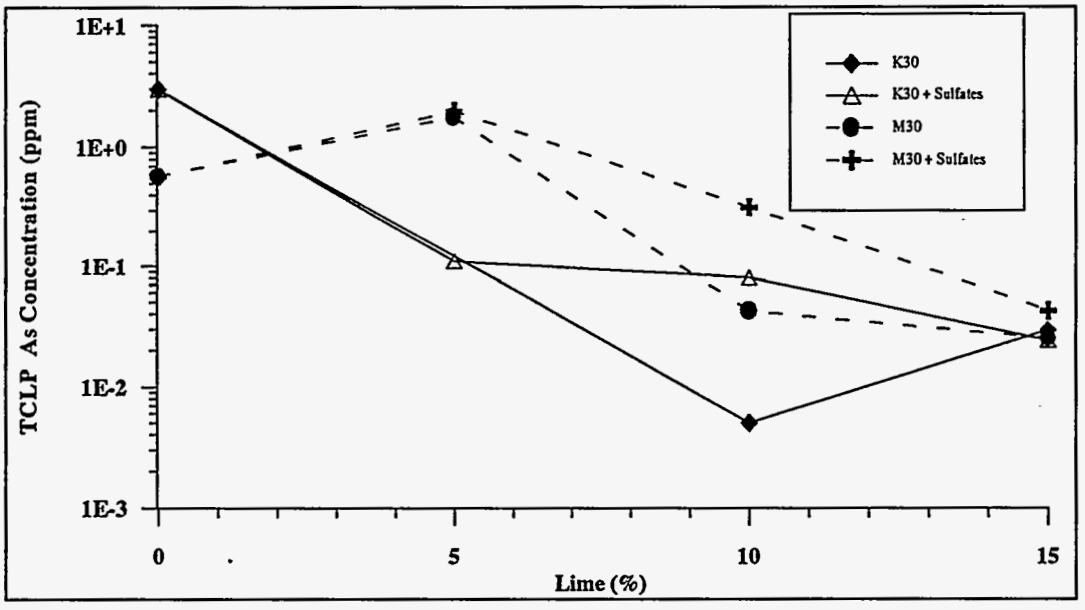

Figure 26. Effect of Sulfate Addition on the TCLP Arsenic Release from Clay-sand Samples Cured for 28 Days.

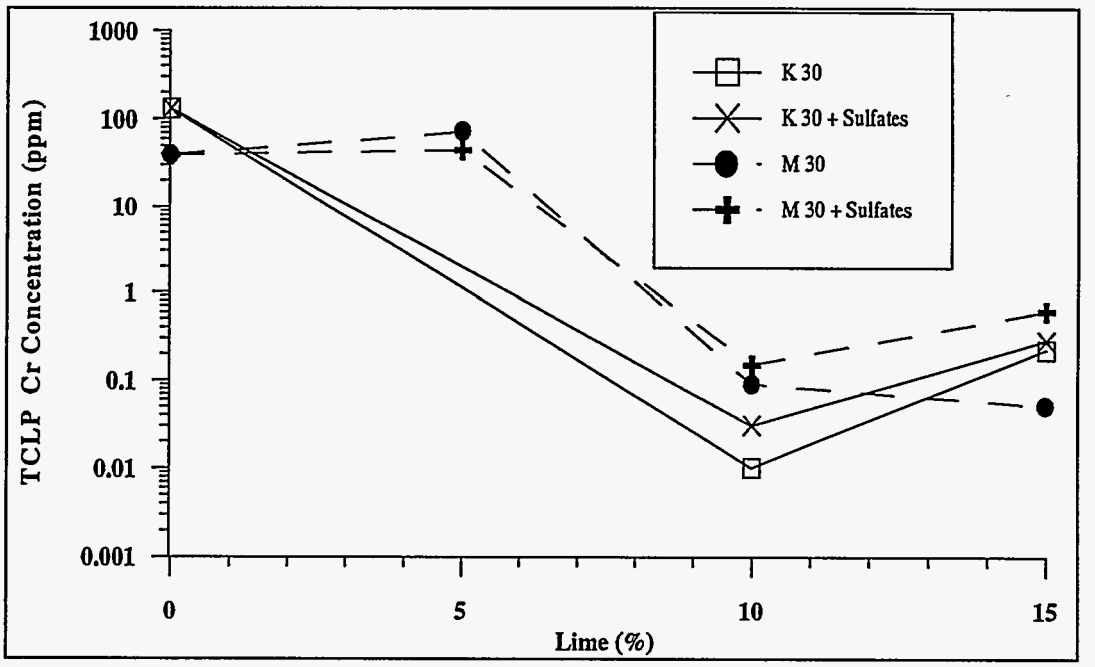

Figure 27. Effect of Sulfate Addition on the TCLP Chromium Release from Clay-sand Samples Cured for 28 Days.

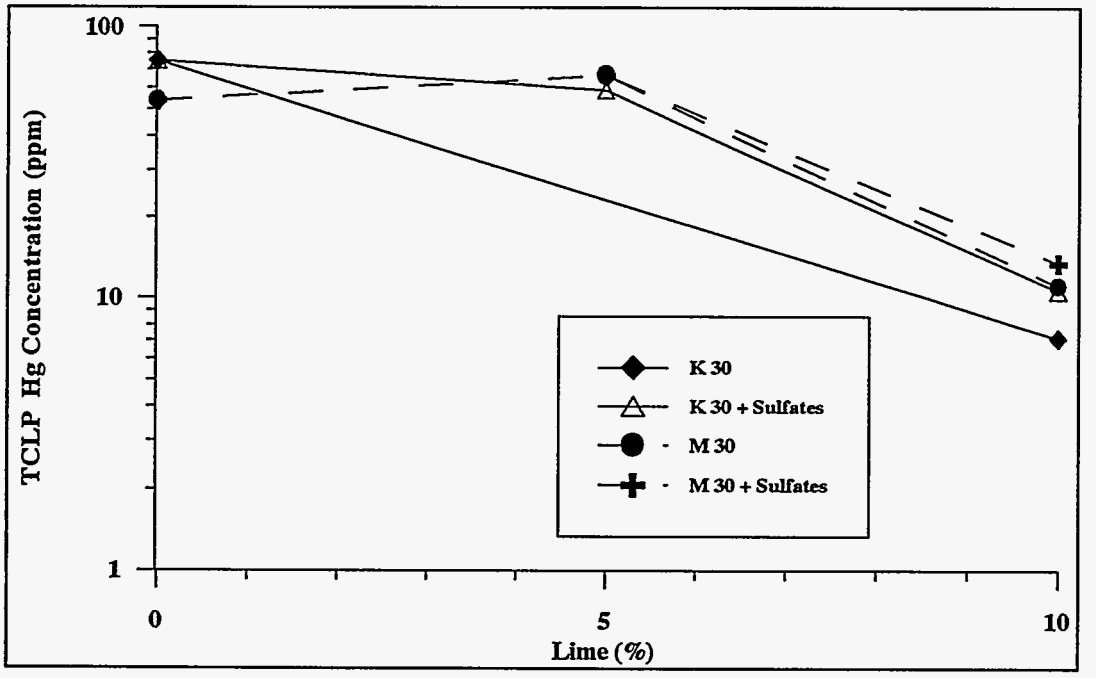

Figure 28. Effect of Sulfate Addition on the TCLP Mercury Release from Clay-sand Samples Cured for 28 Days.

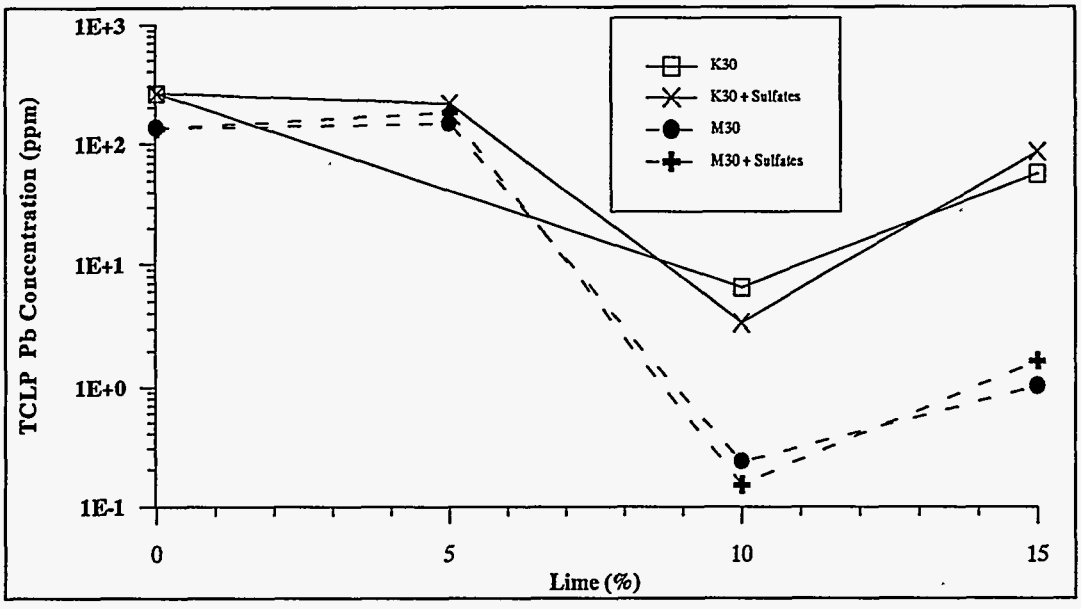

Figure 29. Effect of Sulfate Addition on the TCLP Lead Release from Clay-Sand Samples Cured for 28 Days.

To further elucidate the ettringite - heavy metal association, ettringite was precipitated under laboratory conditions in the presence of each of the four heavy metals under study. The ettringite precipitate was then analyzed using both x-ray diffraction (XRD) and scanning electron microscope - energy dispersive x-ray (SEM-EDX) techniques, to establish the nature of the ettringite - heavy metal association, if any.

More specifically, for the trivalent chromium case, ettringite was formed in a 1 g CaO/L and 5 mM of $Al_2(SO_4)_3$ solution (pH =11.3) in the presence of 1 mM of chromium. The corresponding SEM micrograph (Figure 30) showed both needle-shaped ettringite crystals and nondescript particles were formed. X-ray results suggested both ettringite and Cr (III) substituted ettringite (i. e. bentorite, $[Ca_3Cr(OH)_6]_2(SO_4)26H_2O$) formed. However, energy-dispersive x-ray analyses suggested the chromium content on the nondescript particles was more than twice as much as that detected on ettringite or bentorite crystals (Table 3). The EDX - derived surface chemical composition and corresponding XRD analyses both suggested the nondescript particles were mixtures of aluminum and calcium hydroxides close to the composition of amorphous pozzolanic calcium aluminate hydrate products (CAHs). In other experiments, lead, mercury and arsenic behaved similarly, however, contents detected on the ettringite surface were mostly lower than chromium.

Overall, our results suggest heavy metal immobilization is not mainly controlled by ettringite formation. Instead, heavy metal surface adsorption or even isomorphous substitution on freshly formed amorphous pozzolanic products, seems to be the controlling mechanism of the heavy metal - solid surface interaction.

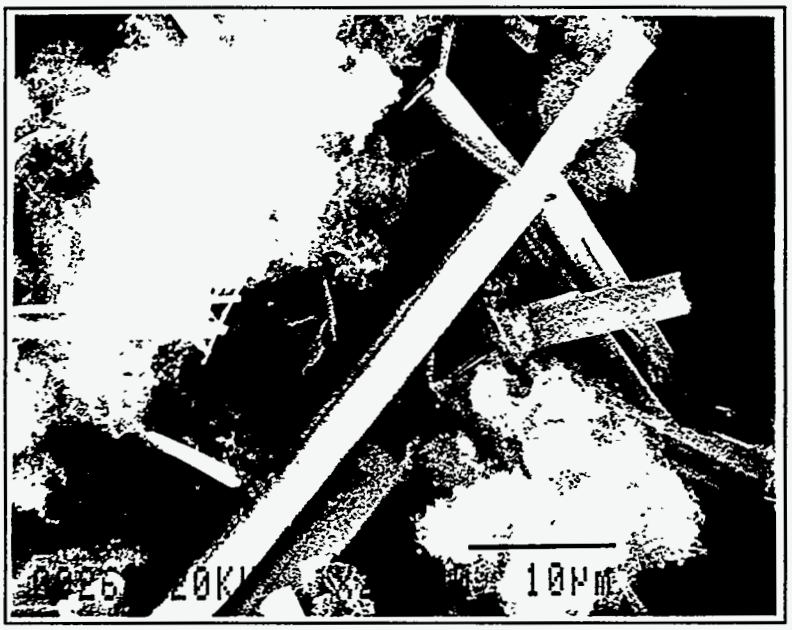

Figure 30. SEM Micrograph of Ettringite and Nondescript Particles Formed in CaO, $Al_2(SO_3)_4$ and $Cr(NO_3)_3$ Solution.

Table 3. Chemical composition of particle in Figure 28.

Particles	Al%	Ca%	S%	Cr%
Nondescript	62	29	5	3.9
Needle-shaped	11.8	69.5	17	1.8

4.1.4 Effect of Soil Heavy Metal Contents on TCLP Release

As discussed in section 4.1.1, the level of heavy metal release is not only a function of total heavy metal contents in the contaminated solid. However, the level of heavy metal presence may affect the corresponding levels of release, and therefore, treatment level requirements. In the present study, the effect of soil heavy metal contents on the effectiveness of quicklime treatment was evaluated by performing TCLP tests on selected samples contaminated using different than "reference state" amounts of heavy metal addition. The "reference state" heavy metal contents used for the bulk of the samples are listed in Table 4. These metal contents constitute the upper limits of contamination levels reported for DOE soil sites [DOE/ER-0547T]. Since heavy metal immobilization was more pronounced in treated montmorillonite-sand samples at "reference

state" heavy metal presence, these contents were doubled for selected montmorillonite samples. Conversely, heavy metal contents in selected kaolinite-sand mixes were reduced by half of the "reference state" values to establish if release could be further reduced.

Table 4. Heavy Metal Contents in the Artificial Soils.

Contaminant Source	Metal Contents (mg/kg soil)	
	Chemicals	Metal Elements
As_2O_3	164	124
$Cr(NO_3)_3$	30814	4007
HgO	1969	1823
PbO	7587	7046

The TCLP release results did not reveal a significant heavy metal content effect on As and Cr leachability for both kinds of clay samples (Figures 31 and 32). Arsenic and chromium leachabilities in all the samples tested were very low, irrespective of the heavy metal content. The insignificant differences between sample TCLP heavy metal release concentration values could be caused by sampling and analytical errors.

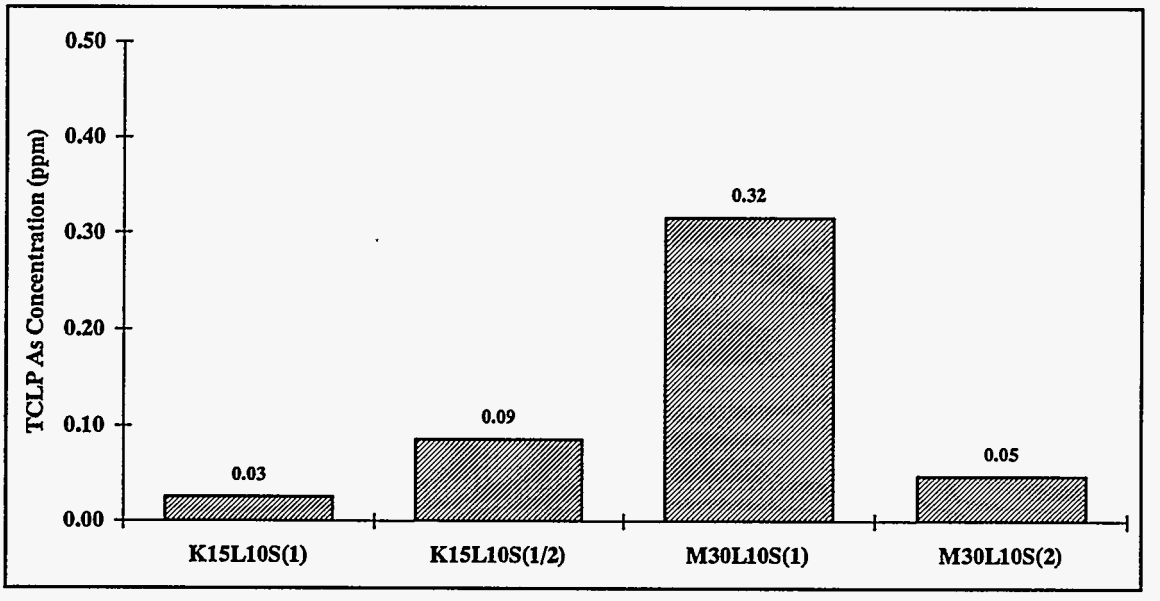

Figure 31. Effect of Heavy Metal Contents in the Solid on As Release.

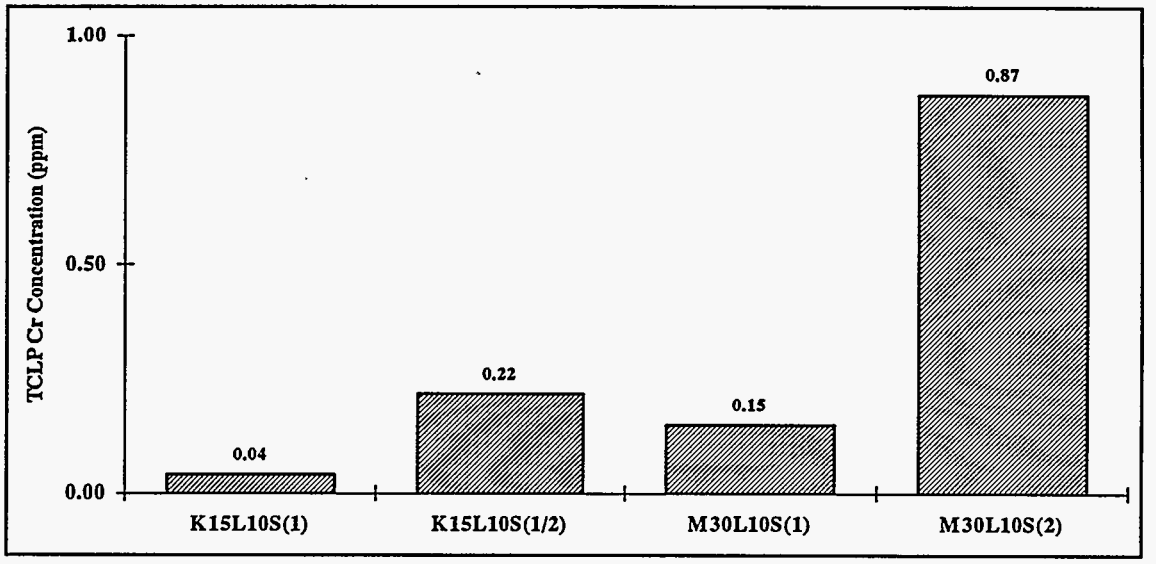

Figure 32. Effect of Heavy Metal Contents in the Solid on Cr Release.

In contrast to As and Cr TCLP release results, the level of heavy metal presence in the kaolinite-sand samples had a considerable effect on Pb leachability (Figure 33). When the metal contents were reduced by half, Pb concentration in the TCLP leachant decreased from 50 ppm to less than 10 ppm for the treated kaolinite-sand sample. The higher metal content montmorillonite sample had higher Pb leachability than the montmorillonite sample with "reference state" metal contents, however, both release concentrations were very low.

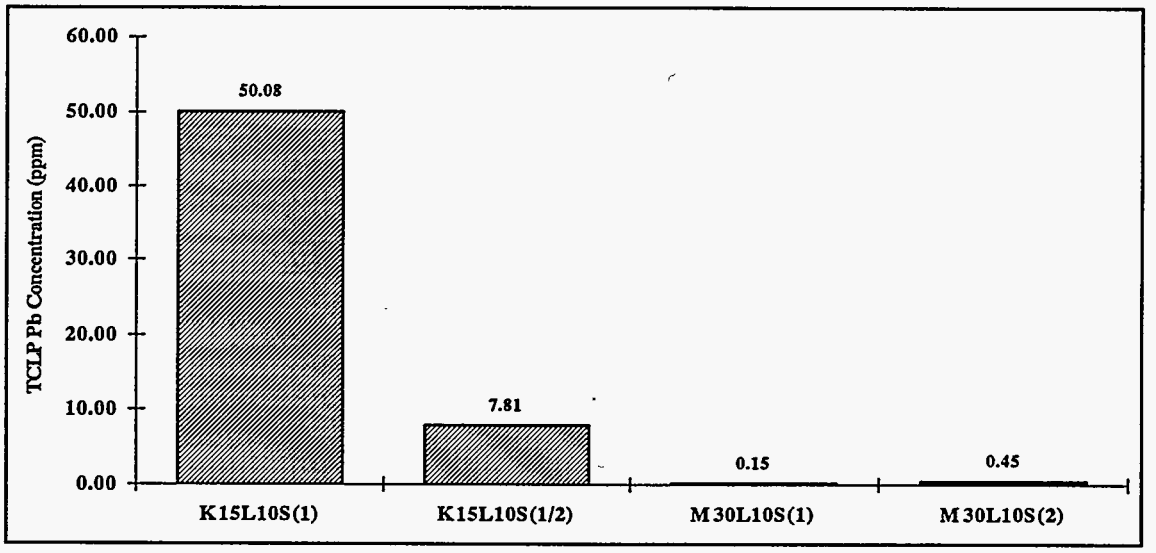

Figure 33. Effect of Heavy Metal Contents in the Solid on Pb Release.

The leaching results obtained for samples with variable heavy metal contents are in general agreement with the metal immobilization mechanisms discussed before. Since As and Cr release from the treated solids was controlled by precipitation, their leachability should not be affected by the contents of these metals in the solids. Based on the effect of clay types and clay content on Pb leachability, we have assumed that Pb leachability was controlled by adsorption. Therefore, when more Pb is added in the solids, more surface sites will be occupied by Pb. As shown for quicklime-sulfate treated kaolinite-sand samples where the activity (CEC) of the surface is low, and therefore the Pb adsorption sites are limited, treatment effectiveness will be a function of the Pb content. In other words, for a given contaminated solid matrix, there seems to be a Pb immobilization capacity which is a function of the availability of reactive surface area. When the Pb content is high enough as to saturate the existing adsorption sites, the solid matrix has reached its capacity for immobilizing Pb and no more lead can be immobilized irrespective of treatment levels. Consequently, the Pb content in contaminated soils has to be carefully considered when designing quicklime treatment applications. That is, in the event that the Pb immobilization capacity in the soil is not high enough to satisfy treatment requirements, some additional reactive surface area (i.e., clay or fly ash) has to be added. In the following section, fly ash addition and its effect on Pb release will be discussed.

4.1.5 Improvement of the Quicklime Treatment Using Fly ash

The results in section 4.1.1.2 showed that for samples with very low clay contents, Pb leachability could not be reduced to meet the TCLP limit. Therefore, fly ash was added into low clay content samples to improve the effectiveness of quicklime treatment in immobilizing Pb leachability. Coal burning fly ash is a industrial waste, having a high surface capacity for heavy metal adsorption. In order to avoid heavy metal dilution caused by the addition of fly ash, heavy metals were added on the total weight of clay, sand and fly ash basis.

As shown in Figure 34, Pb leachability was only reduced from 292 ppm to 124 ppm when 5% kaolinite- 95% sand samples were treated using 10% quicklime. The addition of 25% fly ash alone (no quicklime) reduced TCLP Pb release to the same level as the quicklime treated kaolinite-sand sample (K5L10). Lead leachability was reduced to lower than the TCLP limit when both fly ash and quicklime were added to treat the contaminated sample. Lead TCLP leachability from 5% montmorillonite samples was also reduced effectively below the 5 ppm limit by the quicklime-fly ash treatment (Figure 35).

The addition of fly ash to the untreated samples reduced Cr leachability (Figures 36 and 37) by as much as 80%, probably due to the inherent alkalinity of the fly ash (fly ash contains 25% by weight CaO). However, no dramatic reduction in Cr leachability was achieved when fly ash was added to quicklime treated samples. The Cr leachability was already very low in the quicklime (10%) treated samples due to the formation of Cr precipitates. The addition of fly ash

did not have an obvious effect on As leachability for both treated and untreated samples (Figures 38 and 39), as As concentrations were very low to start with.

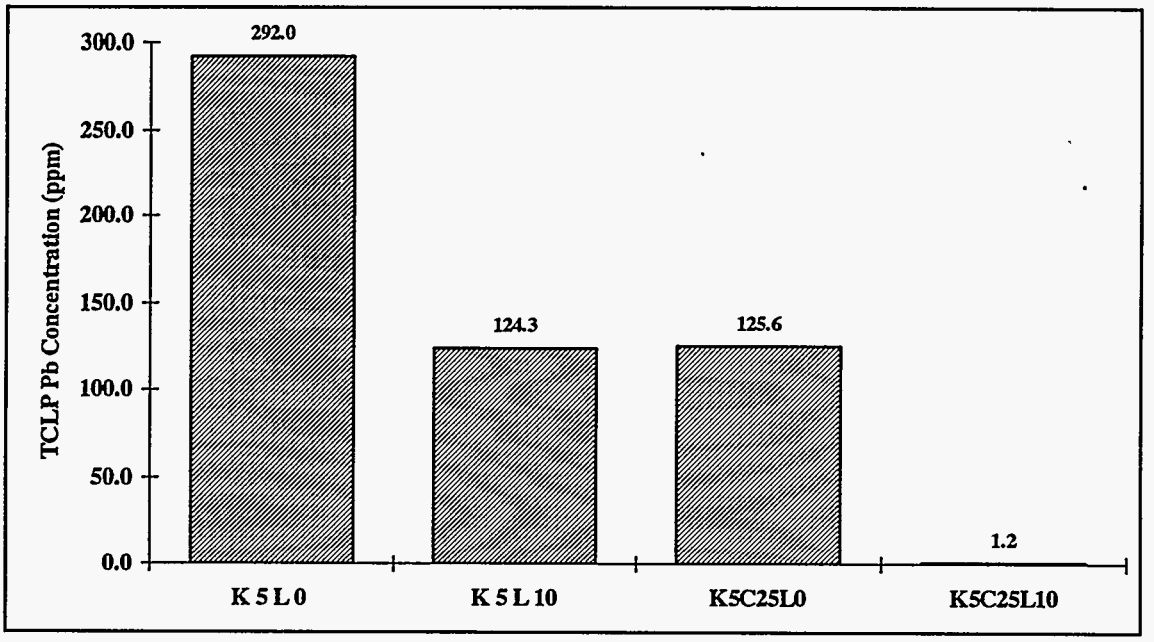

Figure 34. Effect of Fly Ash Addition on Pb Release for Kaolinite (5%) - Sand Mixes.

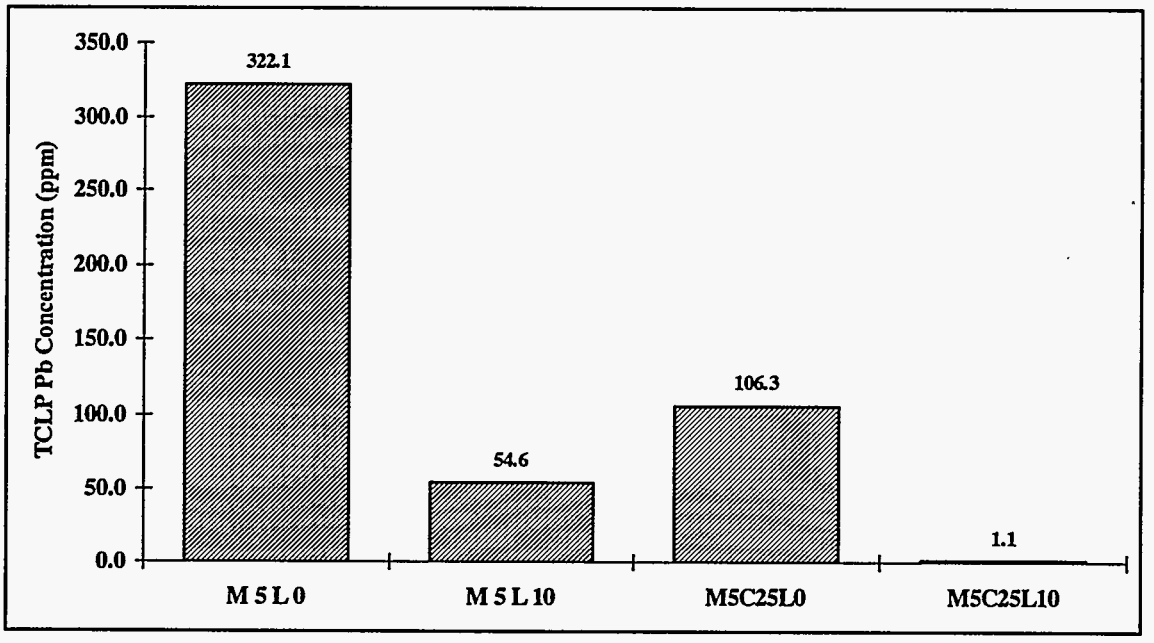

Figure 35. Effect of Fly Ash Addition on Pb Release for Montmorillonite (5%) - Sand Mixes.

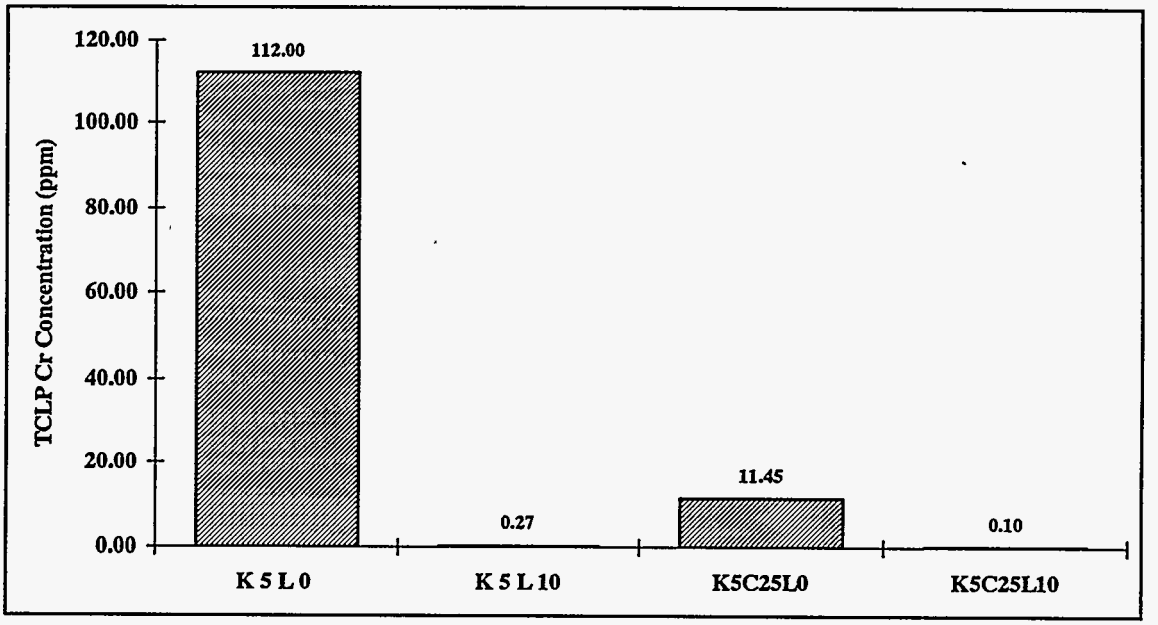

Figure 36. Effect of Fly Ash Addition on Cr Release for Kaolinite (5%) - Sand Mixes.

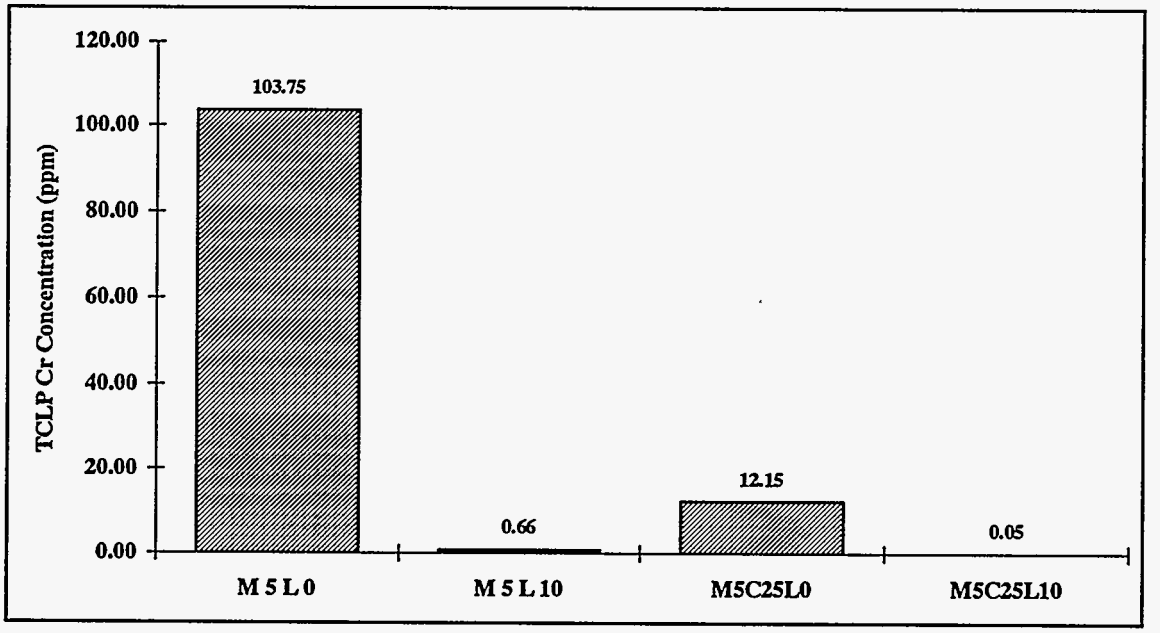

Figure 37. Effect of Fly Ash Addition on Cr Release for Montmorillonite (5%) - sand Mixes.

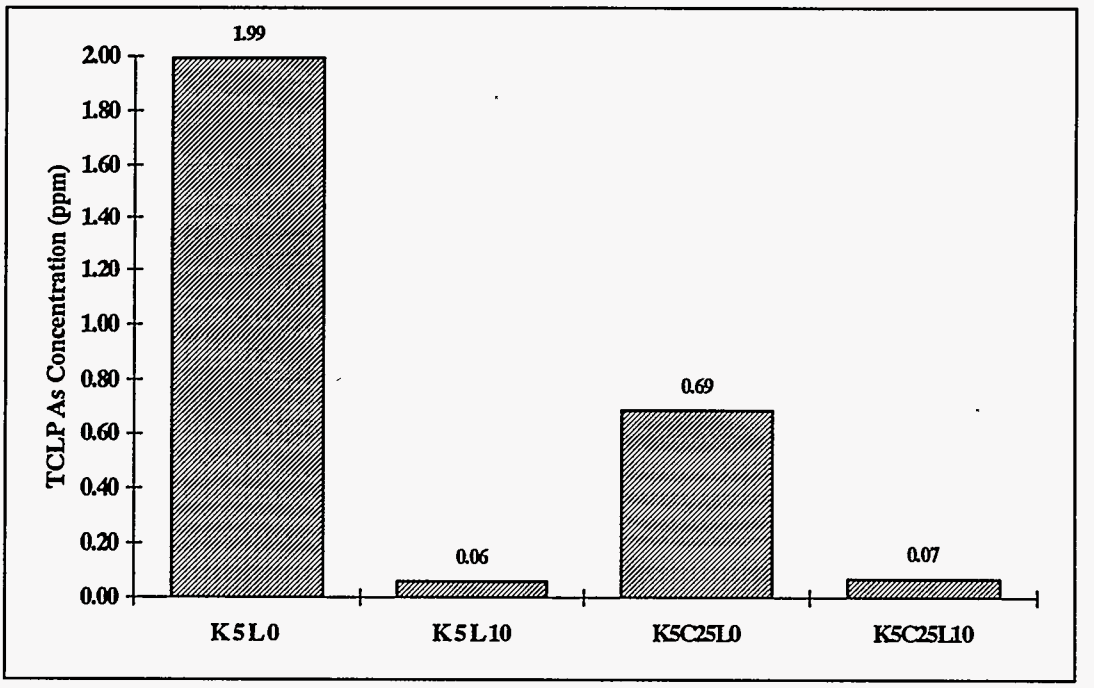

Figure 38. Effect of fly ash addition on As release for kaolinite (5%) - sand mixes.

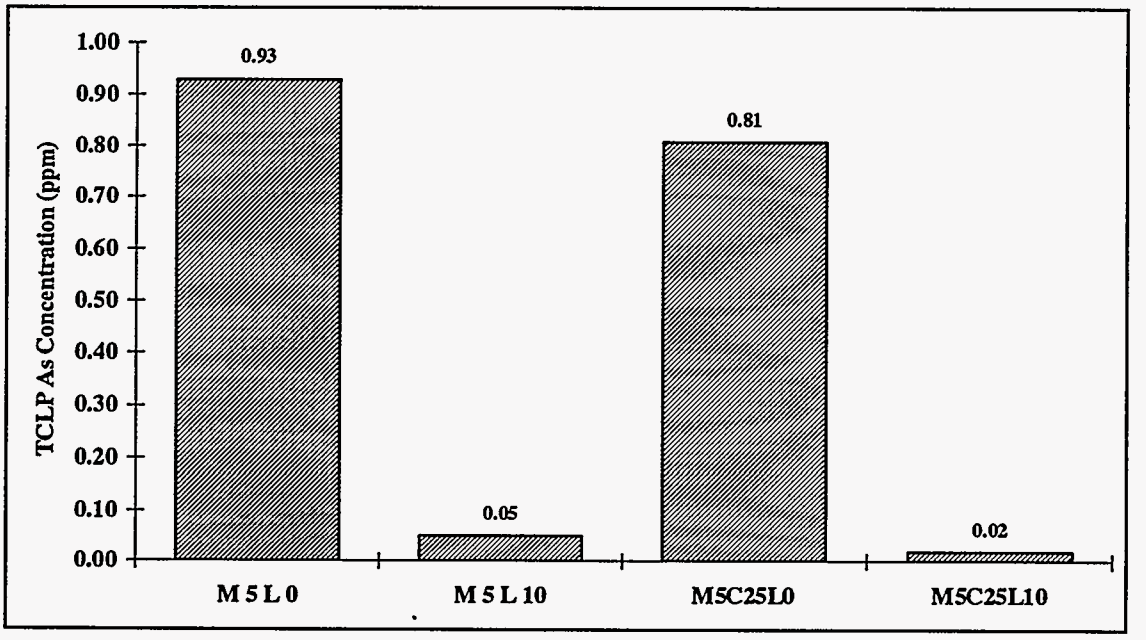

Figure 39. Effect of fly ash addition on As release for montmorillonite (5%) - sand mixes.

Overall, the TCLP release results showed that for Pb contaminated coarse-grained soils, it may be necessary to add both quicklime and fly ash to

effectively immobilize Pb. The addition of fly ash increases the surface area for Pb fixation. However, quicklime has to be added along with fly ash in order to increase the ANC of the waste.

4.1.6 Summary

Overall, the TCLP release results showed that the quicklime-sulfate treatment is effective in immobilizing As, Cr and Pb in contaminated soils. The results were obtained for soil heavy metals contents corresponding to the maximum concentrations reported within the DOE complex. The results reported herein, can be safely extended to include other solid wastes generated within the DOE complex, such as coal and incinerator fly ash, boiler slags, flue gas desulfurization (FGD) wastes, etc. These wastes have a similar texture, physical and chemical properties, and composition with the clay-sand and clay-fly ash-sand mixes used during the present study. As already demonstrated, the proposed quicklime-sulfate salt treatment, if properly designed can immobilize As, Cr and Pb at double the maximum contents reported within the DOE complex. Therefore, the additional heavy metal loading due to the incorporation of other solid wastes during treatment application, will not adversely affect heavy metal immobilization.

4.2 Strength Development in the Quicklime Treated Solids

As already demonstrated in preceding sections, the proposed quicklime-sulfate treatment is effective in producing a solid form that meets the non-hazardous TCLP criteria for As, Cr and Pb. Moreover, it was shown that a wide range of other waste by-products generated within the DOE complex such as fly ash, boiler slag, FGD wastes, etc., could be also successfully incorporated in the proposed quicklime-based treatment scheme. Overall, upon treatment application, solid wastes at DOE sites will be effectively converted from hazardous to non-hazardous. Following treatment, the resulting solid could be safely left in place, or landfilled as non-hazardous, or reused as a readily available construction material. Obviously, the optimum alternative, concerning the ultimate fate of the treated solids, is reusing them.

To reuse the treated solids as construction materials, such as road base or engineering fill, the treated solid forms have to meet certain physical criteria. Among the pertinent physical parameters, compressive strength is the single most important parameter needed to assess the reusability of the treated soils. According to EPA, an unconfined compressive strength of at least 350 kPa (~50 psi) is considered adequate for S/S material reuse. During the present study, a minimum unconfined compressive strength of 500 kPa (~70 psi) had to be attained in order for treatment to be deemed successful. Satisfying this minimum strength requirement indicates the viability of reusing the quicklime-sulfate treated solids in construction applications. In the following sections, the effect of various treatment parameters on the resulting strength of the solids will be discussed. It should be noted that all unconfined compressive strength values reported herein were obtained as average values by testing specimen duplicates.

4.2.1 Effect of Quicklime Content, Curing Time and Sulfate on Strength Development

Unconfined compressive strength values for montmorillonite-sand specimens, cured for 28 days following quicklime-sulfate treatment, are presented in Figure 40 as a function of quicklime treatment levels. When quicklime content was increased from 0 to 10% in specimens containing 15% and 30% montmorillonite, strength of the compacted specimens increased from less than 400 kPa to values higher than 2,400 kPa. However, the strength decreased when the quicklime content was further increased from 10% to 15%. This was expected, since the relationship between lime content, curing time and strength is known to be quite complex. Previous research (Dermatas, 1992) has established that unreacted lime can be responsible for lower strengths at short curing times in higher lime-content specimens relative to lower lime-content specimens. At longer times however, the strength of high lime content specimens (Figure 42) may be considerably higher as a result of increased pozzolanic product (CSH and CAH) formation. For the 5% montmorillonite specimens, quicklime treatment resulted in insignificant strength development. This is probably due to the absence of adequate amounts of alumina and silica needed for the formation of the

cementitious pozzolanic products which are mainly responsible for strength development.

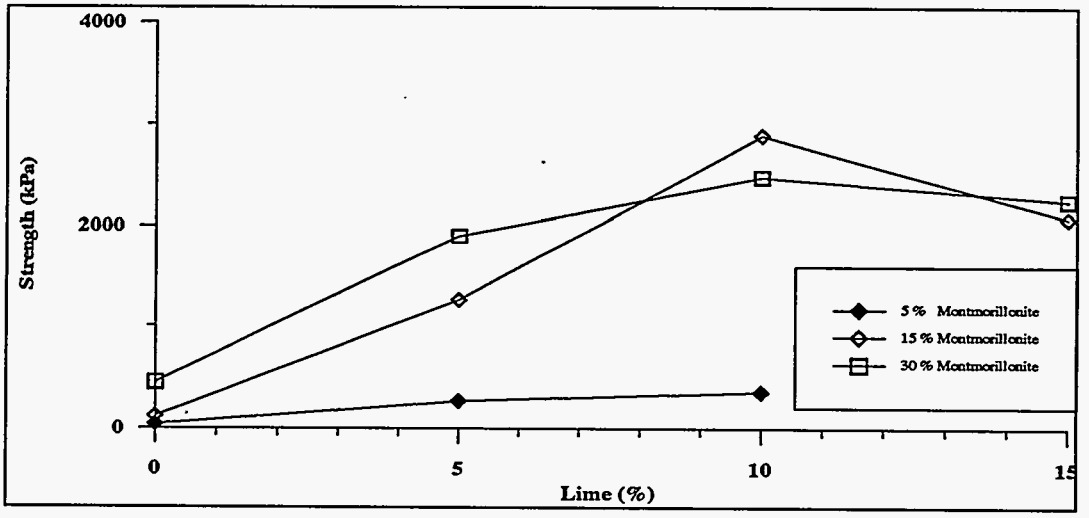

Figure 40. Effect of Quicklime Levels on Unconfined Compressive Strength of Montmorillonite-sand Mixes with Sulfate after 28 Days of Curing.

Lower strength development levels were attained for the quicklime-sulfate treated kaolinite-sand specimens (Figure 41), as opposed to montmorillonite-sand specimens. When kaolinite-sand specimens were treated with 5% quicklime, no obvious strength recovery took place as compared to the strength of untreated specimens. The strength increased significantly when quicklime content was increased to 10% and 15% for specimens containing 15% and 30% kaolinite. Similar to montmorillonite-sand mixes, no significant strength development was observed for the low kaolinite content (5%) specimens.

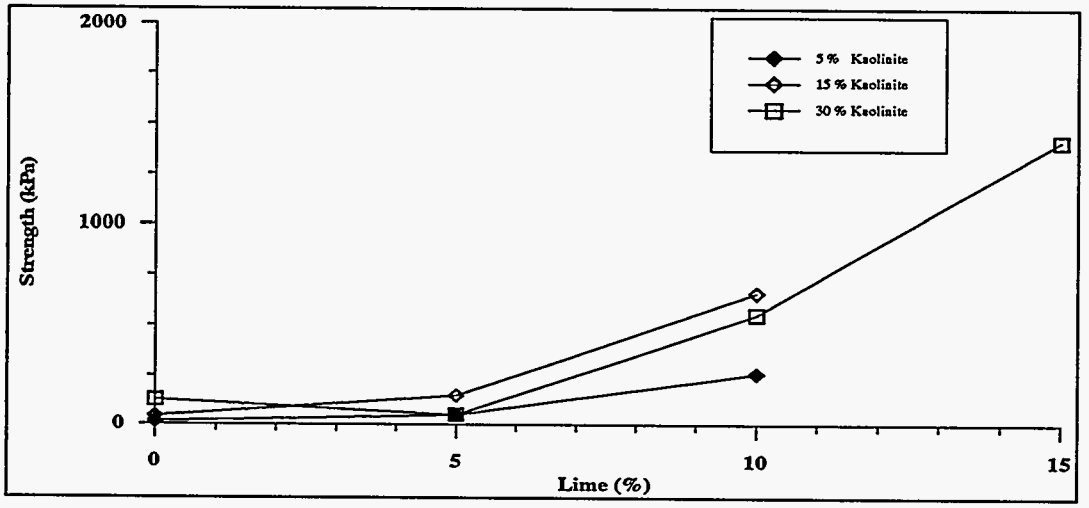

Figure 41. Effect of Quicklime Levels on Unconfined Compressive Strength of Kaolinite-sand Mixes with Sulfate after 28 Days of Curing

To assess the influence of curing time on the resulting levels of unconfined compressive strength, besides testing for 28-day cure specimen strength, specimen replicates were also tested following 6 months of curing. The strength values for specimens tested following 28 days versus 6 months of curing are compared in Figures 42 and 43 for montmorillonite- and kaolinite-sand mixes respectively. As expected, longer curing times did not affect strength development for the untreated specimens, since there is no pozzolanic product formation in these specimens. On the other hand, longer curing times resulted in significant increase of the unconfined compressive strength for all quicklime treated mixes. All the treated montmorillonite specimens, except for the low clay and low lime, M5L5 specimens, developed adequate unconfined compressive strength, as a result of treatment. In fact, strengths were higher than the 500 kPa success criterion after 28 days of specimen curing. Conversely, for kaolinite-sand mixes, it was only after 6 months of curing had elapsed, that the strengths of the quicklime treated specimens were higher than 500 kPa.

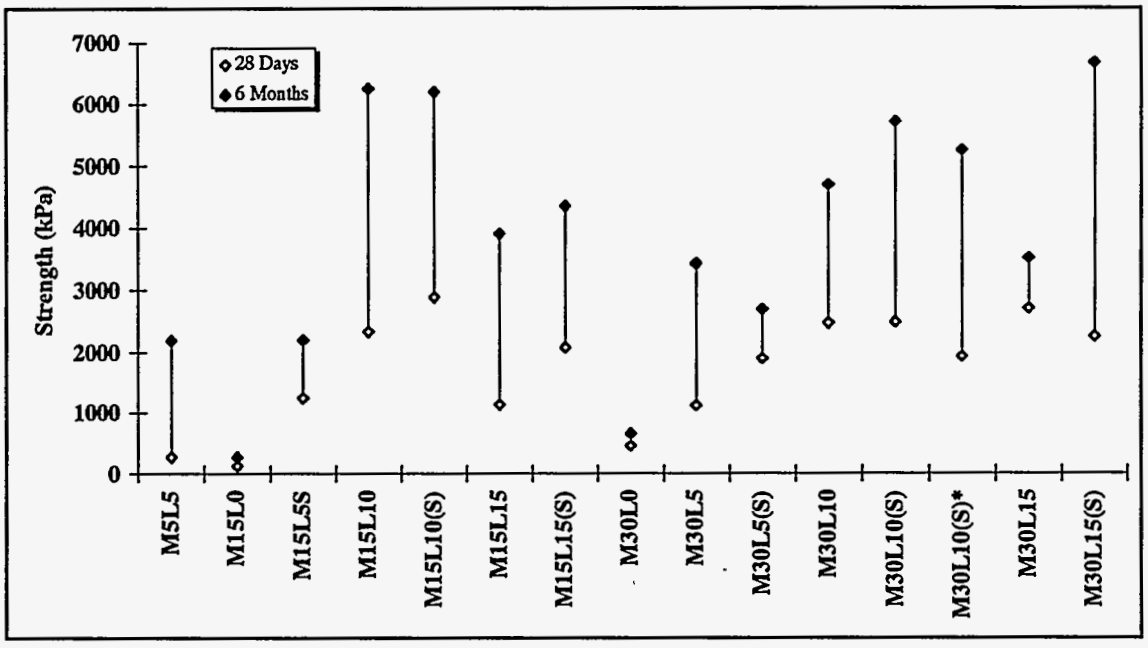

Figure 42. Effect of Curing Time on Unconfined Compressive Strength Development in Montmorillonite-sand Mixes.

Overall, treated montmorillonite-sand specimens attained much higher strength values than kaolinite-sand specimens. Furthermore, in most cases, increasing the clay content of a specimen mix resulted in increased levels of strength gain. Both of these observations are attributed to the higher surface area available for pozzolanic reactions, as clay content increases and as we switch from kaolinite to montmorillonite presence in the soil mixes.

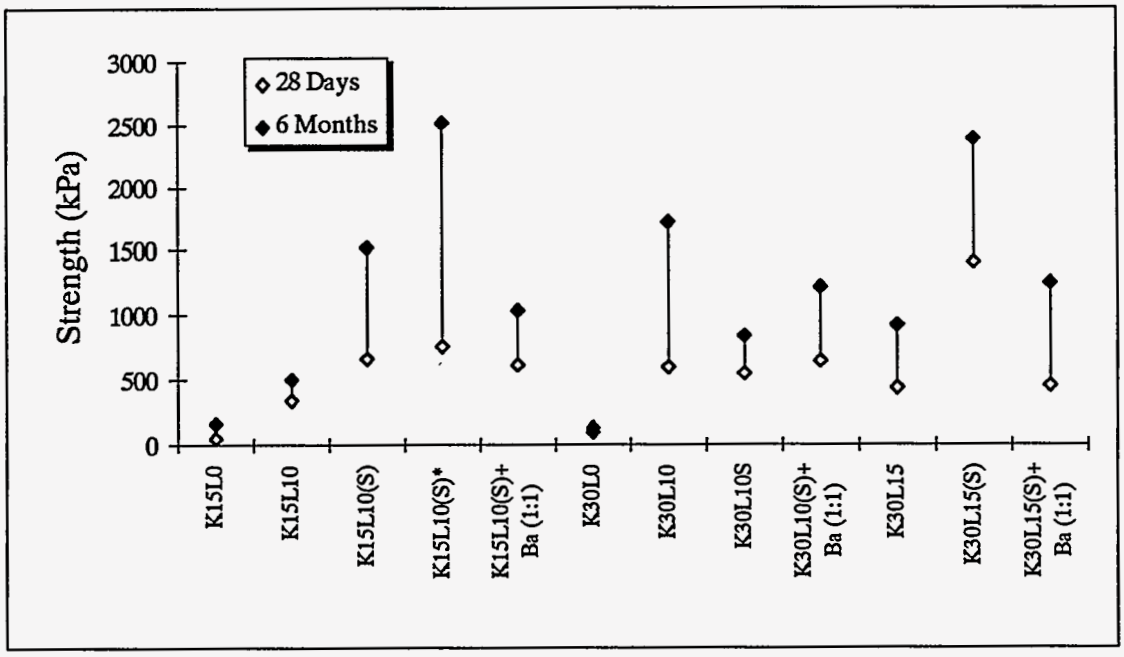

Figure 43. Effect of Curing Time on Unconfined Compressive Strength Development in Kaolinite-sand Mixes.

The x-ray diffraction and SEM results, discussed previously in section 4.1.3, demonstrated that in the presence of sulfates, the mineral ettringite formed in the quicklime treated clay-sand mixes. It has been reported (Dermatas, 1992) that the formation of needle shaped ettringite in lime treated solids may increase their strength due to crystal interlocking. Therefore, specimens with and without sulfate were prepared to evaluate the effect of ettringite formation on the resulting strength levels. The results in Figure 44 suggest that sulfate addition (5% by weight) did not have an obvious effect on the strength development in the treated montmorillonite (30%)-sand (70%) specimens, irrespective of the quicklime treatment levels. This was attributed to the limited amount of alumina present in montmorillonite clays. The ettringite extent of formation is proportionally related to the amount of alumina, calcium and sulfate that are present in the solids. Montmorillonite is predominately comprised of silica, which will react to form CSH products, but would not participate in ettringite formation reactions. Alumina released from montmorillonite, along with calcium available from lime dissolution, and sulfates, did react to form ettringite, as confirmed by x-ray diffraction analyses. However, ettringite did not form in large enough quantities to affect the resulting levels of strength gain.

Similar to montmorillonite-sand behavior, sulfate addition did not seem to have a major effect on strength development in quicklime treated kaolinite-sand specimens. However, a significant sulfate effect on strength development was observed for kaolinite-sand specimens treated with 15% quicklime (Figure 45). Kaolinite is predominately comprised of alumina, thus favoring ettringite formation, more so than montmorillonite. Moreover, since both kaolinite and

sulfate contents were identical for all specimens shown in Figure 45, increasing the level of quicklime addition would increase the amount of ettringite formed. Based on our results, 15% of quicklime addition supplied sufficient amounts of calcium for ettringite to form in ample quantities, thus dominating specimen strength development.

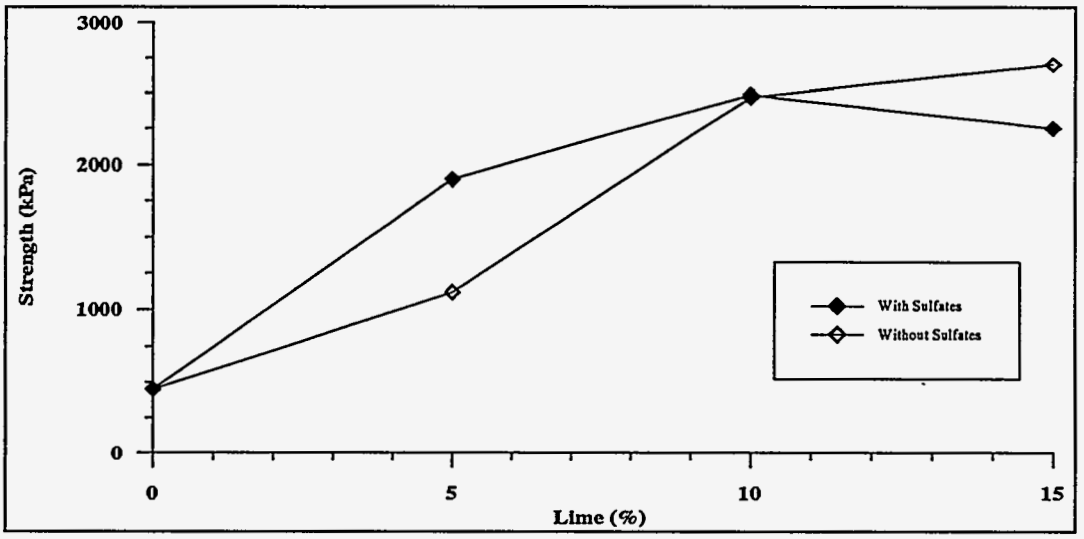

Figure 44. Effect of Sulfate on Unconfined Compressive Strength of Montmorillonite-sand Series after 28 Days of Curing

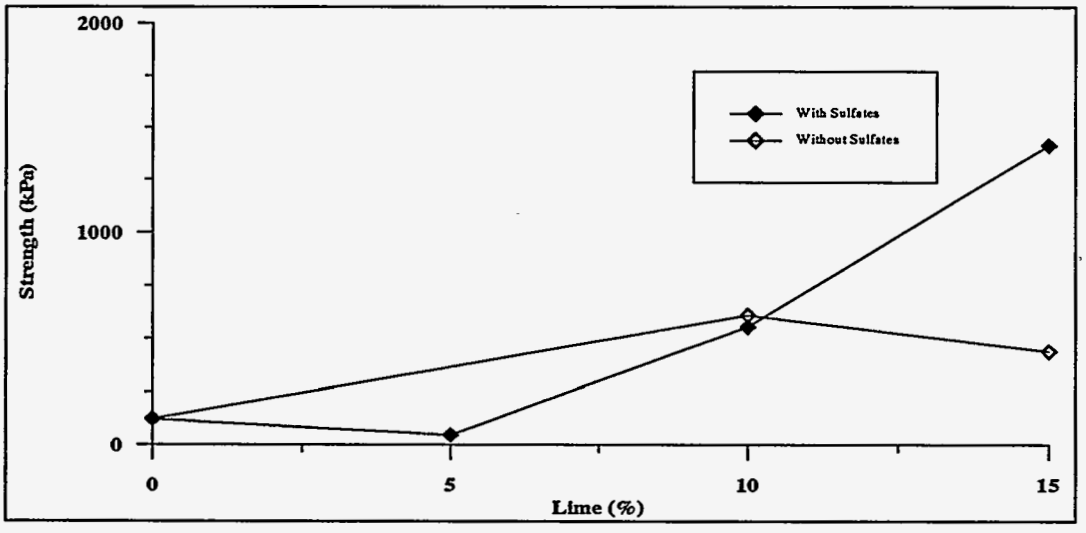

Figure 45. Effect of Sulfate on Unconfined Compressive Strength of Kaolinite-sand Series after 28 Days of Curing.

4.2.2 *Improvement of Strength Using Fly ash*

Since coarse-grained (low clay content) quicklime treated specimens attained very low levels of strength gain, class C fly ash was added in an attempt to

increase the cohesive force in the solids. TCLP leaching results (Figures 34 and 35), have demonstrated that the addition of fly ash can effectively reduce Pb release from coarse-grained specimens, thus enabling regulatory compliance. If fly ash can also act as a cementing agent for these quicklime treated soils, treatment can be used to effectively remediate contaminated coarse-grained soils that may then be reused as readily available construction materials.

The results summarized in Figure 46 indicate the addition of fly ash significantly increased the strength of the low clay content specimens. When 25% of fly ash was added to the treated specimens, their strength increased from less than 350 kPa (M5L10 specimens) to approximately 11,500 kPa (M5C25L10 specimen). These fly ash treated specimens reached strength levels comparable to those of concrete products.

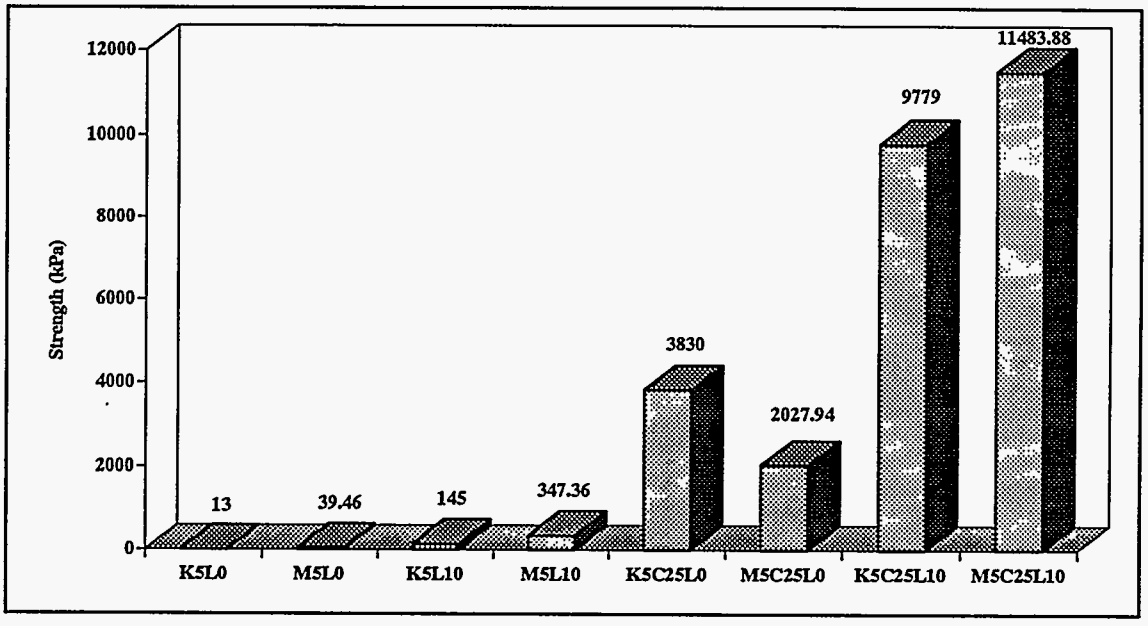

Figure 46. Effect of Fly Ash on the Strength of 5% of Kaolinite and Montmorillonite Mixes.

4.2.3 *Setting Time of Quicklime-Treated Specimens*

When soils are treated with quicklime, a series of reactions will take place, including the hydration of quicklime (short-term reaction) and pozzolanic reactions (long-term reactions). Most of these reactions involve the consumption of water molecules, and result in strength development. Therefore, water content changes in the specimens at different curing time is a meaningful measure of the extent of setting for the treated solid. The water contents of a group of selected specimens were monitored regularly for 10 months. The water content data for both kaolinite and montmorillonite- sand (30% clay content) quicklime (10%)-sulfate (5%) treated specimens are plotted as a function of curing time in Figures 47 and 48 respectively. Statistical analyses were performed to find the best fit equations to describe these experimental results.

The equations obtained for each of the mixes are listed in Table 5, and calculated curves are plotted in the corresponding figures.

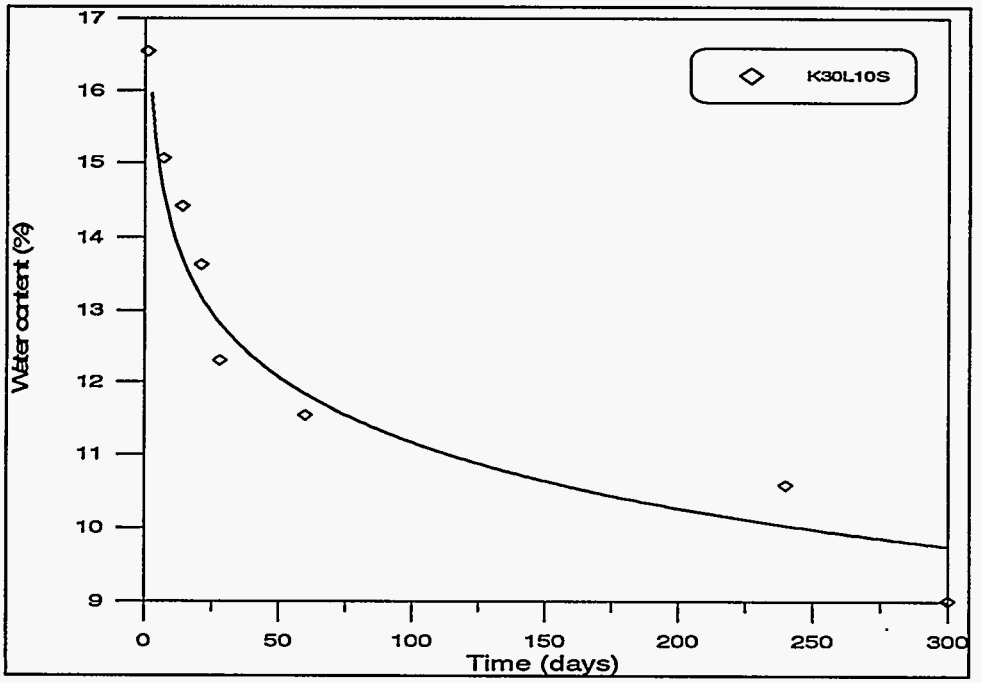

Figure 47. Water Content Change as a Function of Curing Time for K30L0S Specimen.

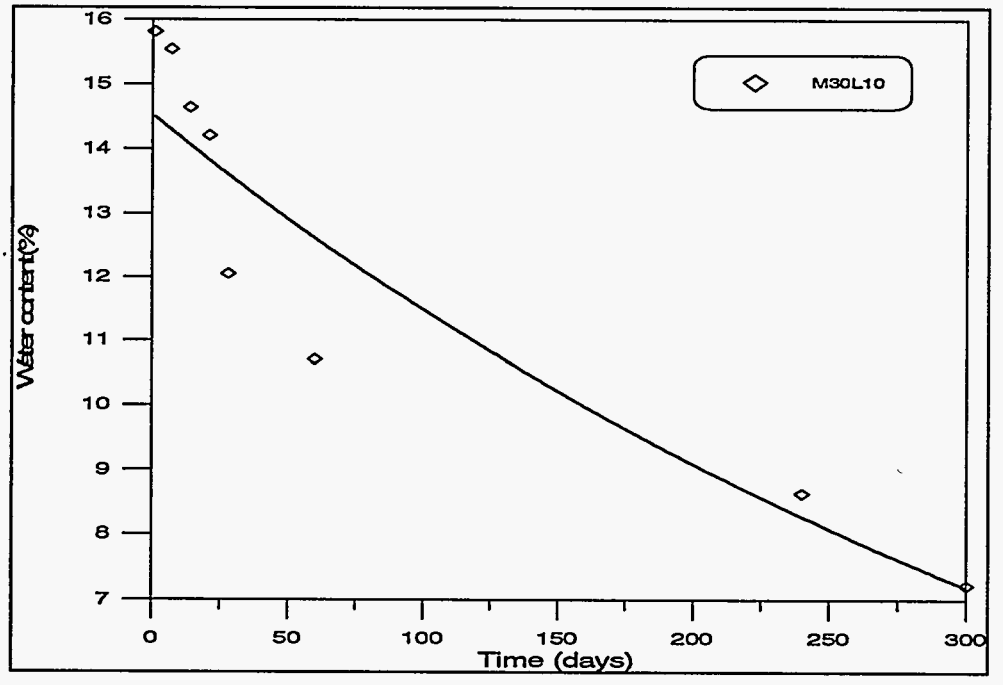

Figure 48. Water Content Change as a Function of Curing Time for M30L10S Specimen.

In general, water contents were reduced significantly during the first 28 days of curing. The decrease in water content tends to level off with increasing curing time. The water content results are in good agreement with the strength development phenomena observed during long term curing. That is, unconfined compressive strength increases with decreasing water content. Statistical analysis of the water content data indicated that the standard deviation for the water content measurement is ±0.45% when water content is about 9%.

Table 5. The Best Fitting Equations Describing Water Content as a Function of Curing Time

Specimens	Equations	R-squared
K30L10S	Y = -1.296 log[X] + 17.1357	0.944
M30L10S	logY = -0.00234X + 2.67	0.897

4.2.4 *Summary*

Treatment strength success criteria were comfortably met for all montmorillonite-sand mixes, following 28 days of specimen curing as long as both the clay and quicklime contents of the mixes were higher than 5%. Strength increased with increased clay content and curing time, whereas sulfate addition and ettringite presence did not have a significant effect on strength development. For kaolinite-sand mixes, treatment strength success criteria could not be met for all specimens following 28 days of curing. However, as long as both the clay and quicklime contents in the mixes were higher than 5%, following 6 months of curing, all specimens attained strength levels higher than 500 kPa, thus satisfying treatment success criteria. Setting time results were in general agreement with the curing time-dependent strength development in the quicklime-sulfate treated solids. Finally, fly ash addition to poor strength mixes was effective in producing treated solids that do not only meet the strength success criteria, but attain strength levels comparable with those characteristic of concrete products.

4.3 Swell Development in the Quicklime Treated Soils

Thus far, it has been demonstrated that quicklime treatment is capable of producing monolithic solids that will satisfy both regulatory heavy metal release and unconfined compressive strength criteria. However, lime-based monolithic solids when exposed to water may swell, especially in the presence of the pozzolanic product ettringite. Assuming the quicklime-sulfate treated soils will be used in construction applications, excessive swell development may result in the deterioration, and possibly the ultimate failure of the construction. Moreover, deterioration of the treated solids will make them increasingly susceptible to rain water and/or other fluid leaching, which in turn may lead to increased levels of contaminant release. Therefore, it is desirable that the quicklime treated solids undergo minimum amounts of swell when soaked in water. In the present study, following a 28 day curing period, compacted cylinder-type specimens were soaked in water-saturated sand bath conditions. The vertical swell of the specimens was measured regularly until steady-state was reached. Treatment was considered effective when maximum vertical swell development levels were lower than 5%.

4.3.1 Effect of Quicklime Content and Sulfate Presence on Swell Development

The swell results for montmorillonite-sand and kaolinite-sand specimens, following 56 days of continuous soaking, are plotted in Figures 49 and 50, respectively. The untreated montmorillonite specimens showed a 10 % to 14% vertical swell development, which increases with increasing clay content. This swell development was due to the expansive nature of the montmorillonite clay (Figure 49). Upon quicklime treatment swelling tendencies were effectively eliminated in all montmorillonite-sand specimens. Levels of vertical swell for specimens prepared with and without sulfate are also shown in Figure 49. These results indicate that the presence of sulfate did not result in additional swell development as compared to the swell development for specimens prepared without adding sulfate. As previously discussed, x-ray diffraction analyses confirmed that in the presence of sulfate, ettringite did form in both montmorillonite-sand and kaolinite-sand specimens. Previous research (Mitchell 1984; Hunter, 1988; Mitchell and Dermatas 1992; Dermatas, 1992) has established that ettringite will expand when brought in contact with water, possibly leading to excessive swelling and subsequent deterioration of lime treated soils. The negligible swell observed for sulfate-bearing montmorillonite specimens indicates restraining pressures, resulting from confinement and cohesive strength development in the quicklime treated montmorillonite-sand specimens, are larger than swelling pressures caused by ettringite hydration. This is attributed to the limited amount of ettringite formation in quicklime treated montmorillonite-sand mixes, due to the relatively low alumina content of montmorillonite clays.

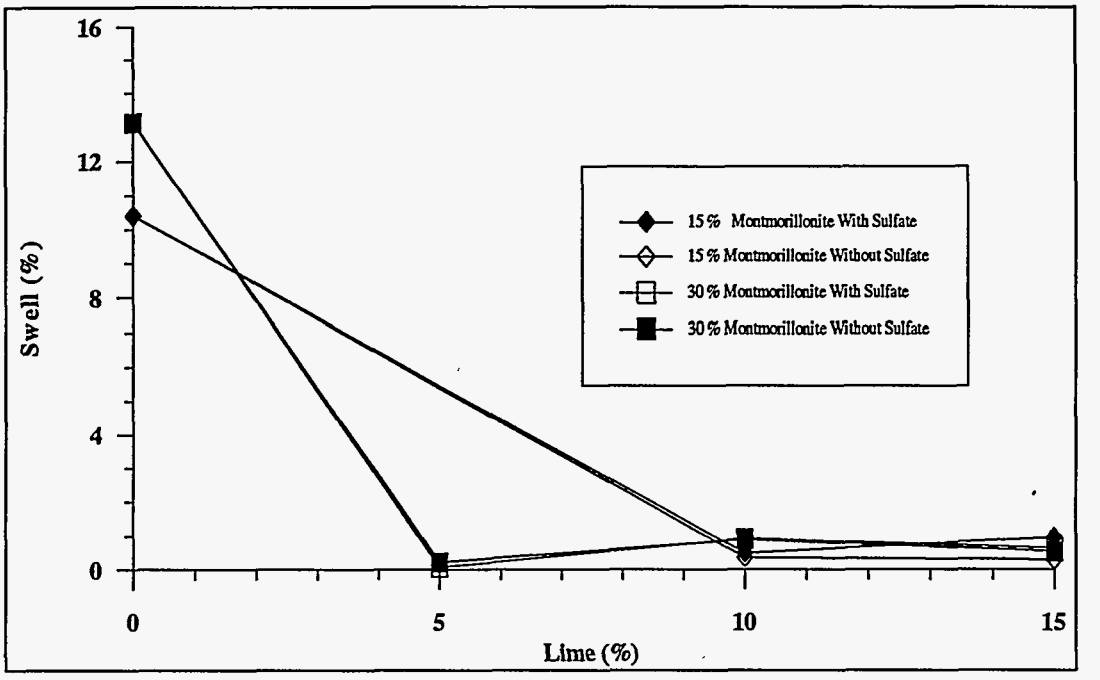

Figure 49. Effect of Quicklime Levels on Swell of Montmorillonite-sand Mixes after 8 Weeks of Soaking in Water-saturated Sand Bath.

In the absence of sulfates, quicklime treated kaolinite-sand specimens also showed negligible swell (Figure 50). However, in the presence of sulfates, the quicklime treated specimens developed 8% to 16% of vertical swell. Everything else being equal, vertical swell increases with increasing quicklime contents, due to the formation of larger amounts of ettringite. Excessive swell development indicates that the restraining forces in the quicklime treated kaolinite-sand matrices were not high enough to overcome the swelling pressures due to ettringite hydration. The compressive strength results discussed in the previous section, also indicated that restraining forces in quicklime treated montmorillonite-sand specimens were higher than in treated kaolinite-sand specimens. Moreover, ettringite is expected to form in larger quantities in kaolinite-sand specimens, due to the increased alumina content and mobility in kaolinite clays.

In order to eliminate swell development, barium hydroxide ($Ba(OH)_2$) was added into sulfate-bearing kaolinite specimens. As previous research has demonstrated (Dermatas, 1992), a barium hydroxide pretreatment of sulfate-bearing soils is successful in eliminating ettringite formation and subsequent swell. In the presence of sulfates and barium, the formation of barium sulfate, $BaSO_4$, is thermodynamically favored over ettringite formation. The barium sulfate precipitate attains a very low solubility in water, and will therefore eliminate the formation of ettringite by consuming the free sulfate ions present in solution. As shown in Figure 50, addition of barium hydroxide was indeed effective in eliminating ettringite-induced swell in all quicklime treated sulfate-bearing kaolinite-sand specimens.

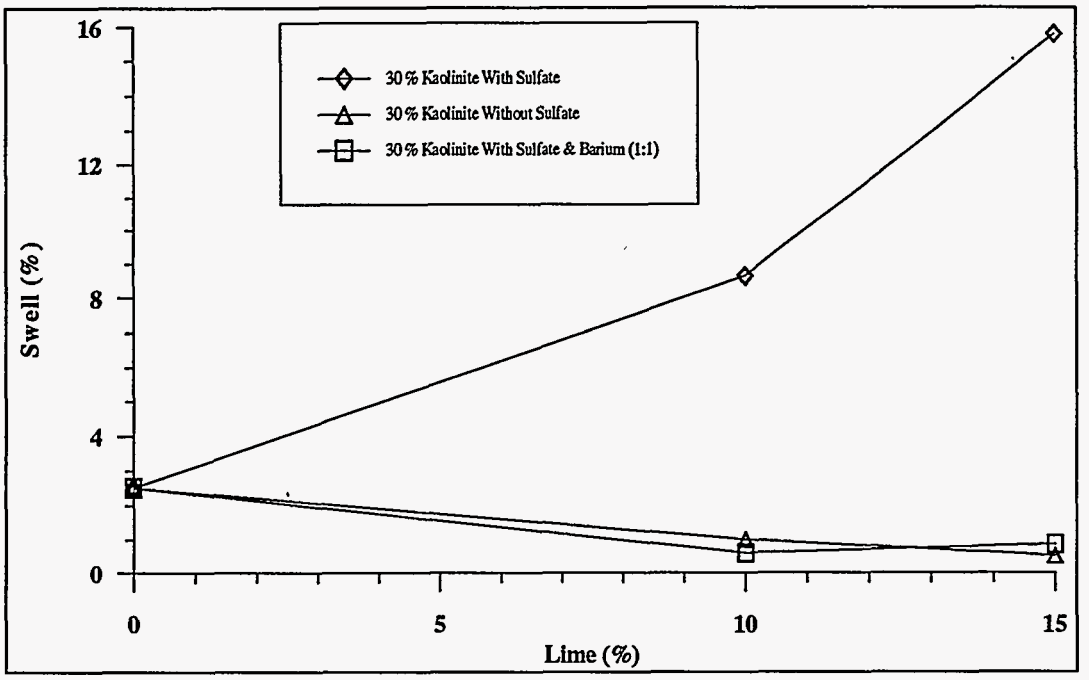

Figure 50. Effect of Quicklime Levels on Swell of Kaolinite-sand Mixes after 8 Weeks of Soaking.

The effect of varying the level of barium addition on the resulting K30L10S specimen swell is depicted in Figure 51. Overall, a Ba^{2+} to SO_4^{2-} molar ratio of 0.2 was effective in eliminating swell development in kaolinite-sand specimens. In other words, ettringite-induced swell can be effectively controlled by the addition of minimum amounts of barium hydroxide.

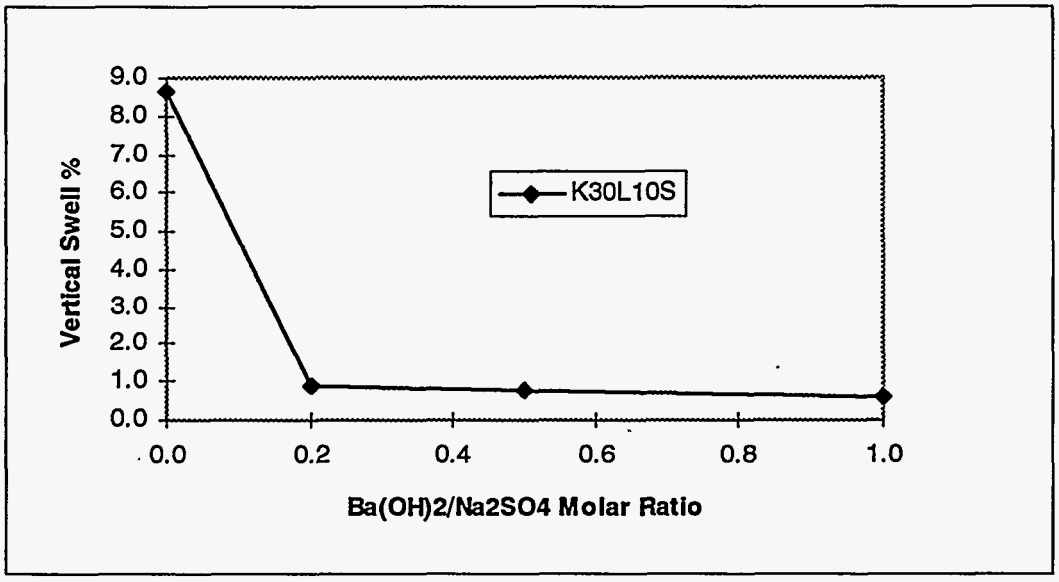

Figure 51. Effect of Barium Content on Swell of Kaolinite(30%)-sand Mixes Treated with Quicklime (10%) and Sulfate (5%).

4.3.2 *Effect of Fly Ash Addition on Swell Development*

In preceding sections it has been demonstrated that the addition of fly ash to quicklime treated clay-sand mixes could significantly reduce the heavy metal leachability and effectively improve the strength of coarse-grained soils. It remains to be seen if the swell of the quicklime-fly ash treated solids also satisfied the less than 5% vertical swell success criterion. The main issue concerning fly ash addition and swell development, involves previously reported swell-induced failures of fly ash containing matrices, attributed to the excessive formation of ettringite (Ferguson, 1993). Relatively recent changes in combustion system technology, such as the incorporation of fluidized bed combustion or dry scrubber systems, resulted in relatively high (5% to 10%) concentrations of soluble sulfates in fly ash. The presence of soluble sulfates, calcium and alumina in fly ash, would ensure ettringite formation, which in turn may lead to excessive swell development in fly ash treated solids.

The swell results of the quicklime/fly ash treated specimens are presented in Figure 52. It is obvious that none of the fly ash and/or quicklime/fly ash treated specimens showed significant swell development. Even the sulfate-bearing kaolinite-sand specimens that were treated with quicklime and fly ash, showed negligible swell. X-ray diffraction and scanning electron microscope-energy dispersive x-ray analyses confirmed the presence of ettringite for all specimens shown in Figure 52. However, as is the case with montmorillonite-sand quicklime-sulfate treated specimens, levels of cohesive force development within the fly ash treated specimen matrix were sufficiently large as to overcome the ettringite hydration swelling pressures.

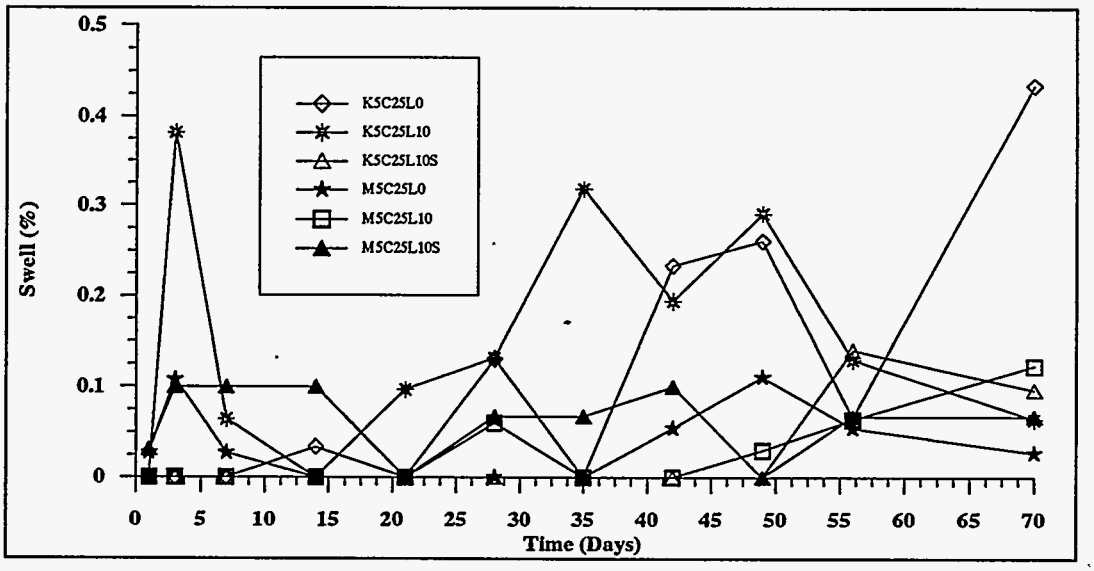

Figure 52. Swell of Fly Ash Treated Specimens as a Function of Soaking Time.

4.3.3 *Summary*

Swell success criteria were easily met for all quicklime treated montmorillonite-sand specimens, whether sulfates were added or not. For kaolinite-sand specimens swell criteria were not always met. In fact, swell increased with increasing the quicklime and/or clay content. This excessive swelling was attributed to the formation of the expansive mineral ettringite, coupled with the existence of weak cohesive forces in the kaolinite-sand solid matrices. However, the use of a barium hydroxide pretreatment scheme was effective in eliminating any adverse swell development and specimen deterioration for the kaolinite-sand mixes. Finally, the addition of fly ash to the low clay content mixes did not result in excessive swell development and swell success criteria were comfortably met for all quicklime/fly ash treated specimens.

4.4 Durability of the Treated Solids

Durability testing evaluates the resistance of a stabilized/solidified waste mixture to degradation due to external environmental stresses. These environmental stresses are simulated by subjecting the S/S treated solid to aggressive physical weathering conditions in the form of wetting, drying, freezing, and thawing processes. These processes may cause disintegration and/or deterioration of the treated solid. In our case, degradation of the quicklime-sulfate treated solid may adversely affect the long-term immobilization of the heavy metals. Heavy metal immobilization requires both stabilization of the heavy metals in the soil, as well as solidification of the waste to reduce the contact area of the solid with the leachant. Therefore, loss of the physical integrity of the treated solids will almost definitely lead to increased levels of heavy metal release. In the present study, aggressive weathering tests (wet/dry and freeze/thaw) were used to evaluate the resistance of the quicklime-treated soil specimens. Evaluation was performed based on observations of the swell development and physical integrity of the tested specimens. Since swell development alone cannot fully account for the physical disintegration of the test specimens, their physical integrity was monitored by taking specimen photographs, following each testing cycle. Photographs of representative specimen response to durability testing can be found in the durability testing Appendix of the present report.

4.4.1 Freeze/Thaw and Wet/Dry Testing

Following a 3 month water soaking period, swell test specimens were subjected to freezing and thawing tests to evaluate their swell behavior under accelerated weathering conditions. Freeze/thaw testing was conducted according to the ASTM standard method D 560-82 for compacted soil-cement mixtures (ASTM, 1986a). Each cycle included 24 hours of specimen freezing at 0°C (for kaolinite-sand) or -5°C (for montmorillonite-sand) and 24 hours of specimen thawing at 22°C. The two sets of freezing conditions used, reflected the unconfined compressive strength magnitude differences between the two types of clay-sand mixes. That is, montmorillonite-sand specimens attaining higher levels of strength than kaolinite-sand specimens, were expected to also exhibit a greater resistance to degradation due to freeze/thaw. An environmental chamber (Model HB/12, Standard Environmental System Inc., NJ) was used during the freezing cycles. Following each freezing cycle, specimens were thawed in a temperature control room. Specimens which withstood the first 12 freeze/thaw cycles, were subjected to an additional 24 cycles of more severe temperature changes (-15°C to 22°C).

Successive cycles of wetting and drying may also have an adverse impact on the structural integrity of the quicklime-sulfate treated waste forms. Wet/dry testing was conducted according to the ASTM standard method D 559-82 for compacted soil-cement mixtures (ASTM, 1986b). Similar to freeze/thaw testing, following a 3 month water soaking period, swell test specimen duplicates were subjected to wet/dry testing. During these tests, the specimens were dried at 70°C for 24 hours and then soaked in water at 22°C for 24 hours. Overall, 12

dry/wet cycles were conducted for each specimen. For those specimens which withstood the first 12 wet/dry cycles, a higher temperature (110°C) was used for the dry step during a second set of 24 cycles of wet/dry tests. Contrary to freeze/thaw testing, wet/dry testing conditions were identical for all specimens, since preliminary testing indicated no major differences in specimen response to testing conditions.

Table 6. Summary of Durability Test Results

SPECIMEN DESIGNATION	Swell (%) Before Freeze/ Thaw Tests	FREEZE AND THAW TESTS			Swell (%) Before Wet/Dry Tests	WET AND DRY TEST		
		MAX. SWELL (%)	FAILURE	CYCLE AT WHICH FAILS		MAX. SWELL (%)	FAILURE	CYCLE AT WHICH FAILS
M5L5	0.3	2.15	YES	4	1.1	1.03	YES	13
M5L5(S)	0.4	0.94	YES	3	0.6	0.79	YES	2
M15L10	0.7	2.02	NO	-	1.5	1.40	YES	4
M15L10(S)	1.4	3.84	NO	-	0.6	20.10	YES	2
M15L15	0.4	2.39	YES	3	0.7	3.22	NO	-
M15L15(S)	1.8	4.91	YES	2	1.9	1.65	YES	5
M30L5	0.6	3.31	YES	9	0.2	8.17	NO	-
M30L5(S)	0.4	3.81	YES	16	0.2	2.71	YES	12
M30L10	0.4	3.65	NO	-	2	6.51	NO	-
M30L10(S)	1.0	11.80	NO	-	1.6	2.96	YES	16
M30L10(S)*	0.3	7.02	NO	-	0.3	13.86	YES	16
M30L15	1.1	4.68	YES	26	2	2.47	NO	-
M30L15(S)	1.2	2.40	YES	4	1.2	3.38	YES	16
K15L10	1.7	2.90	YES	14	0.6	10.10	YES	4
K15L10(S)	7.9	1.17	YES	4	7.4	2.44	YES	12
K15L10(S)*	11.2	1.37	YES	4	14.7	5.48	YES	9
K15L10(S)+Ba(1:1)	6.5	3.86	YES	15	0.6	7.15	NO	-
K30L10	0.4	4.72	YES	14	1.2	2.95	YES	3
K30L10(S)	10.6	3.36	YES	4	9.3	5.78	YES	3
K30L10(S)+Ba(1:1)	0.3	7.93	YES	14	1.2	4.94	NO	-
K30L10(S)+Ba(0.5:1)	0.9	8.09	YES	14	7.4	8.20	NO	-
K30L10(S)+Ba(0.2:1)	0.4	4.69	YES	14	0.7	9.52	NO	-
K30L15	0.7	0.58	YES	12	0.4	10.27	YES	4
K30L15(S)	12.9	2.97	YES	4	8.9	9.56	YES	1
K30L15(S)+Ba(1:1)	1.2	7.18	YES	14	1.1	4.26	NO	-

Both swell results and visual observations for quicklime treated specimens subjected up to a total of 36 cycles of durability testing, are summarized in Table 6. These specimens had been soaking in water, at room temperature, for 3 months prior to initiation of the durability testing. The specimen swell values attained before durability test initiation are also listed in Table 6. The maximum swell values, as reported in the adjacent column, were calculated by assuming zero swell at the beginning of the durability tests. They therefore represent the

maximum swell development during freeze/thaw or wet/dry cycling. However, significant swell development did not always translate in specimen failure. Specimen failure indicates that the specimens disintegrated or cracked, irrespective of the magnitude of swell development. Photographs showing both failed as well as intact specimens following the durability testing, are included in the durability section of the appendices.

The freeze/thaw results in Table 6 indicate many of the treated montmorillonite specimens developed negligible swell and kept intact throughout the duration of the durability tests. Moreover, specimen failure was never in the form of surface cracking. Specimen failure took place in the form of specimen mass loss due to surface pealing and deterioration. Specimens treated with 15% of quicklime and 7.5% of $Na_2SO_4 \cdot H_2O$ failed during the freeze/thaw tests, possibly due to the large amount of ettringite formation, leading to excessive swell pressure development. In fact, most of the mixes treated with quicklime and sodium sulfate, for which ettringite presence was confirmed, loosened and failed. Moreover, specimens treated at the highest level of quicklime addition (15%) but containing no sulfates also failed. However, these specimens resisted degradation for much longer times than the 15% quicklime-sulfate treated specimens. However, sulfate-bearing specimens treated with 10% of quicklime did not fail in spite of the significant swell development. Overall, during freeze/thaw testing, the addition of sulfates was detrimental leading to montmorillonite-sand specimen degradation, only at different than optimum levels of quicklime (i.e., 5% and 15%). All specimens treated at optimum quicklime content, i.e. 10%, kept intact following 36 cycles of freezing and thawing.

For kaolinite-sand specimens the story is quite different, as all specimens failed, at some point or another, during the 36 cycle freeze/thaw testing period. However, there is a definite effect of sulfate addition and subsequent ettringite formation on specimen durability. All kaolinite-sand specimens which were treated with barium hydroxide, or that did not contain sulfates, remained intact following the milder first set of 12 cycles of freeze/thaw testing. Conversely, all specimens that contained sulfates all failed during the first 4 cycles of freeze/thaw. This is attributed to the presence of weak cohesive forces in these specimens. Ettringite formation and subsequent swell development, prior to freeze/thaw test initiation, resulted in weakening of the specimen and substantial losses in cohesive strength levels.

As shown in Table 6, wetting and drying affected montmorillonite-sand specimens in a different way than freezing and thawing did. Specimens that did not contain sulfates remained intact throughout the test duration. Interestingly enough, all sulfate-bearing specimens failed irrespective of the other compositional attributes. Moreover, montmorillonite-sand sulfate-bearing specimen failures were mostly in the form of surface cracking, indicating some swell pressure development mechanism. Previous research (Dermatas, 1992) demonstrated the adverse effect of temperature and relative humidity changes on swell development of sulfate-bearing lime treated montmorillonite-sand soils, similar to the soils used during the present study. Even though ettringite

presence was confirmed for sulfate-bearing montmorillonite-sand specimens, no swell development was observed during regular swell testing. Wet and dry durability results indicated such testing conditions were more amenable to ettringite-induced swelling for the specimens tested.

For kaolinite-sand specimens wetting and drying had lesser of an impact to specimen durability than freezing and thawing did. For sulfate-bearing specimens this was expected as failure had already taken place during the three month period of regular swell testing. Specimens with no sulfates failed due to the weak cohesive force development as already evidenced by their low strength values (Figure 43). All barium pretreated sulfate-bearing specimens remained intact during wetting and drying. This further demonstrated the effectiveness of the barium hydroxide pretreatment in eliminating ettringite formation and subsequent specimen swelling and deterioration.

A closer look at some of the durability test results further illustrates the importance of both sulfate presence and cohesive strength development on the specimen structural integrity under accelerated weathering conditions. In Figure 53, the swell development for the 30% montmorillonite 70% sand untreated, quicklime treated and quicklime-sulfate treated specimens is shown as a function of elapsed testing cycles. The untreated specimen swelled excessively immediately upon soaking. This was expected since montmorillonite clays are known to be very expansive when brought in contact with water. However, the addition of 10% quicklime was effective in eliminating excessive swell development throughout the test duration. The presence of sulfates seems to lead to some swell development, picking up following the 22nd freeze/thaw cycle. However, such swell development was not accompanied by any visible signs of specimen deterioration.

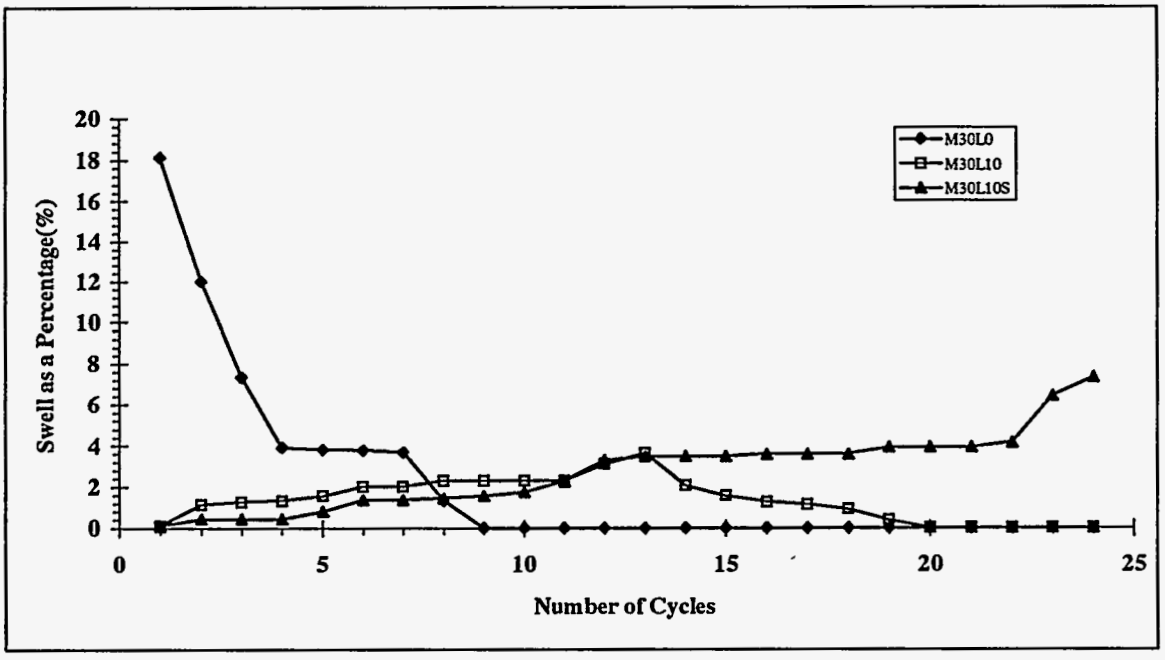

Figure 53. Effect of Freeze and Thaw Cycles on the Swell of M30-mixes.

For kaolinite (30%)- sand (70%) specimens, the story was quite different, as it can be seen in Figure 54. Specimens did not develop excessive swell during the freeze/thaw cycling, but they all failed somewhere in between 12 and 15 cycles of freezing and thawing. The sulfate-bearing specimen (K30L10S) failed first, and the other specimens followed. The limited swell development and early sudden failure that is characteristic of the kaolinite-sand specimens, signifies the inadequate levels of cohesive strength development, as was also evidenced by the strength test results (Figure 43).

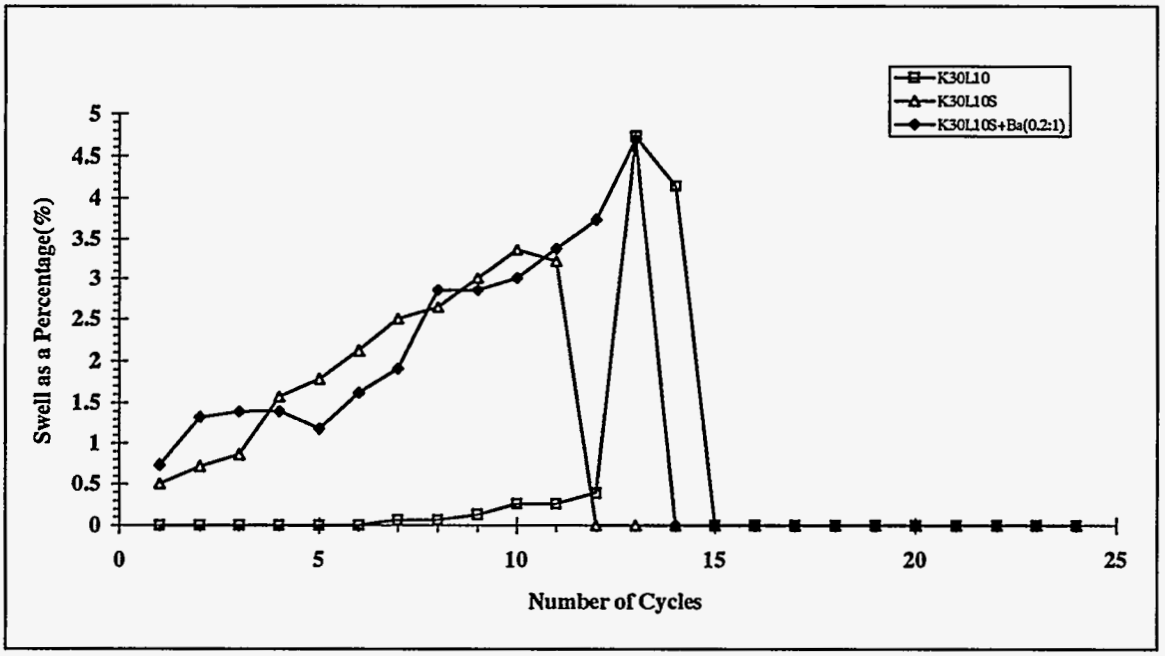

Figure 54. Effect of Freeze and Thaw Cycles on the Swell of 30% of Kaolinite-sand Mixes.

The swell development in montmorillonite specimens containing 30% of clay are plotted in Figure 55, as a function of elapsed wet/dry cycles. The untreated specimens showed significant swell after the first cycle of wet/dry. When these untreated specimens were subjected to additional wet/dry cycles, the swell reading decreased as the result of further specimen disintegration. Both M30L10 and M30L10S specimens developed approximately 2% swell during the first 12 cycles of wet/dry tests. After the first 12 wet/dry cycles, the swell of M30L10 specimen increased gradually under the more severe drying conditions (110°C), but was not accompanied by specimen failure. Conversely the M30L10S specimen failed after 4 cycles of the severe wet/dry tests (total 16 cycles).

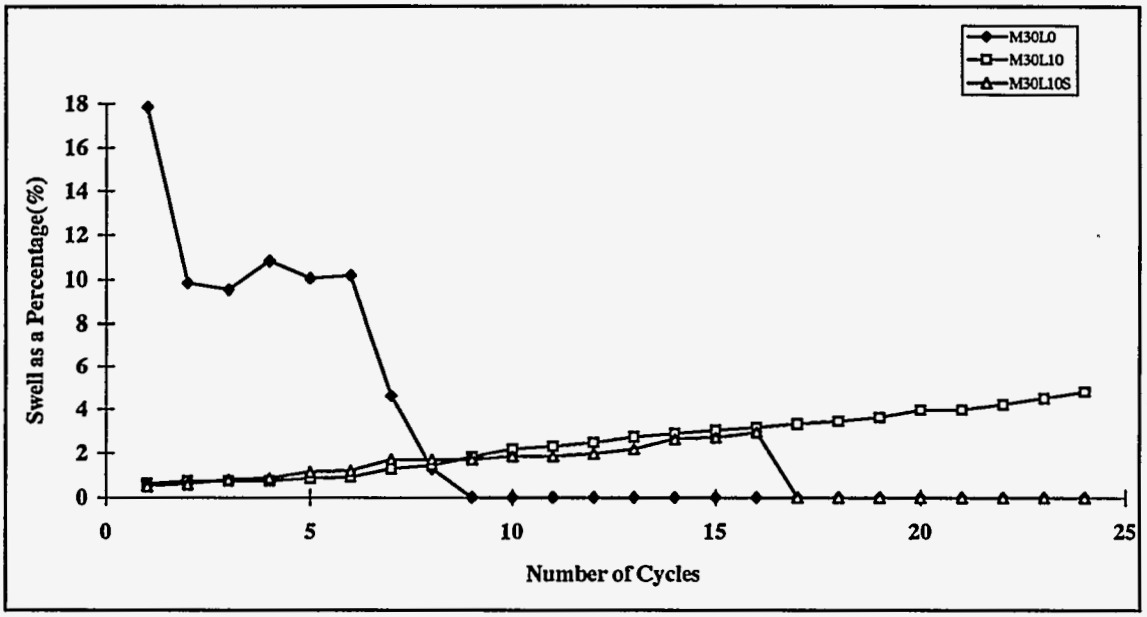

Figure 55. Effect of Wet and Dry Cycles on the Swell of M30-mixes

Both quicklime treated kaolinite-sand specimens (K30L10 and K30L10S) developed 3% to 5.5% swell during the first 12 cycles of milder conditions of wet/dry testing (Figure 56), but did not fail. However, both of these specimens failed in the first cycle of the severe, second set of wet/dry testing. Upon barium hydroxide addition to the treated specimen, the swelling of the kaolinite mixes was reduced to less than 5% swell after 24 cycles of testing. Moreover, the barium hydroxide pretreated specimen remained intact throughout the wet/dry test duration.

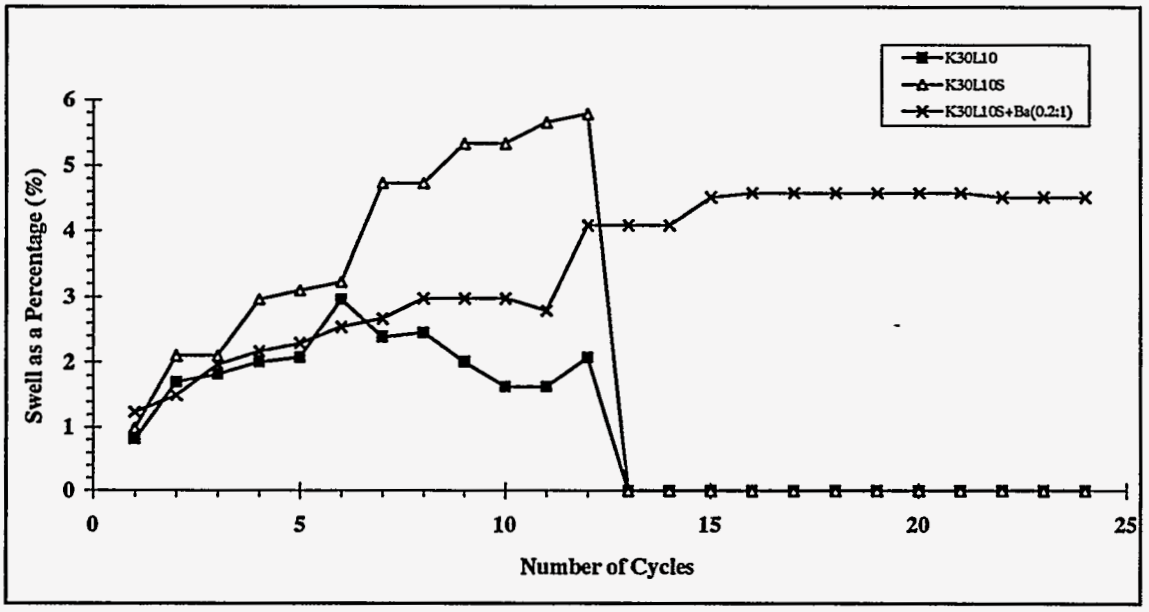

Figure 56. Effect of Wet and Dry Cycles on the Swell of K30-mixes.

4.4.2 *Effect of Fly Ash Addition on Specimen Durability*

Following a 3 month soaking period, low clay content (5%) specimens having been treated using both quicklime and fly ash, were also subjected to both freeze/thaw and wet/dry durability cycling. This was done in order to assess the possible effect of fly ash addition to specimen durability. The testing conditions were identical with the conditions that the montmorillonite-sand specimens were subjected to, as outlined in the previous section. As it can be seen in Figure 57, all clay-sand quicklime/fly ash treated specimens withstood the severe freeze/thaw conditions without any obvious signs of specimen failure. Interestingly enough, all specimens developed some limited magnitude of vertical swell, which however, was not accompanied by any signs of physical deterioration. Swell development was less pronounced for specimens to which sulfates were added. Most likely, the observed swell was a direct response of the solid matrices to ice formation during freezing, and not to ettringite-induced deformations.

The effect of wet/dry on the quicklime/fly ash treated kaolinite- and montmorillonite-sand specimens is depicted in Figure 58. As it can be seen, wetting and drying cycles lead to some swell development, but more importantly, to kaolinite-sand specimen failures. Following approximately 12 to 15 wet/dry cycles, all kaolinite-sand specimens failed. No obvious explanation for such behavior has been drafted to this date. Conversely, in spite of some limited swell development, all montmorillonite-sand specimens withstood the wet/dry weathering conditions. These results suggest that the montmorillonite-sand specimens were more resistant to the wet/dry weathering than the kaolinite-sand specimens. They also suggest that wetting and drying conditions are more critical than freezing and thawing, with respect to fly ash treated specimen durability.

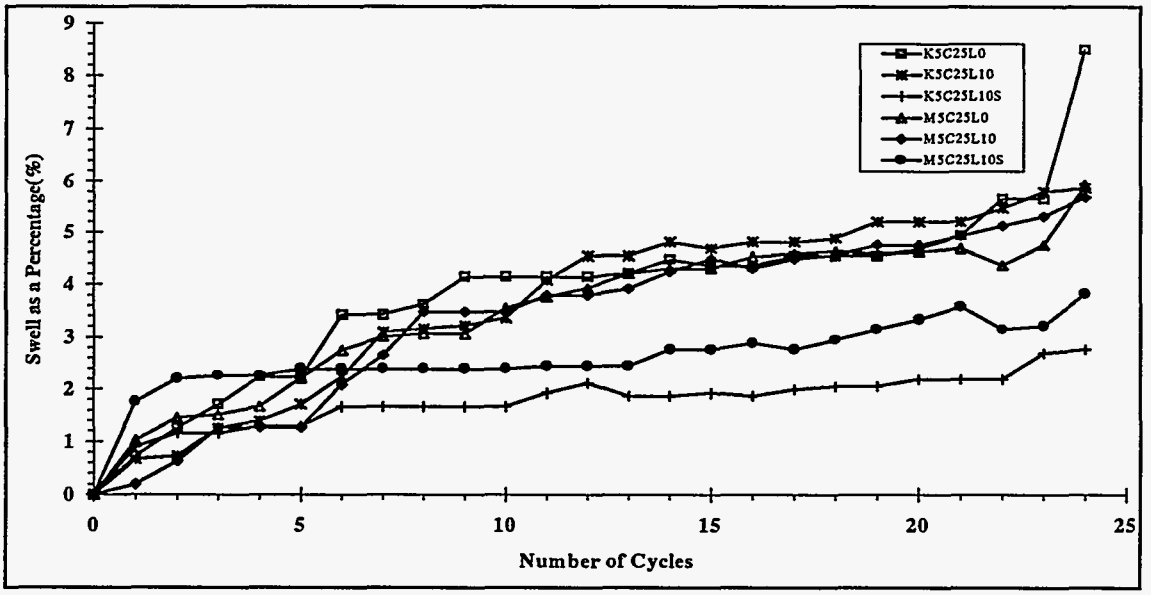

Figure 57. Effect of Freeze and Thaw Cycles on the Swell of K5C25 and M5C25 Mixes.

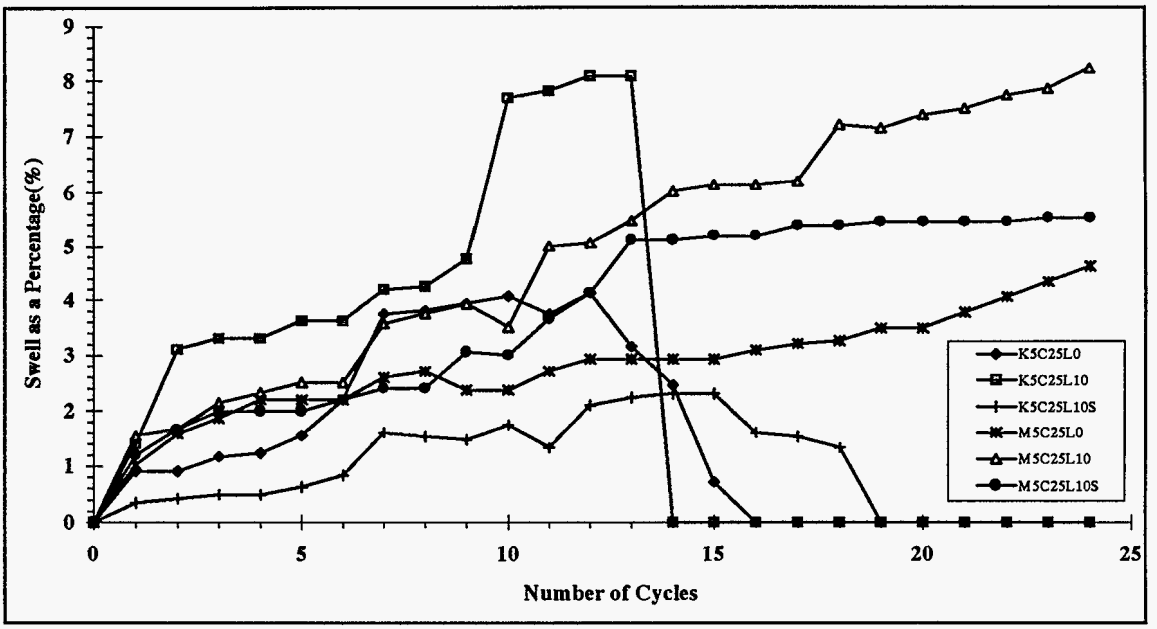

Figure. 58. Effect of Wet and Dry Cycles on the Swell of Mixes with Fly Ash (class C).

4.4.3 Summary

Specimen durability is a strong function of the specimen mix compositional attributes. Montmorillonite-sand specimens were more resistant to the severe weathering conditions than the kaolinite-sand specimens, following treatment application. The development of strong cohesive forces within the montmorillonite-sand matrix, signified by high values of specimen strength, successfully restrained any swell tendencies due to the aggressive temperature and relative humidity changes. Moreover, the presence of sulfates and the subsequent formation of the expansive mineral ettringite, may adversely affect the specimen structural integrity during wetting and drying, more so than during conventional swell testing. Most quicklime treated clay specimens and the quicklime/fly ash treated clay specimens could withstand the moderate wet/dry and freeze/thaw conditions without any signs of specimen deterioration. The kaolinite-sand sulfate-bearing specimens which were subjected to the barium hydroxide pretreatment scheme, successfully withstood the 36 cycles of wet/dry and the first 14 cycles of freeze/thaw. This further demonstrated the effectiveness of the barium pretreatment scheme in controlling ettringite-induced swelling and specimen deterioration. Overall, only a few quicklime treated clay specimens and the quicklime/fly ash treated montmorillonite specimens could withstand the severe weathering conditions without disintegration. However, the severe weathering conditions used during testing, temperature changes from -15°C to 22°C within a few hours during freeze/thaw and an 110°C drying temperature for wet/dry, are not likely to occur in natural environments. These destructive tests were mainly used to evaluate the durability of the treated specimens in a timely fashion.

4.5 Heavy Metal Release from Monolithic Solids under Static Leaching Conditions

The TCLP results, as already discussed in previous sections, have demonstrated that the quicklime-based treatment was effective in immobilizing As, Cr, and Pb. However, the TCLP testing and extraction conditions are quite different than the leaching scenarios the treated solids will experience in the real world. When a low permeability compacted waste form is subjected to hydraulic flow conditions, it is most likely that only the outer surface of the monolithic solid will interact with water or any other leachant. Under such circumstances it is generally expected that diffusion through the solid matrix will be the main mechanism of contaminant release.

To understand the leaching behavior of the quicklime treated solids under such moderate leaching conditions, a static leaching test program was designed and undertaken in our laboratory facilities. More specifically, the American Nuclear Society (ANS 16.1, 1986) static leaching procedure for hazardous wastes was modified and used to simulate diffusion-controlled conditions. During this leaching test, compacted specimens with 4.70±0.05 cm diameter by 4.0±0.4 cm height were used. After the specimens were cured for 28 days, they were immersed in distilled water for 30 seconds to rinse out any loose particles from the specimen surface. A Nylon mesh harness was used to support each specimen near the centroid of approximately 950 mL of the acetic acid solution (0.014 N, pH = 3.45) in a polyethylene container. The leachant volume to the specimen's external surface ratio was maintained at 10±0.2 cm. During the experiment, the leachant was replaced at designated time intervals (2, 7, 24, 48, 72, 99, 456, 1128, and 2160 hours). Throughout the test duration heavy metal concentrations in the leachate were measured and pH changes were recorded.

4.5.1 Cumulative Release of Heavy Metals

Based on the static leaching results, the cumulative leachability, expressed as the percentage of heavy metals released over the total amount present in each specimen, was calculated. The release data in Figure 59 suggests that under static leaching conditions, significant amounts of As were released from the untreated montmorillonite (15%)-sand specimen. The amount of As released increased with increasing leaching time. After 90 days of leaching, more than 30% of the As in the solid was released. On the other hand, quicklime treatment significantly reduced the leachability of As (Figure 59). Approximately 2% of As was leached out from the treated specimens during the first 4 days of leaching. No further release of As was observed for the treated specimens. The release behavior of Cr and Pb from the untreated montmorillonite specimens (Figures 60 and 61) was quite different than that for As. For both heavy metals, significant levels of release were observed during the first day of leaching. This means the 20% Cr and 40% Pb were readily extractable under the static leaching conditions. In contrast to the leaching results for the untreated specimens, negligible Cr and Pb were leached out from the treated specimens.

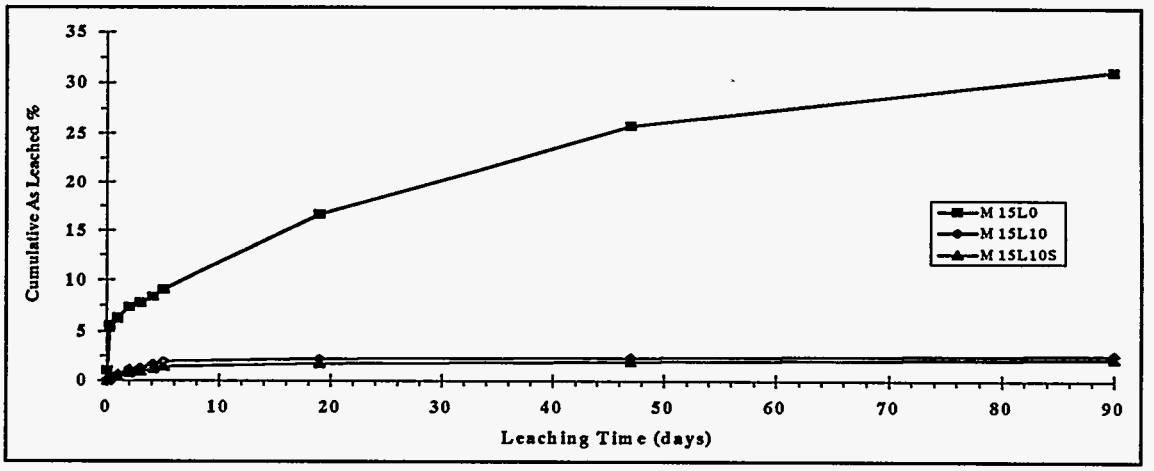

Figure 59. Effect of Quicklime Treatment (with and without sulfates) on As Release from Montmorillonite (15%) Mixes during Static Leaching.

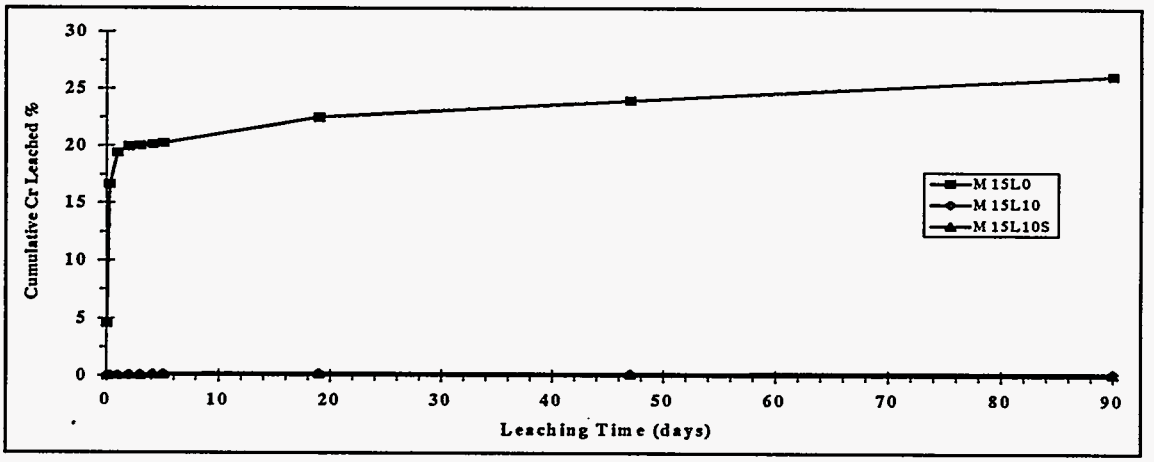

Figure 60. Effect of Quicklime Treatment (with and without sulfates) on Cr Release from Montmorillonite (15%) Mixes during Static Leaching.

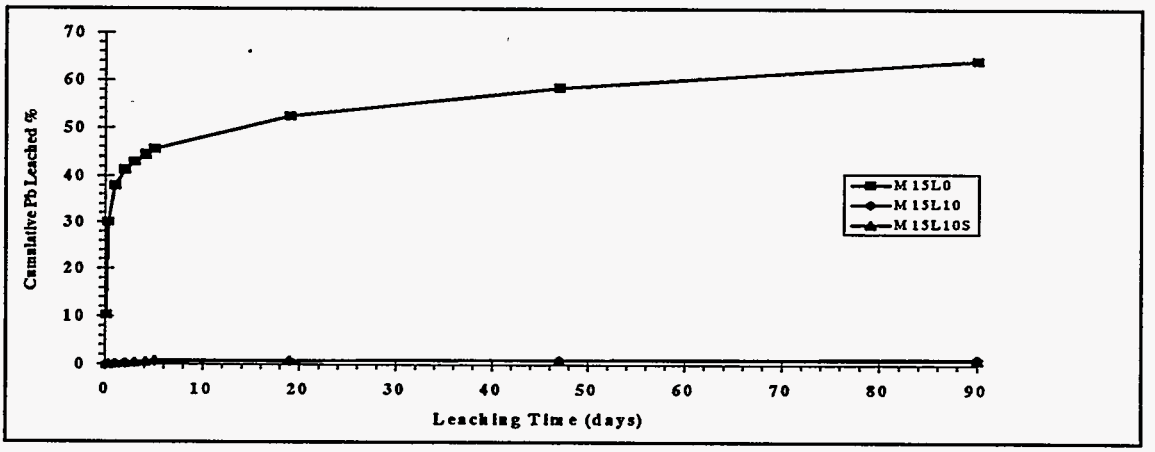

Figure 61. Effect of Quicklime Treatment (with and without sulfates) on Pb Release from Montmorillonite (15%) Mixes during Static Leaching.

The results in Figures 62 and 63 show As and Cr release from kaolinite (15%) specimens was also effectively eliminated by quicklime treatment. There are only two points presented for the untreated specimens since testing was discontinued following 7 hours of soaking, owing to specimen disintegration. Conversely, the amount of Pb released from the treated kaolinite-sand specimens was relatively high (Figure 64), indicating treatment ineffectiveness. These results agree with the TCLP data which indicated that Pb in low kaolinite content (5 and 15%) specimens could not be immobilized effectively by the quicklime-sulfate treatment. These relatively high levels of Pb release warranted some additional testing aimed at the reduction of Pb release. During these additional tests, the kaolinite content was increased or fly ash was added to the specimen mixes.

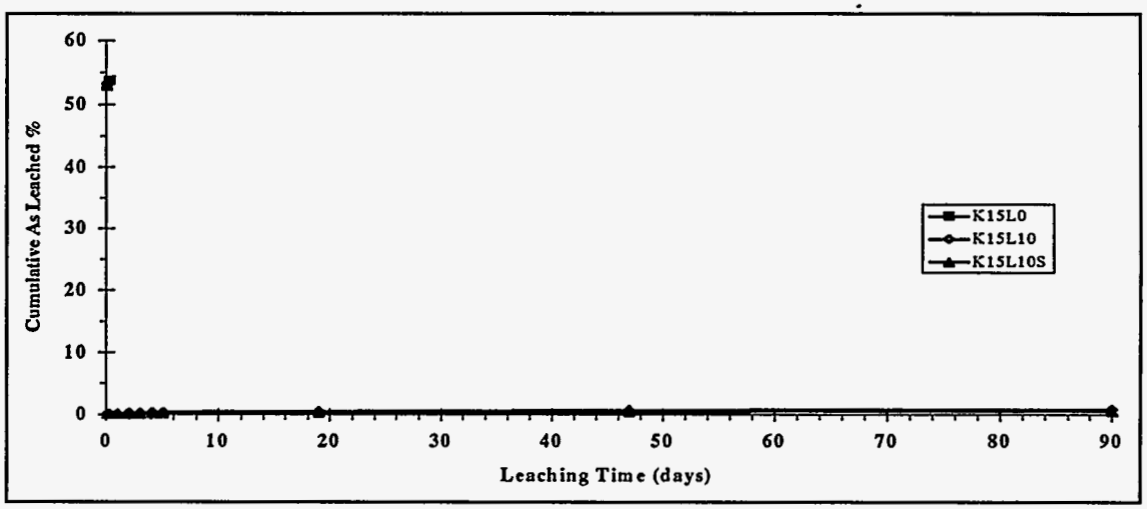

Figure 62. Effect of Quicklime Treatment (with and without sulfates) on Arsenic Release from Kaolinite (15%) Mixes during Static Leaching.

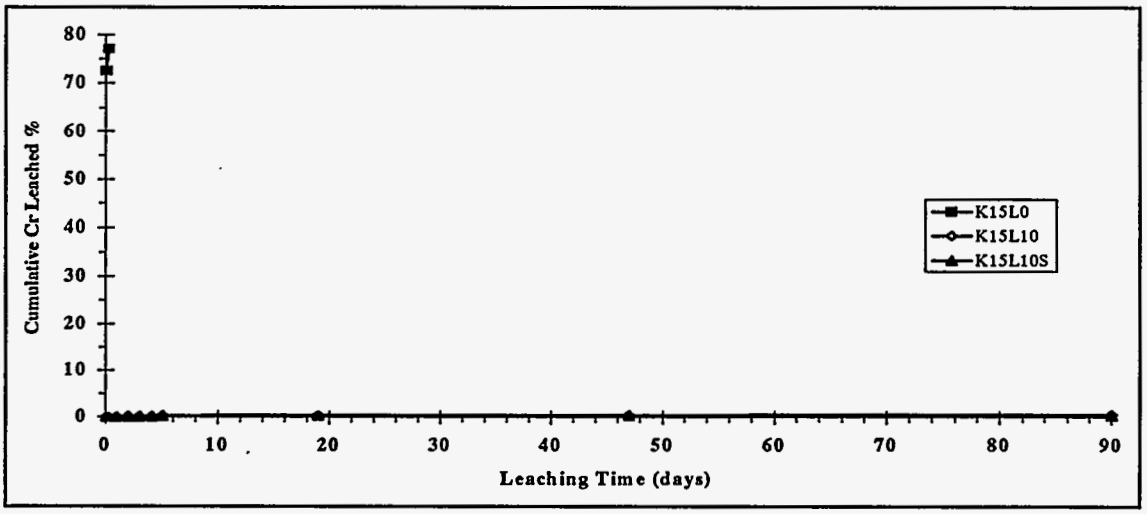

Figure 63. Effect of Quicklime Treatment (with and without sulfates) on Chromium Release from Kaolinite (15%) Mixes during Static Leaching.

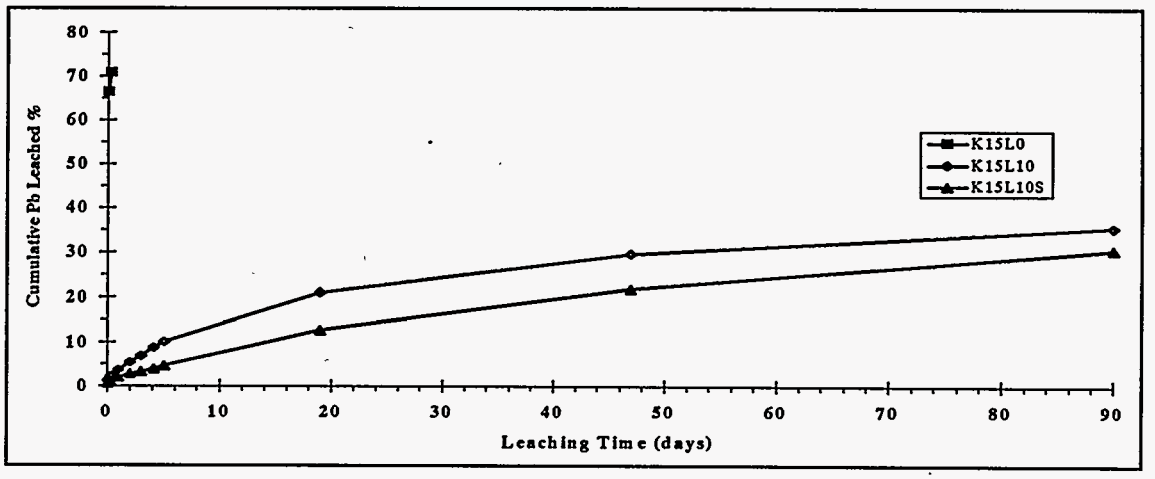

Figure 64. Effect of Quicklime Treatment (with and without sulfates) on Lead Release from Kaolinite (15%) Mixes during Static Leaching.

The clay content and fly ash presence effect on Pb release is illustrated in Figure 65 for kaolinite-sand specimens. When the kaolinite content increased from 15% to 30%, Pb leachability showed a six-fold decrease. Moreover, 5% kaolinite-sand specimens treated with 25% of fly ash attained significantly lower Pb release levels than the K30L10 specimens, limiting release to less than 1% of the total amount of lead present in the specimen.

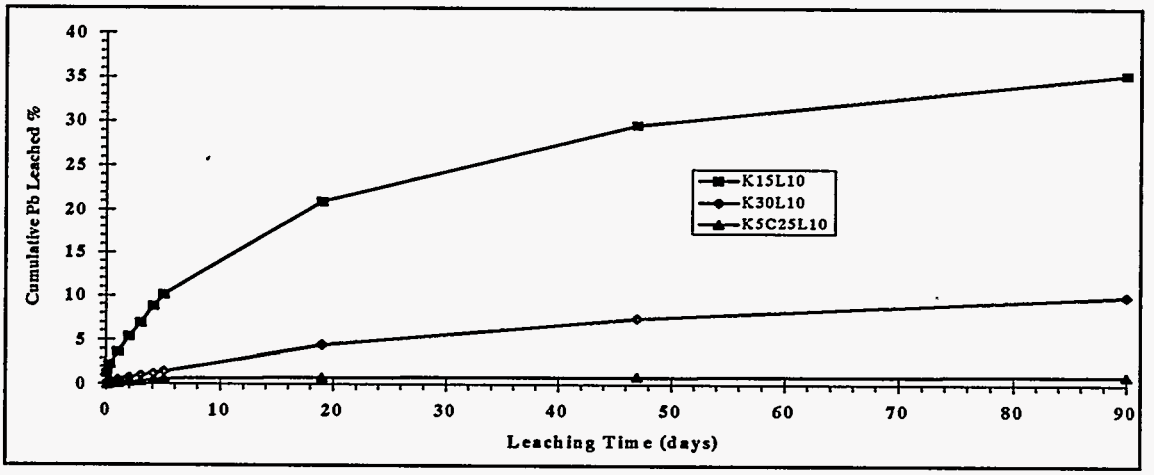

Figure 65. Effect of Kaolinite Content and Fly Ash on Lead Release from Quicklime Treated (10%) Mixes, Static Leaching Test.

Similar to lead release, increasing the kaolinite content or adding fly ash to the specimen resulted in further reductions of the release of Cr (not shown here), which however, was very low to begin with. Conversely, the release of As from quicklime/fly ash treated specimens was higher than that from the quicklime

treated specimens (Figure 66). Moreover, the increased kaolinite content (K30L10) specimens showed higher As release than the lower clay content (K15L10) specimens. Again with As, as was the case with Cr, levels of release were very low irrespective of the specimen compositional attributes. Similar results (not presented here) were obtained for montmorillonite-sand specimens, however, release levels were much lower than kaolinite-sand specimens.

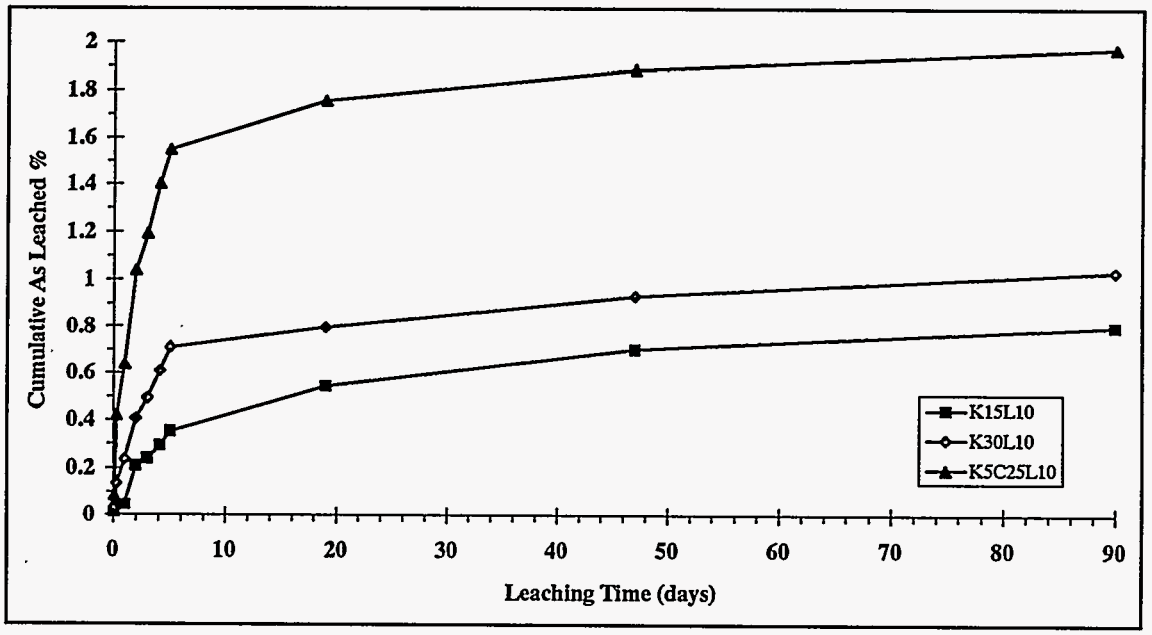

Figure 66. Effect of Kaolinite Content and Fly Ash on Arsenic Release from Quicklime Treated (10%) Mixes, Static Leaching Test.

Thus far we have been expressing heavy metal release as a percentage of the total metal content. However, heavy metal concentration levels in the leachate are also important to be considered, especially when assessing the overall impact of heavy metal contamination to the surrounding environment. The static leaching results in Figure 67 indicate that the As concentration in the leachate for the untreated montmorillonite specimen was approximately 1,000 ppb. The quicklime treatment reduced the As concentration to less than 80 ppb, a more than ten-fold concentration reduction. Moreover, a two order of magnitude reduction in Cr leachate concentrations was achieved by quicklime treatment application(Figure 68). When the untreated specimen came in contact with the acetic acid leachant, Cr concentrations reached approximately 50,000 ppb in the leachate. Conversely, Cr concentrations in the leachate for all treated specimens were always lower than approximately 300 ppb. Quicklime treatment reduced Pb concentrations in the leachate from 100,000 ppb to approximately 1,000 ppb (Figure 69). Similar results were observed for kaolinite-sand specimens (results are not presented here).

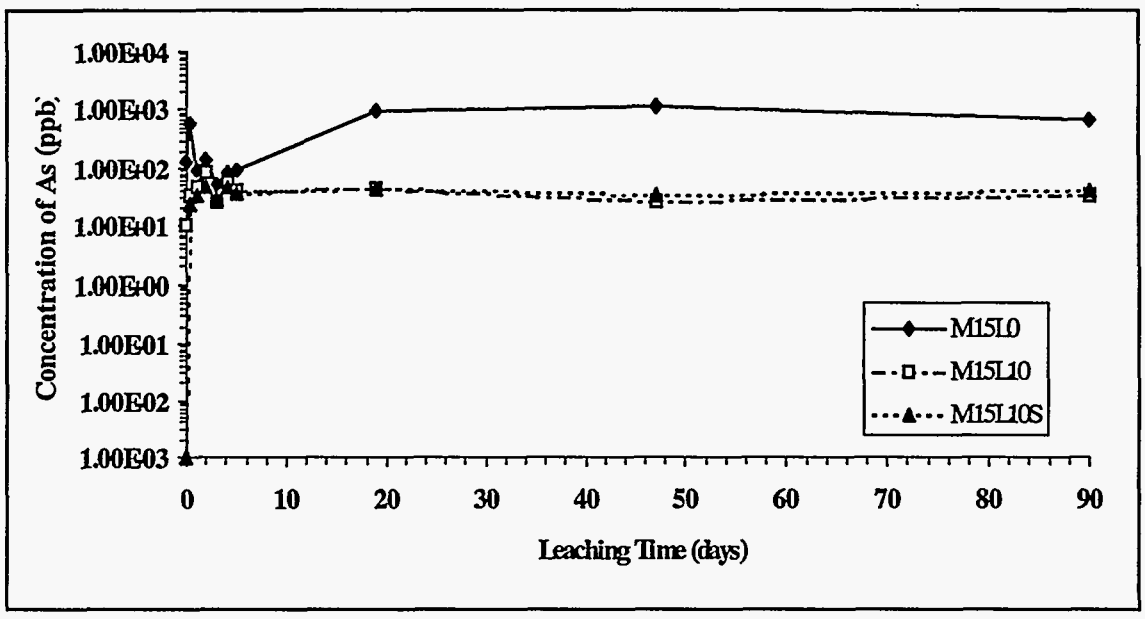

Figure 67. As Concentrations in the Leachate under Static Leaching Conditions, Montmorillonite(15%)-sand Mixes.

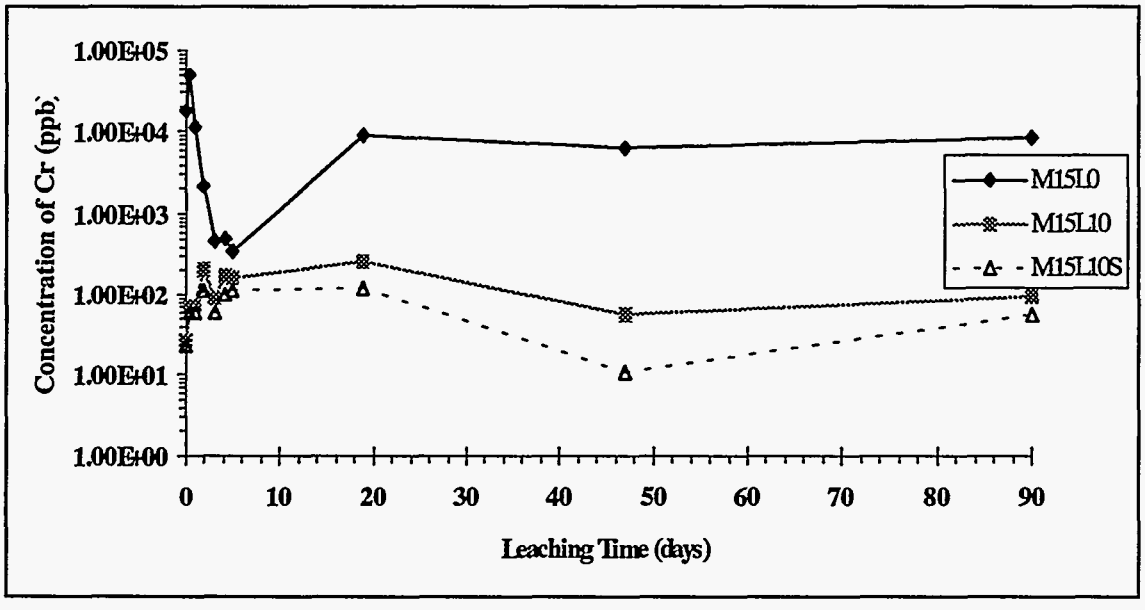

Figure 68. Cr Concentrations in the Leachate under Static Leaching Conditions, Montmorillonite(15%)-sand Mixes.

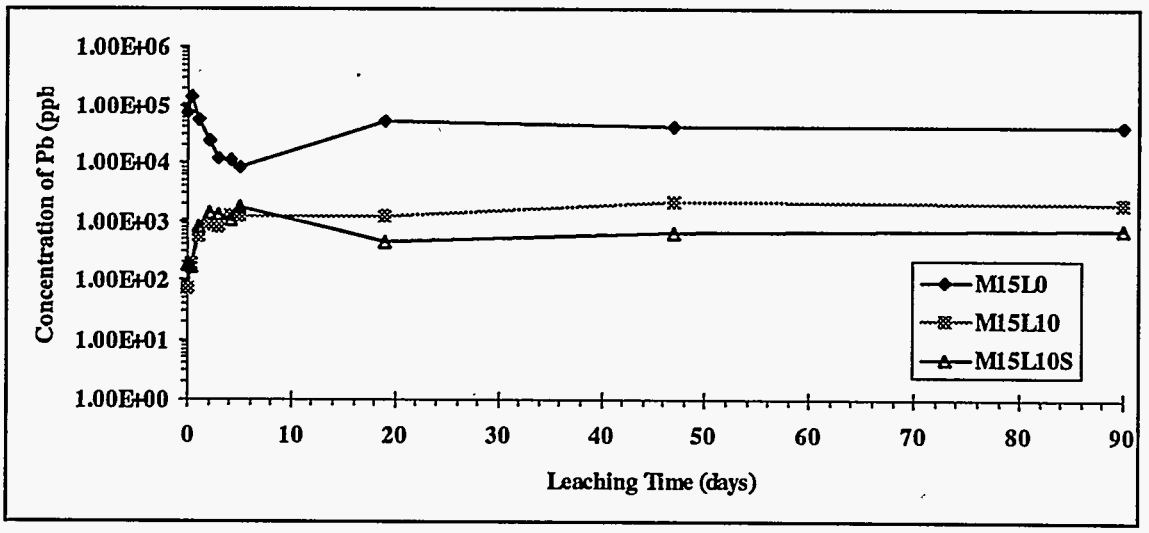

Figure 69. Pb Concentrations in the Leachate under Static Leaching Conditions, Montmorillonite(15%)-sand Mixes.

4.5.2 *Transport of Heavy Metals from Solid to Solution*

To elucidate the mechanisms controlling heavy metal release from the treated soils, the data obtained from the static leaching experiments was further evaluated using a diffusion model (Crank, 1975). The specific model was derived based on diffusion from a product with semi-infinite dimensions, and was used to evaluate the release process of heavy metals from the quicklime-treated specimens. Since in our diffusion-controlled leaching experiments, the amount of heavy metals release was much less than total amount of heavy metals present in each specimen, our leaching system can be safely assumed to be similar to a specimen with semi-infinite dimensions. For a solid specimen with uniform heavy metal distribution, under diffusion-controlled leaching (or tank leaching) conditions, the concentration in the solid-solution interfacial region can be described by Equation 1 (Crank, 1975):

$$\frac{C - C_1}{C_0 - C_1} = erf \frac{x}{2 \cdot \sqrt{(D \cdot t}} \qquad (1)$$

where, $C(x,t)$ = the concentration as function of place and time, C_1= the concentration at x=0 (surface), C_0= the initial concentration at t=0 in the product (uniformly distributed), D= the diffusion coefficient, t= the time, x= the distance to surface (positive values), and *erf*= the standard error function.

When the solution is not perfectly mixed, the concentration near the solid surface can be significantly higher than zero, especially for the diffusion-controlled leaching experiment in which the solution is under static conditions. According to Groot and van der Sloot (1992), the upper limit of C_1 will be $\frac{1}{2} \cdot C_0$ because diffusion in the leachate is at least as fast as diffusion in the solid.

The resulting diffusion equation from Equation 1 for the boundary conditions $C_1=1/2C_0$ is:

$$D_e = \frac{\pi \cdot B_t^2}{t \cdot (U_{max} \cdot d)^2} \qquad (2)$$

or

$$B_t = U_{max} \cdot d \cdot \sqrt{(D_e/\pi)} \cdot \sqrt{t} \qquad (2b)$$

where D_e= the effective diffusion coefficient for component x in m^2/s, B_t= the cumulative maximum release of the component in mg/m^2, t= the contact time in seconds, U_{max}= the leachable quantity in mg/kg (= availability f times total concentration in product)., d= the bulk density of the product in kg/m^3.

Equation 2b can be transformed to a logarithm form:

$$\log(B_t) = 1/2 \cdot \log(t) + \log[U_{max} \cdot d \cdot \sqrt{(D_e/\pi)}] \qquad (3)$$

The type of leaching mechanism which controls the heavy metal release can be determined by looking at the slope of $\log(B_t)$ versus $\log(t)$ line. If the slope of the curve is 0.5, the release of heavy metals will be slow and can be described by the diffusion model. According to Groot and van der Sloot (1992), a slope of 1 for $\log(B_t)$ versus $\log(t)$ line indicates a dissolution process. This is because the dissolution of material from the surface proceeds faster than diffusion through the pores of the matrix. In some other cases, the surface of the solid is covered with a layer of relatively soluble material. Most of the soluble material on the surface will be dissolved in the initial phase of the leaching experiment. This phenomenon is called surface washoff, and the process typically results in a slope of 0.0 the release-time plot. In many cases, the subsequent to surface washoff release is diffusion controlled. Both dissolution and surface washoff will result from the dissolution of relatively highly soluble materials and will lead to high levels of heavy metal release. However, during the dissolution process the material will not be depleted during the leaching experiment.

The cumulative release of As, Cr and Pb from untreated, quicklime treated and quicklime-sulfate treated specimens containing 15% of montmorillonite is plotted as a function of leaching time in Figures 70 to 72 (in logarithmic scales). A regression analysis shows a high linear correlation between $\log(B_t)$ and $\log(t)$ for all the specimens. The slopes of the linear lines are between 0.4 and 0.6 for all the treated specimens, except for Pb release from M15L10 where the slope is slightly higher. Overall, the results indicate the release of As, Cr, and Pb from the quicklime treated specimens is mainly controlled by diffusion. It has been reported that in most pozzolanic-based materials, the leaching process should be diffusion controlled for treatment to be considered effective (Groot and van der Sloot, 1992).

In contrast to the slope values for the treated specimens, the slopes of $\log(B_t)$ versus $\log(t)$ curves for Cr and Pb release from the untreated specimens (M15L0, Figures 71 and 72) are approximately 0.2. This implies that the release of Cr and Pb was mainly controlled by surface washoff of relatively soluble metal oxides or hydroxides. However, a slope value of 0.42 suggests As release from M15L0 was mainly controlled by a diffusion process (Figure 70). This is because the solubility of As_2O_3 used as the As contaminant source is very low. In separate solubility experiments, the obtained experimental results indicated the solubility of As_2O_3 is lower than 1 ppm of As, when the solution pH is between 5 and 11. Similar results were obtained for kaolinite-sand specimens but are not presented herein.

In Figures 73 to 75, the cumulative release of As, Cr, and Pb from quicklime treated specimens containing 15%, 30%, and 5% montmorillonite and 25% class C fly ash is plotted as a function of leaching time. Increasing the amount of clay content or adding fly ash to the solid mix results in slope values of 0.5 or so, indicating heavy metal release is still controlled by molecular diffusion. Similar results were obtained for kaolinite-sand mixes but are not presented herein.

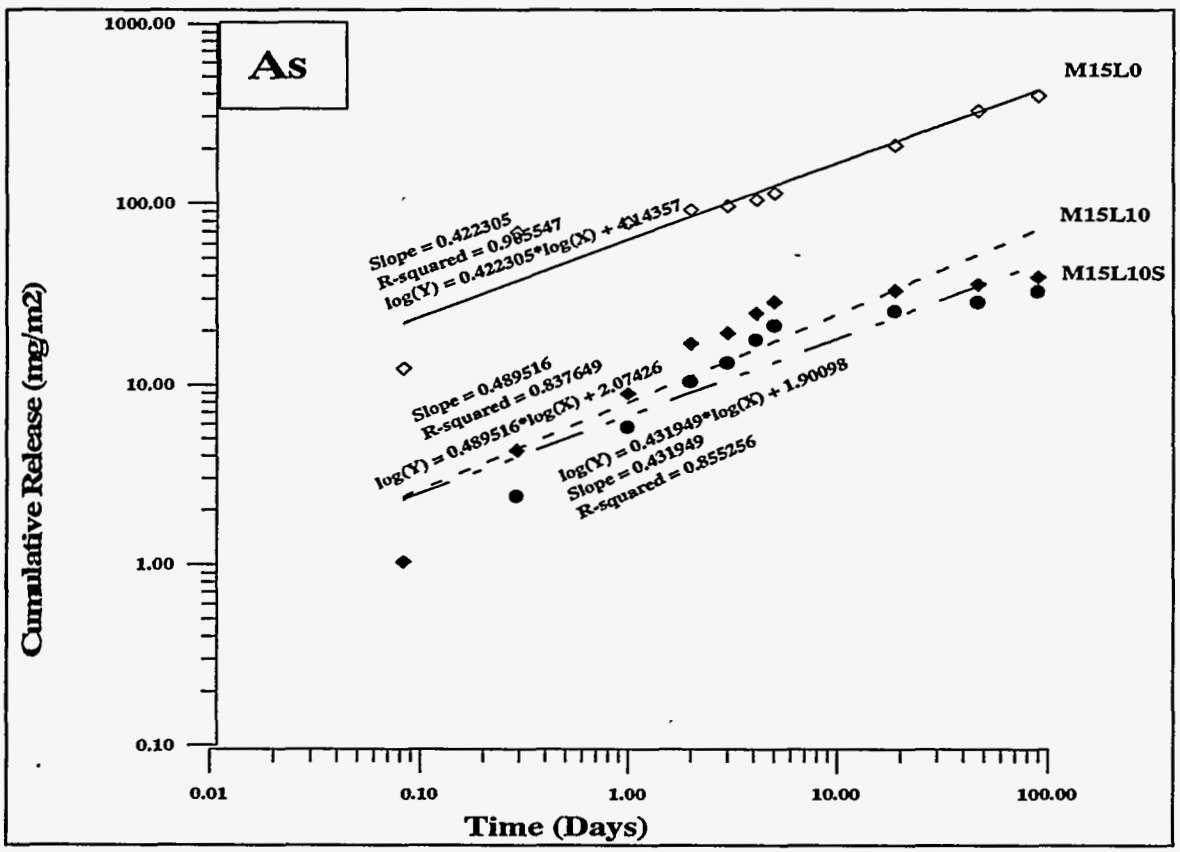

Figure 70. Linear Regression Analyses of Static Leaching Results for Arsenic Release from Montmorillonite (15%) Mixes.

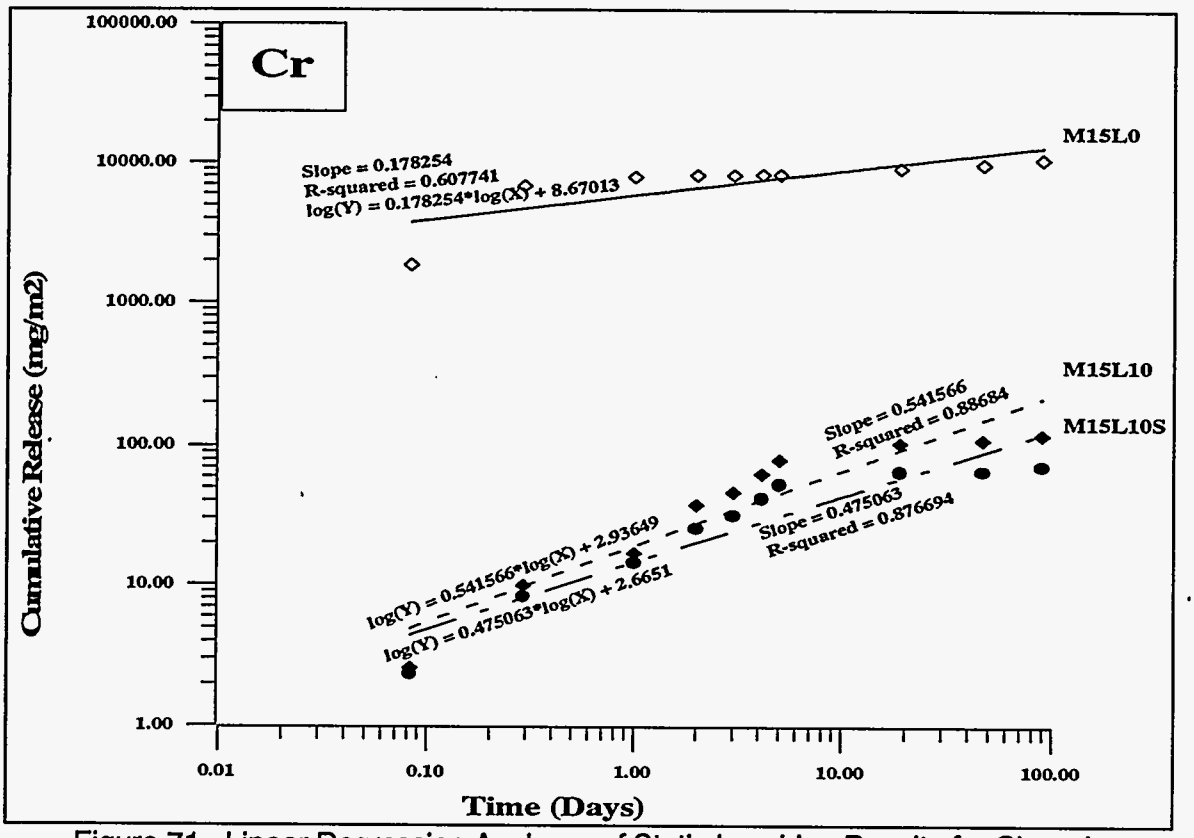

Figure 71. Linear Regression Analyses of Static Leaching Results for Chromium Release from Montmorillonite (15%) Mixes.

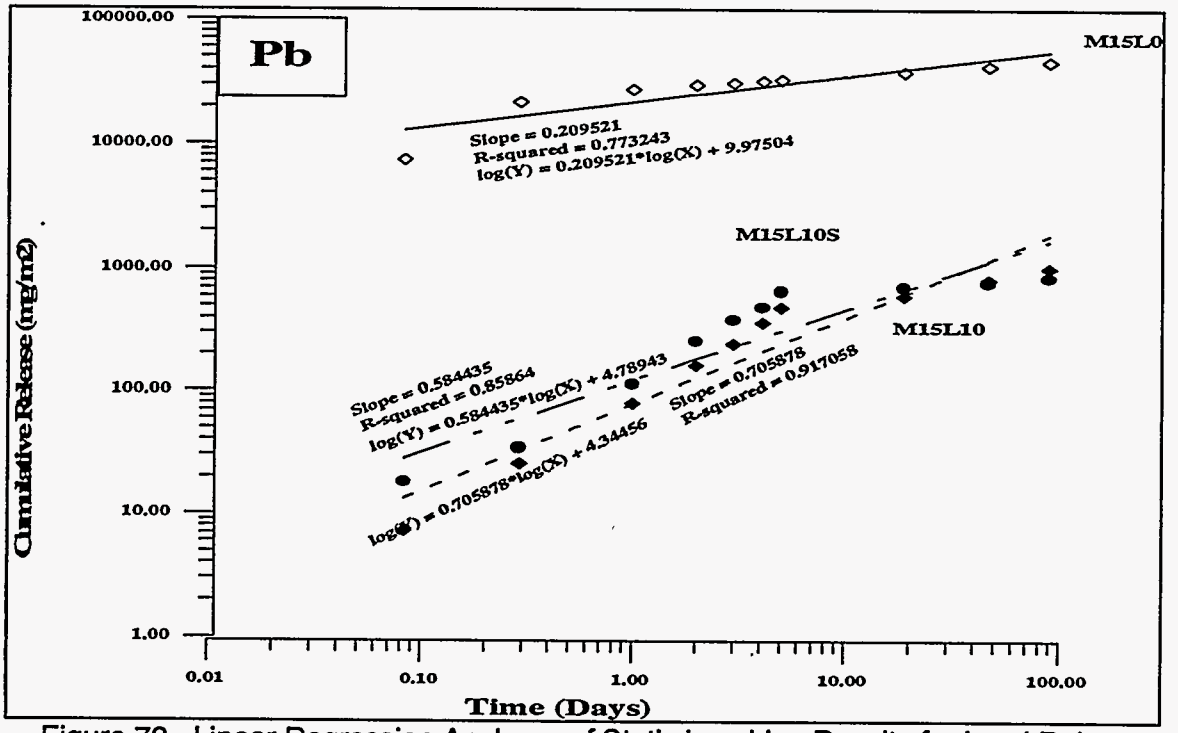

Figure 72. Linear Regression Analyses of Static Leaching Results for Lead Release from Montmorillonite (15%) Mixes.

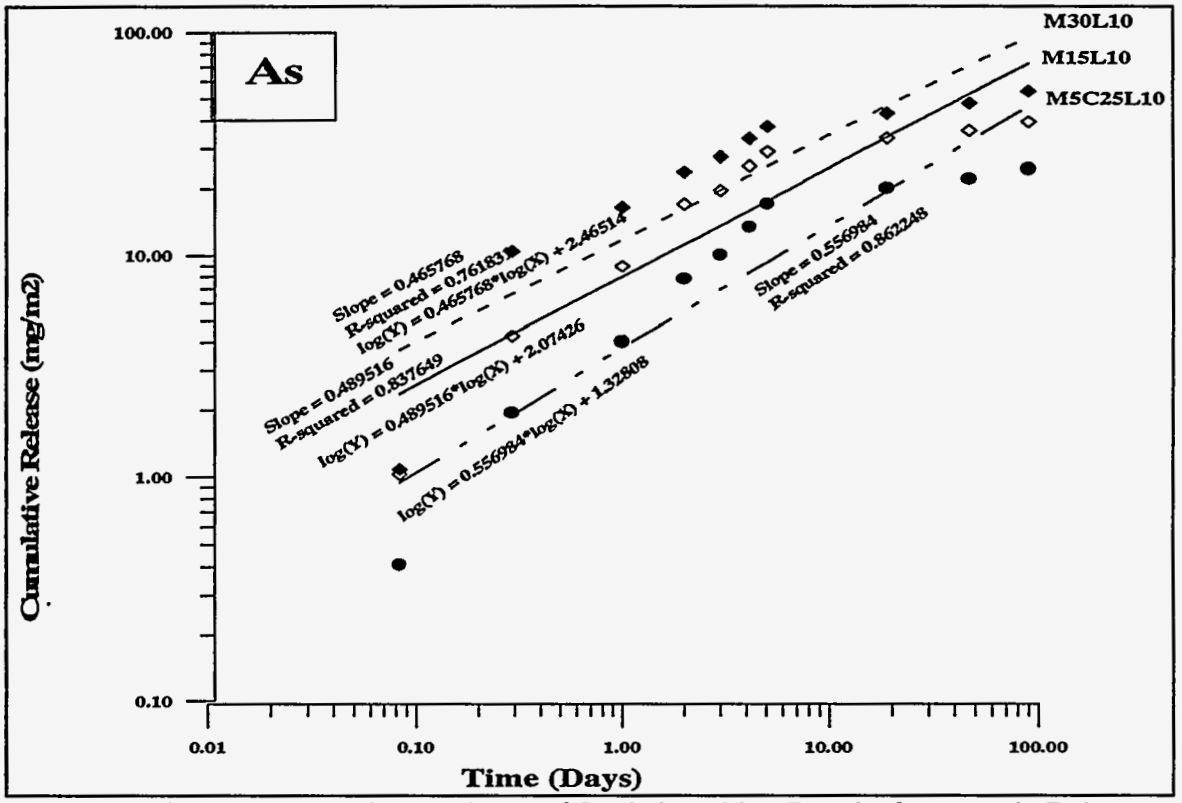

Figure 73. Linear Regression Analyses of Static Leaching Results for Arsenic Release from Montmorillonite-lime Mixes.

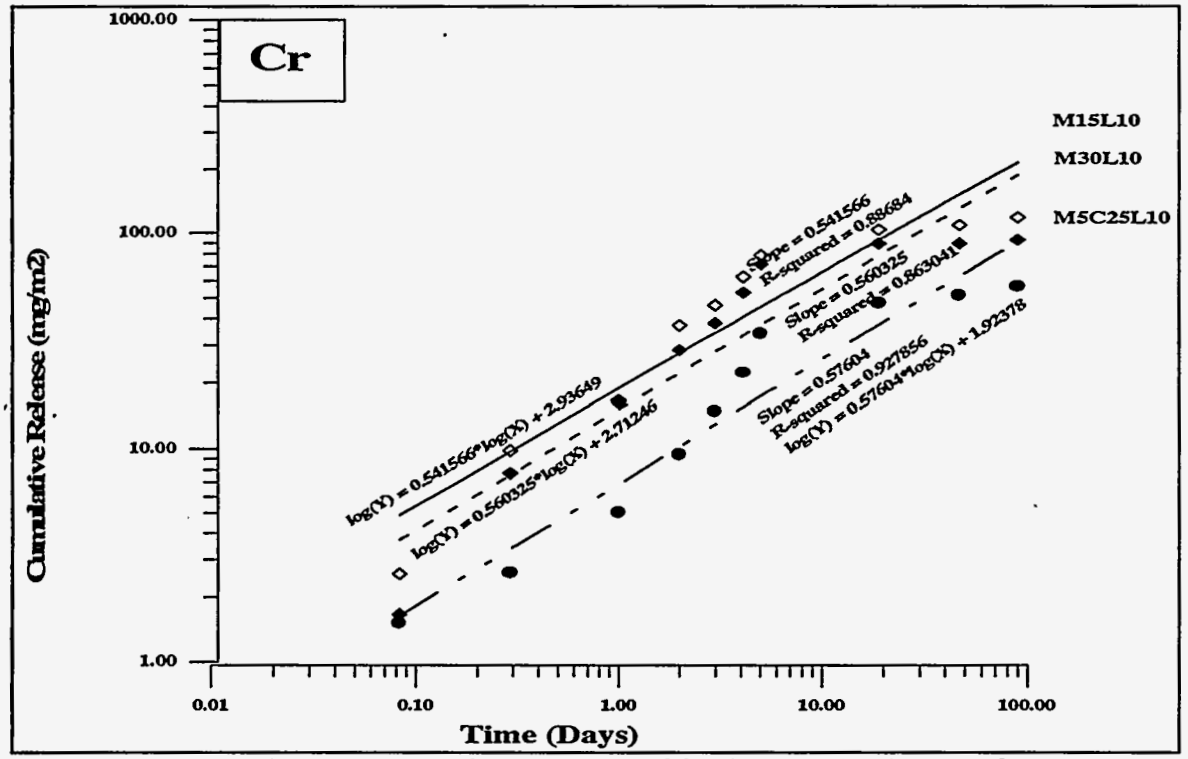

Figure 74. Linear Regression Analyses of Static Leaching Results for Chromium Release from Montmorillonite-lime Mixes.

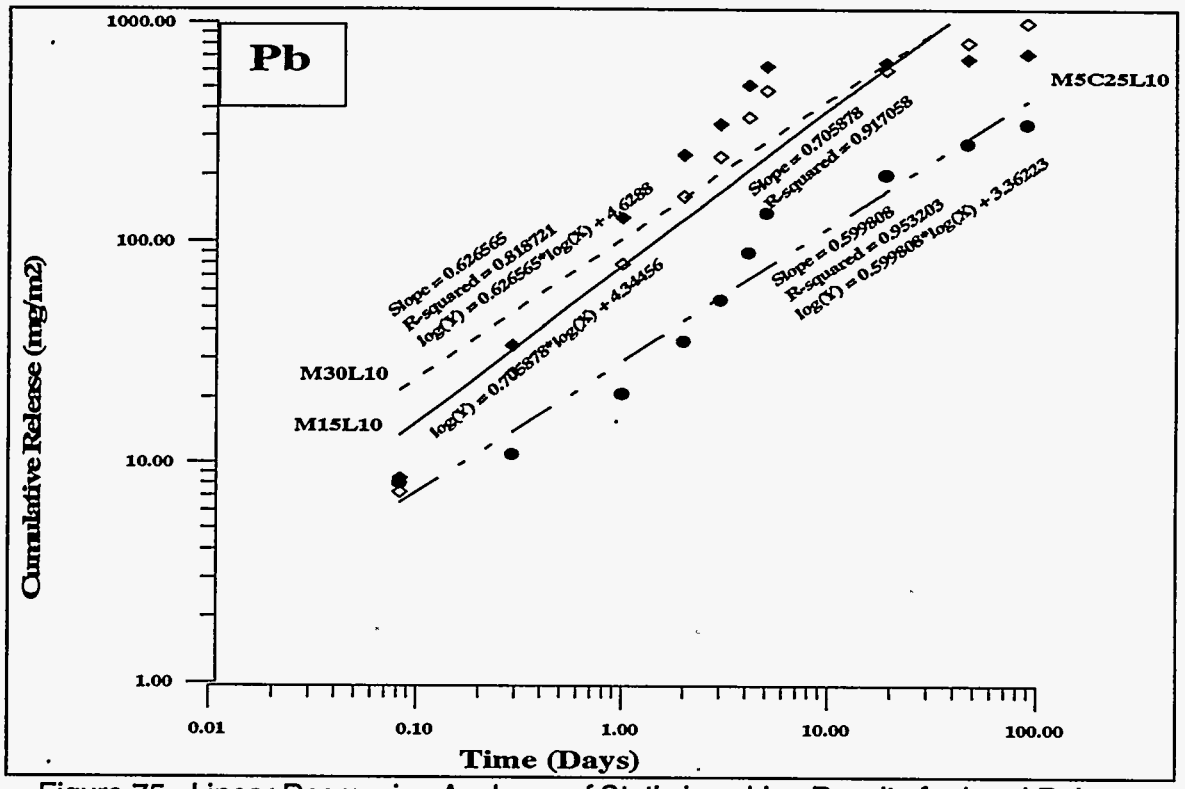

Figure 75. Linear Regression Analyses of Static Leaching Results for Lead Release from Montmorillonite-lime Mixes.

According to ANS 16.1 (1986), the effective diffusion coefficient for heavy metals being released from the solid to solution can be calculated from Equation 4:

$$D_e = \pi\left[\frac{a_n / A_0}{(\Delta t)_n}\right]^2\left[\frac{V}{S}\right]^2 T \qquad (4)$$

where a_n= the activity of a metal ion released from the specimen during leaching interval n, A_0= the total activity of a given metal ion in the specimen at the beginning of the first leaching interval, $(\Delta t)_n = t_n - t_{n-1}$, V= the volume of specimen in cm³, S= the geometric surface area of the specimen as calculated from measured dimensions in cm², and

$$T = \left[\frac{1}{2}(t_n^{1/2} + t_{n-1}^{1/2})\right]^2 \qquad (4a)$$

The leaching characteristics of a given specimen can be qualified by the leachability index (ANS 16.1, 1986). The leachability index is defined according to ANS 16.1, as:

$$L_i = \frac{1}{n}\sum_{1}^{n}[\log(\beta / D_{ei}]_n \qquad (5)$$

where β is a defined constant (1.0 cm^2/s). The correlation coefficient, r, for L_i is calculated according to:

$$r = \frac{\sigma_{Lt}}{\sigma_L \sigma_t} \tag{6}$$

$$\sigma_{Lt} = \frac{1}{9}\sum_{1}^{10}(L_n - L_i)(t_n - t_m) \tag{7}$$

σ_{Lt} is the covariance of the ten sets of L and t, s.

$$\sigma_L = \frac{1}{3}\left[\sum_{1}^{10}(L_n - L_i)^2\right]^{1/2} \tag{8}$$

σ_L is the standard deviation of the ten values of L_n, dimensionless.

$$\sigma_t = \frac{1}{3}\left[\sum_{1}^{10}(t_n - t_m)^2\right]^{2} \tag{9}$$

σ_t is the standard deviation of the ten values of t_n, s.

The 99.9% confidence range of the leachability index is defined by the expression:

$$C = L_i \pm 4.781\sigma_L n^{-1/2} = L_i \pm 1.51\sigma_L \tag{10}$$

where Li is the mean of the ten values of L_n.

Table 7. Leachability Parameters Calculated from Static Leaching Results

Specimen Designation	Mean of Li			r			Range of Li		
	As	Cr	Pb	As	Cr	Pb	As	Cr	Pb
K15L0	7.33	6.49	6.55	0.35	0.35	0.35	5.097-9.57	4.83-8.16	4.9-8.21
K15L10	12.87	12.94	9.50	0.06	0.15	0.06	9.68-16	10.9-14.99	6.97-12.02
K15L10S	14.58	13.45	10.00	-0.04	0.14	-0.03	4.38-24.79	11.57-15.32	6.9-13.1
K30L10	12.32	13.48	12.99	0.12	0.12	-0.03	8.8-15.84	11.29-15.68	10-15.93
K30L10S	12.27	13.34	10.00	0.11	0.08	0.00	10-14.51	11.58-15.11	6.58-13.43
K30L10S+Ba(0.5:1)	13.56	13.85	10.18	-0.02	0.09	-0.02	6.63-20.48	11.82-15.87	6.43-13.94
M15L0	10.02	10.53	9.19	0.02	0.04	0.07	5.62-14.42	2.23-18.83	2.95-15.43
M15L10	11.50	13.62	10.33	0.13	0.15\	0.14	7.5-15.48	10.31-16.93	9.18-11.47
M15L10S	12.38	14.07	12.45	0.01	0.14	0.12	5.37-19.39	9.8-18.33	8.75-16.14
M30L10	11.18	14.72	12.64	0.12	0.12	0.13	7.46-14.9	3.39-26.05	7.94-17.34
M30L10S	11.23	14.43	13.91	0.10	0.13	0.12	7.9-14.53	7.2-21.65	0.34-27.48
M5L5	11.92	12.74	11.17	0.11	0.13	0.17	9.69-14.14	10.54-14.94	9.28-13.07

The calculated mean of the leachability index, L_i, the correlation coefficient, r, and the confidence range of L_i are all listed in Table 7 for the respective specimens. Taking into account that a high leachability index indicates low release, the results in Table 7 suggest that the release of As, Cr, and Pb from quicklime-treated specimens is much lower than the release of the metals from untreated specimens (M15L0 and K15L0). For the quicklime-treated specimens containing 15% of kaolinite (K15L10) and 15% of montmorillonite (M15L10), the presence of sulfates (S) increases the leachability index, hence decreasing the anticipated heavy metal release. However, the effect of sulfate is not obvious for specimens with 30% of clay content.

A closer look at the correlation coefficient (r) values listed in Table 7, provides some additional information concerning the rate of heavy metal release. Theoretically, the correlation coefficient, r, should vary from -1 to +1. The sign indicates whether L_n is tending to increase (+r) or to decrease (-r) as t_n (time) increases. The results in Table 7 show the r values are positive for most of the specimens. This clearly indicates the release rate of heavy metals decreases with increasing leaching time.

However, the diffusion of heavy metals from solid to solution can be reduced by physical retardation (tortuosity) and/or chemical retention (geochemical attenuation). The general equation for the effective diffusion coefficient as a function of the physical retardation and chemical interaction is:

$$D_e = D_{o,x} \cdot \frac{1}{R \cdot \tau} \qquad (11)$$

where $D_{O,X}$ = the diffusion coefficient of component x in water in m^2/s, R = the chemical retention factor of component x in the solid, and τ = the physical retardation in the solid.

If $D_{o,x}$ values are known, the $R \cdot \tau$ term can be calculated by using Equation 2. The $D_{o,x}$ values of Pb^{2+} and $Cr^{3+}$are 9.45E-6 cm^2/s and 5.95E-6 cm^2/s, respectively (CRC Handbook of Chemistry and Physics, 1994). However, the $D_{o,x}$ value for $H_2AsO_3^-$ was not found. Therefore, $D_{o,x}$ value (9.05E-6 cm^2/s) for $H_2AsO_4^-$ was used to calculate $R \cdot \tau$. The mean values of D_e and calculated $R \cdot \tau$ data are listed in Table 8.

The effective diffusion coefficients of Cr, Pb, and As for the untreated specimens (K15L0 and M15L0) are significantly larger than those for the treated specimens (Table 8). The data in Table 8 also indicates the values for the physical and chemical retardation factors ($R \cdot \tau$) for the treated specimens are much higher than those for the untreated specimens. For the release of Cr from K15L0, the retardation factor is approximately 1. This implies the release rate of Cr from the untreated specimen is similar to the diffusion of Cr^{3+} in water. Quicklime treatment increased the retardation factor by approximately six orders of magnitude for Cr release. Moreover, the retardation factors for Pb and As

release for the treated specimens are 4 to 7 orders of magnitudes higher than those for the untreated specimens. The results therefore suggest quicklime treatment was effective in significantly reducing the mobility of the heavy metals, so that only trace levels were released.

Table 8. Mean Effective Diffusion Coefficients and Retardation Factors

Specimen Designation	Cr		Pb		As	
	Mean D_e (cm^2/s)	$R\tau$	Mean D_e (cm^2/s)	$R\tau$	Mean D_e (cm^2/s)	$R\tau$
K15L0	7.29E-06	8.16E-01	6.12E-06	1.54E+00	3.87E-06	2.34E+00
K15L10	2.18E-13	2.73E+07	1.12E-09	8.44E+03	4.52E-13	2.00E+07
K15L10S	6.04E-14	9.85E+07	3.28E-10	2.88E+04	7.05E-14	1.28E+08
K30L10	8.31E-14	7.16E+07	3.91E-13	2.42E+07	1.77E-12	5.11E+06
K30L10S	1.36E-13	4.38E+07	6.69E-10	1.41E+04	1.46E-12	6.20E+06
K30L10S+Ba(0.5:1)	3.02E-14	1.97E+08	3.12E-10	3.03E+04	3.95E-13	2.29E+07
M15L0	1.32E-08	4.51E+02	5.28E-08	1.79E+02	1.24E-09	7.30E+03
M15L10	6.69E-14	8.89E+07	5.55E-11	1.70E+05	1.21E-11	7.48E+05
M15L10S	3.90E-14	1.53E+08	1.04E-12	9.09E+06	4.75E-12	1.91E+06
M30L10	4.64E-14	1.28E+08	8.98E-13	1.05E+07	4.27E-11	2.12E+05
M30L10S	9.58E-14	6.21E+07	2.03E-11	4.66E+05	2.67E-11	3.39E+05
M5L5	3.41E-13	1.74E+07	1.06E-11	8.92E+05	2.64E-12	3.43E+06

4.5.3 Summary

Overall, the monolithic static leaching test results further demonstrated the proposed treatment effectiveness. First, in terms of cumulative release, less than 1% of the total amount of heavy metals present was released from the quicklime treated specimens during the duration of the static leaching tests. Conversely, throughout the test duration, 25% to 75% of the total amount of heavy metals present was released from the untreated specimens. It was shown that this (translates into two and three orders of actual release concentration magnitude reduction) upon treatment application. Furthermore, through some additional data manipulation using a diffusion model, it was concluded that treatment resulted in a diffusion controlled, very slow release of the heavy metals. In the absence of treatment, Cr and Pb release was fast and mainly controlled by surface washoff of the soluble heavy metal species. For As, and in the absence of treatment, release was diffusion controlled , mainly due to the low solubility of the arsenic oxide. However, As release was still effectively minimized by treatment application. Finally, based on the obtained results, effective diffusion coefficients and the corresponding retardation factors were calculated for the heavy metals and solid matrices under study. Such parameters can be effectively used to predict the ultimate fate and transport of the released heavy

metal species in subsurface environments when used as inputs for subsurface flow deterministic, as well as stochastic models.

4.6 Heavy Metal Release under Flow-Through Leaching Conditions

The TCLP is a simple batch extraction test aimed at establishing regulatory levels of heavy metal release. However, it cannot be used to predict the actual long term leaching behavior of the treated solids in the field. When considering actual field behavior, heavy metal release would have to be evaluated by testing the solid material under actual field conditions. This entails testing the solid in its monolithic, rather than its pulverized form. It also entails testing under actual conditions of contact between the leachant and the solid. Since we are dealing with low permeability materials, both advective and diffusive modes of contact are possible. Heavy metal levels during diffusion-controlled release have already been evaluated by means of conducting monolith static leaching tests, as discussed in the previous section. However, the worst field leaching condition is infiltration of a leachant or rain water through the treated solid form. During infiltration, heavy metal release is triggered by a coupled flow process, which includes advective, as well as diffusive flow components. Therefore, flow-through leaching tests were designed and undertaken to establish the levels of heavy metal release under infiltration conditions.

During these flow-through tests, 0.014 M of acetic acid solution (pH = 3.45) was continuously passed through a compacted solid disc (4.75 cm diameter by 2.0 cm height) placed in a flexible wall apparatus which was similar to a flexible-wall permeameter. The hydraulic gradients applied to the specimens were unrealistically high, and varied between 15.0 and 280.0, in an attempt to attain reasonable testing duration times as a function of the anticipated specimen soil permeability values. Overall, the flow-through tests simulated the behavior of the treated solid under severe, "worst case" infiltration field conditions (low pH, continuous leaching, and high hydraulic gradients). A limited number of tests were also carried out using distilled water as the leachant, mainly for comparison purposes.

The main difference between the flow-through test used in the present study and the conventional column leaching test is that in the flow-through test, treated monolithic specimens instead of pulverized loose solids were tested. The advantage of the test used is the solids were not disturbed, so the actual hydraulic properties and leaching behavior of the specimens could be determined at the same time. During more than one year of continuous infiltration leaching, the effluent leachate was collected regularly and leachate volume, pH, and heavy metal levels of release were measured and recorded.

4.6.1 Long-Term Permeability of the Quicklime-Treated Solids

The permeability of the treated soil would directly affect the rate of infiltration, and therefore the capacity of the soil to withstand chemical leaching and physical weathering changes. However, most of the column leaching research conducted in the S/S field neglects this fundamental soil property. The soil permeability changes with elapsed testing time, during the flow through column experiments, are depicted in Figure 76. All test results correspond to acetic acid

leaching conditions unless indicated otherwise in the figure. Kaolinite sand specimens, whether treated or untreated, showed limited variability in hydraulic conductivity values, from approximately $4x10^{-7}$ to $2x10^{-8}$ cm/sec. As expected, soil permeability increased following lime treatment, since lime treatment will generally result in a more flocculated fabric due to exchange of monovalent cations by Ca^{2+}, and thus increased flow through the intracluster pores (Mitchell, 1993). There is no apparent effect of sulfate addition on the permeability, as the observed variability is not significant and could potentially be attributed to differences in the water content of compaction (the lime-sulfate specimen was compacted wet of optimum whereas the lime specimen was compacted at dry of optimum). However, the effect of acid leaching versus water leaching is more clear. Acid leaching results in increased hydraulic conductivity values with respect to time, as kaolinite flocculates in an edge-to-face fashion at low pHs [11].

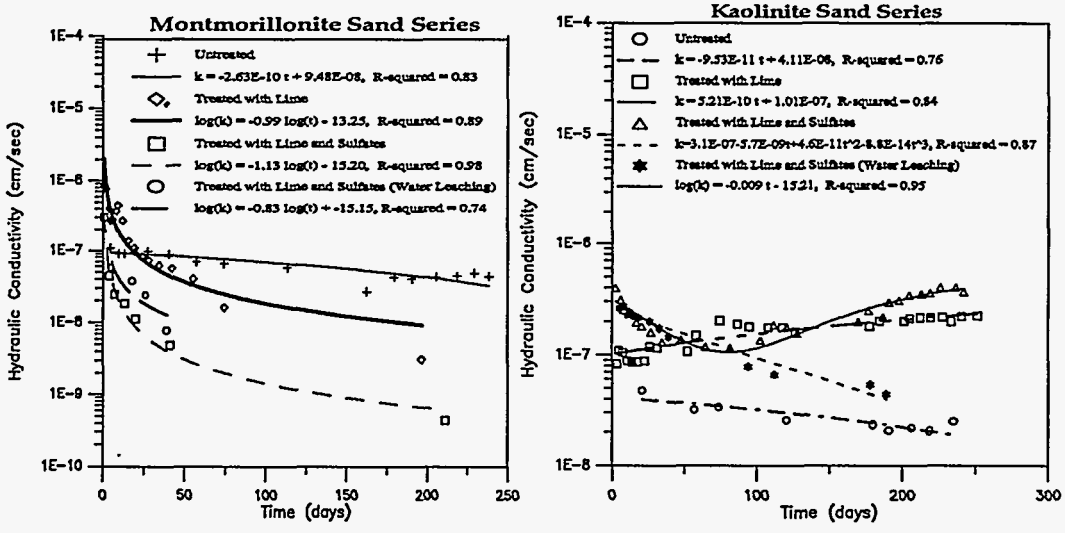

Figure 76. Flow Through Hydraulic Conductivity as a Function of Elapsed Time; *Left:* Montmorillonite Sand Series; *Right:* Kaolinite Sand Series

For the montmorillonite sand series, the variability of permeability values was much more pronounced as values ranged from $2x10^{-6}$ to $5x10^{-10}$ cm/sec. As expected, treatment resulted in a marked increase in hydraulic conductivity values immediately following test initiation. However, as time elapsed permeability decreased significantly for all lime treated specimens, whereas it effectively remained constant for the untreated specimen. This can be explained if we assume the divalent calcium, present in the montmorillonite exchange sites as a result of lime treatment, is slowly being exchanged for the monovalent hydrogen cation due to mass action. Such a cation exchange process would result in a transition from a flocculated fabric to a dispersed one. It could be however, that acid flows disintegrate clay particles, which in turn leads to clogging of the pore space by disintegrated mobile fines. It could also be that specimen consolidation is responsible for such a permeability decrease. Even though the water leaching results are limited, since the flow through experiment

is still in progress, so far there is no marked difference between water versus acetic acid leaching permeabilities. Overall, based on the permeability results, an effective average permeability value of 10^{-7} cm/sec was assigned for both kaolinite and montmorillonite specimen mixes, to be later used for long term heavy metal release predictions.

4.6.2 *Leachate pH Change during Long-Term Flow-Through Leaching*

The pH of the leachate is an important parameter and a convenient indicator of the amount of alkalinity still available in the solids. A low leachate pH would indicate the alkaline solid attributes, in this case lime, are exhausted by the acidity of the leachant. A low pH in the effluent would also be accompanied by increased heavy metal release levels. Even though there are marked exceptions to the rule, heavy metal species are mostly mobile at the lower pH region. Therefore, resisting pH decrease tendencies would also ensure the lowest possible levels of heavy metal release from the treated solids.

The effluent leachate pH, for montmorillonite-sand specimen tests, is plotted as a function of leachate volume in Figure 77. Since the untreated specimens had negligible levels of ANC (Figure 3), the leachate pH was always about 4.0, throughout the duration of the flow-through leaching test. For all the treated specimens, leachate pH was between 10.0 and 12.0 upon testing initiation and shortly thereafter. As additional leachant passed through, leachate pH gradually decreased, following a similar pattern and rate of decrease amongst the different specimens. The pH dropped to 7.0 after approximately 3,250 mL of the acetic acid (approximately 270 pore volumes) passed through the M30L10 specimen. The leachate pH for the M30L10S and M5C25L10S specimens is still higher than 8.0, mainly due to the limited volume of acid infiltration, owing to the lower specimen hydraulic conductivity values. Different amounts of leachate were collected for different specimens due to permeability and hydraulic gradient differences.

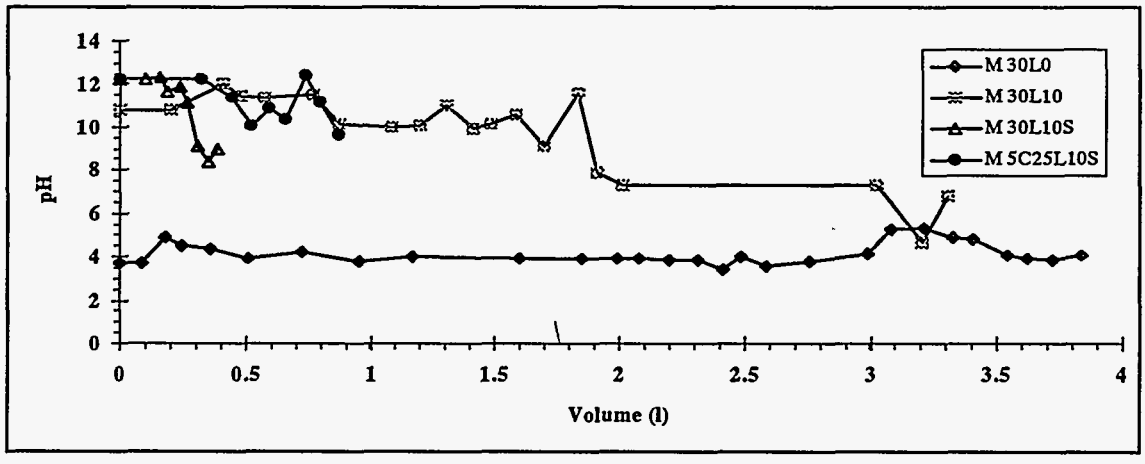

Figure 77. Flow-through Leachate pH as a Function of Leachate Volume for Montmorillonite-sand Specimens.

Whereas leachate pH was about 4.0 throughout the test duration for the untreated specimen, significant leachate pH decreases occurred as the leachant passed through the treated kaolinite-sand specimens (Figure 78). It seemed that the amount of free lime available to neutralize the acidic leachant, in both the K30L10 and K30L10S specimens, was thoroughly exhausted after 10 L (800 to 850 pore volumes) of the leachant had passed through. On the other hand, the quicklime/fly ash treated specimen showed a much higher acid neutralization capacity. Following 25 L (1,800 pore volumes) of flow-through leaching the pH of the effluent is still higher than 9.0, thus keeping heavy metal release at minimum levels.

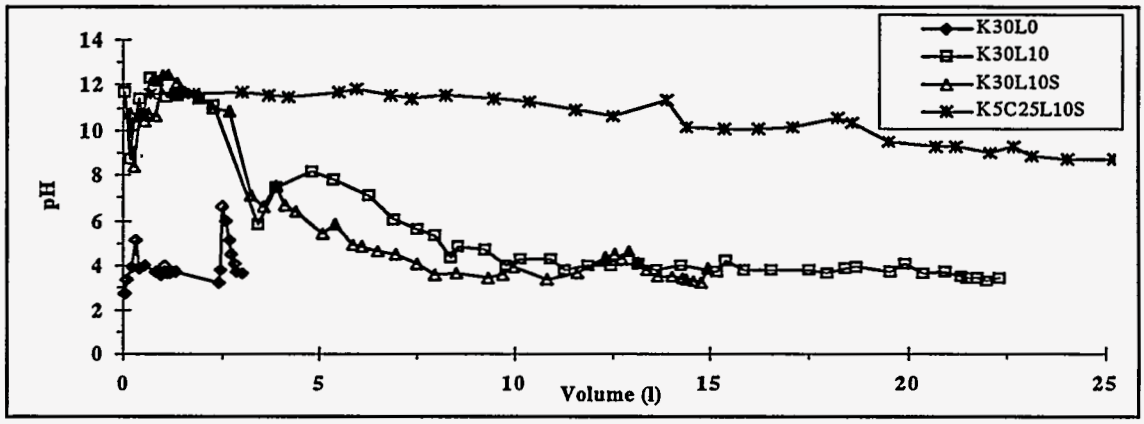

Figure 78. Flow-through Leachate pH as a Function of Leachate Volume for Kaolinite-sand Specimens.

The leachate pH changes for acid versus distilled water leaching are compared in Figure 79. As expected, the leachant pH for acid leaching was much lower than for water leaching.

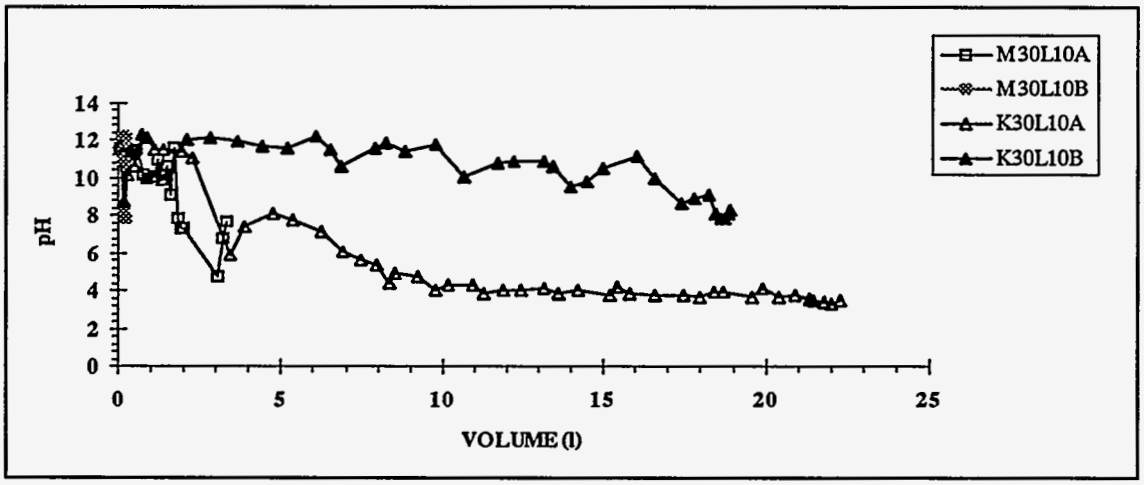

Figure 79. Effect of Different Leachants (A-acetic Acid, B-distilled Water) on the Effluent pH.

4.6.3 *Heavy Metal Release during Long-Term Flow-Through Leaching*

The cumulative percentage of As leached from untreated and quicklime treated montmorillonite sand specimens is plotted in Figure 80 as a function of leachate volume collected. The amount of As leached out from the untreated specimens increased from 5% to 75% after an acetic acid leachant volume of 4 L had passed through the specimen. Conversely, the amount of As released from all quicklime treated specimens was very small. After 3.3 L of acetic acid leachant had passed through the M30L10 specimen, only 5% As was leached out. For the rest of the specimens, As release was even lower mainly due to the lower permeability of these specimens which limited the volume of leachant passing through.

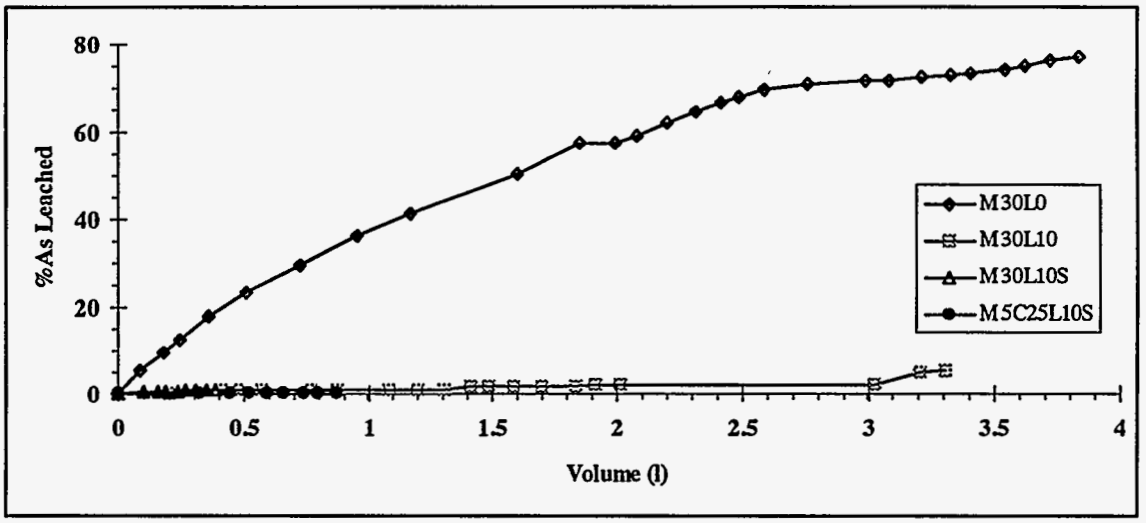

Figure 80. Percentage of Arsenic Leached as a Function of Effluent Volume for the Montmorillonite Specimens.

Approximately 4% Cr was leached out from the untreated specimen during the first 88 mL of leachant infiltration (Figure 81). No significant Cr release was observed from that point and on. These results suggest that approximately 4% of the total Cr was readily leachable from the untreated specimen. Negligible amounts of Cr (less than 0.05%) were leached out from all treated specimens. The release of Pb from both untreated and treated specimens was similar to that of As. Overall, very small amounts of heavy metals were released from the treated montmorillonite-sand specimens. These results agree with the leachate pH values (Figure 77), which showed the pH did not drop to low enough values for heavy metal release to be favored, following more than one year of acid leaching.

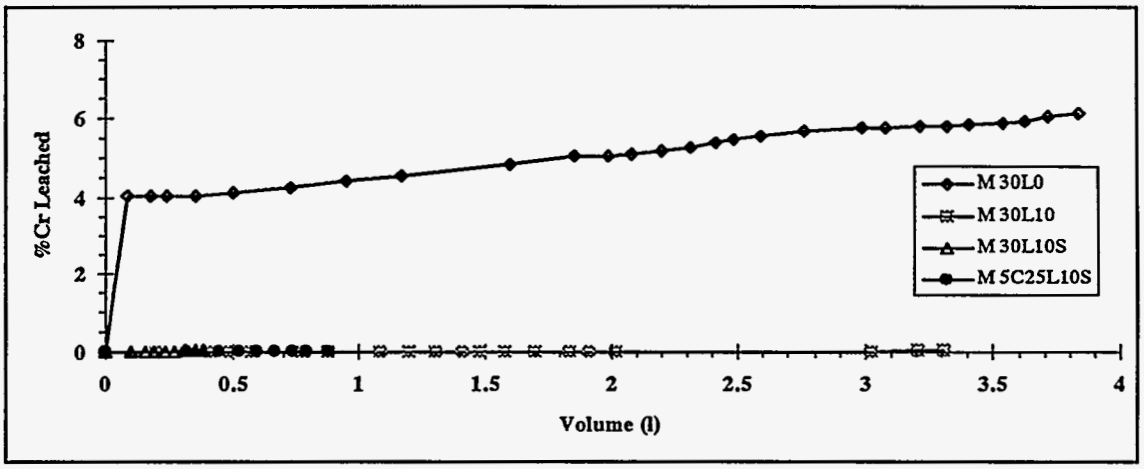

Figure 81. Percentage of Cr Leached as a Function of Effluent Volume for the Montmorillonite Specimens.

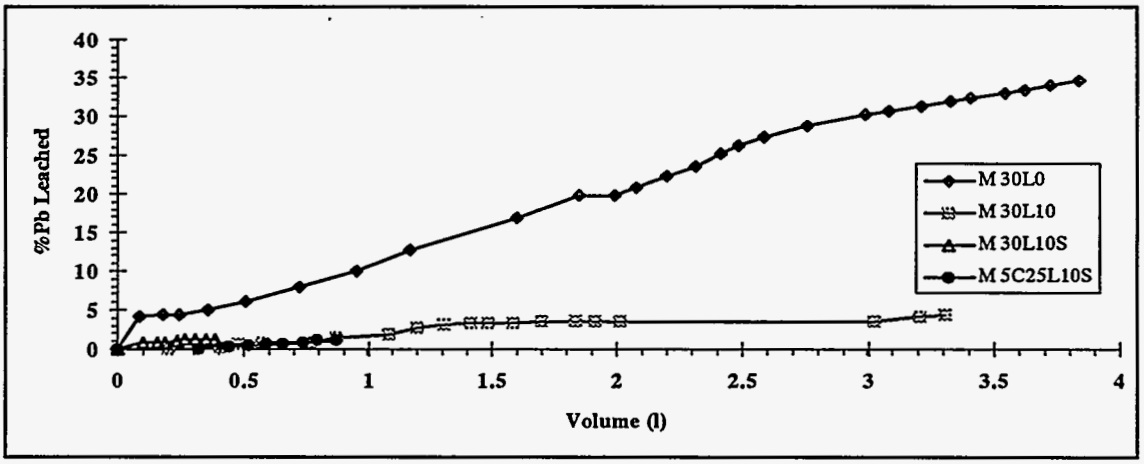

Figure 82. Percentage of Lead Leached as a Function of Effluent Volume for the Montmorillonite Specimens.

In contrast to the leaching results for montmorillonite-sand specimens, the results in Figure 83 show that larger amounts of As were released for both untreated and treated kaolinite-sand specimens. For the untreated specimen, 80% of the arsenic was released with less than 3 L of acid leaching through the specimen (~370 pore volumes). For the treated specimens, As break through release occurred following approximately 5 L of acid leachant infiltration through the K30L10S specimen (~ 400 pore volumes). Following some time after the break through, the cumulative release leveled off at 28%, and no more As was released thereafter. The break through in As release was caused by the corresponding pH decrease (Figure 78), following the exhaustion of specimen alkalinity. Similarly, for the K30L10 specimen, As break-through took place after approximately 12 L of acid leaching (~ 1,000 pore volumes), and cumulative release leveled of at 48%. For the specimen treated with quicklime/fly ash, no As break through occurred with more than 63 L (~4,500

pore volumes) of the leachant passing through the specimen. However, about 20% of the total As has been released.

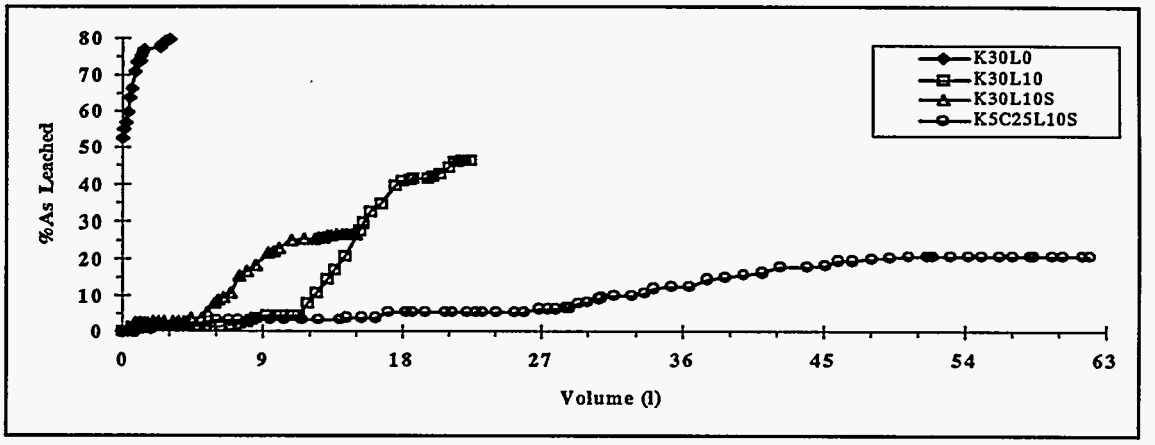

Figure 83. Percentage of Arsenic Leached as a Function of Effluent Volume for the Kaolinite-sand Specimens.

Chromium break through also took place following approximately 5 L of acidic flow-through leaching for both the K30L10 and K30L10S specimens (Figure 84). Following break through, almost all of the Cr present in the specimens was released. A typical pattern of Cr release for the untreated kaolinite-sand specimen is that most of the leachable portion of the metals was released during the first few days of flow-through test. However, after 35% of the total Cr present was released, Cr release seemed to level off. For the quicklime/fly ash treated specimen, break through has not taken place yet, even though more than 4,500 pore volumes of leachant passed through. The main reason for such behavior is the higher pH (~8) of the leachate. The quicklime/fly ash treatment significantly increased the capacity of the solid to withstand pH drops due to acidic leaching (Figure 78), resulting in higher leachate pH values.

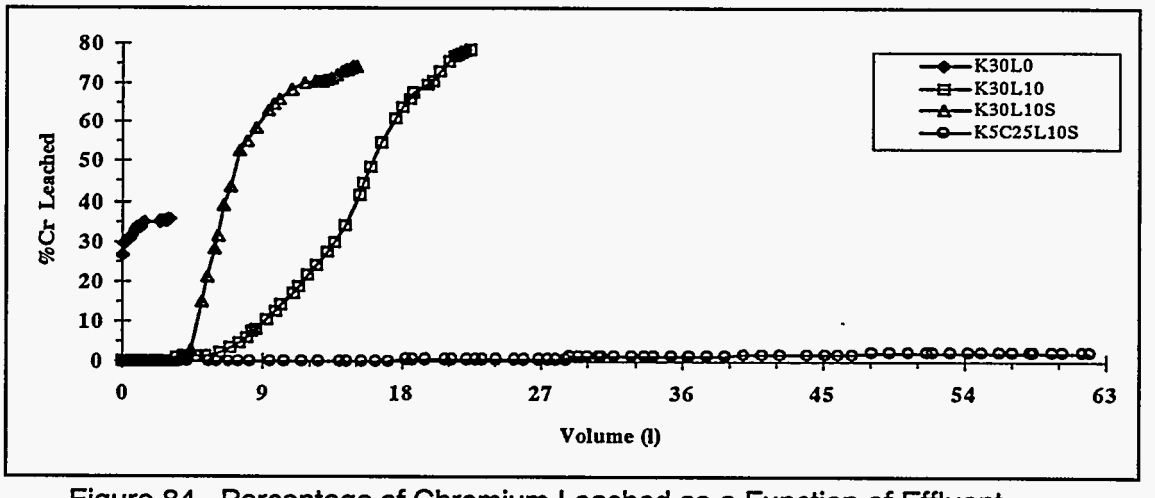

Figure 84. Percentage of Chromium Leached as a Function of Effluent Volume for the Kaolinite-sand Specimens.

Lead release levels were high from the start of the flow-through tests. This was due to the initially high pH of the leachate. Lead, due to its amphoteric behavior

can be released at both high and low pH, as discussed in the opening section of Chapter 4. Lead cumulative release from the K30L10S specimen was actually higher than for the untreated (K30L0) specimen. Lead release from the K30L0 specimen leveled off at 77%, whereas the K30L10 specimen seemed to level off at about 45%. For K30L10S, all of the lead present in the specimen was released. Conversely, upon addition of fly ash and quicklime, lead release was kept below 5%. This further demonstrates the ability to deal with the increased levels of lead release by the addition of fly ash, as was also shown in a previous section, based on our TCLP results.

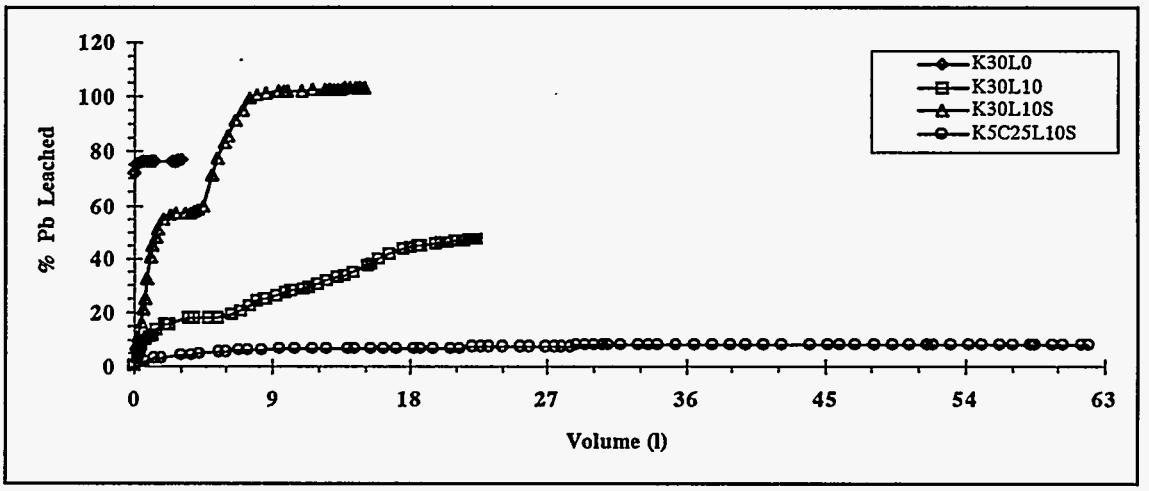

Figure 85. Percentage of Lead Leached as a Function of Effluent Volume for the Kaolinite-sand Specimens.

Heavy metal release levels for specimen duplicates, using acid versus water as the leachant during the course of the leaching tests, are compared in Figures 86 to 88. As expected, when distilled water was used, the amount of heavy metals released from both quicklime treated clay-sand specimens was significantly lower than when using acid solution as the leachant medium. This difference was much more significant for kaolinite-sand specimens, where the levels of heavy metal release were higher. The most dramatic difference in release levels was for Cr. For the quicklime treated kaolinite-sand specimens, Cr release levels dropped from close to 80% during acid leaching down to 0.3% during distilled water leaching. For As, levels of cumulative release dropped from close to 50% during acid leaching down to less than 10% during water leaching. For Pb, release decreased from close to 50% down to 14%. For the montmorillonite-sand specimens, differences between acid versus water leaching were generally less pronounced, even though lower heavy metal levels were released during water leaching.

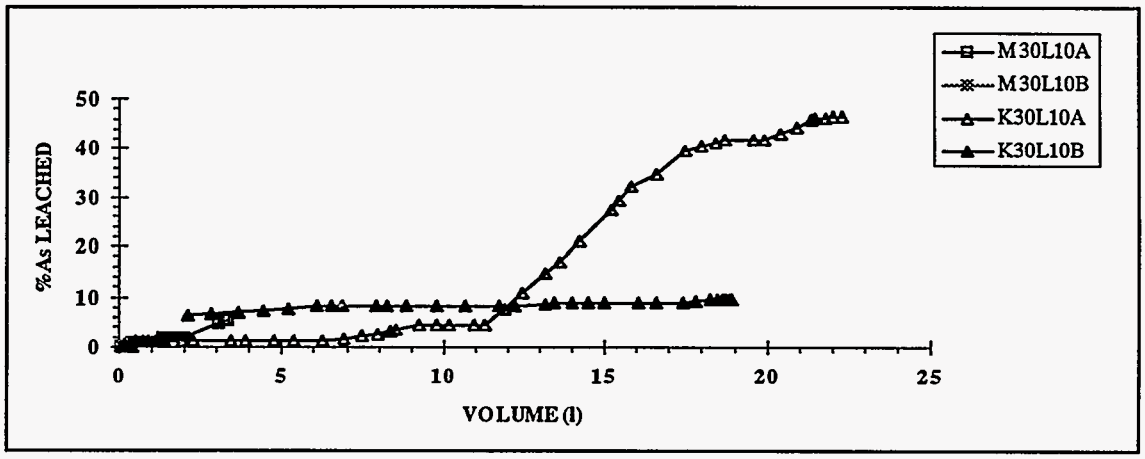

Figure 86. Effect of Leachant Acidity (A-acetic Acid, B-distilled Water) on Arsenic Release during Flow-through Test.

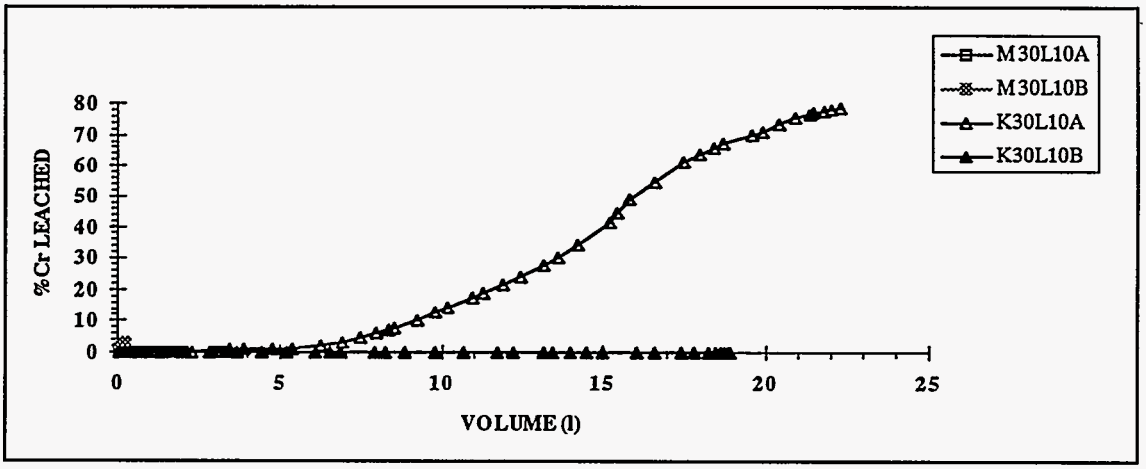

Figure 87. Effect of Leachant Acidity (A-acetic Acid, B-distilled Water) on Chromium Release during Flow-through Test.

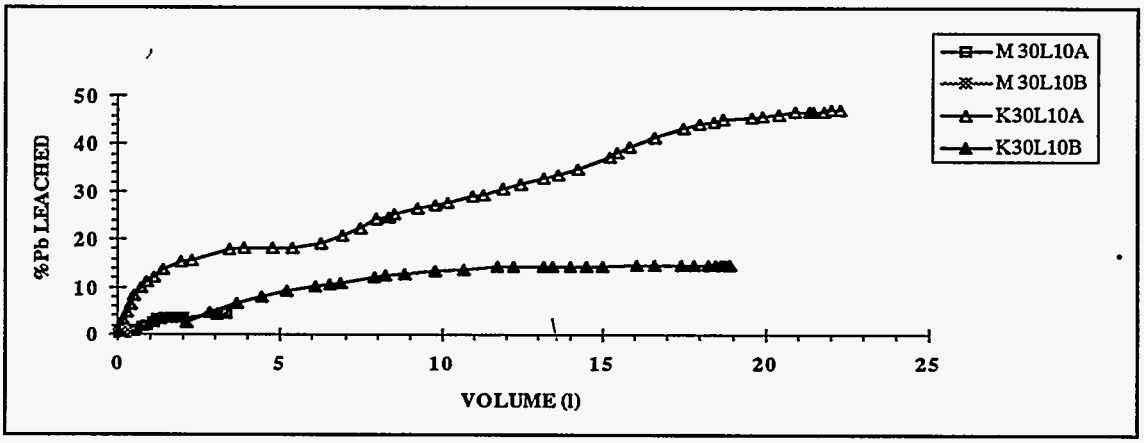

Figure 88. Effect of Leachant Acidity (A-acetic Acid, B-distilled Water) on Lead release during flow-through leaching.

4.6.4 *Summary*

Overall, the flow through leaching results demonstrated that heavy metal leachability is significantly reduced by quicklime treatment, especially in the presence of fly ash. Heavy metal release levels are also majorly influenced by the type of clay mineral present in the artificial soils. Whereas, for kaolinite sand specimens, lead release break-through was a continuous process, so far montmorillonite-sand lime treated specimens have not shown any indication of a concentration break through. The lower heavy metal leachability in the montmorillonite-sand matrices versus the kaolinite-sand matrices was expected. It can be attributed to the fact that montmorillonite has a much higher surface area and cation exchange capacity than kaolinite. In terms of physicochemical behavior, montmorillonite is a much more active mineral than kaolinite. When fly ash was added to the clay-sand specimens, heavy metal release was significantly reduced. Furthermore, heavy metal release was further reduced when water was used as the leachant medium. For As and Cr, the amount of pore volumes leached through the treated test specimens before break through took place, ranged from 300 up to 4,500 pore volumes. On the other hand, break through took place within the first pore volume of leachant passing through the untreated specimens. Under actual field conditions, it could take less than a year for a single pore volume to pass through 1 m^3 of soil, whereas it may take thousands of years for 300 pore volumes to pass through. This time dimension with respect to treatment effectiveness will be dealt with more extensively in the following section.

4.7 Prediction of Long-Term Leachability of the Treated Soils

A successful S/S technological application should produce treated solids that can last for a long period of time without significant release of heavy metals. Thus far, it has been demonstrated that As, Cr and Pb leachabilities in the clay-sand specimens could be effectively reduced below the TCLP limits. However, TCLP results cannot be used for assessing how long the treated solid can last under natural leaching conditions. Therefore, the experimental data obtained from the flow-through leaching, acid neutralization capacity and TCLP tests were combined, analyzed and used to obtain a methodology of predicting the duration of the treated solid under typical leaching conditions in the field.

4.7.1 pH Effect on Leachability

Heavy metal leachability is very sensitive to pH changes, since both the solubility and adsorption behavior of the heavy metals are strong functions of solution pH. When the leachability is controlled by the solubility of the heavy metals, the nature and extent of solid surface presence will not significantly affect their leachability. However, the nature and extent of the solid surface may have a significant effect on heavy metal release when their leachability is mainly controlled by adsorption. The mechanisms controlling heavy metal release from quicklime treated soils can be established by studying the effect of the surface type and extent on heavy metal leachability. However, to effectively control heavy metal release, the pH range for immobilization should also be established for different soil matrices.

In order to elucidate the pH effect on the heavy metal leachability during the TCLP batch test, the heavy metal concentrations in the TCLP leachate were plotted as a function of leachate pH in Figures 89 to 91. The results in Figures 89 and 90 show that when leachate pH was between 5.0 and 13.0, As and Cr concentrations in the TCLP leachate were very low. In the absence of quicklime treatment, when the pH level was near 5.0, a dramatic increase in As and Cr concentrations occurred in the leachate. Moreover, the pH boundaries for As and Cr release were the same for specimens with different montmorillonite and kaolinite contents. Therefore, these results suggest that As and Cr release at pH 5.0 was dissolution - controlled, and that the heavy metals are effectively immobilized by the quicklime treatment over a wide pH range.

The results in Figure 91 indicate Pb could be effectively immobilized only when pH was between 7.0 and 11.5. When the pH level was outside this range, a dramatic increase in lead concentration in the TCLP leachate was observed. A closer look at Figure 91 revealed that the high Pb concentration points correspond to TCLP release from kaolinite-sand specimens when leachate pH was between 11.5 and 12.0. Pb was released from montmorillonite (30%) specimens when pH was higher than 12.0. Moreover, in the low pH range, clay type and contents did not have a significant effect on Pb concentrations in the leachate. Overall, strong adsorption of montmorillonite for Pb shifted the Pb release boundary to a higher pH range, as compared to the release boundary for kaolinite specimens. When pH was lower than 7.0, the release of Pb was mainly

controlled by Pb dissolution. To effectively immobilize Pb in quicklime treated soils, leachate pH should be controlled between 7.0 and 11.0.

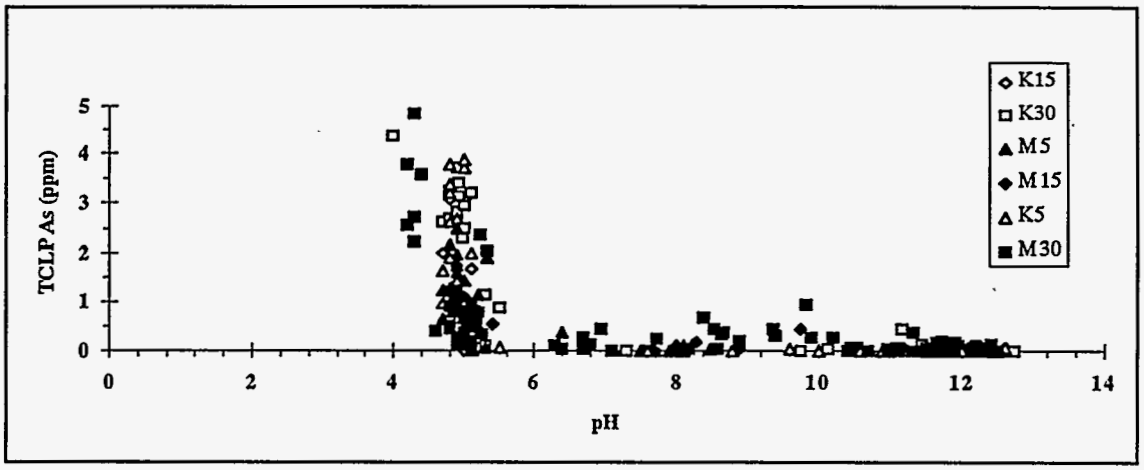

Figure 89. Effect of Leachate pH on TCLP Arsenic Concentration.

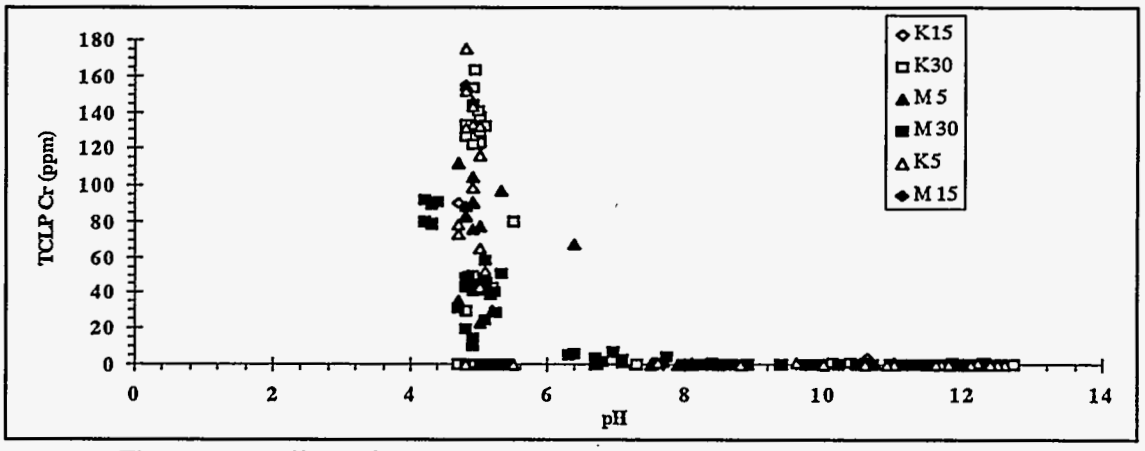

Figure 90. Effect of Leachate pH on TCLP Chromium Concentration.

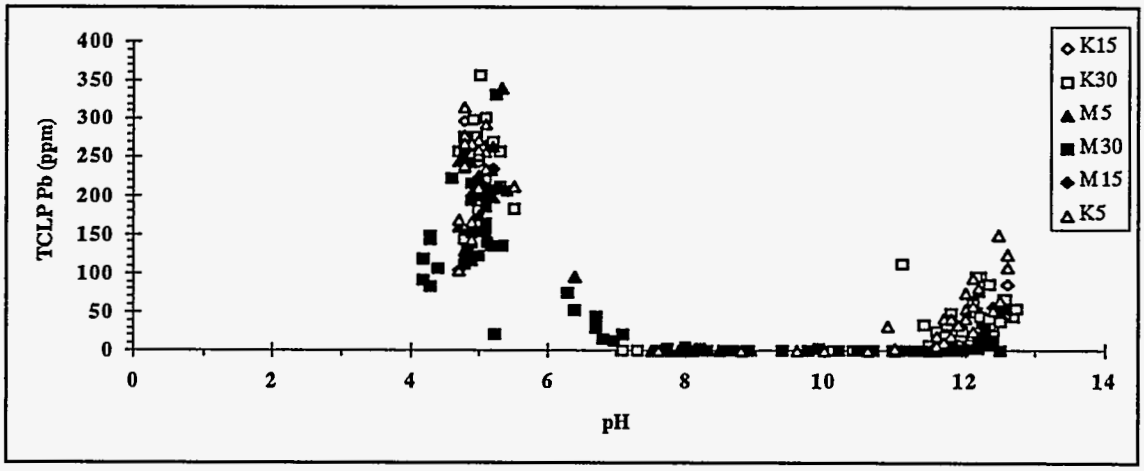

Figure 91. Effect of Leachate pH on TCLP Lead Concentration.

Similar heavy metal release plots, showing release concentrations versus leachate pH, were also constructed using the flow-through leaching data. During flow-through leaching (Figure 92), As was released only when the pH level was lower than 4.0. However, the immobilization pH range for Cr was smaller than the one obtained based on the TCLP results, as Cr release was imminent when the pH level was lower than 6.0 (Figure 93). The Pb release upper boundary was approximately at pH=10.0 (Figure 94), which was 1.5 pH units lower than Pb release pH under TCLP leaching conditions. Overall, Cr and Pb release was more favored under flow-through leaching conditions than under TCLP leaching conditions. Therefore, a safety factor of at least 2.0 pH units has to be considered when TCLP results are used to design quicklime treatment for Pb in the higher pH range or for Cr in the lower pH range.

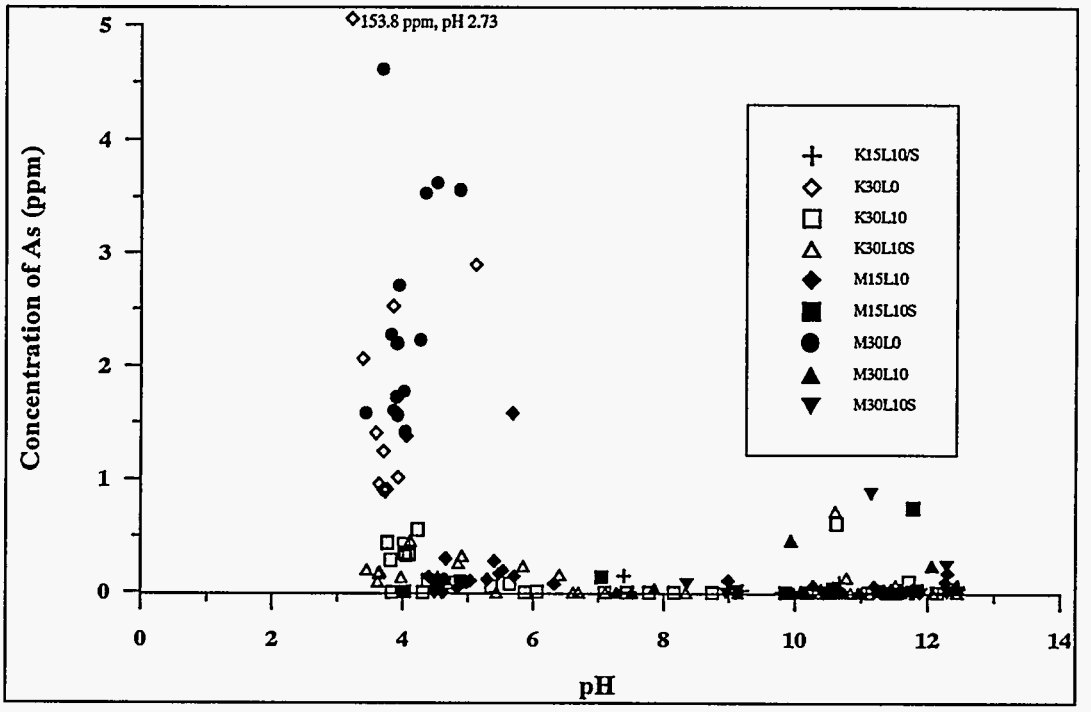

Figure 92. Effect of Flow-through Leachate pH on As Effluent Concentrations.

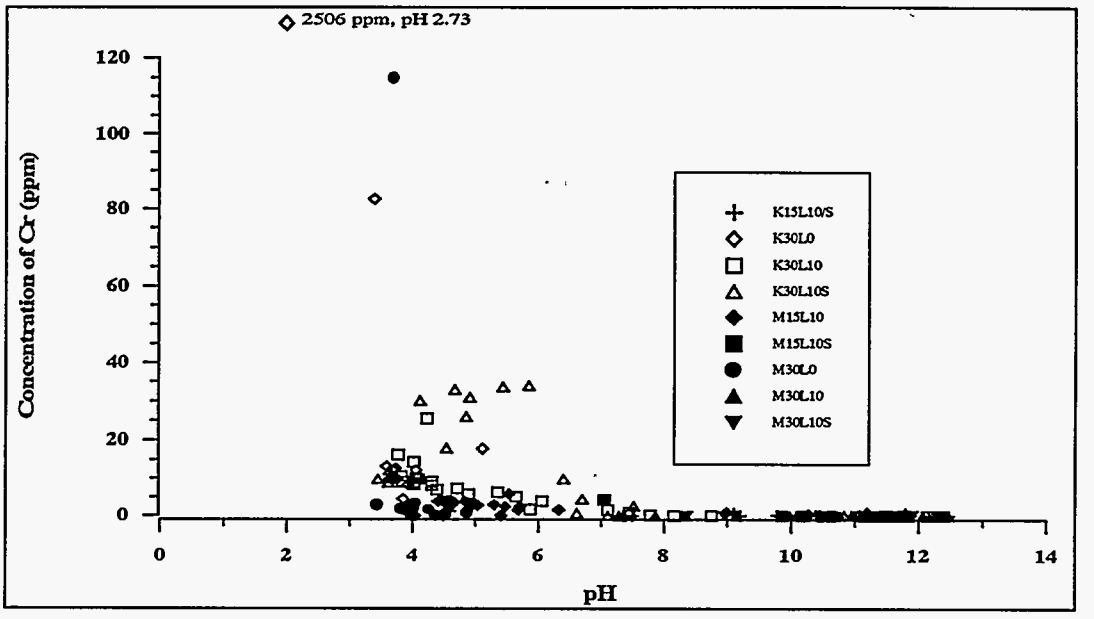

Figure 93. Effect of Flow-through Leachate pH on Cr Effluent Concentrations.

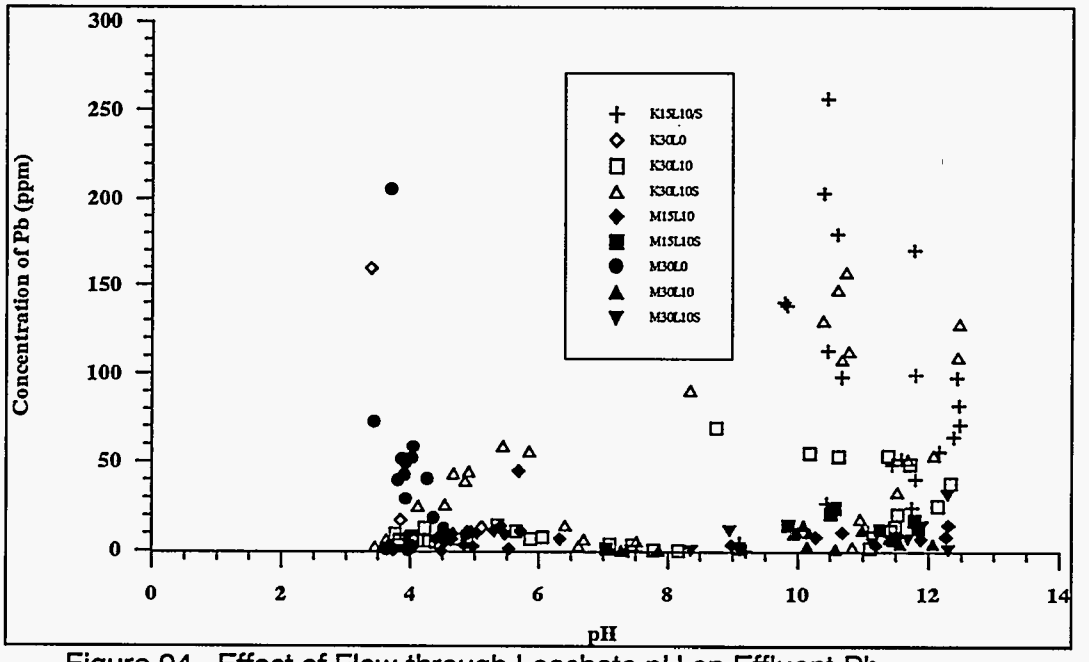

Figure 94. Effect of Flow-through Leachate pH on Effluent Pb Concentrations.

The fact that under flow-through conditions, the Cr and Pb pH immobilization range is narrower than under TCLP leaching conditions, may be explained by the two following factors. First, during the course of flow-through testing, the leachant volume to solid mass ratio was much higher than the ratio (solution : solid = 20) used for the TCLP test. Second, during flow-through leaching, contact time between the leachant and the solid was lower than during TCLP testing. These hypotheses were confirmed by the results in Figures 95 and 96, where the pH changes during flow-through versus TCLP batch titration

conditions are compared. When the same amount of equivalents of acid contacted the solids, leachate pH for the flow through test was consistently lower than leachate pH for the TCLP batch titration.

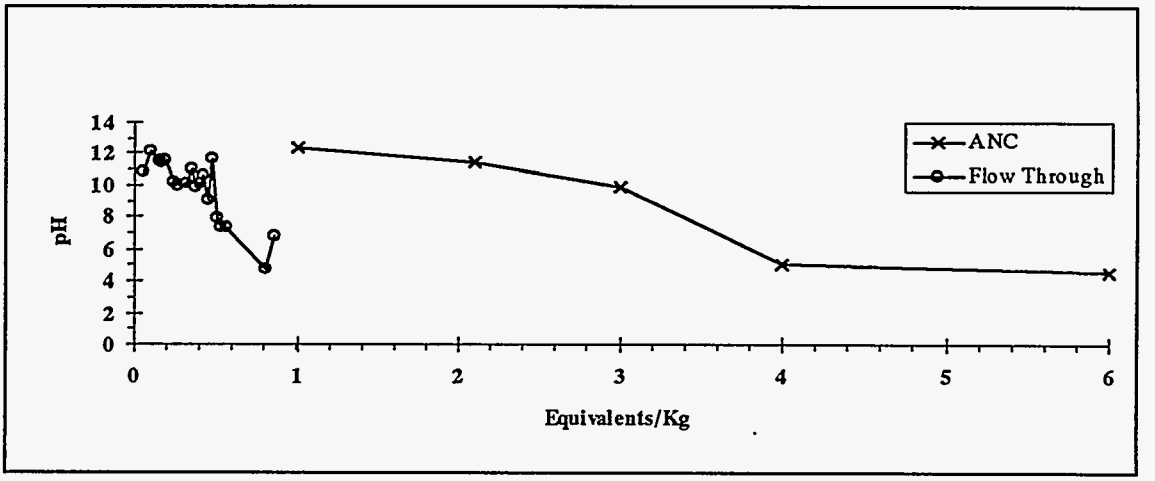

Figure 95. Comparison of Leachate pH for Flow-through Leaching and Batch Titration, M30L10.

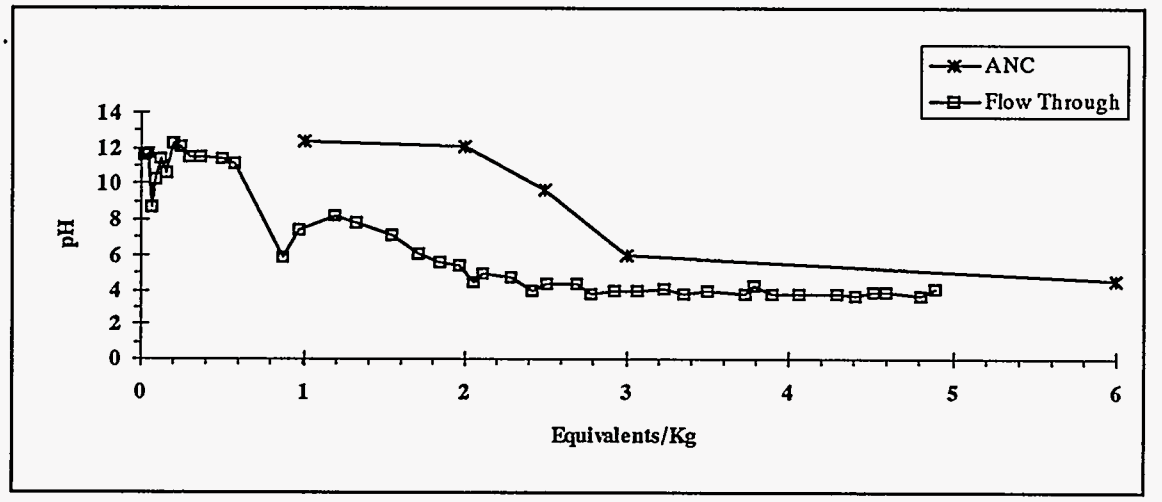

Figure 96. Comparison of Leachate pH for Flow-through Leaching and Batch Titration, K30L10.

4.7.2 *Prediction of Duration of the Quicklime Treated Solids*

Both TCLP and flow-through results show that the heavy metals can be immobilized as long as the pH level is maintained within a certain range. Therefore, based on the acid neutralization capacity and the permeability of the treated solid, and the acidity of leachant, the duration of treatment effectiveness under actual field conditions could be predicted. Duration of treatment effectiveness is the time period it takes for heavy metal concentration break-through to occur.

First, the flow-through results were used to calculate the duration of treatment effectiveness under actual field conditions. Since heavy metal concentration break through occurred only for kaolinite-sand specimens under acidic leaching, their respective leachate volume at the break-through point was used for the duration calculation. The duration of the treated montmorillonite specimens will be much longer than the treated kaolinite specimens. According to Figures 83 and 84, for the treated kaolinite sand specimens As and Cr, break-through occurred when 4.4 L of acetic acid (0.014 N) passed through the specimen. The weight of the solid specimens was 64 g. This means the treated specimens (10% quicklime) can neutralize 965 eq acid/1000 kg of the solid without obvious release of As and Cr.

To predict the durability of the treated solids, two leachant media (i.e. rainwater and landfill leachate) were used for calculation purposes. The acidities of typical rainwater and landfill leachant were 0.1 and 100 meq/L, respectively (Bishop, 1986). Assuming the rainfall intensity was 1.0 m/year and all rainfall penetrated through the quicklime treated compacted solid cube (very conservative assumption) with a volume of 1.0 m^3, the leachant velocity would be 1000 L/m^3 of solid. Since the density (bulk unit weight) of the treated solid is 1.9 gr/cm^3, the amount of acid passed through the solid would be 526 L/1000 kg of solid per year. The annual flow rate of acid would be 0.0526 eq/1000 kg for the rainwater, and 52.6 eq/1000 kg for the landfill leachant. Therefore, the lime kaolinite-sand (1.0 m thick) layer can withstand 18,346 years of rainfall leaching and 18.3 years of landfill leachate leaching without any significant release of As and Cr.

The calculation steps used above are summarized in the following equation:

$$Duration(years) = \frac{ANC \times \gamma_{bulk} \times V}{C \times P \times A} \qquad (12)$$

where, ANC = the acid neutralization capacity value in meq/gr of soil, for which heavy metal release exceeds regulatory standards, γ_{bulk} = the soil wet unit weight, in gr/cm^3, V = the volume of the remediated layer in cm^3, C = the acidity of leaching solution expressed as meq/cm^3, P = the rainfall intensity equaling 1.0 m/year, and A = the intersection area of the remediated solid in cm^2.

The long term leaching behavior of the treated specimens was also assessed by combining the TCLP and ANC batch test results. The acid neutralization capacity (ANC) experimental results presented in Figure 4, indicated approximately 4 equivalents of acetic acid per kg of soils treated with 10% of quicklime were required to lower the suspension pH level down to a value of 5.0. Combining the ANC results and the TCLP results (Figures 92 and 93), we can estimate that one kg of the solids treated with 10% of quicklime could withstand 4 equivalents of acid leaching while meeting the As and Cr TCLP criteria for non-hazardous waste. A simple calculation shows this kind of treated solid can last 76,000 years and 76 years for the typical rain water and landfill leachant leaching, respectively.

Overall, the elapsed time to break-through release calculated based on the TCLP and ANC results is about 4 times as long as the time predicted based on the flow-through results. This may indicate under flow-through leaching

conditions, less lime was available to neutralize the acid than under TCLP leaching conditions. If testing time were not an issue and a more realistic (close to field values) hydraulic gradient was used, the resulting flow velocity would have been lower and the reaction time between the leachant and the soil would have been substantially longer. Under such conditions, the break-through time (duration of the remediation application) may have been closely predicted by the TCLP and ANC plots (Figures 92, 93 and 94).

In the above duration calculation, it was assumed all rainwater passes through the remediated solid (the worst leaching scenario). However, the actual leaching rate follows Darcy's Law:

$$U = k \times i \tag{13}$$

where, U = the flow rate (cm/year), k = the average hydraulic conductivity of the waste form (cm/year), $i = Dh/L$, or the hydraulic gradient (dimensionless). Based on the hydraulic conductivity of the treated solid, the field hydraulic gradient, and acid-base properties of the waste and leachant, the duration of waste form can be calculated using Equation 14a.

$$Duration(years) = \frac{ANC \times \gamma_{bulk} \times V}{C \times k \times i \times A} \tag{14a}$$

or

$$Duration(years) = \frac{ANC \times \gamma_{bulk} \times H}{C \times k \times i} \tag{14b}$$

Using the above equation (14b), a hydraulic conductivity value of 10^{-7} cm/sec, which is an average value for the specimens tested during the present study, an ANC value of 4 eq/L as derived from the batch leaching tests, and the actual specimen height and bulk density data as determined during the present study, we can plot the expected duration of the lime treated soils tested during the present study, versus the hydraulic gradient and infiltration acidity scenarios (Figure 97).

In Figure 97, we also plotted separate lines indicating the value of the hydraulic gradient (i = 270) and the test duration time (200 days), for which the flow-through leachate for the kaolinite sand lime-treated specimen dropped to a value lower than 5.0, thus indicating the end of treatment effectiveness. The fact that this point of intersection, A is lower than the one predicted based on Figure 97 (point B), signifies the fact that the ANC value of 4.0, as determined during batch leach testing, is not appropriate for actual flow-through leaching conditions. Overall, treatment effectiveness becomes more pronounced when we consider the actual field hydraulic gradient regimes (i.e., hydraulic gradient, i = 0.1), and rainwater infiltration. Under such conditions, treatment effectiveness is expected to last for hundreds of thousands of years (Figure 97).

For treatment design purposes, a modified *extended ANC* test can be performed on a given waste form, where except for the extract solution pH, heavy metal concentrations in the extract solution are also measured so the amount of acidity that needs to be percolated through the given waste matrix for regulatory compliance to

be jeopardized, could be established. Based on the obtained ANC value, the leachant acidity input, and the waste form permeability using Figure 97, we can predict the duration of the remediation scheme (for how long it will be effective). Conversely, Figure 97 can be also used to design for the level of treatment, drainage conditions, etc. As more results are obtained upon conclusion of the remaining tests, and as new tests are currently designed where actual soils will be used, it is expected that Figure 97 will be augmented, and the factor quantifying the difference between batch and flow-through based predictions would be more accurately established. Then we could potentially evaluate and/or design a remediation treatment scheme by performing the *extended ANC* test described above (short duration and easy to perform test), estimating hydraulic conductivity and obtaining the infiltration rate and acidity input.

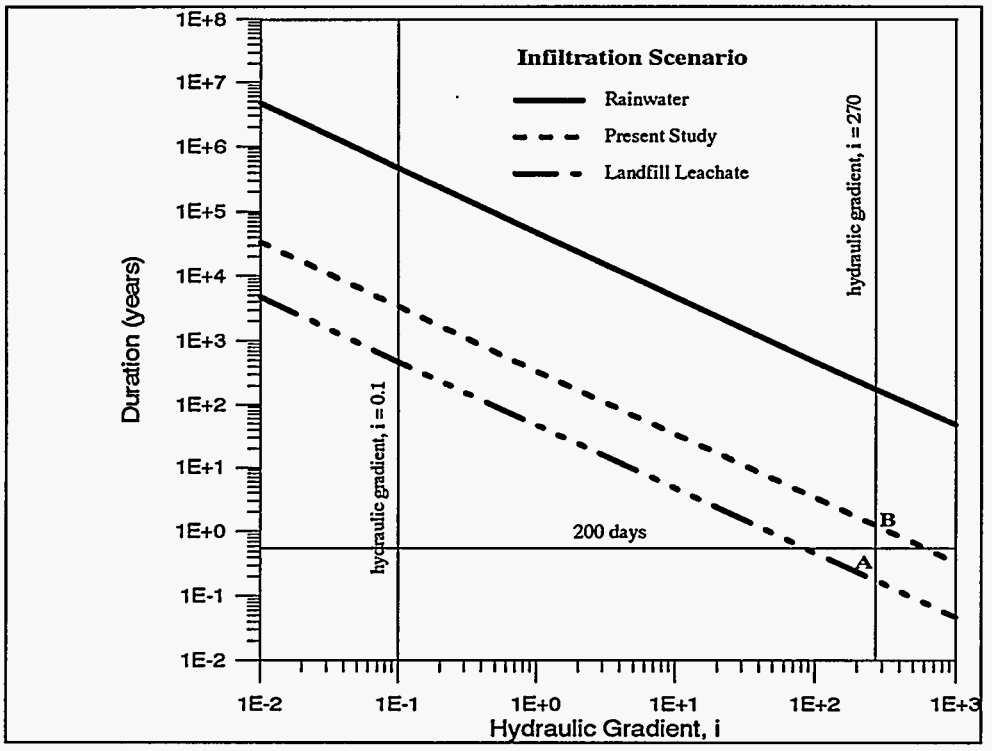

Figure 97. Prediction of the Duration of Lime-treated Soils under Different Hydraulic Gradients ($k = 10^{-7}$ cm/sec).

4.7.3 Summary

Based on the results obtained during the present study, heavy metal immobilization in the quicklime treated soils was evaluated following three distinct approaches. First, to test for regulatory compliance, heavy metal release was established following the TCLP batch testing approach. To establish actual field levels of heavy metal release, specimen monoliths were tested under both static and flow-through leaching conditions. Out of these three approaches, "worst case" heavy metal release scenarios were achieved during flow-through leaching. Conversely, "best

case" heavy metal release conditions were observed during static leaching. Moreover, heavy metal release was maximum for the kaolinite-sand solid matrices.

In lieu of the above, predictions were made to establish treatment duration effectiveness under actual field conditions. These predictions were mainly based on the kaolinite-sand flow-through testing results, since they provide the "worst case", maximum heavy metal release conditions. Based on such an approach, it was found that under actual field conditions of rainwater infiltration, treatment will be effective for at least hundreds of thousands of years (Figure 97). However, since flow-through testing is a time consuming endeavor, predictions of treatment duration were also made based on TCLP and ANC batch results. Treatment effectiveness duration is consistently overpredicted by a factor of about 4, when TCLP-based predictions are made. However, performing TCLP and ANC batch extraction is a much simpler and less time consuming process as compared to conducting flow-through experiments. Therefore, we propose a modified extended ANC test to be used as a prediction tool for treatment effectiveness duration, and as a design tool ensuring long-term treatment effectiveness.

4.8 Quicklime Treatment of Contaminated Field Samples

The results obtained for the artificial soil mixes have amply demonstrated the quicklime-based treatment is an effective technique to immobilize As, Cr, and Pb, and to improve the geotechnical properties of the soils. However, the chemical and mineralogical compositions of contaminated field soils may be quite different from the artificial soils used during our laboratory studies. Therefore, it was necessary to conduct a laboratory treatability study using contaminated field soils before a pilot scale field treatment scheme will be designed and undertaken. In May 1994, four heavy metal contaminated samples (2 kinds of heavy metal sludges from the Crystal Mine site, tailings from the Cataract Creek tailing facility, and a soil sample from Anaconda, Montana) were received from MSE, Inc., Butte, Montana. The samples were tested for water content, TCLP leachability, particle size distribution, soil pH and optimum water content. Batch treatment experiments were also conducted to establish the quicklime content that should be used during the compaction treatment step. Finally, the effectiveness of the quicklime-based treatment to stabilize/solidify the contaminated field samples was evaluated based on our testing results.

4.8.1 Physical and Chemical Properties of the Contaminated Materials

The water content of the samples was measured by drying the samples at 110°C for 24 hours in accordance with ASTM D 2216-92 (ASTM, 1992b). The sludge samples had 72 to 74% of water which was consistent with the values reported by the contaminated sample provider, MSE, Inc. (Table 9). The tailing and soil samples contained moderate to low percentages of water.

The liquid and plastic limit tests were performed in accordance with the ASTM D 4318-84 multipoint method (ASTM, 1984) using air-dried samples. The samples were sieved and the portion of solid that passed through #40 sieve was used for these tests. Sludge samples (#1 and #2) had very high liquid limit values (Table 9), mainly because of their fine particle gradation (about 80% finer than US sieve No. 200). It was impossible to perform liquid limit tests on the Cataract Creek tailing sample and the Anaconda soil sample. Owing to their silty sand texture and gradation, these samples possessed no plasticity whatsoever (similar to a quartz clean sand). The plastic limit for the sludge (#1) was determined to be 69%. A similar value was assumed for the other sludge sample (#2). Plastic limits could not obtained for the soil and tailing samples and they were determined to be non-plastic.

The pH level of the soils and sludges is an important parameter controlling the leachability of heavy metals in these materials since the solubility and adsorption behavior of the heavy metals is mainly affected by soil pH. pH determination is also important towards estimating the amount of quicklime needed for addition to the contaminated materials in order to successfully immobilize the heavy metals. According to ASTM D 4972-89 (ASTM, 1989) the pH level of the samples was measured by mixing 10 grams of air dried sample

with 10 mL of distilled and de-ionized water. The pH level of the suspension was measured after the suspension had been agitated for one hour. The sludge and soil samples had very low pH values (Table 9). The pH level of the tailing was also relatively low (pH = 5.9).

Table 9. Physico-chemical Properties of the Field Soil Samples

Sample Designation	Water Content %	Specific Gravity	Natural Soil pH	Liquid Limit %	Plastic Limit %
Sludge 1	74.5	2.70	2.6	105	69
Sludge 2	72.3	2.64	2.5	101	69
Anaconda Soil	3.4	2.66	3.7	ND	ND
Cataract Creek Tailing	9.7	2.72	5.9	ND	ND

ND - not determined

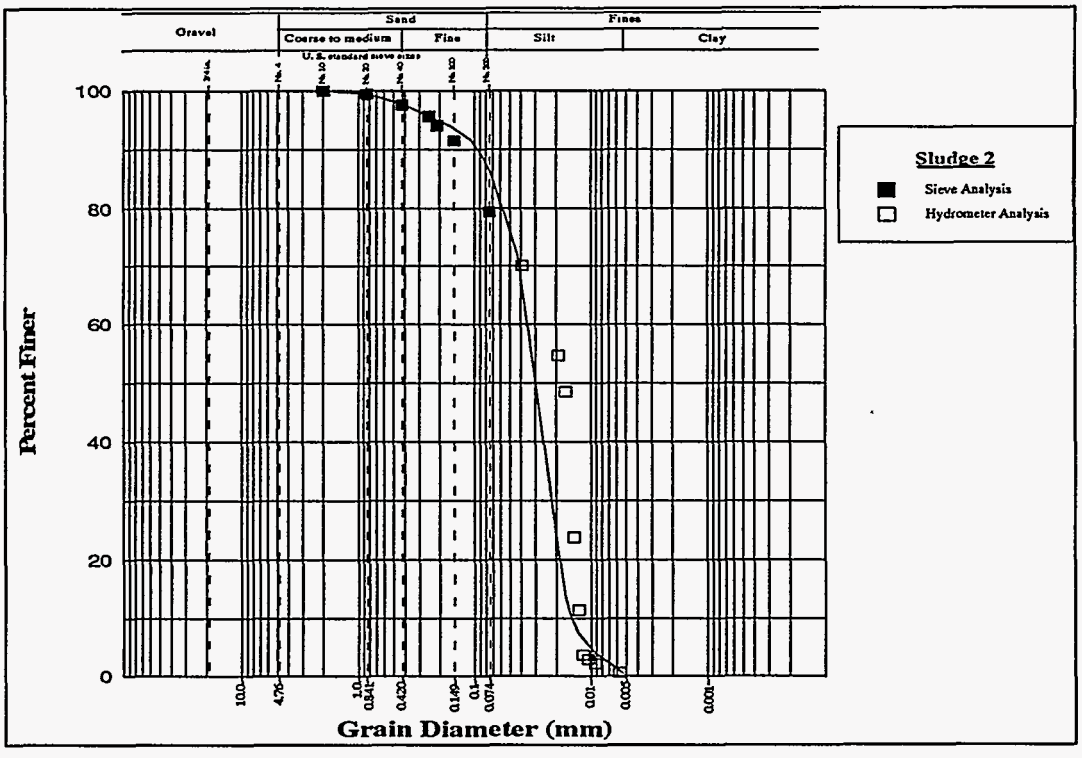

Figure 98. Particle Size Distribution of Sludge 2 Sample.

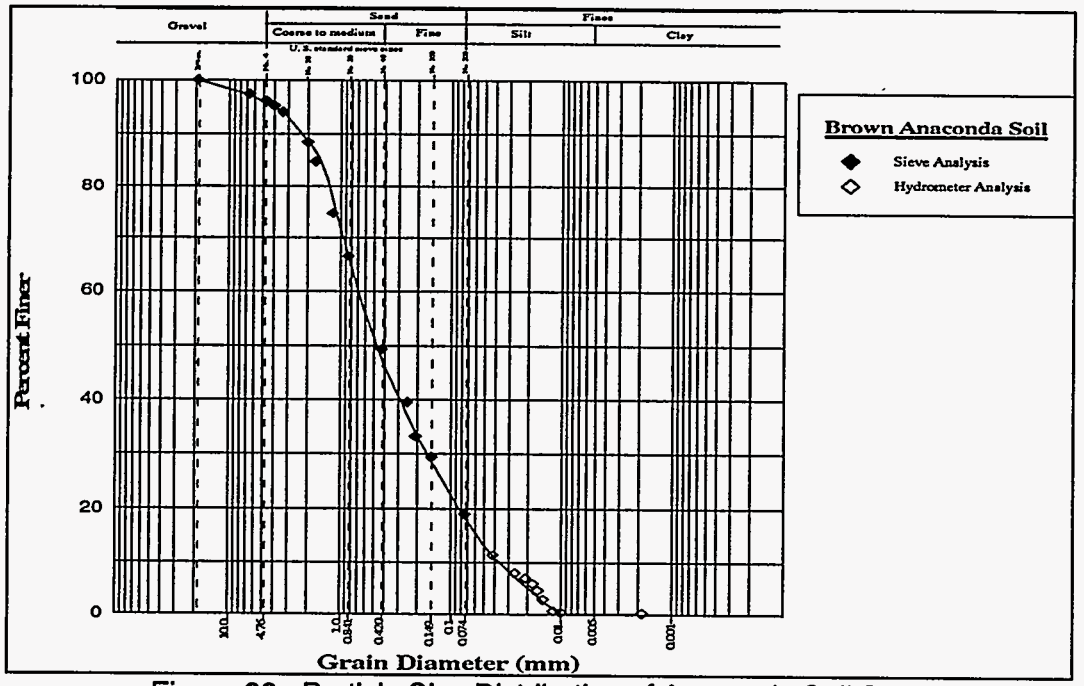

Figure 99. Particle Size Distribution of Anaconda Soil Sample.

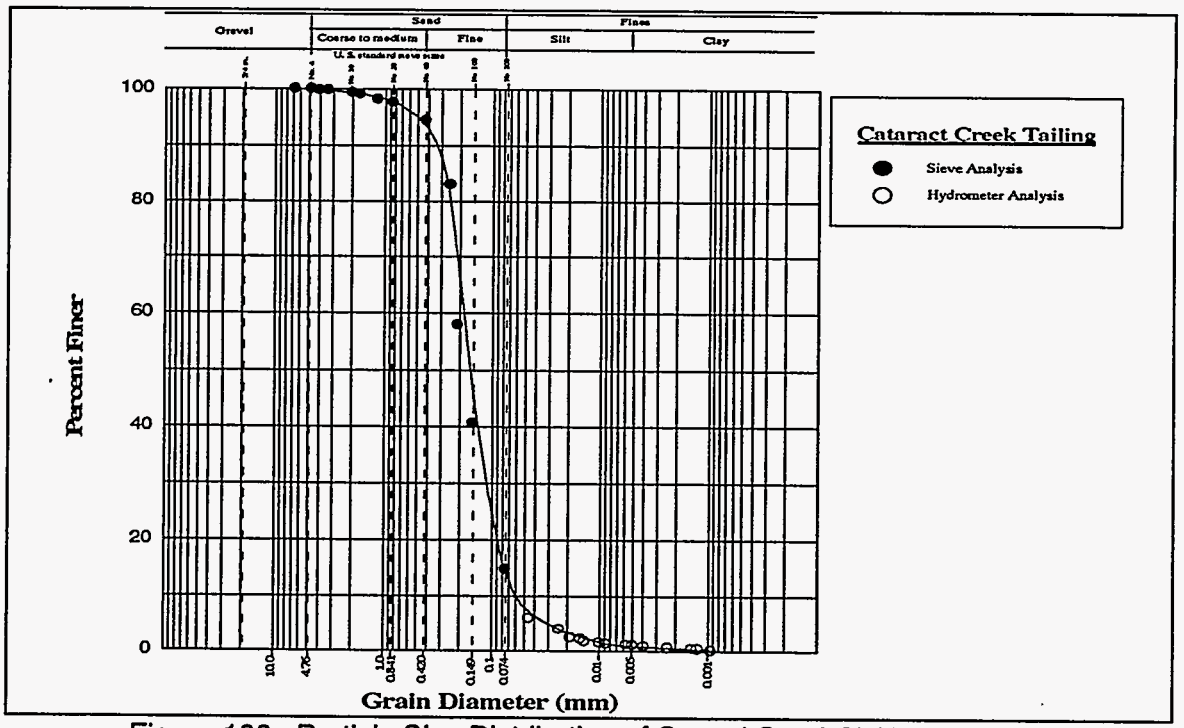

Figure 100. Particle Size Distribution of Crystal Creek Tailing Sample.

All particle size analyses were conducted on oven-dried samples in accordance with ASTM D 2217-85 (ASTM, 1985a), ASTM D 421-85 (ASTM, 1985b) and ASTM D 422-63 (ASTM, 1963). For the mechanical sieve analysis, the wet method of sample preparation was followed. Soil samples were washed with DI water on the #10 sieve and separated solids were dried in the oven. After the

solid was pulverized, a mechanical sieve analysis was performed on the soil samples using a combination of sieves. The finer portion of the solid (finer than #200 sieve) was then used for hydrometer analysis. Since the soil pH level was lower than 7.0 for all samples, sodium metasilicate (water glass) was used as the dispersing agent. A concentrated solution of sodium metasilicate was prepared for the hydrometer analysis. The results of the combined particle size analysis indicated sludge 2 was essentially a fine-grained soil with more than 79% passing through the #200 sieve (Figure 98). Hydrometer results indicated the fine fraction of the sludge was predominantly silt-size material with a negligible clay fraction. Grain size distribution results for the Anaconda soil indicated it was essentially a well graded fine-silt sand (Figure 99). It can be classified as SM or SC group symbol based on the Unified Soil Classification System. The Cataract Creek tailing is a uniformly graded fine-silty sand (Figure 100).

The leachability of heavy metals in the contaminated solids was evaluated using the US EPA TCLP. As and Cr concentrations in the TCLP leachate were less than 1 ppm for all samples (Table 10). The leachability of lead in the samples was also low. Overall, none of the tested samples failed the TCLP criteria for non-hazardous waste (5 ppm). TCLP results suggested the leachable fraction of the heavy metals in the contaminated sludges, soil, and tailing had already been leached out in the field, as can be seen by the low pH level of the samples (Table 9).

To determine the total amount of heavy metals in the waste samples, the lithium tetra borate fusion method was used to digest the solids in accordance with ASTM E 886-88 (ASTM, 1988). Sludge samples and the Cataract Creek tailing sample contained high contents of As and Pb (Table 10). Heavy metal contents in the soil sample were significantly lower than those in sludge and tailing samples. TCLP and total digestion results (Table 10) indicate only small fraction of the As, Cr, and Pb in the contaminated materials was leachable under TCLP leaching conditions.

Table 10. TCLP and Total Digestion of The Field Soil Samples

Sample Designation	TCLP Concentration				Total Digestion concentration*		
	As (ppm)	Cr (ppm)	Pb (ppm)	TCLP pH	As mg/kg	Cr mg/kg	Pb mg/kg
Sludge 1	0.08	0.07	1.19	4.12	4,3420	972.4	3,068
Sludge 2	0.23	0.50	0.64	4.26	2,6940	204.0	2,570
Anaconda Soil	0.50	0.09	1.31	4.85	814	252.6	459
Cataract Creek Tailing	0.12	0.02	0.71	4.90	2,964	299.2	3,530

* Lithium tetra borate fusion method

4.8.2 *Optimum Lime Content Study*

The optimum lime content tests were conducted according to ASTM C 977-89 (ASTM, 1990) standard procedure for soil-lime stabilization. The basic thrust of the pH procedure is to add sufficient lime to the soil to ensure a pH level of 12.4

for sustaining the strength producing soil-lime pozzolanic reaction (Transportation Research Board, 1987). This test method usually provides a soil-lime proportion for stabilization and gives an indication whether the soil in question can be effectively stabilized.

For the sludge #1 sample, approximately 4% of lime was needed to raise the pH level of the mix to 12.0 (Figure 101). However, much more lime (~9%) had to be added to sludge #2 to reach a pH level of 12.0. The minimum amount of lime needed for the soil and tailing was approximately 3% (Figure 102).

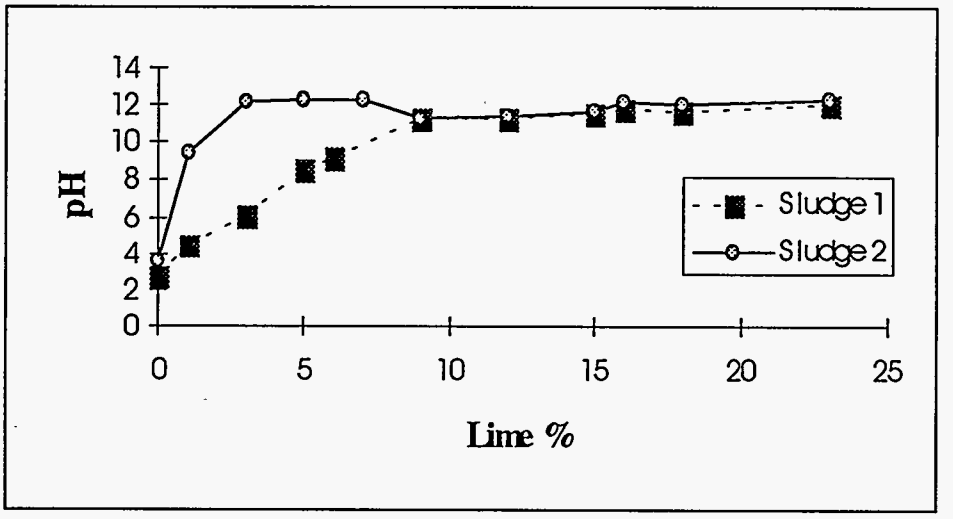

Figure 101. Optimum Lime Content Results for Sludge Samples.

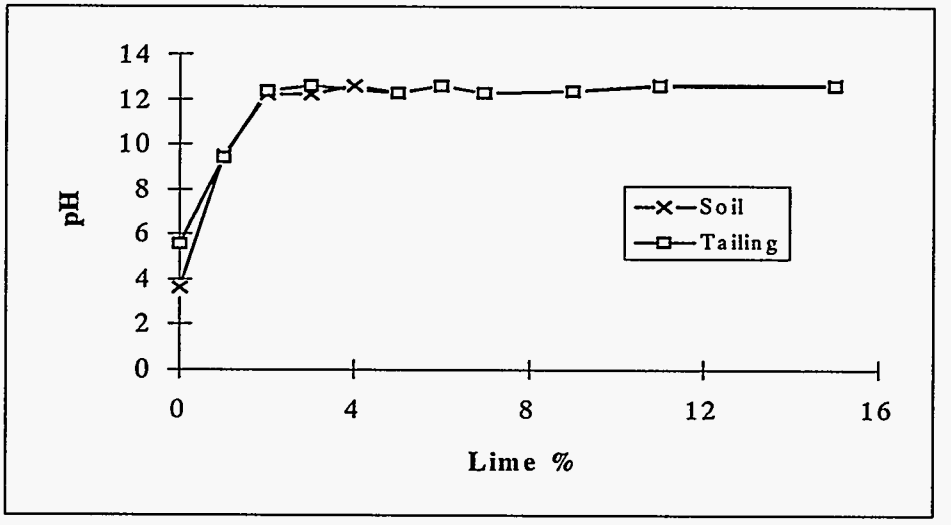

Figure 102. Optimum Lime Content Results for Soil and Tailing Samples.

4.8.3 *Micromorphological Properties of Contaminated Field Materials*

SEM micrographs (Figures 103 and 104) show that the Crystal Mine sludges mainly contained aggregates of fine particles. The size of the primary particles was in the range of 0.2 to 0.5 μm. Both the Anaconda soil and Cataract Creek tailing samples contained large sand as well as fine particles (Figures 105 and 106). However, the surface properties of the sand in these two samples were quite different. While the sand in the tailing sample showed smooth uncovered surfaces, the sand of the Anaconda soil sample was coated with fine particles.

Energy Dispersive X-ray (EDX) analyses indicated (Table 11) that both sludge samples contained approximately 50% of iron (Fe) and a high arsenic content (approximately 14%). The silicon content in the sludge samples was only 10 to 20%. Both SEM micromorphological and EDX chemical results suggested that the sludges attain a high capacity to contain heavy metals within the solid phase, because of their high surface area (fine particles) and their high Fe oxide content. The Anaconda soil sample consisted mainly of Si, Fe, Ca and Al (Anaconda Soil, average in Table 11). When EDX analyses were conducted on the Anaconda soil sand surface, only 48.7% of Si was detected (Anaconda Soil, sand in Table 11). Significant amounts of Fe, Ca and Al were also detected on the soil sand surface. The surface composition results agreed with the SEM observations (Figure 106), showing that Fe, Ca and Al minerals were formed on the sand surface. The Cataract Creek tailing surface had higher Si and Fe contents (Cataract Creek Tailing, average in Table 11) than the soil sample. The tailing sand surface contained 97.3% of Si, which confirmed that the sand was not covered by other minerals.

Overall, based on the micromorphological and surface chemical properties of the samples, it can be predicted that the sludges should have higher capacity to contain heavy metals than the soil and tailing samples. However, the heavy metal leachability can not be predicted based only on the physical and chemical properties of the materials. Total heavy metal content and previous leaching history of the materials in the field are also important factors towards assessing heavy metal release.

Table 11. Surface Chemical Composition of Contaminated Samples Determined Using EDX.

Samples	Al%	As%	Ca%	Cu%	Fe%	K%	S%	Si%	Ti%	Zn%
Crystal Mine Sludge 1	4.2	14.2	0.0	6.5	54.1	1.1	4.8	10.9	0.0	4.2
Crystal Mine Sludge 2	7.2	13.0	4.9	0.0	49.0	2.5	3.9	19.4	0.0	0.0
Anaconda Soil, average	6.1	0.0	24.1	2.1	23.8	4.1	3.5	35.4	0.8	0.0
Anaconda Soil, sand	11.0	0.0	17.1	0.0	15.9	4.2	3.1	48.7	0.0	0.0
Cataract Creek Tailing, Average	3.3	0.0	0.0	0.0	28.5	3.6	3.2	61.4	0.0	0.0
Cataract Creek Tailing, Sand	0.0	0.0	0.0	0.0	2.7	0.0	0.0	97.3	0.0	0.0

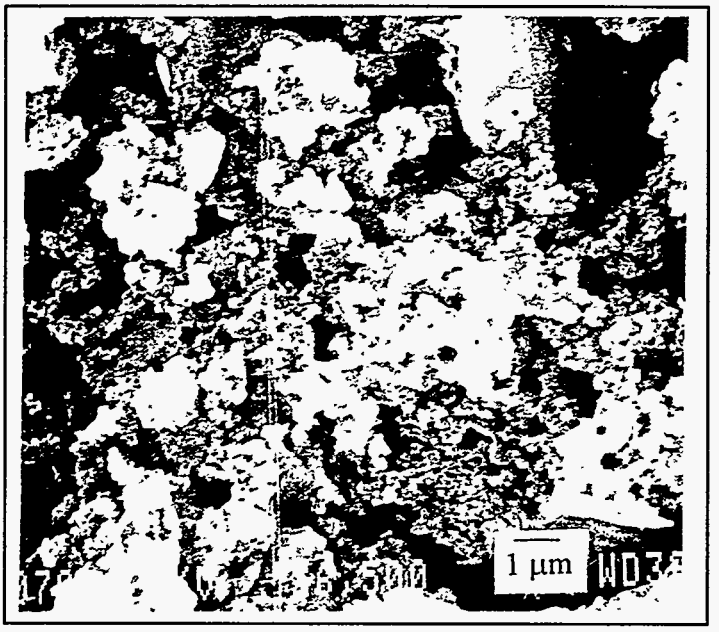

Figure 103. SEM Micrograph of Crystal Mine Sludge #1.

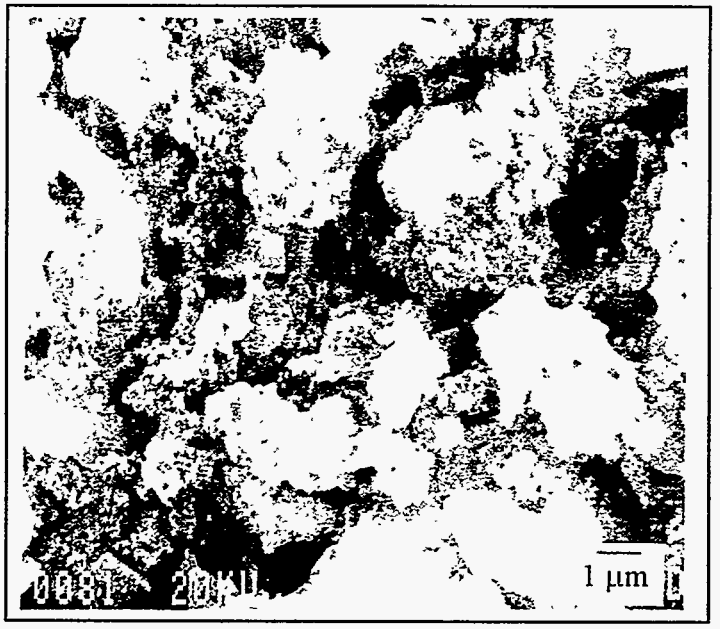

Figure 104. SEM Micrograph of Crystal Mine Sludge #2.

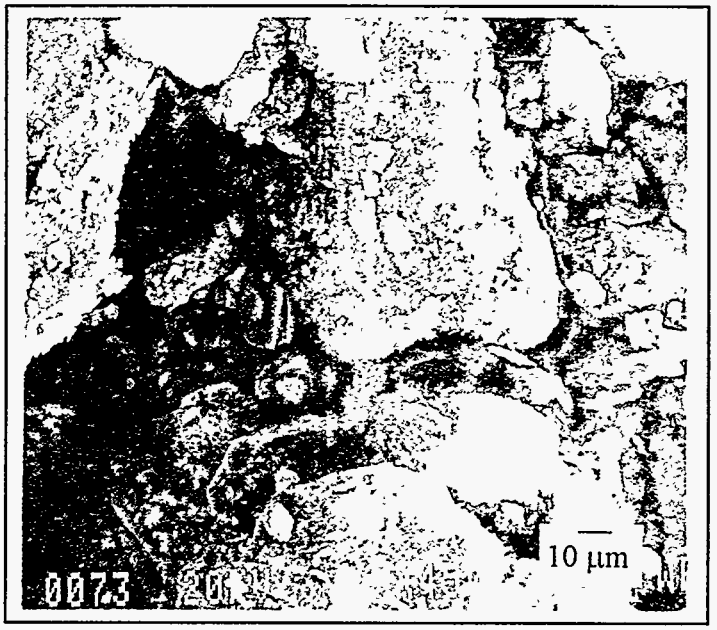

Figure 105. SEM Micrograph of Anoconda Soil.

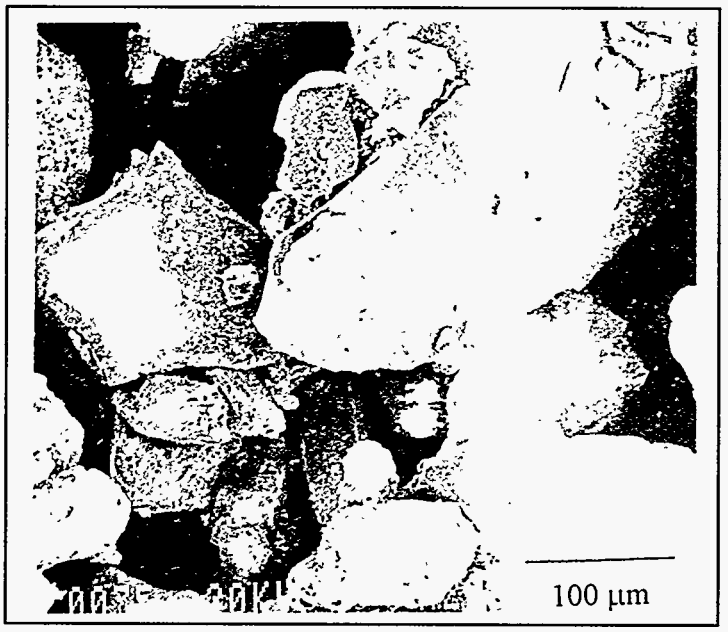

Figure 106. SEM Micrograph of Cataract Creek Tailing.

4.8.4 *Mineralogical Properties of Contaminated Field Materials*

New mineral formation following treatment of the contaminated soils is an important factor controlling the solubility and adsorption/inclusion behavior (mobility) of the heavy metals in the solid matrix. The understand of soil mineralogical properties are also necessary for the proper design of S/S applications for hazardous wastes. Therefore, the four contaminated field samples were analyzed using X-ray diffraction techniques to obtain their mineralogical compositions prior to as well as following treatment. Clear X-ray scans were obtained for both the Cataract Creek tailing and Anaconda soil samples (Figures 107 and 108). However, many small and poorly resolved peaks were observed in the X-ray scans for the Crystal Mine sludges (Figures 109 and 110). These results indicated that a large amount of poorly crystallized minerals are present in the Crystal Mine sludges.

The main minerals identified in both the Cataract Creek tailing and Anaconda soil were quartz, mica (roscoelite), and iron oxides (ferrihydrite) (Figures 107 and 108). Arsenic oxide (As_2O_5) was also detected for the Anaconda soil sample, which suggested the presence of the oxidized As(V) form in the solid. Quartz and mica (roscoelite) were the main minerals identified in the Crystal Mine sludges as well (Figures 109 and 110). In addition, several kinds of iron oxides (ferrihydrite, maghemite and hematite) were detected in the sludges. According to the information provided by the sample supplier (MSE), the Crystal Mine sludges contained approximately 263 g Fe/kg sludge (Table 12). However, the pertinent iron oxides peaks did not show high intensities in the X-ray scans. This indicates most of the iron oxides are present in the sludges in their amorphous or poorly crystallized forms. Quantitative X-ray analyses have to be performed in order to determine the percentage of iron in both mineral and amorphous forms. A chemical equilibrium calculation predicts that the $FeAsO_3 \cdot H_2O$ mineral should form when both ferric and arsenate ions are abundant in a solid. However, only arsenic oxide (As_2O_5) was detected for the sludges. The mineralogical information and low As leachability data suggested that As was associated with amorphous iron oxides.

Table 12. Chemical Composition of Contaminated DOE Field Samples

Samples	Chemical Contents (g/kg)												
	Al	As	Ca	Cd	Cu	Fe	K	Mg	Mn	Na	Pb	Si	Zn
Crystal Mine Sludge	--	60.20	--	0.03	0.30	263	--	--	0.21	--	1.82	--	0.82
Anaconda Soil	2.81	0.82	1.71	0.00	0.77	15.2	1.58	1.16	0.17	0.15	--	0.79	0.71
Cataract Creek Tailing	0.62	3.77	0.25	0.01	0.39	32.8	1.58	0.67	1.52	0.02	--	0.51	2.28

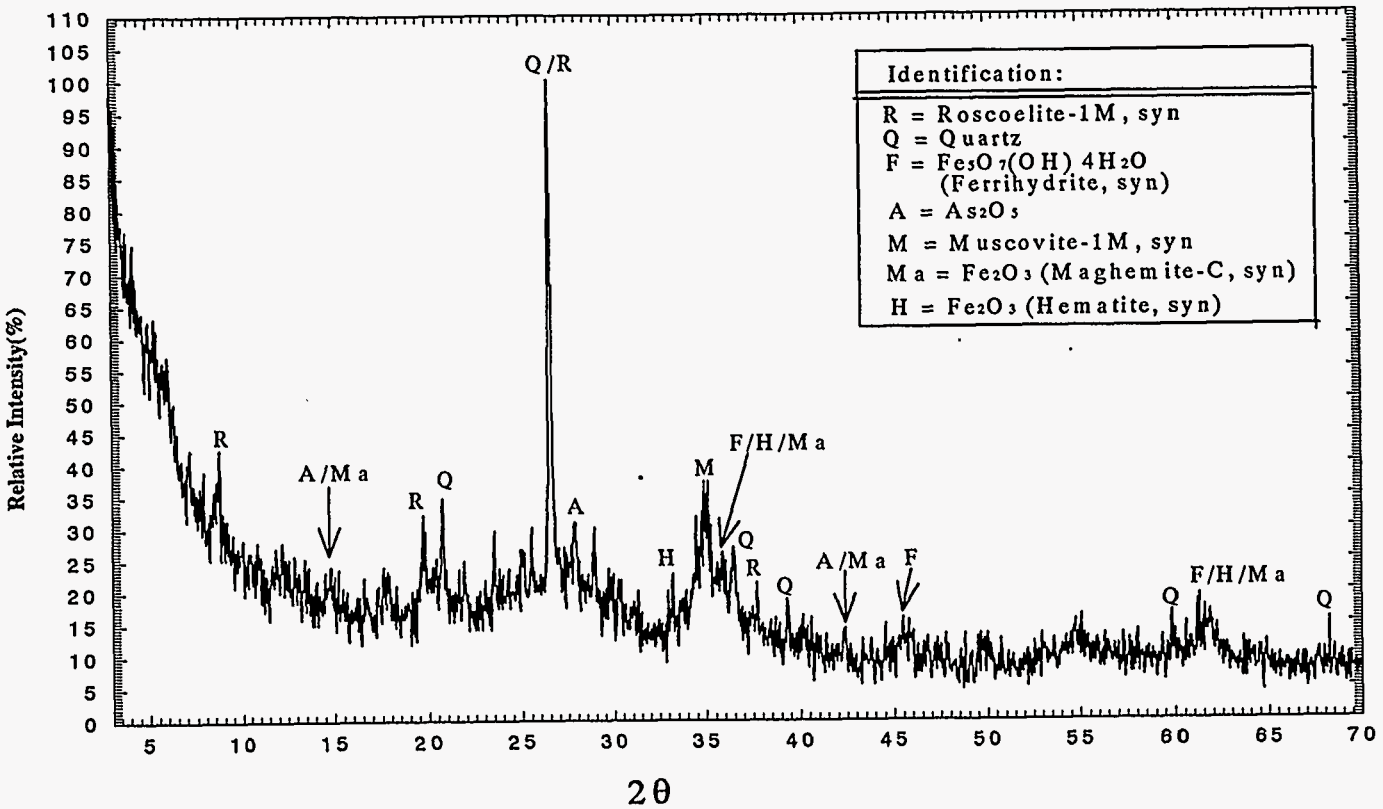

Figure 107: X-ray diffraction scan for Crystal Mine Sludge # 1 sample

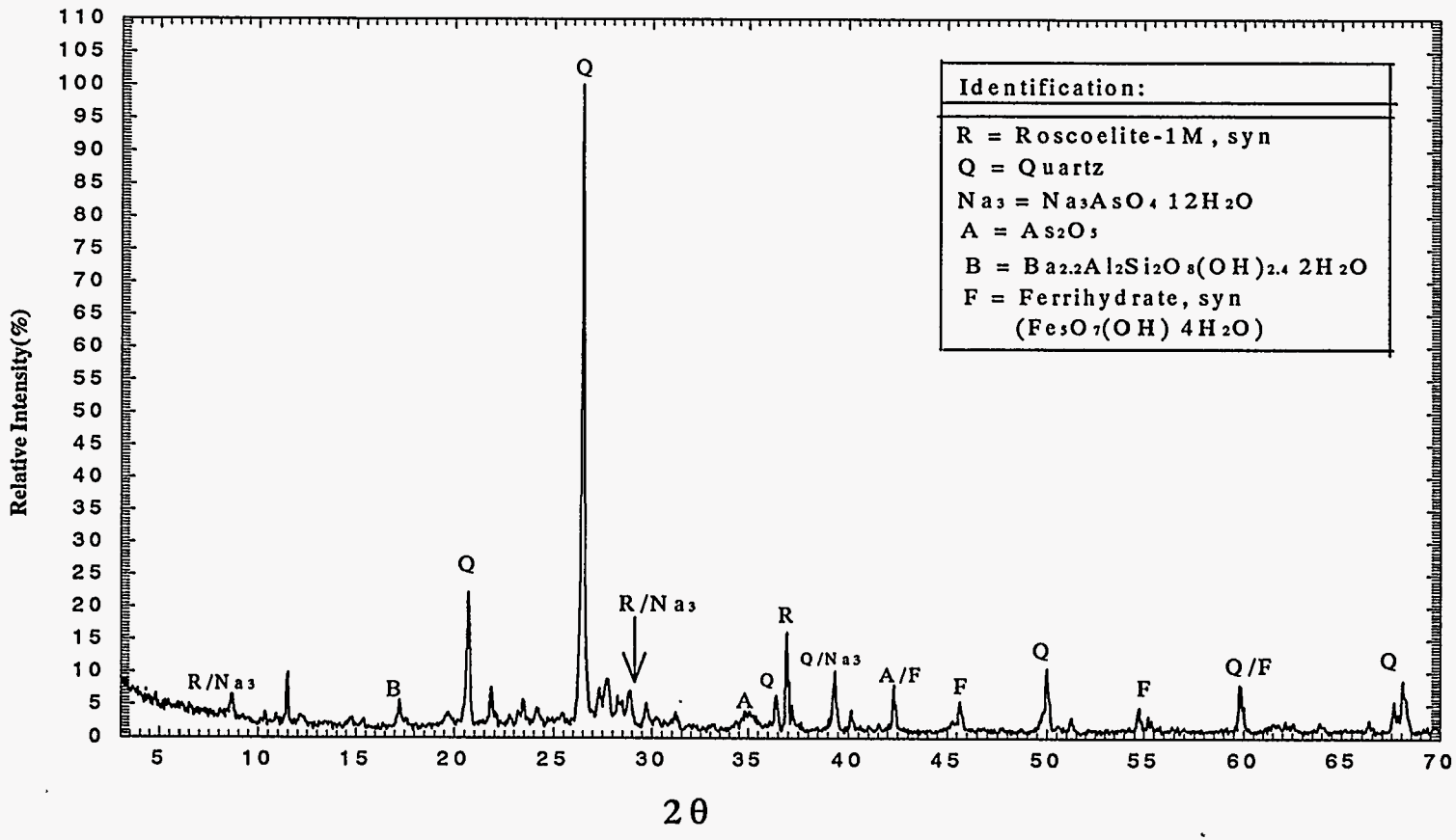

Figure 108: X-ray diffraction scan for Anaconda soil sample

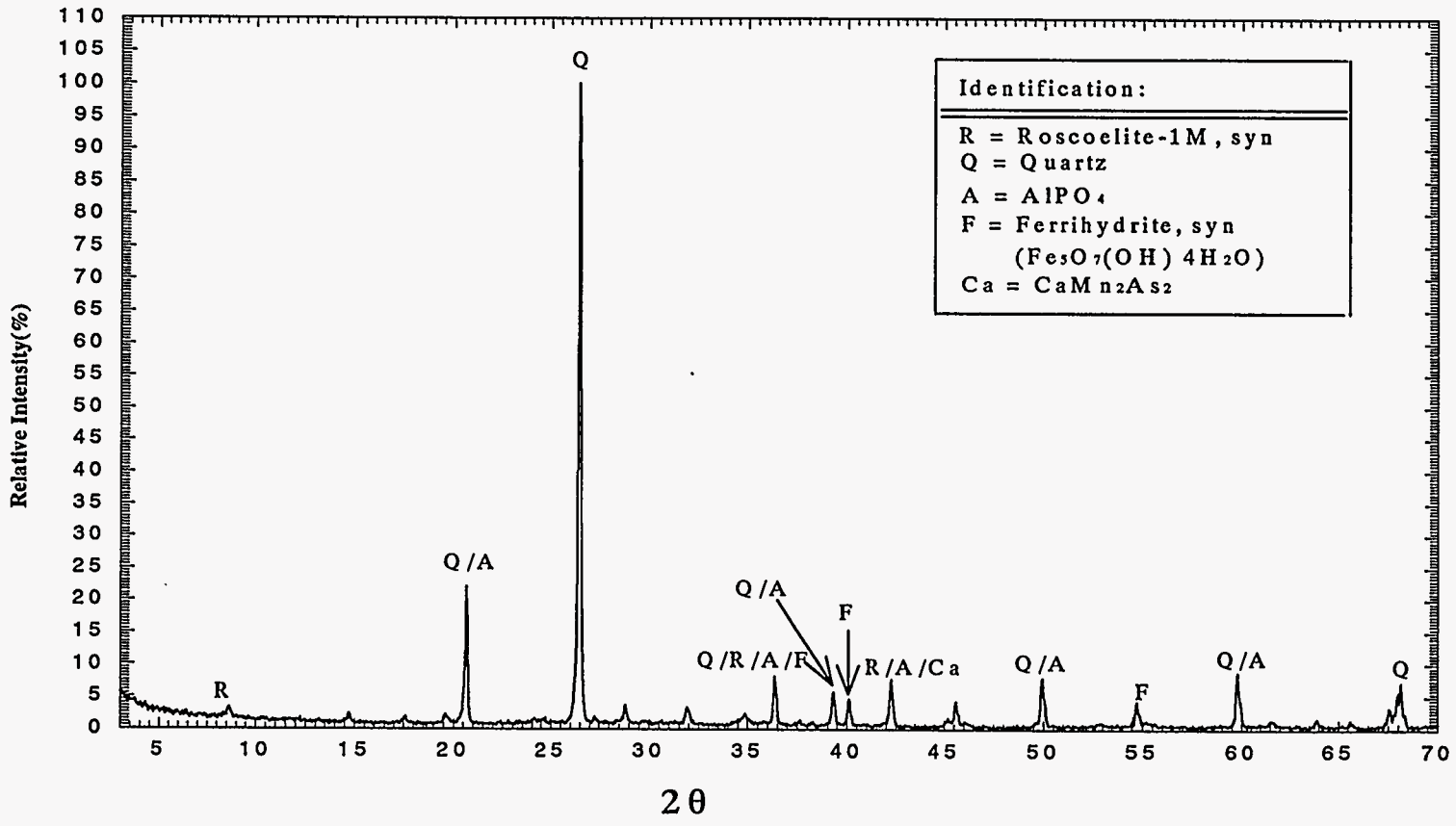

Figure 109: X-ray diffraction scan for Cataract Creek Tailing sample

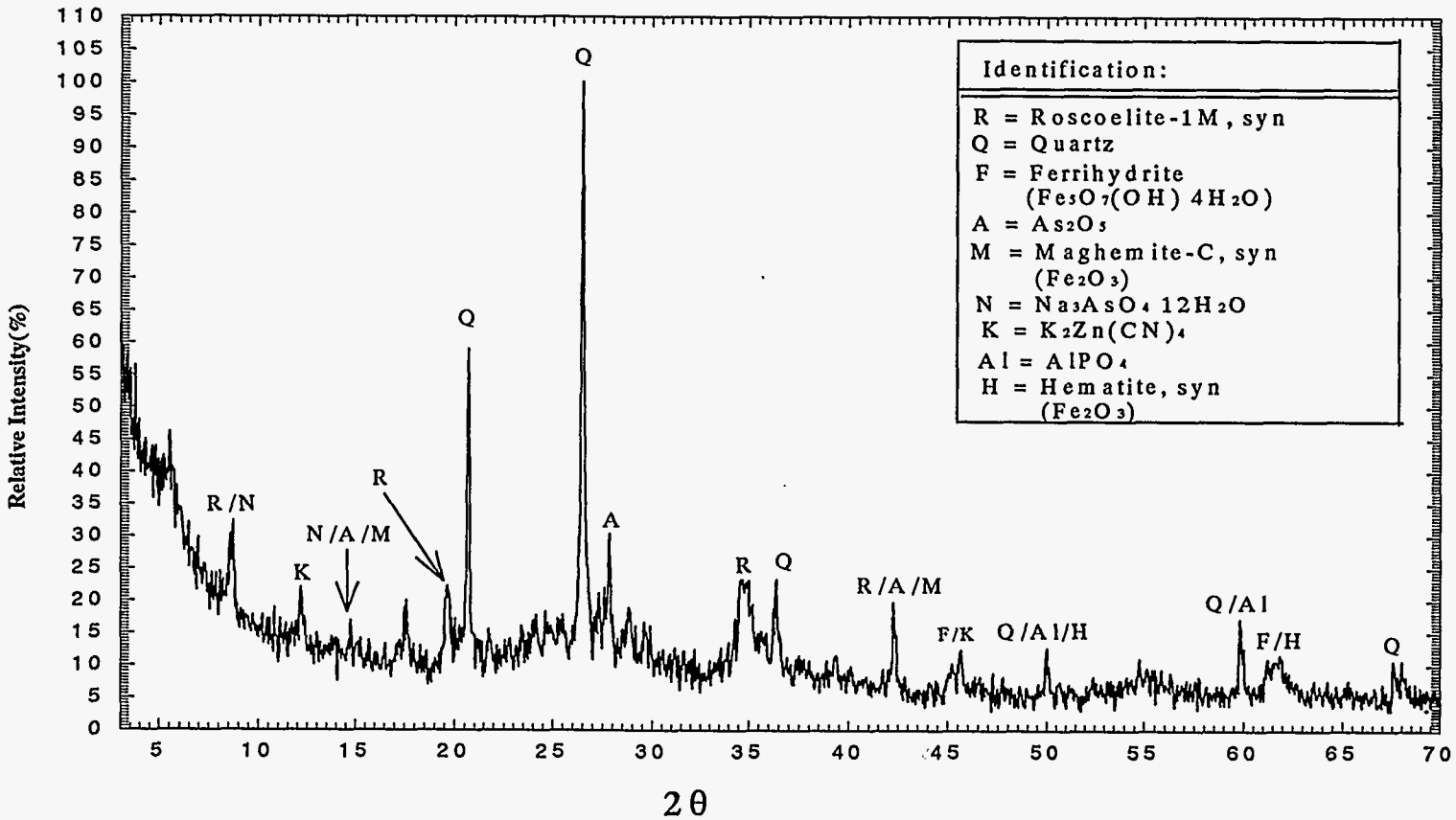

Figure 110: X-ray diffraction scan for Crystal Mine Sludge # 2 sample

4.8.5 *Heavy Metal Release at Different pHs*

TCLP results do not provide information on heavy metal leachability at various pH values, because the TCLP test is a single point batch extraction. Therefore, an "extended" TCLP test was conducted, in which heavy metals were extracted in a wide pH range. The extraction solution and other procedures used in this extended TCLP experiment were identical to those used in TCLP test.

The experimental results indicated that As concentration was low in the leachate when extraction solution pH was between 2 and 11 (Figure 111). When the pH was higher than 11 or lower than 2, significant amount of As was released from the sludge samples to the leachate. The release of Cr from the samples was low when pH was between 1 and 13 (Figure 112). A slight increase in Cr leachability was observed in the lower pH range. On the other hand, Pb release from the samples was increased when the pH was lower than 4 (Figure 113). The leachability of Pb from the Cataract Creek tailing was much higher than from any of the other samples.

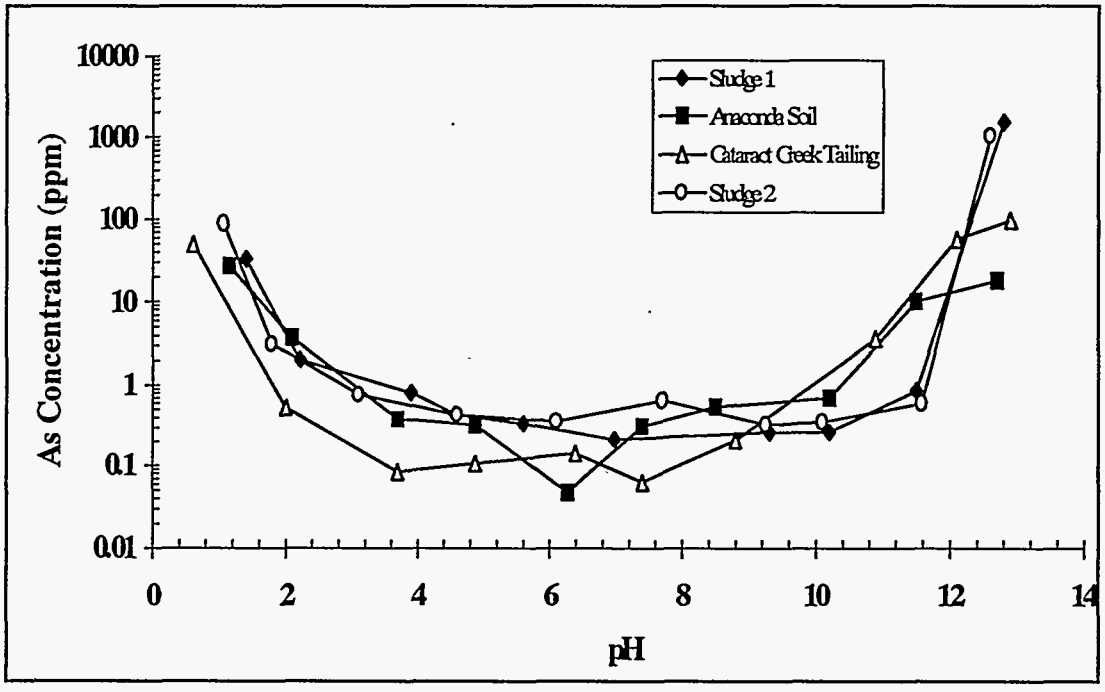

Figure 111. As Leachability in the Contaminated Samples as a Function of Leachate pH, Extended TCLP Extraction.

4.8.6 *Strength Development of the Treated Specimens*

It has been determined that both the Anaconda soil and the Cataract Creek tailings attain a fine-silty sand gradation (Section 4.8.1 of the topical report). Sandy materials are more vulnerable to leaching because of their high hydraulic

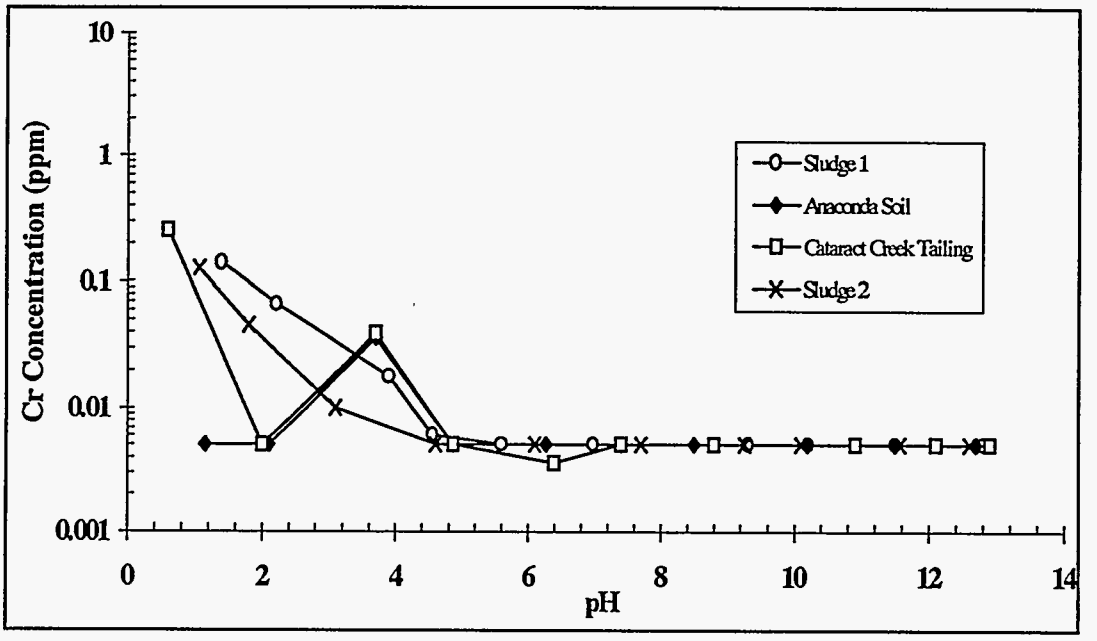

Figure 112. Cr Leachability in the Contaminated Samples as a Function of Leachate pH, Extended TCLP Extraction.

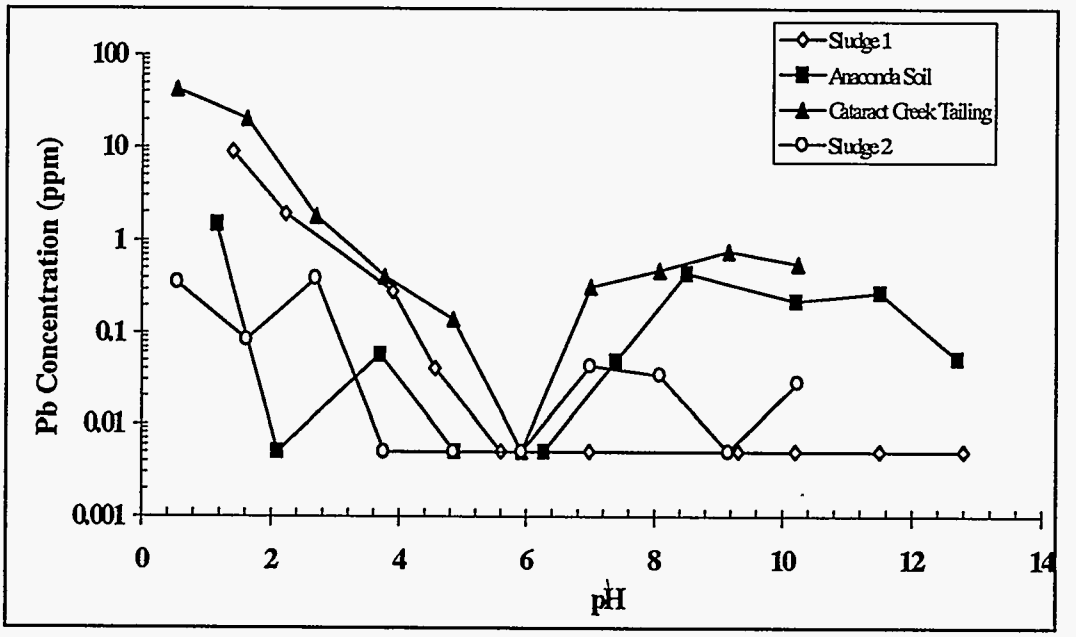

Figure 113. Pb Leachability in the Contaminated Samples as a Function of Leachate pH, Extended TCLP Extraction.

conductivity. Both the soil and tailings were treated in an attempt to produce monolithic solids with high strength and low hydraulic conductivity so as to limit the contact between the leachant and the contaminated soils. The levels of strength development in the quicklime treated and quicklime-fly ash treated samples are presented in Figures 114 and 115. When only quicklime was added, the treated soil and tailings showed only moderate strength development. This was due to the low clay content in the samples, which limits the formation of pozzolanic products. On the other hand, no obvious strength development was observed when fly ash itself was added into the samples. This was expected because the alkaline content in the fly ash was not high enough to raise the pH of the soil and tailings to 12. It is known that pozzolanic reactions will only take place in soils when the pH is higher than 12.0 or so.

The results in Figures 114 and 115 show that the combined addition of quicklime and fly ash led to a significant increase in the strength of both the soil and tailings. A maximum strength (706 psi and 335 psi for Anaconda soil and Cataract tailing, respectively, treated with 5% quicklime and 25% fly ash) was observed when quicklime content was 5%. When quicklime content increased from 5% to 10%, the strength of the quicklime treated specimen decreased. The results demonstrated that both binding materials (in this case fly ash and quicklime) had to be used to obtain significant strength gain for the sandy solids. Since the clay content in the soils and tailings was very low, the addition of excessive amount of quicklime resulted in strength loss. This observation is consistent with the strength results obtained for low montmorillonite (15%)-sand samples [2]. For M15 samples, strength decreased when quicklime content increased from 10% to 15%.

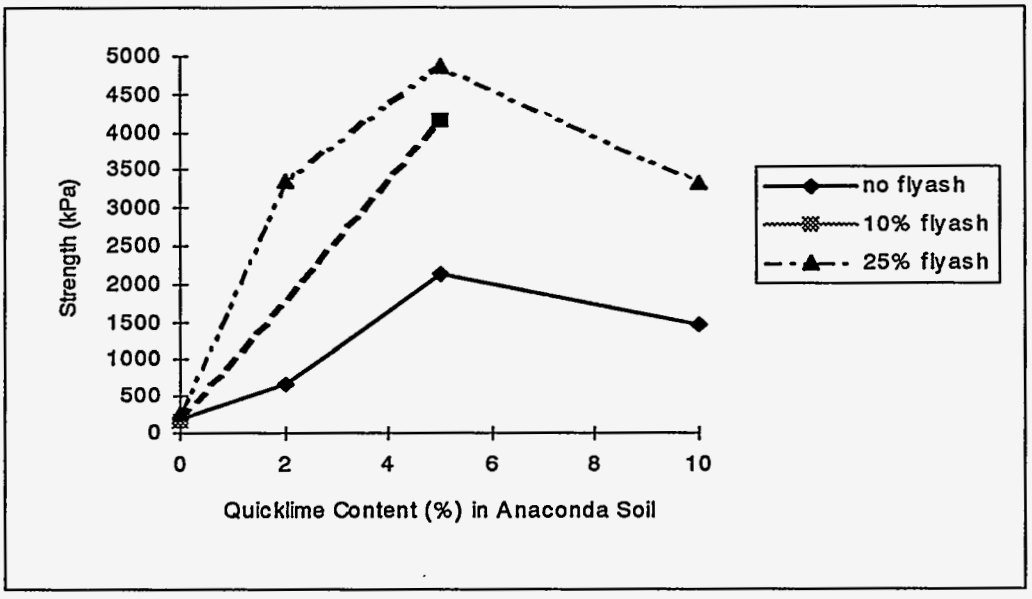

Figure 114. Strength Development of Quicklime/Fly Ash Treated Anaconda Soil, 28 Days Curing.

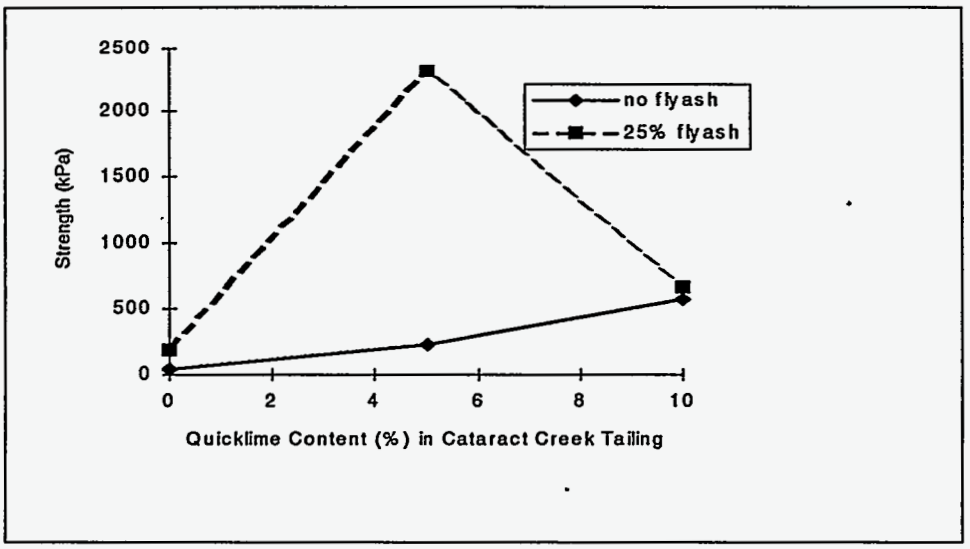

Figure 115. Strength Development of Quicklime/Fly Ash Treated Cataract Creek Tailing, 28 Days Curing.

4.8.7 *Vertical Swell of the Treated Specimens*

Swell is an important factor affecting the reuse potential of the treated solids as construction materials. High swell means that the solids may disintegrate under wet/dry weathering conditions. The disintegration of the solids may cause failure of the construction application altogether. Moreover, the immobilization of heavy metals will also be significantly affected by the disintegration of the treated solids. It is important to keep the solid in intact form in order to eliminate infiltration leaching, and to minimize the surface area exposed to leaching.

Swell tests were conducted by soaking the cured specimens in a water-saturated sand bath. The height of the specimens was measured on a weekly basis, and any visual observations, such as crack formation, were also noted. The swell results plotted in Figures 116 and 117 correspond to 5 weeks of continuous soaking. Overall, no swell was observed for any of the specimens. This is mainly because both the Anaconda soil and Cataract Creek tailings are sandy solids with minimum clay content. In addition, for all the specimens, except SC25L5 (S - soil, C25 - 25% class C fly ash, L5 - 5% quicklime), no ettringite formation was observed.

The swell results (Figures 116 and 117) indicate that the quicklime/fly ash treatment significantly improved the cohesive force in the solids. The untreated soil and tailing specimens (no quicklime and fly ash) disintegrated when they soaked in water. For the soil sample, the addition of 10% fly ash (SC10L0) or addition of 2% quicklime (SL2) resulted in adequate strength development. The specimens treated with 25% fly ash, or more than 5% quicklime, or a combination of 2% quicklime and 10% fly ash could withstand more than 5 weeks of soaking without any obvious signs of disintegration.

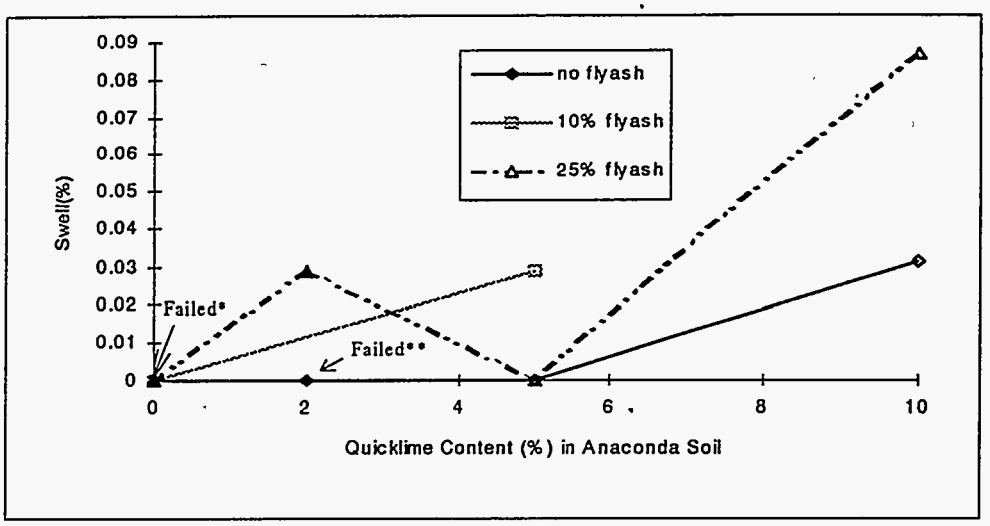

Figure 116. Swell of Quicklime/Fly Ash Treated Soil Specimens, 5 Weeks Soaking. * SL0 Sample (Untreated) Disintegrated in the Second Day of Soaking; SC10L0 Sample (Treated with 10% Fly Ash only) Disintegrated in the First Day of Soaking, ** SL2 Sample (Treated with 2% Quicklime only) Disintegrated in the Third Week of Soaking.

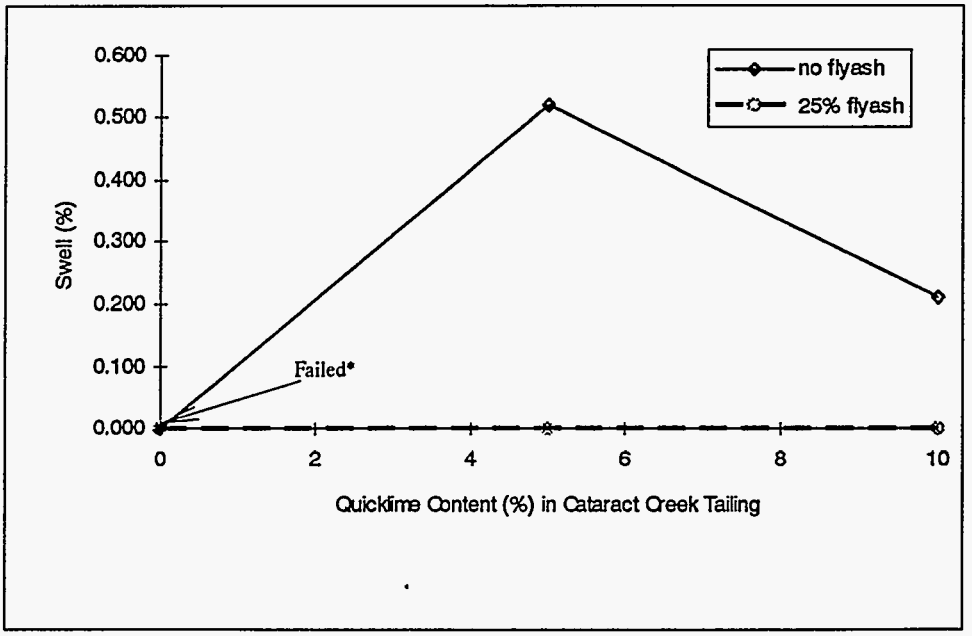

Figure 117. Swell of Quicklime/Fly Ash Treated Tailing Specimens, 5 Weeks Soaking. * TL0 samples (Untreated) Disintegrated in the First Day of Soaking.

4.8.8 *Heavy Metal Leachability of Quicklime/Fly Ash Treated DOE Samples*

Immediately following the strength test performance, samples were taken from the failed strength specimens, and tested for heavy metal leachability using the TCLP method. The leachability of heavy metals in the quicklime treated and quicklime-fly ash treated Anaconda soil samples are presented in Figures 118 to 120. Quicklime treatment obviously decreased the leachability of As, Cr and Pb. Lead concentration was reduced from 4.1 ppm to 0.4 ppm when the soil was treated with 2% of quicklime (Figure 120). No further reduction in Pb leachability was observed when quicklime content increased from 2% to 10%. Similar results were obtained for As (Figure 118) and Cr (Figure 119). When both quicklime and fly ash were used to treat the soil, no further reduction in As and Cr leachability was obtained comparing to the leachability of quicklime or fly ash treated samples. This was because As and Cr leachabilities in the quicklime or fly ash treated soils were already very low. The leachability of Pb in the quicklime-fly ash treated soil was lower than that in quicklime treated soil.

Heavy metal leachability in the treated tailing samples was different than that in the treated soil. When 5% quicklime was used to treat the tailings, no obvious reduction in heavy metals leachability was obtained (Figures 121 to 123). Lead leachability was actually increased when the tailing was treated with 5% quicklime (Figure 123). The leachability of the heavy metals was reduced when 10% of quicklime was used to treat the samples. Similar as the Pb leaching results in quicklime-fly ash treated soil, the addition of fly ash effectively reduced Pb leachability in the tailings (Figure 123).

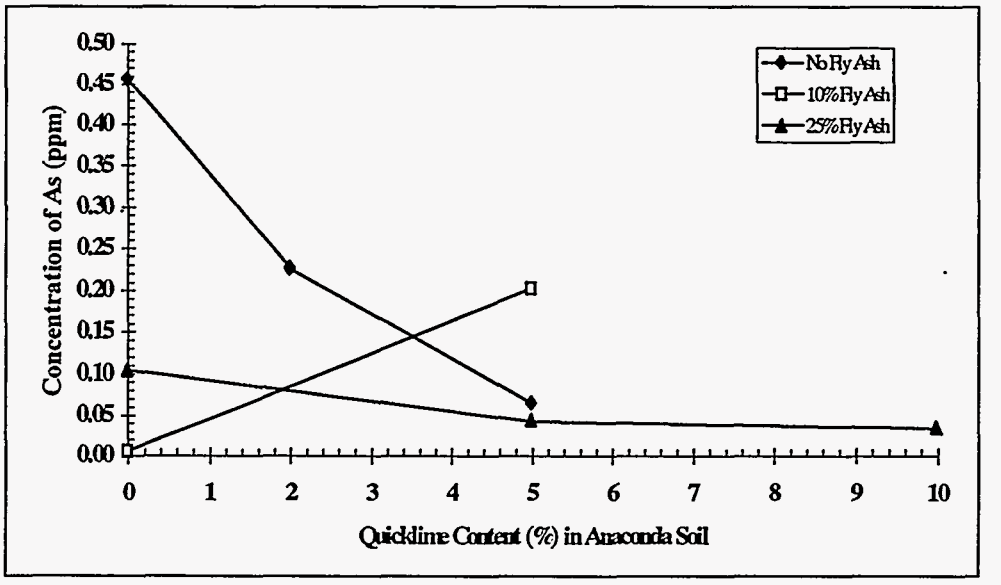

Figure 118. Arsenic Concentration in the TCLP Leachate for Quicklime/Fly Ash Treated Soil, 28 Days Curing.

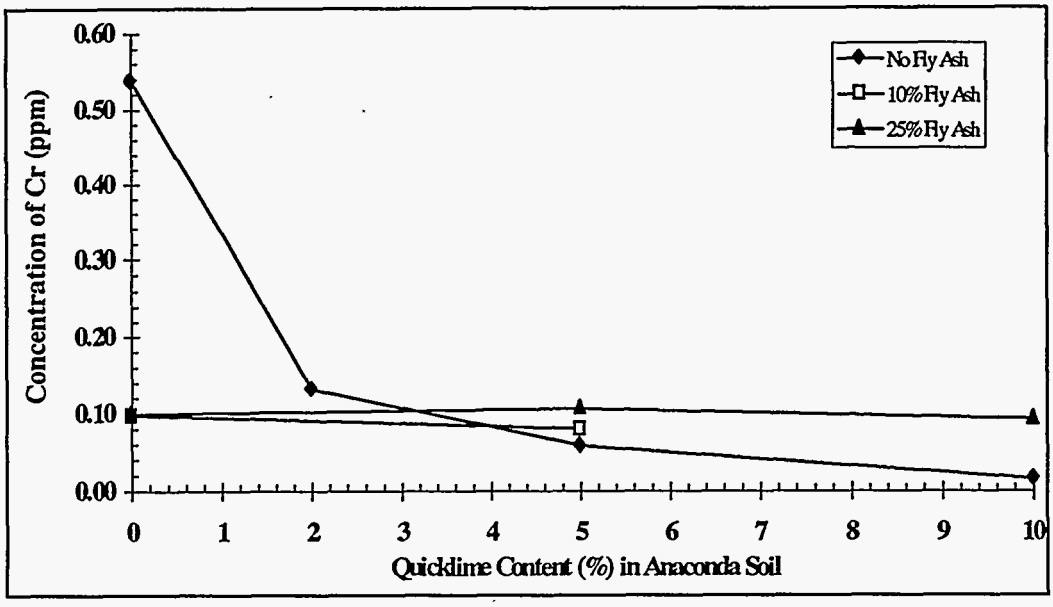

Figure 119. Chromium Concentration in the TCLP Leachate for Quicklime/Fly Ash Treated Soil, 28 Days Curing.

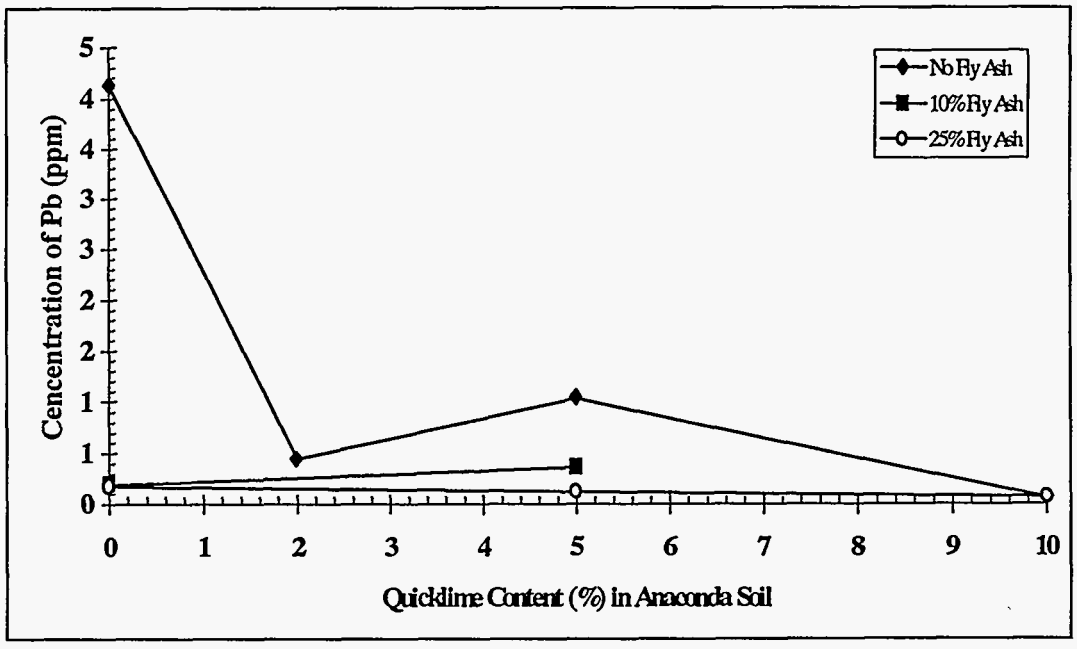

Figure 120. Lead Concentration in the TCLP Leachate for Quicklime/Fly Ash Treated Soil, 28 Days Curing.

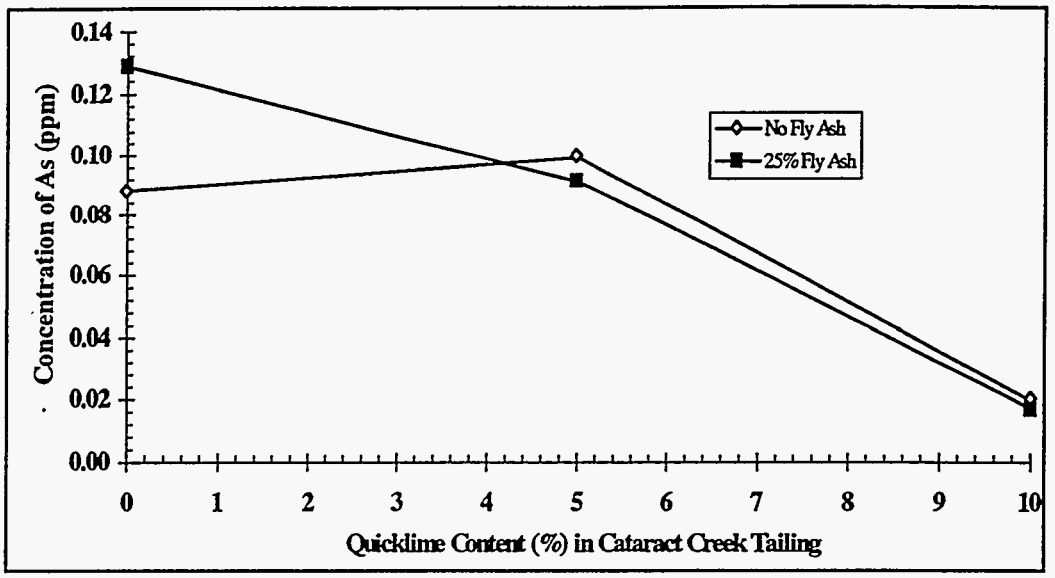

Figure 121. Arsenic Concentration in the TCLP Leachate for Quicklime/Fly Ash Treated Tailing, 28 Days Curing.

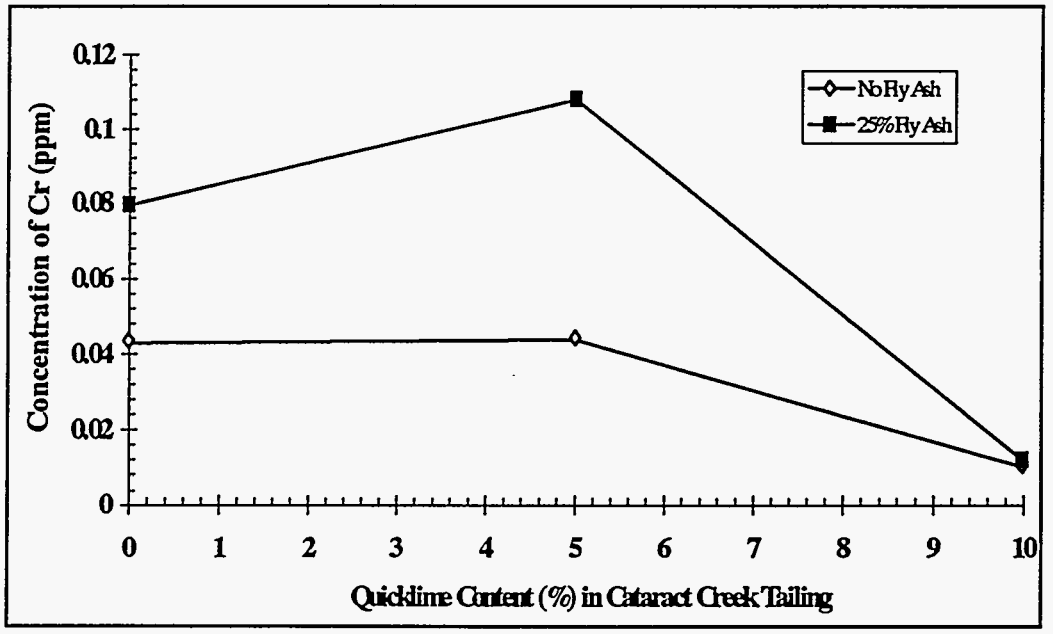

Figure 122. Chromium Concentration in the TCLP Leachate for Quicklime/Fly Ash Treated Tailing, 28 Days Curing.

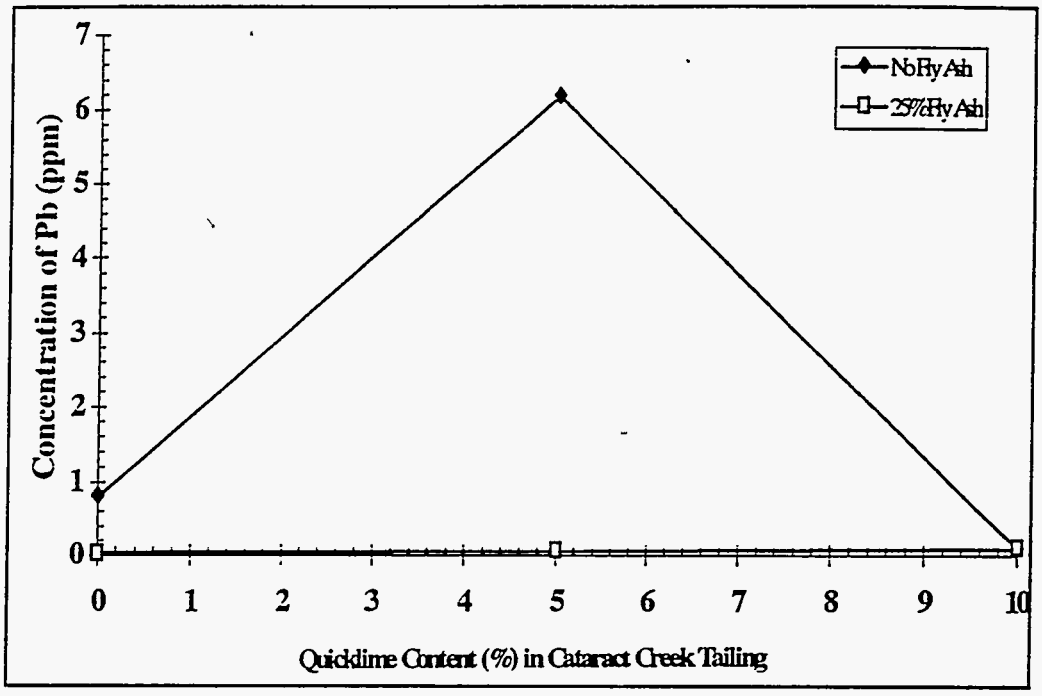

Figure 123. Lead Concentration in the TCLP Leachate for Quicklime/Fly Ash Treated Tailing, 28 Days Curing.

4.8.9 Mineralogical and Micromophological Properties of the Treated DOE Specimens

It has been previously reported that the main minerals in both Cataract Creek tailing and the Anaconda soil were quartz, mica (roscoelite), and iron oxides (ferrihydrite). An oxidized form of arsenic (As_2O_5) was also detected in the Anaconda soil sample. The same minerals were identified for the untreated soil and tailing specimens that had been compacted at optimum water content and cured for 28 days (Table 13). This is expected because no major chemical reactions were expected to take place due to water addition and compaction. Hydrated lime was identified in all the specimens treated with 10% and 25% fly ash, which is due to the lime content of fly ash. Quicklime treatment resulted in the formation of magnesiocarpholite, $(Mg,Fe)Al_2Si_2O_6(OH)_4$, in the soil specimens. Ettringite was detected only for the soil specimen treated with 25% fly ash and 5% quicklime. No other pozzolanic reaction products, such as calcium silicate hydrate (CSH) and calcium aluminum silicate hydrate (CASH), were positively identified in the specimens.

Treatment changed the chemical forms of arsenic in the soil specimens. In the quicklime/fly ash treated soil specimens, new As minerals, such as $Na_4As_2O_7$, $Na_{1.5}Al_2(OH)_{4.5}(AsO_4)_3{\cdot}7H_2O$ and $CaAsO_3(OH){\cdot}2H_2O$, were formed. As the result of these new As minerals formation, As_2O_5 disappeared. In the TCLP results discussed above, it was observed that As leachability was obviously reduced by the quicklime/fly ash treatment. This may be caused by As incorporation into the crystal lattice of the new minerals. However, no As minerals were detected in the tailing specimens although the tailing sample has higher As content (2964 mg As/kg) than the soil sample (814 mg As/kg). The results indicate that the As forms in the tailing and soil samples are quite different. No Pb and Cr minerals were detected, which may suggest that these heavy metals are present in the soils in amorphous forms, or that the amounts of the metal crystals are too low to be detected.

In order to evaluate the effect of quicklime treatment on the mineralogical changes of the solids, SEM micrographs of the untreated field samples are presented. One of the important minerals that can be formed in the quicklime treated solids is ettringite. Ettringite is an important mineral for strength development of quicklime treated soils. The formation and hydration of ettringite can also cause swell problems in the treated solids. Furthermore, the cations (Al^{3+} and Ca^{2+}) and anions (SO_4^{2-}) in the ettringite crystal lattice can be replaced by heavy metals through isomorphous substitution. As a result of this isomorphous substitution, heavy metals can be immobilized. Ettringite crystals (usually with needle shape) can be identified using SEM and X-ray diffraction analysis. Figure 124 shows that needle type crystals were formed in the Anaconda soil specimen that was treated with 10% of quicklime and cured for 3 months. However, no obvious needle crystals were observed for the tailing specimen when it was treated with 10% of quicklime and cured for 3 months (Figure 125). The formation of ettringite requires the presence of soluble aluminum, sulfate and calcium at high pH. The soil pH's of the treated (10% quicklime) the soil and tailing specimens were 12.75 and 12.57, respectively. At such high pH, Al can be released from the clay minerals and aluminum oxides in the soil. However, since the tailings mainly consist of sand, no enough aluminum was released to form ettringite. EDX analyses indicate that Al content on the tailing particle surface is much less than that on the soil particle surface (Table 14).

Table 13. Mineralogical Properties of the Treated and Untreated DOE Samples

Sample identification	SL0	SL5	SL10	SC25L0	SC25L5	SC25L10	TL0	TL10	TC25L0	TC25L5	TC25L10
Roscaelite-1M, syn	X	X	X	X	X	X	X	X	X	X	X
Sand	X	X	X	X	X	X	X	X	X	X	X
Na2Se.9H2O	X	X	-	-	-	-	-	-	-	-	-
As2O5	X	-	-	-	-	-	-	-	-	-	-
NaNilO6	X	X	X	X	-	-	-	-	-	-	-
Ba2.2Al2SiO8(OH)2.4 .2H2O	X	X	-	-	-	-	-	-	-	-	-
AlPO4	X	X	X	X	X	X	X	X	X	X	X
Ferrihydrite,syn [Fe5O7(OH) .4H2O]	X	X	X	X	X	X	X	X	X	X	X
Mg2Ge	X	X	X	X	X	X	-	-	-	-	-
CaSb2O6	X	X	X	X	X	X	X	X	X	X	X
(NH4)2.S2O7	X	X	X	X	X	X	-	-	-	-	-
CaO	-	X	X	-	X	X	-	X	-	X	X
Ca(OH)2	-	X	X	X	X	X	-	X	X	X	X
KCa3H(P2O7)2. 4H2O	-	X	-	-	-	-	-	-	-	-	-
Magnesiocarpholite[(Mg,Fe)Al2Si2O6(OH)4]	-	X	X	-	X	X	-	-	-	-	-
Li3Mg0.5SiO4	-	X	-	-	-	-	-	-	-	-	-
Na2CuFe(CN)6	X	X	X	X	X	X	-	-	-	-	-
Na1.5Al2(OH)4.5(AsO4)3. 7H2O	-	X	X	X	X	X	-	-	-	-	-
Ca(Zr(H2PO2)6)	X	X	X	-	-	-	-	-	-	-	-
Na3NbO4	-	-	X	-	-	-	-	-	-	-	-
CaAsO3(OH).2H2O	-	X	-	X	-	X	-	-	-	-	-
SrAl2Si2O8	-	X	-	-	X	X	-	-	-	-	-
CaMn2As2	X	X	X	-	-	X	X	-	-	-	-
d-Al196O288N4	X	X	X	X	X	X	X	X	X	X	X
CdFe2O4	X	X	X	X	X	X	X	X	X	X	X
Ettringite, syn	-	-	-	-	X	-	-	-	-	-	-
Ca(Cu, Zn)4(SO4)2(OH)6 3H2O	-	X	X	X	X	X	X	-	X	X	X
Na4As2O7	-	X	X	-	X	-	-	-	-	-	-
K2CdCl4	-	-	-	-	-	-	X	-	-	-	-
MgSO4 zMg(OH)2 xH2O	X	X	X	X	X	X	X	-	-	-	-
NaCa2Mg5Si7AlO22F2	-	-	-	-	-	X	-	-	-	-	-

S - Soil; T- Tailing; C - Class C Fly Ash; L - Quicklime

Table 14. Surface Chemical Composition of Specimens Determined Using EDX

Samples	Al%	Pb%	Ca%	Cu%	Fe%	K%	S%	Si%	Ti%	Mg%
Untreated Anoconda soil	6.1	0.0	24.1	2.1	23.8	4.1	3.5	35.4	0.8	0.0
SL10	3.2	0.0	60.4	0.0	12.5	3.2	3.9	16.8	0.0	0.0
SC25L10	4.7	0.0	56.4	0.0	13.9	2.4	1.6	20.1	1.0	0.0
Untreated Cataract Creek Tailings	3.3	0.0	0.0	0.0	28.5	3.6	3.2	61.4	0.0	0.0
TL10	3.2	0.0	49.4	0.0	15.3	4.0	0.0	28.0	0.0	0.0
TC25L10	4.9	0.0	48.1	0.0	16.1	2.9	1.6	25.4	0.9	0.0

S- Anoconda soil
L-Quicklime
C-Class C Fly Ash
T- Cataract Creek tailings
Numbers after the letters indicate the percent content of the additives.

Figure 124. SEM Micrograph of the Anaconda Soil Treated with 10% Quicklime, 3 Months of Curing.

Figure 125. SEM micrograph of the Cataract Creek tailing specimen treated with 10% quicklime, 3 months of curing.

4.8.10 Flow-through Leaching Results

4.8.10.1 Permeability of the Treated Field Samples

One of the most important factors concerning the immobilization of heavy metals in soil environments is the permeability of the contaminated materials. In order to reduce infiltration leaching through the contaminated materials, the treated solids should attain very low permeability values. The permeability is also an important factor concerning the reuse potential of the treated solid. The permeability of the quicklime/fly ash treated and untreated Anaconda soil specimens was determined based on the flow-through test results. The setup and the operation conditions of the flow-through system were described in detail in Appendix A4. The compacted untreated soil specimen had an initial permeability of 6.2E-7 cm/s (SL0 specimen in Figure 126). When 1,400 pore volume of 0.014 M acetic acid solution leached through the untreated specimen at a hydraulic gradient of 118, the permeability of the untreated specimen increased significantly. When the soil was treated with 10% of quicklime, the initial permeability was measured to be 2.3E-7 cm/s (SL10 specimen in Figure 126). The permeability was decreased to 1.6E-7 cm/s (SC25L0 specimen in Figure 126) when the soil sample was treated with fly ash. However, a small increase in permeability was observed for SC25L0 specimen during the leaching test. The initial permeability of the quicklime/fly ash treated specimen (SC25L10) was similar as that of the fly ash treated specimen (SC25L0). The permeability of the SC25L10 specimen decreased significantly as more leachant was passed through the specimen.

Overall, during 50 days of flow-through experiment 2299 pore volumes of leachant (15.3 L) passed through the untreated specimen at a hydraulic gradient of 118. The untreated specimen disintegrated completely after 50 days of flow-through leaching. In contrast to the leaching results for the untreated specimen, only 139 pore volume of the leachant (1.7 L) passed through the SC25L10 specimen in 51 days of test. The hydraulic gradient applied to the SC25L10 specimen (i = 246) was approximately twice as high as that for the untreated specimen.

4.8.10.2 Heavy Metal Leachability during Flow-Through Leaching Tests

The chemical behavior of the treated specimens was determined by measuring the pH and heavy metal concentration in the leachate. The quicklime treatment resulted in an increase of the leachant pH from 3.4 for the untreated specimen to 11.8 (Figure 127). When the soil was treated with 25% fly ash, the initial leachant pH was also increased to 11.8 (SC25L0 specimen in Figure 127). However, the leachant pH dropped to 4.6 when 587 pore volume of the leachant passed through the specimen. This was due to the rapid consumption of alkalinity in the fly ash treated specimens by the acidic leachant. Therefore, quicklime should be added in order to effectively control the pH of the treated solids during acid leaching.

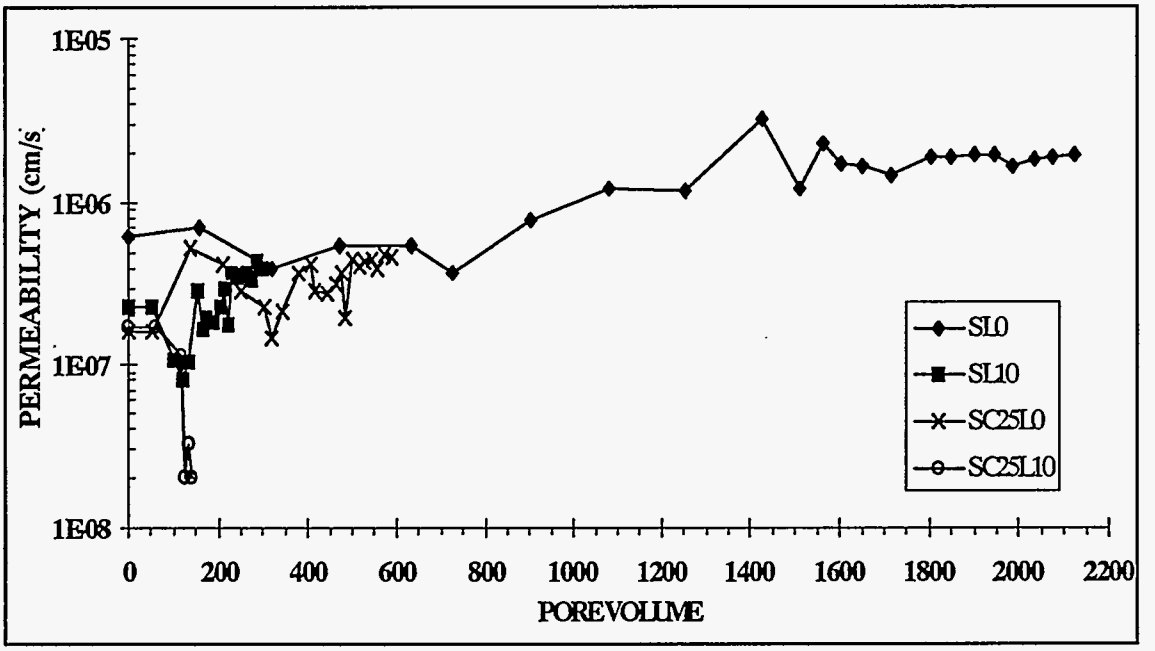

Figure 126. Permeability of Untreated and Quicklime/Fly Ash Treated Anaconda Soil Specimens.

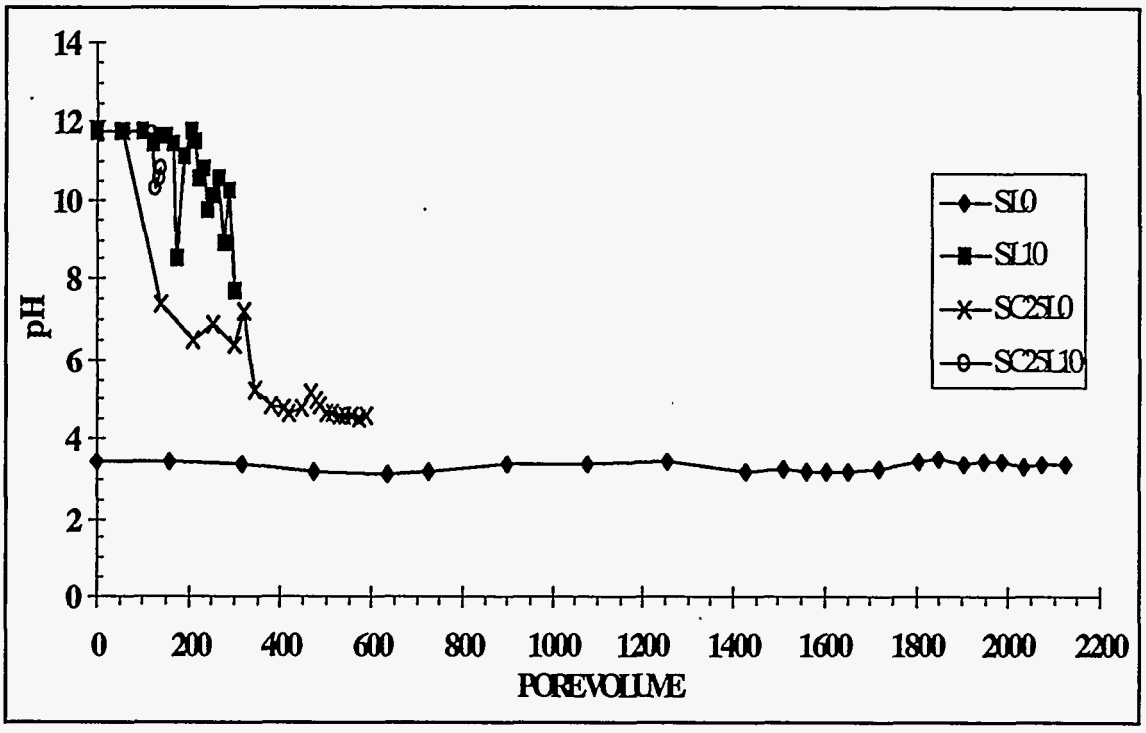

Figure 127. Leachant pH of Untreated and Quicklime/Fly Ash Treated Anaconda Soil Specimens.

The effect of the quicklime treatment on As leachability is shown in Figure 128. The cumulative percentage of the As released during the flow-through tests was calculated using the amount of As in the leachant and total amount of As in the specimen. Only 1% of As was leached out from the untreated soil specimen after more than 2000 pore volume of leachant passed through the specimen. The As released from the fly ash treated specimen (SC25L0) was slightly higher than that from untreated specimen when equal pore volume of the leachant passed through the SC25L0 and SL0 specimens. On the other hand, the amount of As released from the quicklime and quicklime/fly ash treated specimens (SL10 and SC25L10) was negligible. The leachability of Cr and Pb from the untreated and the treated specimens is compared in Figures 129 and 130. More Cr and Pb were also released from the SC25L0 specimens than from untreated specimens. Among the specimens tested, the SC25L10 specimen had the lowest leachability.

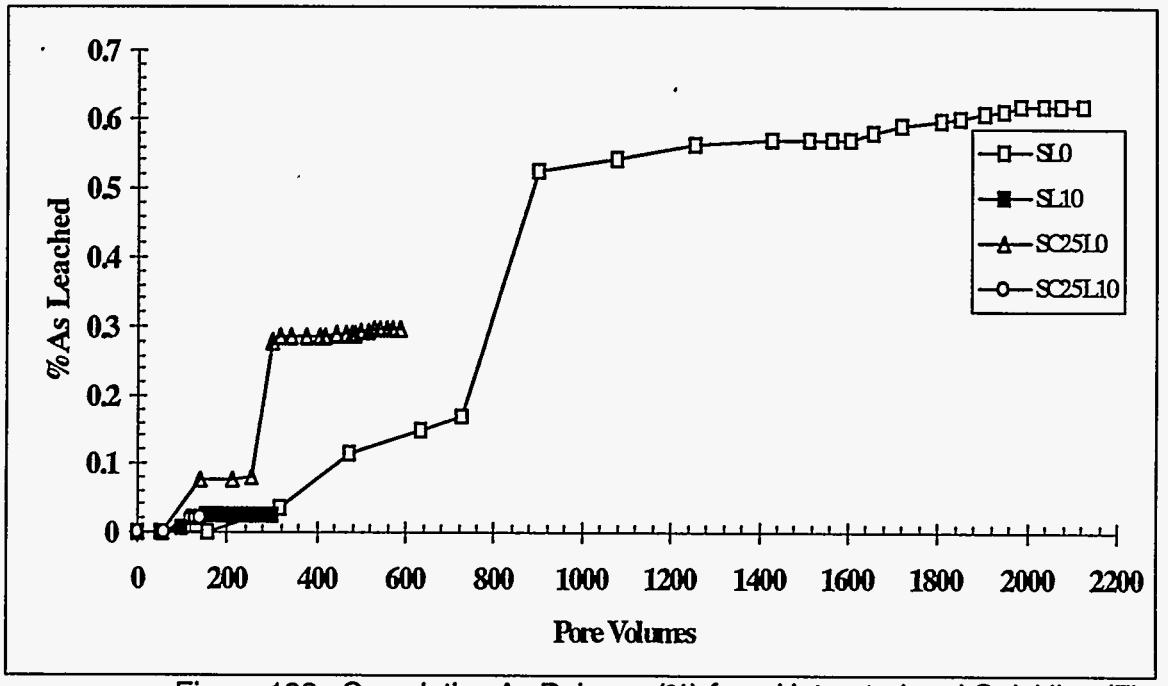

Figure 128. Cumulative As Release (%) from Untreated and Quicklime/Fly Ash Treated Anaconda Soil Specimens.

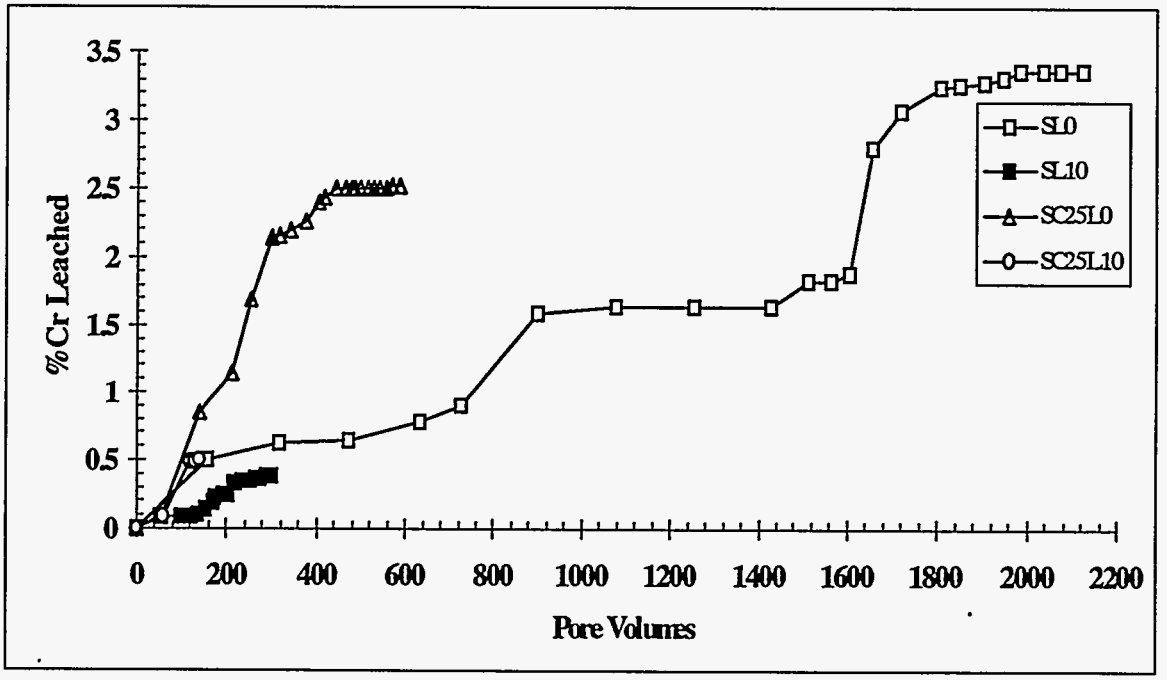

Figure 129. Cumulative Cr Release (%) from Untreated and Quicklime/Fly Ash Treated Anaconda Soil Specimens.

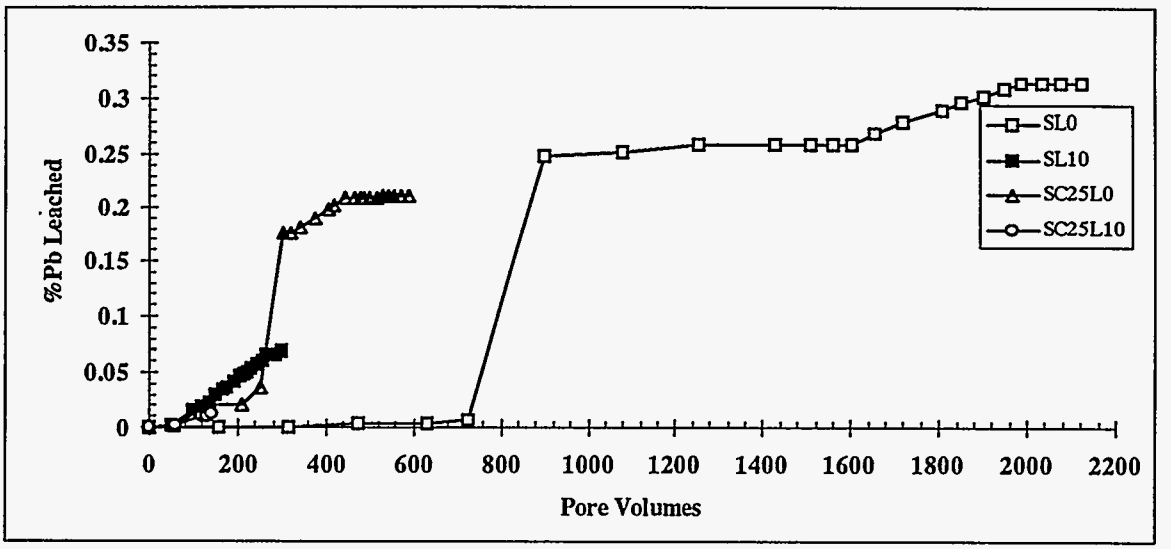

Figure 130. Cumulative Pb Release (%) from Untreated and Quicklime/Fly Ash Treated Anaconda Soil Specimens.

4.8.11 Heavy Metal Release from Monolithic Solids under Static Leaching Conditions

The results, as already discussed in previous sections, have demonstrated that when the contaminated DOE soil and tailings were treated using quicklime/fly ash, high strength and low permeability solids were formed. When the treated solid forms are subjected to hydraulic flow conditions, it is most likely that only the outer surface of the monolithic solids will interact with water or any other leachant due to their low permeability. In order to understand the leaching behavior of the quicklime/fly ash treated solids under such moderate leaching conditions, a static leaching test program was designed and undertaken in our laboratory. More specifically, the American Nuclear Society (ANS 16.1, 1986) static leaching procedure for hazardous wastes was modified and used to simulate diffusion-controlled conditions. The details of the static leaching procedures have been described in the appendix A.5 of this report.

4.8.11.1 Cumulative Release of Heavy Metals

Based on the static leaching results, the cumulative leachability, expressed as the percentage of heavy metals released over the total amount present in each specimen, was calculated. The release data in Figure 131 suggest that under static leaching conditions, moderate amounts of As were released from the untreated soil specimen (SL0). The amount of As released increased significantly within the first few days of test. After 88 days of leaching, approximately 2% of the As in the solid was released. On the other hand, quicklime treatment reduced As leachability to less than 1%. A combined treatment of quicklime and fly ash was more effective to reduce the leachability of As (Figure 132). As release from the quicklime/fly ash treated specimen was less than 0.3%.

of As (Figure 132). As release from the quicklime/fly ash treated specimen was less than 0.3%.

The release of Cr and Pb from both untreated and treated soil specimens were very low (Figures 133 to 136). Therefore, no obvious difference in Cr and Pb leachability was measured between the untreated and quicklime treated specimens.

The release of As from untreated tailings (TL0 specimen in Figure 137) was much higher than that from untreated soil specimen (Figure 131). Arsenic leachability was effectively reduced to less than 1% when the tailings were treated with 5% and 10% quicklime (Figure 137). The leachability of As treated with 25% fly ash treatment (TC25L0 specimen in Figure 137) is even lower than that from the quicklime treated specimen. The leachability of Cr and Pb from the tailing were also significantly reduced by quicklime and fly ash treatment (Figures 138 and 139).

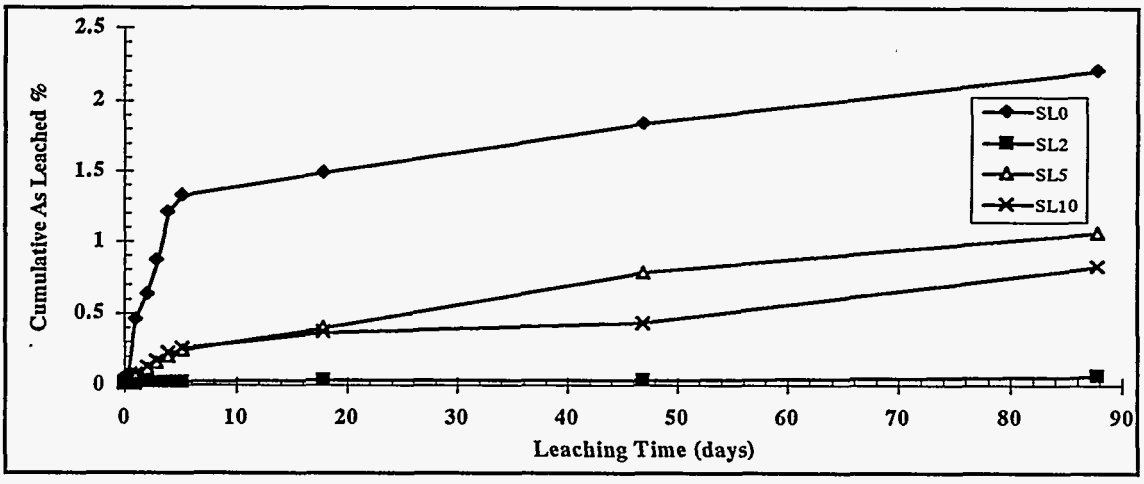

Figure 131. Effect of Quicklime Treatment on As Release from Contaminated Anaconda Soil Specimens During Static Leaching.

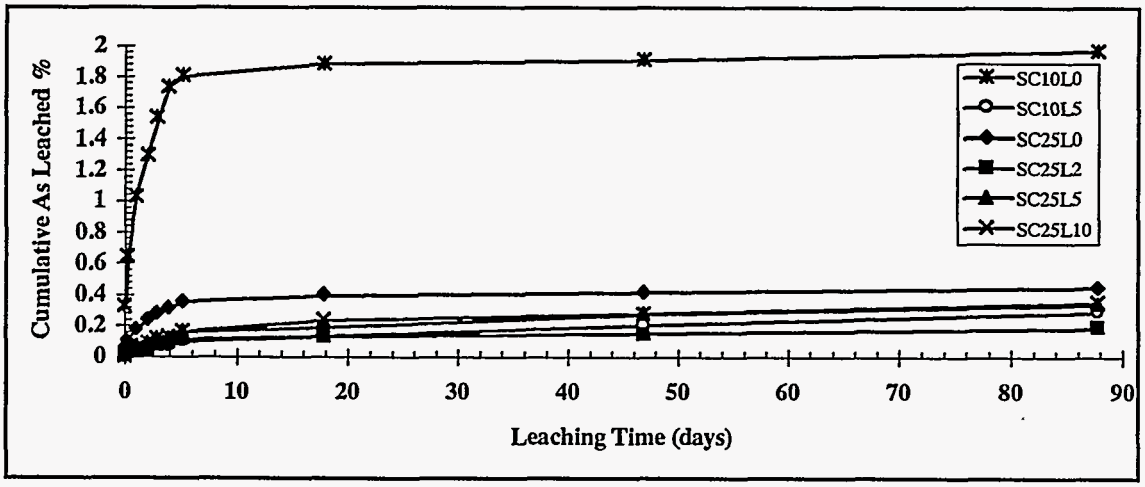

Figure 132. Effect of Quicklime/Fly Ash Treatment on As Release from Contaminated Anaconda Soil Specimens During Static Leaching.

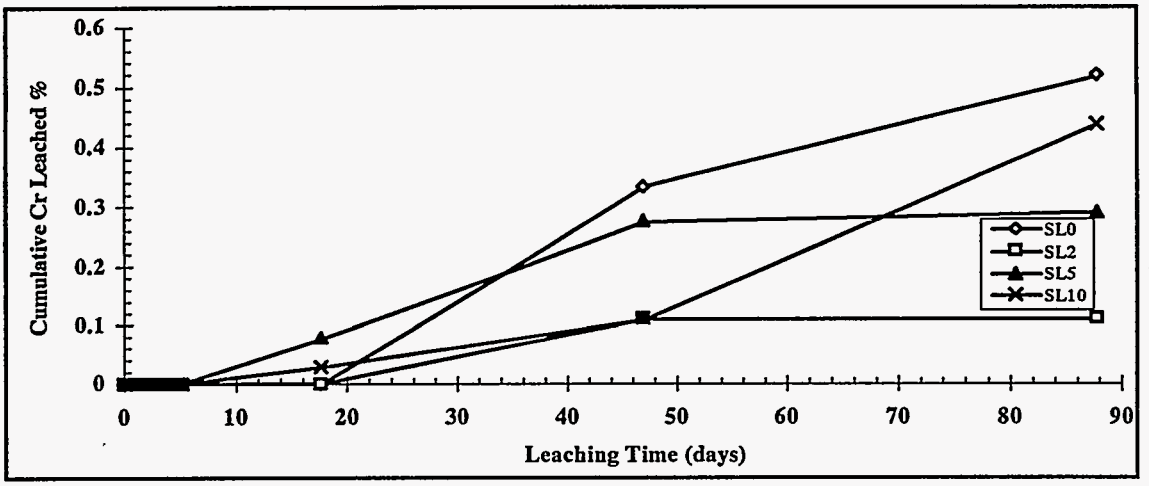

Figure 133. Effect of Quicklime Treatment on Cr Release from Contaminated Anaconda Soil Specimens During Static Leaching.

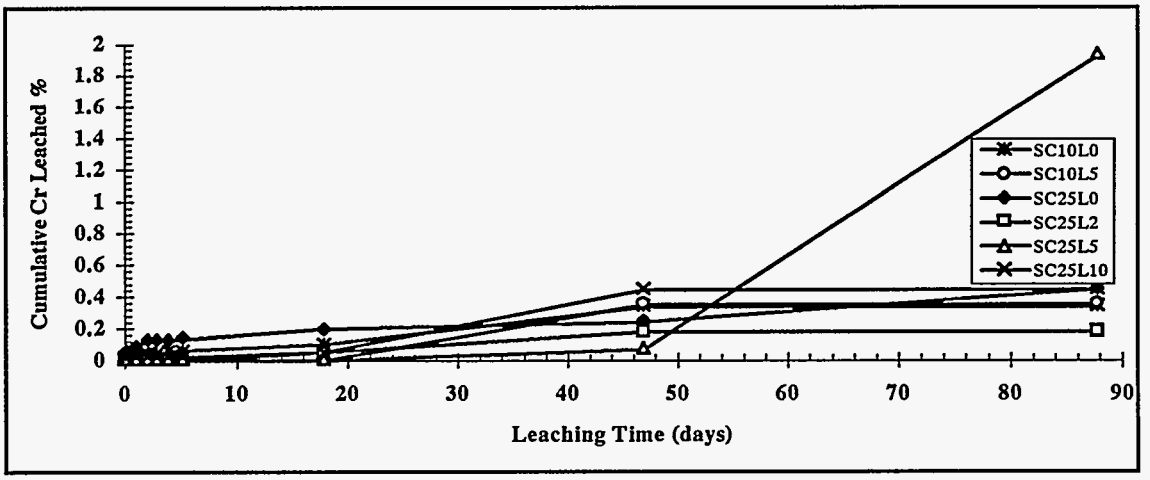

Figure 134. Effect of Quicklime/Fly Ash Treatment on Cr Release from Contaminated Anaconda Soil Specimens During Static Leaching.

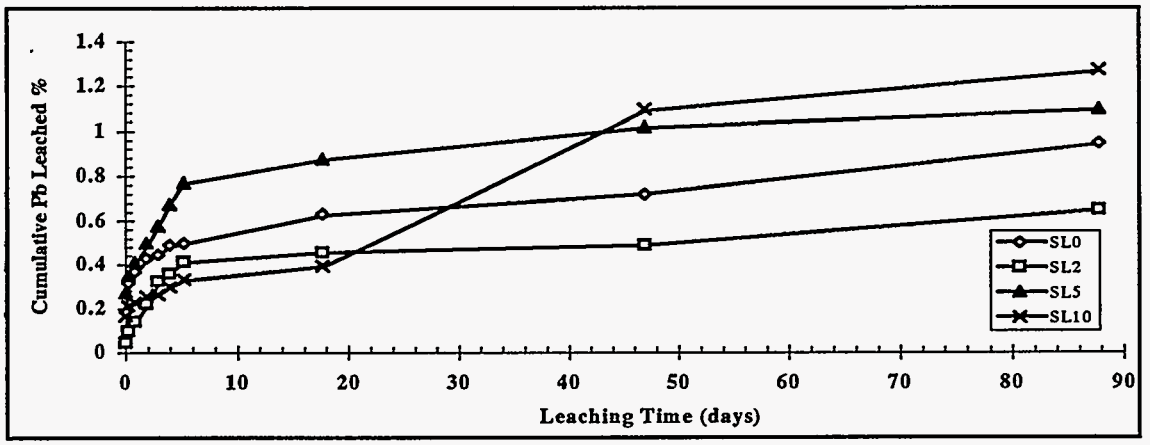

Figure 135. Effect of Quicklime Treatment on Pb Release from Contaminated Anaconda Soil Specimens During Static Leaching.

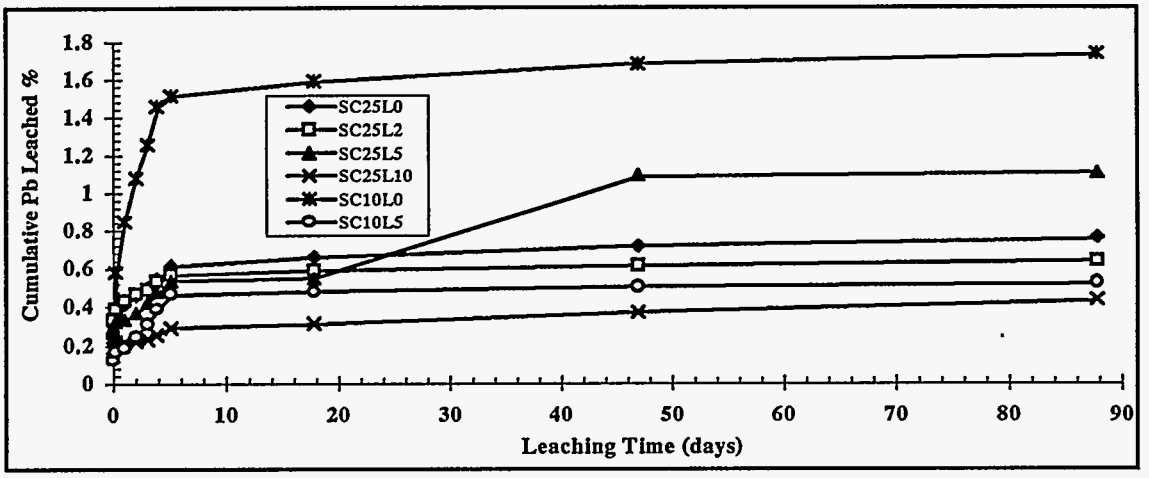

Figure 136. Effect of Quicklime/Fly Ash Treatment on Pb Release from Contaminated Anaconda Soil Specimens During Static Leaching.

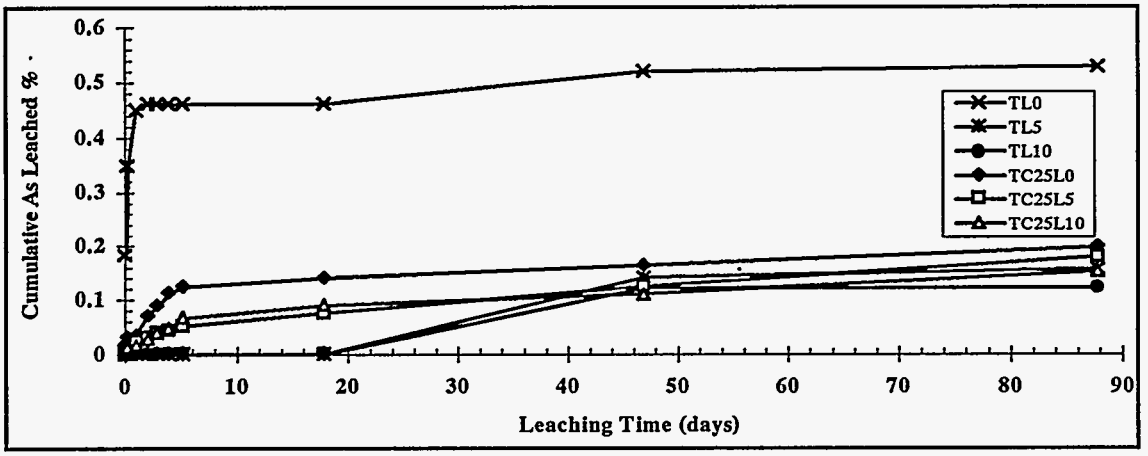

Figure 137. As Release from Contaminated Cataract Creek Tailing Specimens During Static Leaching.

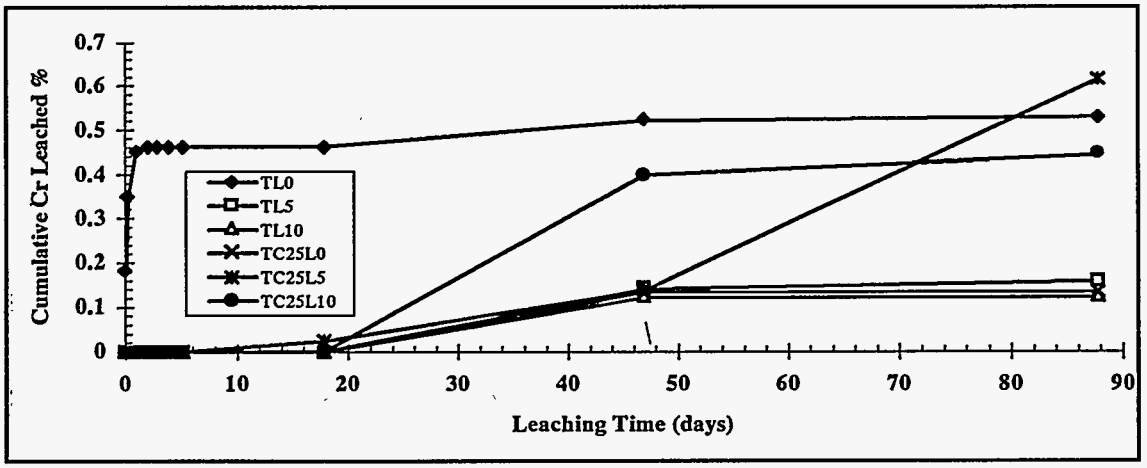

Figure 138. Cr Release from Contaminated Cataract Creek Tailing Specimens During Static Leaching.

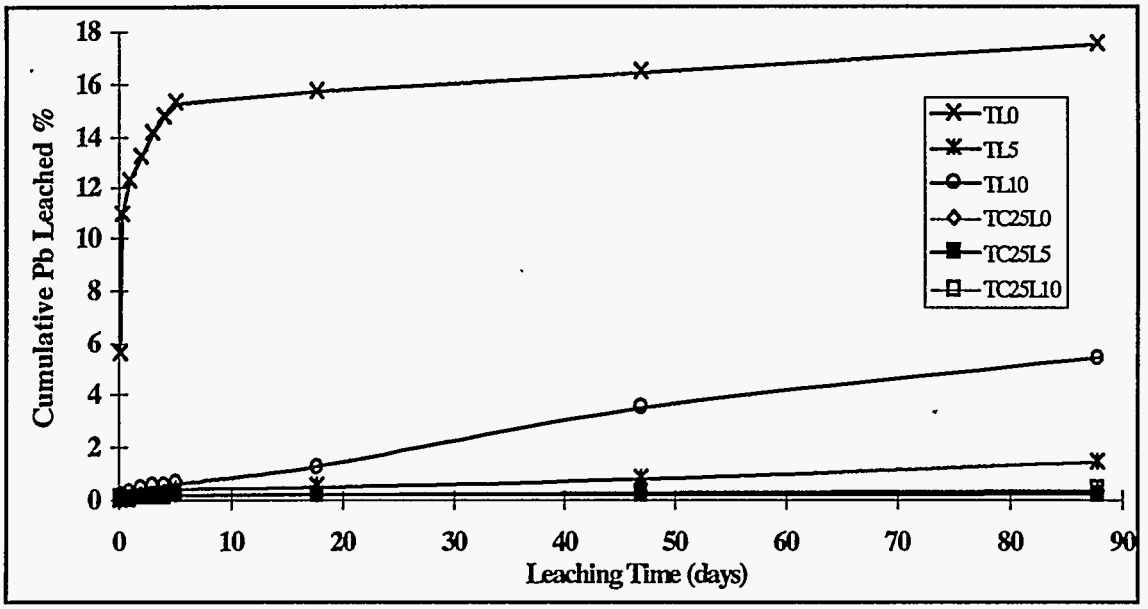

Figure 139. Pb Release from Contaminated Cataract Creek Tailing Specimens During Static Leaching.

4.8.11.2 Transport of Heavy Metals from Solid to Solution

In order to elucidate the mechanisms controlling heavy metal release from the treated soils, the data obtained from the static leaching experiments was further evaluated using a diffusion model (Crank, 1975). The model assumptions and equations were discussed in detail in Section 4.5.2 of the report.

The cumulative release of As from untreated and quicklime treated soil specimens is plotted as a function of leaching time in Figure 140 (in logarithmic scales). A regression analysis shows a high linear correlation between $\log(B_t)$ and $\log(t)$ for all the specimens (Table 15). The slopes of the linear lines are between 0.5 and 0.7 for untreated and quicklime treated soil specimens. The results indicated that the release of As from the specimens is mainly diffusion controlled. When the soil was treated with 10% fly ash (SC10L0 specimen in Figure 141), a slope of 0.24 was observed, which suggests that As release from the specimen was a mixed process of diffusion and surface wash off during the static leaching test. Arsenic release from the quicklime/fly ash treated specimen (SC10L5 specimen in Figure 141) was mainly controlled by a diffusion process.

In contrast to As release from untreated soil specimen, As release from untreated tailing specimen was mainly controlled by surface wash off (Figure 142). The quicklime treatment reduced As release by eliminating the surface wash off process (TL5 and TL10 specimens, in Figure 142). The results in Figure 142 indicate that As release from the fly ash treated and quicklime/fly ash treated tailings specimens are controlled by diffusion.

Quicklime and quicklime/fly ash treatment of the soil samples did not result in obvious changes in the Pb release processes since the slopes of untreated and the treated specimens are between 0.2 and 0.4 (Figures 143 and 144). On the other hand, Pb release from the tailings specimens was changed from the surface

wash off for untreated specimen to a diffusion process in the quicklime treated specimen (Figure 145). However, fly ash treatment did not result in a consistent change in Pb release process (Figure 145). Very poor correlation between $\log(B_t)$ versus $\log(t)$ was obtained for Cr leaching data because the Cr concentration in the leachate was very low. Therefore, model analysis of the Cr release from the specimens is not reported.

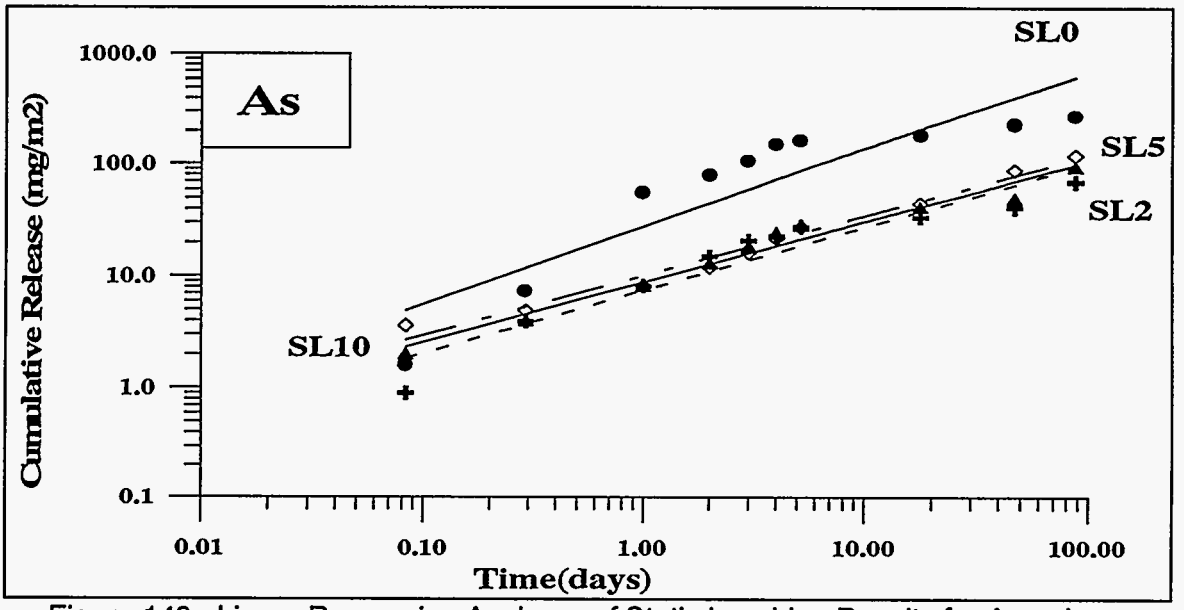

Figure 140. Linear Regression Analyses of Static Leaching Results for Arsenic Release from Contaminated Anaconda Soil Specimens, Quicklime Treatment.

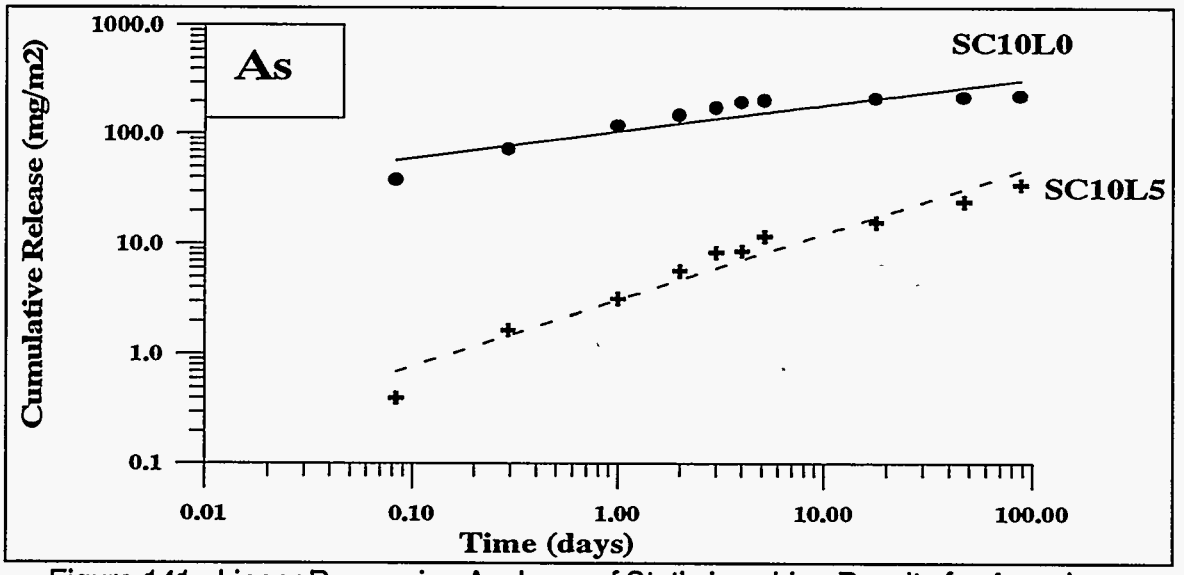

Figure 141. Linear Regression Analyses of Static Leaching Results for Arsenic Release from Contaminated Anaconda Field Soil Specimens, Quicklime/Fly Ash (10%) Treatment.

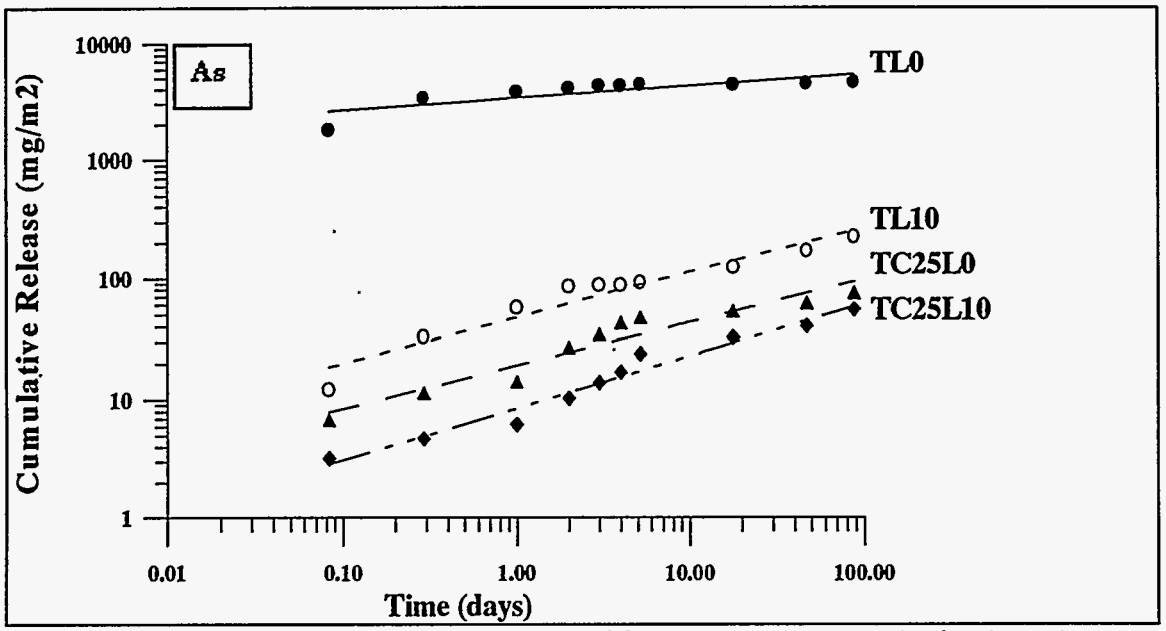

Figure 142. Linear Regression Analyses of Static Leaching Results for Arsenic Release from Contaminated Cataract Creek Tailing Specimens, Quicklime/Fly Ash Treatment

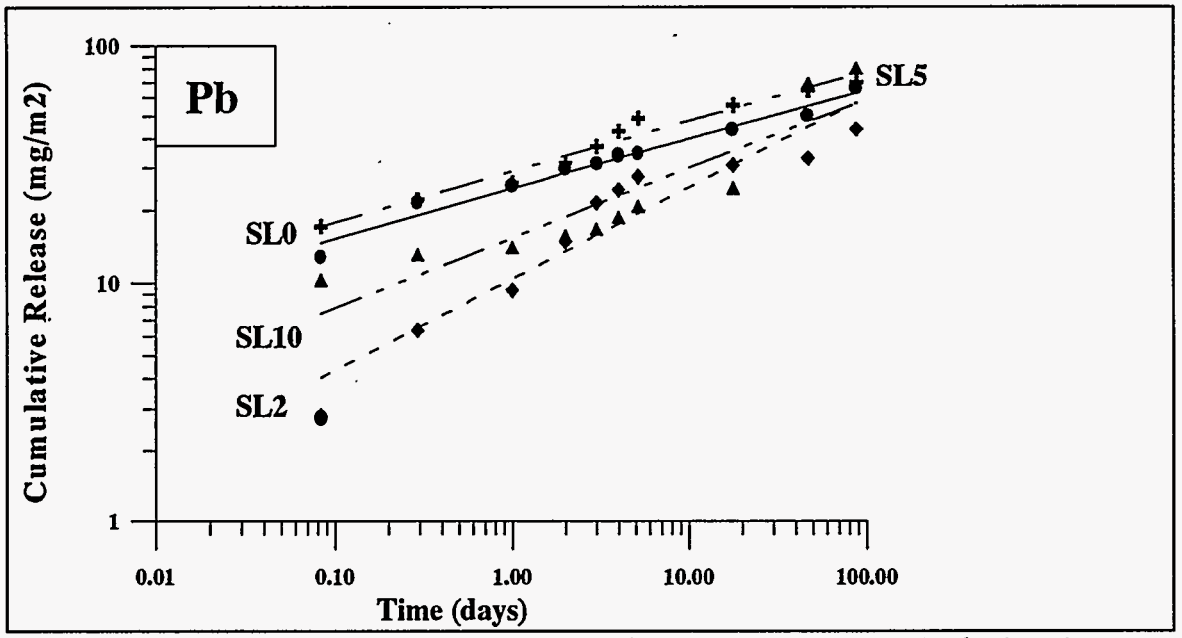

Figure 143. Linear Regression Analyses of Static Leaching Results for Lead Release from Contaminated Anaconda Soil Specimens, Quicklime Treatment.

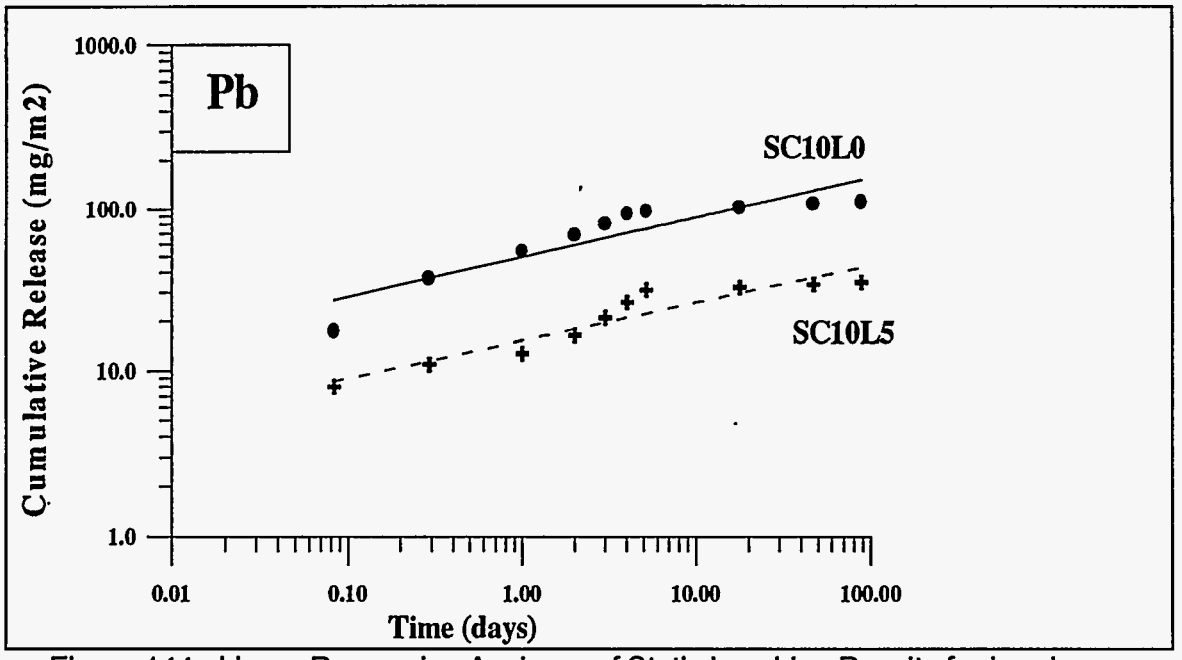

Figure 144. Linear Regression Analyses of Static Leaching Results for Lead Release from Contaminated Anaconda Soil Specimens, Quicklime/Fly Ash Treatment.

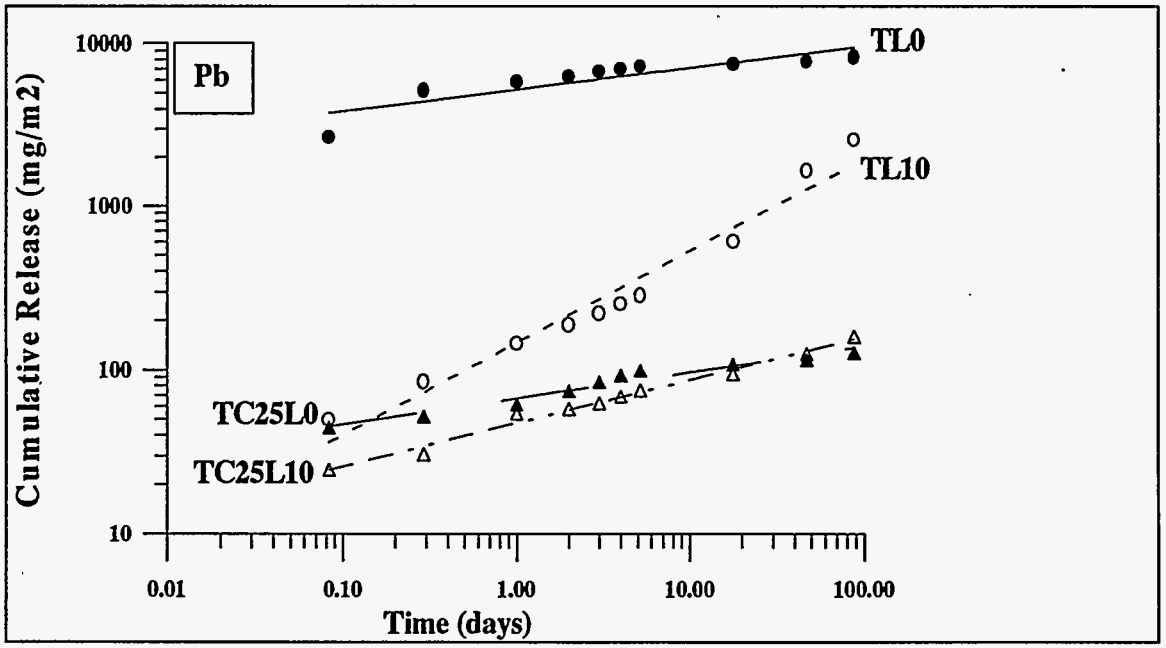

Figure 145. Linear Regression Analyses of Static Leaching Results for Lead Release from Contaminated Cataract Creek Tailing Specimens, Quicklime/Fly Ash Treatment.

Table 15. Regression Analyses Results for As and Pb Release Data in Figures 140 to 156

As			
Sample ID	Slope	Intercept	R^2
SL0	0.70	3.31	0.82
SL2	0.56	2.00	0.91
SL5	0.53	2.31	0.98
SL10	0.54	-2.17	0.97
SC10L0	0.24	4.65	0.81
SC10L5	0.60	1.13	0.95
SC25L0	0.28	3.00	0.90
SC25L2	0.36	1.62	0.95
SC25L5	0.57	1.56	0.87
SC25L10	0.47	1.88	0.85
TL0	0.11	8.12	0.65
TL5	0.29	4.10	0.94
TL10	0.38	3.86	0.93
TC25L0	0.36	2.94	0.92
TC25L5	0.48	2.03	0.99
TC25L10	0.43	2.13	0.97

Pb			
Sample ID	Slope	Intercept	R^2
SL0	0.21	3.20	0.97
SL2	0.38	2.34	0.90
SL5	0.21	3.39	0.97
SL10	0.29	2.73	0.83
SC10L0	0.25	3.90	0.83
SC10L5	0.23	2.72	0.89
SC25L0	0.16	3.32	0.95
SC25L2	0.09	3.37	0.95
SC25L5	0.21	3.20	0.87
SC25L10	0.11	2.63	0.89
TL0	0.13	8.56	0.77
TL5	0.52	3.98	0.98
TL10	0.56	4.98	0.96
TC25L0	0.16	4.20	0.95
TC25L5	0.52	2.63	0.90
TC25L10	0.26	3.86	0.99

The calculated mean of the leachability index, L_i, the correlation coefficient, r, and the confidence range of L_i are all listed in Table 16 for the respective specimens. Equations 5, 6, and 10 were used for the calculations. Taking into account that a high leachability index indicates low release, the results in Table 16 suggest that the release of As and Pb from quicklime treated specimens are much lower than the release of the metals from untreated specimens (SL0 and TL0). The leachability of the metals from the quicklime/fly ash treated specimens is obviously lower than that from the quicklime treated specimens. The leachability index for Cr is not reported in the table because the Cr concentration for most of the specimens was too low to be measured accurately using even a graphite atomic absorption spectrometer.

The diffusion of heavy metals from the stabilized/solidified solid to solution can be reduced by physical retardation (tortuosity) and/or chemical retention (geochemical attenuation). The general equation for the effective diffusion coefficient as a function of the physical retardation and chemical interaction is given in Equation 11.

The mean values of D_e and calculated $R \cdot \tau$ data are listed in Table 17. The effective diffusion coefficients of As for the untreated specimens (SL0 and TL0) are significantly larger than those for the treated specimens (Table 17). The effective diffusion coefficient for Pb release from untreated soil specimen was very low. Therefore, quicklime and fly ash treatment did not result in obvious reduction of the effective diffusion coefficient for Pb release. Pb diffusion coefficient from tailings specimens was reduced by 2 to 4 orders of magnitudes by the quicklime and fly ash treatment. The data in Table 17 also indicates that the values for the physical and chemical retardation factors ($R \cdot \tau$) for the treated specimens are much higher than those for the untreated specimens. The results therefore suggest that quicklime and fly ash treatment was effective in significantly reducing the mobility of the heavy metals, so that only trace levels were released.

Table 16. Leachability Parameters Calculated from Static Leaching Results

Specimen Designation	Mean of Li		r		Range of Li	
	As	Pb	As	Pb	As	Pb
SL0	10.44	11.17	0.05	0.06	6.30-14.58	7.98-14.35
SL2	11.62	11.29	0.03	0.09	8.85-14.39	7.74-14.84
SL5	11.26	10.79	-0.03	0.12	9.62-12.89	6.99-14.60
SL10	11.38	11.30	0.01	0.00	9.22-13.54	8.01-14.59
SC10L0	10.45	10.46	0.12	0.13	3.94-16.97	4.86-16.06
SC10L5	12.30	11.53	0.00	0.12	9.57-15.04	5.41-17.66
SC25L0	11.54	11.20	0.13	0.13	6.90-16.18	6.60-15.81
SC25L2	12.36	11.60	0.08	0.12	8.69-16.02	6.47-16.72
SC25L5	11.96	11.40	0.07	0.03	9.04-14.75	6.43-17.98
SC25L10	11.89	12.2	0.07	0.03	9.04-14.75	6.43-17.98
TL0	9.37	8.66	0.11	0.11	2.52-16.23	3.65-13.67
TL5	11.72	10.96	0.01	-0.03	7.79-15.64	8.73-13.20
TL10	11.78	10.20	0.02	-0.15	8.35-15.21	8.67-11.73
TC25L0	12.28	12.05	0.09	0.12	8.64-15.93	7.94-16.17
TC25L5	12.63	12.32	0.03	0.10	11.83-13.44	8.20-16.44
TC25L10	12.66	11.94	0.06	0.07	10.22-15.10	9.49-14.39

Table 17. Mean Effective Diffusion Coefficients and Retardation Factors

Specimen Designation	As		Pb	
	Mean De (cm^2/s)	Rτ	Mean De (cm^2/s)	Rτ
SL0	1.66E-10	5.45E+04	3.69E-11	2.56E+05
SL2	5.11E-12	1.77E+06	1.42E-11	6.65E+05
SL5	8.07E-12	1.12E+06	7.28E-11	1.30E+05
SL10	7.12E-12	1.27E+06	2.34E-11	4.04E+05
SC10L0	2.80E-10	3.23E+04	2.14E-10	4.42E+04
SC10L5	1.36E-12	6.65E+06	2.38E-11	3.97E+05
SC25L0	1.00E-11	9.05E+05	5.45E-11	1.73E+05
SC25L2	1.52E-12	5.95E+06	7.48E-11	1.26E+05
SC25L5	3.94E-12	2.30E+06	6.22E-11	1.52E+05
SC25L10	2.81E-12	3.22E+06	2.68E-11	3.53E+05
TL0	2.75E-08	3.29E+02	4.71E-08	2.01E+02
TL5	8.27E-12	1.09E+06	2.11E-11	4.48E+05
TL10	5.84E-12	1.55E+06	1.03E-10	9.17E+04
TC25L0	1.40E-12	6.46E+06	7.38E-12	1.28E+06
TC25L5	2.64E-13	3.43E+07	4.31E-12	2.19E+06
TC25L10	5.63E-13	1.61E+07	3.37E-12	2.80E+06

4.8.12 Summary

Overall, the MSE heavy metal contaminated field samples were all highly acidic materials, having very poor geotechnical properties and minimum surface area attributes. For the purposes of the proposed quicklime-sulfate salt S/S treatment, such materials would be on the fringes of treatment applicability. In addition, all samples had unusually high As, Cr, and Pb total contents, much higher than those reported within the DOE sites. In the case of the sludge samples, such high contents of heavy metals and other metal minerals present might suggest that a viable alternative would be resource recovery, if the economics work out. However, the leachability of the heavy metals is very low when the pH level of the leachant was between 2.0 and 10.0. In fact, none of the field samples tested thus far would even remotely classify as hazardous waste according to the TCLP rule. This suggests the leachable portion of the heavy metals has already been released, and the remaining portion is strongly immobilized in iron hydroxide matrices. In other words, the heavy metals are already immobilized, or rather as immobilized as possible, given their very high total contents. Therefore, the only advent of treatment for such soils is to provide with treated solids that attain satisfactory geotechnical properties, enabling their reuse in construction applications.

The experimental results demonstrated that the quicklime/fly ash treatment was an effective method to improve the geotechnical properties of the contaminated tailing and soil. The quicklime/fly ash treatment significantly increased the compressive strength levels of the soil. The permeability of the solids was also significantly reduced by the quicklime/fly ash treatment, which effectively reduced the volume of leachant infiltration through the solids. Both quicklime and fly ash had to be used to treat the sandy materials to attain satisfactory geotechnical properties. The TCLP, flow-through, and monolithic static leaching results all demonstrated that quicklime/fly ash treatment can significantly reduce heavy metal leachability in the contaminated tailing and soil.

REFERENCES

American Society of Testing Materials, (1963), Standard D 422-63, "Particle-Size Analysis of Soils." Section 4, Vol. 4.08, pp. 93-99.

American Society of Testing Materials, (1984), Standard D 4318-84, "Liquid Limit, Plastic Limit, And Plasticity Index of Soils." Section 4, Vol. 4.08, pp. 682-692.

American Society of Testing Materials, (1985a), Standard D 2217-85, "Wet Preparation of Soil Samples for Particle-Size Analysis and Determination of Soil Constants." Section 4, Vol. 4.08, pp. 298-300.

American Society of Testing Materials, (1985b), Standard D 421-85, "Dry Preparation of Soil Samples for Particle-Size Analysis and Determination of Soil Constants." Section 4, Vol. 4.08, pp. 91-92.

American Society for Testing and Materials, (1986a), "Annual Book of ASTM Standards" Vol. 4.08, Soil and Rock; Building Stones, Philadelphia, PA. PP. 160-165.

American Society for Testing and Materials, (1986b), "Annual Book of ASTM Standards" Vol. 4.08, Soil and Rock; Building Stones, Philadelphia, PA. PP. 154-159.

American Society of Testing Materials, (1988), Standard E 886-88, "Dissolution of Refuse-Derived Fuel (RDF) Ash Samples for Analyses of Metals." Section 11, Vol. 11.04, pp. 516-519.

American Society of Testing Materials, (1989), Standard D 4972-89, "pH of soils." Section 4, Vol. 4.08, pp. 1163-1165.

American Society of Testing Materials, (1990), Standard C 977 - 89, "Standard Specification for Quicklime and Hydrated Lime for Soil Stabilization." ASTM Standards on Soil Stabilization With Admixtures, pp. 8-9.

American Society for Testing and Materials, (1992a), "Annual Book of ASTM Standards" Vol. 4.08, Soil and Rock; Building Stones, Philadelphia, PA.

American Society of Testing Materials, (1992b), Standard D 2216-92, "Laboratory Determination of Water (Moisture) Content of Soil and Rock." Section 4, Vol. 4.08, pp. 294-297.

ANS 16.1 (1986), American National Standard for the Measurement of the Leachability of Solidified Low-Level Radioactive Wastes by a Short-Term Tests Procedure, *ANSI/ANS-16.1, 1986*, American National Standards Institute, New York, NY.

Arizumi et al. (1977). "Solidification of Harmful Wastes and Muds by means of the Formation of Cement Bacillus and its Application". Proc. of Specialty Session of Geotech. Eng and Env. Control, 9th ICSMFE, Tokyo, Japan, pp. 253-263.

Bishop, P. L. (1986), "Prediction of Heavy Metal Leaching Rates from Stabilized/Solidified Hazardous Wastes", *Proceedings of the 18th Mid-Atlantic Industrial Waste Conference*, pp. 236-252.

Cote, P. and Constable, T. (1982), "Evaluation of Experimental Conditions in Batch Leaching Procedures", *Resources and Conservation*, Elservier Scientific Publishing Company, Amsterdam, Netherlands, pp. 59-73.

Culliane, M. J. and Jones, L. W., (1986), "Stabilization/Solidification of Hazardous Wastes," US EPA Hazardous Waste Engineering Research Laboratory, EPA/600/D-86/028.

Crank, J., *The Mathematics of Distribution*, 2nd ed., Clarendon Press, Oxford, 1975.

Dermatas, D. and Meng, X. G. (1994), "Stabilization/Solidification of Chromium Contaminated Soils." *J. Soil Contamination*, (under review).

Dermatas, D. (1992), "An Experimental Study to Elucidate and Eliminate Ettringite-Induced Swelling in Lime-Stabilized Sulfate-Bearing Clayey Soils", *Ph. D Thesis*, submitted to the faculty of the University of California at Berkeley, Berkeley, CA 94720, May 1992.

Diamond, S. and Kinter, E. B. (1966), "Mechanisms of Soil-Lime Stabilization, An Interpretive Review", Public Roads, Vol. 33, No. 12, 1966, pp 260.

Ferguson, G. (1993), *"Use of Self-Cementing Fly Ashes as a Soil Stabilization Agent"*, ASCE Geotechnical Special Publication No. 36: "Fly ash for Soil Improvement", ASCE, New York, pages 1-14.

Groot, G. J. de and Sloot, H. A. van der, (1992), "Determination of Leaching Characteristics of Waste Materials Leading to Environmental Product Certification," *stabilization and Solidification of Hazardous, Radioactive, and Mixed wastes, 2nd Volume, STP 1123*, T.M. Gillliam and C.C. Wiles, Eds., American Society for Testing Materials, Philadelphia, 1992, pp.149-170.

Handbook of Chemistry and Physics, 74th ed., CRC Press, 1993-1994, p 5-90.

Hunter, D. (1988)."Lime-Induced Heave in Sulfate-Bearing Clay Soils", J. of Geotechnical Engrg., ASCE, 114(2), pp. 150-167.

Isenburg, J. and Moore, M. (1992), "Generalized Acid Neutralization Capacity Test", *Stabilization and Solidification of Hazardous, Radioactive, and Mixed Wastes, 2nd Volume, ASTM STP 1123*, T. M. Gilliam and C.C. Wiles, Eds., American Society for Testing and Materials, Philadelphia, pp. 361-377.

Kamon et al. (1988), "Reutilization of Waste Concrete Powder by Cement Hardening", Journal of the Japanese Society of Materials Science, Vol. 37, No 422, pp. 1260-65.

Kamon M and Nontananandh S., (1991), "Combining Industrial Wastes with Lime for Soil Stabilization", *J. of Geotechnical Engrg*, ASCE, Vol. 117, No. 1, January, 1991, pp.1-17.

Kumarathasan, P. McCarthy, G., Hassett, D., and Pflughoeft, D.F. (1990). "Oxyanion Substituted Ettringite: Synthesis and Characterization; and Their Potential Role in Immobilization of As, B, Cr, Se and V", *Mat. Res. Soc. Symp. Proc.*, 178, pp. 83-104.

Kujala, K. (1986)."Stabilization of Harmful Wastes and Muds", Proc. of 1st Int. Symposium on Environmental Geotechnology, Vol. 1, pp. 540-548.

Kuroda et al. (1980)."Stabilization Effect of a New Cement Fixing Agent (Parts I & II)", Research Institute of Technology, Tokyo Construction Co Ltd., Japan.

Mitchell, J. K. (1984)."Practical Problems from Surprising Soil Behavior", J. of Geotechnical Engrg., ASCE, 112(3), pp. 250-289.

Mitchell, J. K., (1993), "Fundamentals of Soil Behavior", John Willey & Sons, Inc., 2nd edition.

Mitchell, J. K. and Dermatas, D., (1992), "*Clay Soil Heave Caused by Lime-Sulfate Reactions*", Innovations in Uses for Lime, *ASTM Special Technical Publication 1135*, American Society for Testing and Materials, Philadelphia, PA, pp. 41-64.

Payne J. R. et al. (1992), "DCR Treatment of Oily Wastes and Oil-Contaminated Soils", Hazardous Materials Control Research Institute, to be presented at the Research and Development Conference '92, February 1992, San Francisco, CA, 17 pages.

Shida et al. (1987), "Developing a New-Type Stabilizer Made from Industrial Wastes as a Soft Ground Stabilizer", Proc. of the 22nd Japanese National Conference on Soil Mechanics and Foundation Engrg., Nigata, Japan, 1987, pp. 1881-1884.

Suprenant B. A. et al. (1990), "Oilcrete", ASCE Civil Engineering Magazine, Vol 60, No. 4, April 1990, pp. 61-63.

Transportation Research Board, National Research Board, (1987), "Lime Stabilization, Reaction, Properties, Design, and Construction," Prepared by Transportation Research Board Committee on Lime and Lime-Fly Ash Stabilization.

Turco M. A. and Zenobia K. E. (1985). "A Case Study: Lime-A Hazardous Waste Stabilization Agent", Lime for Environmental Uses, ASTM STP 931, Los Angeles, CA, June 25, 1985, pp. 69-77.

U. S. Environmental Protection Agency (1985), "Solid Waste Leaching Procedure Manual", *SW-924*, U. S. EPA, Cincinnati, OH.

US EPA, (1989), "Stabilization/Solidification of CERCLA and RECRA Wastes: Physical Tests, Chemical Testing Procedures, Technology Screening, and Field Activities," EPA/625/6-89/022, CERI, Cininati, OH.

Welsh, S., Gagnon, J. and Elnabarawy, M. (1981), "Comparison of Three Acid Extraction-Leaching Test Protocols", *Hazardous Solids Waste Testing: First Conference, ASTM STP 760*, pp. 28-39.

Zhou, H. and Colombo, P. (1987),"Solidification of Low-Level Radioactive Wastes in Masonry Cement", Brookhaven National Lab, Upton, NY, USA, prepared for the Dept. of Energy, Washington, DC, March 1987.

Appendix A Experimental protocols

The effectiveness of the proposed quicklime treatment was tested under optimum water content compaction conditions. Tests were performed on artificial soil specimens composed of 5% to 30% of kaolinite or montmorillonite and 70% to 95% quartz fine sand. Mixtures of clay and sand were used, rather than pure clay, to obtain specimens with gradations more comparable to those of naturally occurring soils and to provide materials that could be mixed and compacted easier than pure clays. Lead, chromium, mercury nitrates and oxides, arsenic oxide, and sodium arsenite were used as the contaminant source.

The specimen preparation for the optimum water content compaction experiments involved dry mixing of all constituents in designated percentages, followed by addition of water, mellowing and compaction under standard conditions. The four heavy metals were added in a solid form to the clay-sand mixes at contents based on the untreated weight of the soils (124 mg As(III), 4040 mg Cr^{3+}, 7006 mg Pb^{2+} and 1823 mg Hg^{2+} per kg of solid). Since the heavy metals were added as salts or oxides, the amount of salts needed to provide the required level of contamination was calculated based on the targeted species concentrations. Quicklime (CaO) was added at 5% to 15% and sodium sulfate was added at 4% to 8%, both contents on a by weight basis of the dry mixes. The amounts of water added to the solid mixes were such as to obtain compacted solids with maximum dry density for a given compactive effort.

Specimens were compacted at optimum water content according to ASTM D1557-91 standard (*American Society of Testing and Materials, 1992a*), and cured at 20°C and 95% RH. Specimen dimensions varied depending on the type of tests to be performed. A compacted specimens cylinder with a 3.5 cm diameter and a 7.0 cm height was used for compressive strength tests. The specimens used for swell testing were 4.75 cm in diameter and 4.0 cm in height. A 4 lb. (1.8 kg) compaction rammer with a 12 inch (30.5 cm) drop was fabricated to achieve the required compactive effort of 56,250 lb./ft^2 specified by ASTM D 1557-91. Following 28 days of curing, the compressive strength and swell were determined, and the heavy metal leachability of the treated specimens was evaluated using the TCLP method (US Environmental Protection Agency, 1985), the Acid Neutralizing Capacity (ANC) method (Isenburg and Moore, 1992), the ANS 16.1 method (ANS 16.1, 1986), and by conducting the flow-through flexible wall column experiment as described in the following sections.

A.1 Toxicity Characteristic Leaching Procedure (TCLP)

The U. S. Environmental Protection Agency (EPA) TCLP is a batch leaching test (US Environmental Protection Agency, 1985). In this test, the waste is pulverized and mixed with an acetic acid solution (pH = 3.0 or 5.0) at a solution to solid ratio of 20.0. The suspension is tumbled for 18 hours before the separation of the extract solution from the solid takes place by filtration. The

extract pH was recorded and the heavy metals in the extract were analyzed using an inductively coupled plasma atomic emission spectrometer.

A.2 Strength Testing

After 28 days and 6 months of curing periods, strength specimens were removed from the plastic bags, and their dimensions and weights were recorded. The ASTM standard D2166-85 *(American Standard Test Method for Unconfined Compressive Strength of Cohesive Soil)* was used to determine their unconfined compression strengths. The test was performed under a constant axial strain rate of 2% per minute. The axial load was recorded as a function of axial deformation. The axial strain and stress were calculated based on the load deformation data. A stress-strain curve was drawn to obtain the maximum stress. This stress was taken as the unconfined compressive strength for the specimen. The apparatus used was supplied by Soiltest Company (model no.U-610 168). Water content was measured from the failed specimen.

A.3 Swell Testing

The vertical swell test was conducted by soaking the cured specimen in a water saturated sand-bath. The specimen was placed in the middle of a high density polyethylene cup, and confined laterally by the surrounding sand. The initial reading of the dial gage was recorded. Specimens were allowed to soak for a 24 hour period, after which the final reading of the dial gage was recorded. Dial gage readings were taken periodically, and the swell versus time relationship was established for each specimen.

A.4 Flow-Through Leaching

In the present study, infiltration leaching was simulated with a flow-through leaching system, to enable the prediction of actual field heavy metal leaching and evaluate the effect of soil permeability on the leaching behavior of the compacted solid specimens. Specimen dimensions were based on ASTM D 3877-85 (American Society for Testing and Materials, 1992a). This standard specifies that minimum specimen thickness shall be 1.9 cm and other dimensions to be in accordance with ASTM D 2435-80 (American Society for Testing and Materials, 1992a), which specifies minimum specimen diameter-to-height ratio to be 2.5. The compaction mold used had a diameter of 4.75 cm. Therefore, flow-through leaching specimens were compacted at approximately 2 cm of height to comply with the aforementioned standards. The specimens were compacted in 3 layers at 6 blows per layer resulting in a compactive effort of approximately 57,730 lb./ft^2.

The compacted specimens were placed in a confined chamber and tested in a manner similar to a flexible wall permeability test (Figure 146). During the experiment a 0.014 M acetic acid solution at a pH of 3.45 was passed through the specimens under constant hydraulic head conditions, without prior back pressure specimen saturation. The leachant was collected regularly for leachant volume measurement, pH levels, and heavy metal analyses. The hydraulic

gradients applied to the specimens were unrealistically high and varied between 15.0 and 280.0 in an attempt to attain reasonable testing duration times as a function of the anticipated specimen soil permeability values. The flow-through tests simulated the behavior of the treated solid under severe field conditions (low pH, continuous leaching, and high hydraulic gradients). In addition to the acid leaching, a limited number of tests were carried out using distilled water as the leachate, mainly for comparison purposes.

A.5 Static Leaching Test

A moderate set of leaching conditions is simulated through the contact of the outer surface of monolithic solids with water or other leachant. In natural environments, this can happen when a given waste form lies below the groundwater table in a very low hydraulic gradient flow regime. The American Nuclear Society (ANS, 1986) 16.1 static leaching procedure for hazardous wastes was used to simulate such a scenario. During this test, compacted samples with 4.70 ± 0.05 cm diameter by 4.0 ± 0.4 cm height were used. After the samples were cured for 28 days, they were immersed in distilled water for 30 seconds to rinse out any loose particles on the sample surface. A Nylon mesh specimen harness was used to support each sample near the centroid of approximately 950 mL of the acetic acid solution (0.014 N at pH = 3.45) in a polyethylene container (Figure 146). The leachant volume to the specimen's external geometric surface area ratio was maintained at 10.0 ± 0.2 cm. During the experiment, the leachant was replaced at designated time intervals (2, 7, 24, 48, 72, 121, 456, 1128, and 2160 hours). Heavy metals in the leachate were analyzed using an inductively coupled plasma atomic emission spectrometer or graphite furnace atomic absorption spectrometer, and pH changes were also recorded.

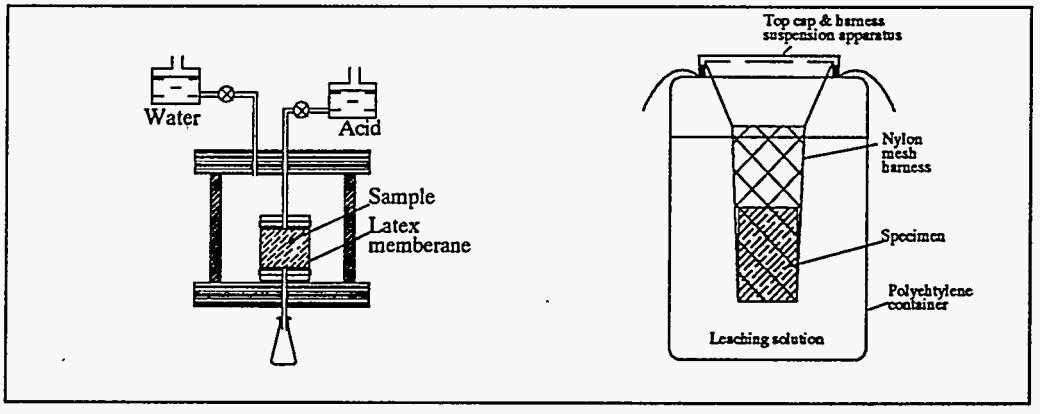

Figure 146. (a) Flow-through Leaching Apparatus (b) Static Leaching Apparatus

A.6 Acid Neutralization Capacity (ANC) Test

The ANC is a measure of a solid sample to resist pH reduction caused by acid leaching. In general, heavy metals found in solid wastes with relatively high ANC are less mobile as the adsorption of the heavy metals on solids is increased and the solubility of the heavy metals is relatively low in alkaline conditions. Quicklime addition increases the soil pH and ANC. However, it is neither economical nor practical to add too much quicklime into the contaminated soil. High quicklime content could also limit the strength development of the treated soils. Therefore, an optimum lime-level should be obtained. Overall, the ANC testing provides useful information on the amount of quicklime to be added to contaminated soils since the leaching behavior of heavy metals is directly related to the soil ANC.

The ANC test procedure reported by Isenburg and Moor (1992) was used in our laboratory. The test was conducted by placing one gram of dry solids in a series of bottles. Then, a certain volume of 2.0 N acetic acid and distilled water are added to the bottles. The total volume of the solution is 20 mL. After the samples are tumbled in the TCLP rotating extractor for 48 hours, the pH of the solution is measured.

A.7 Severe Weathering Tests

Freeze/thaw tests were conducted according to ASTM standard method D 560-82 (American Society for Testing and Materials, 1986a) to evaluate the swell of the treated specimens. Each cycle included 24 hours freeze at 0°C (for kaolinite) or -5°C (for montmorillonite) and 24 hours thaw at 22°C. An environmental chamber (Model HB/12, Standard Environmental System Inc., NJ) was used for conducting the freeze test, and the samples were thawed in a temperature control room. For the samples which withstood the first 12 freeze/thaw cycles, more severe temperature changes (-15°C to 22°C) were used in the second and third 12 cycles to test them.

Wet/dry cycles tests were conducted according to ASTM standard method D 559-82 for wetting-and-drying tests of compacted soil-cement mixtures (American Society for Testing and Materials, 1986b) to evaluate the swell of the samples after they had been soaked in a water saturated sand-bath for three months. During the tests, the samples were dried at 70°C for 24 hours and then soaked in water for 24 hours. Overall, 12 wet/dry cycles were conducted for each sample. For the samples which withstood the first 12 wet/dry cycles, a higher temperature (110°C) was used for the dry step in the second and third 12 cycles of wet/dry tests. Because the swell value could not fully represent the physical disintegration of the samples, photographs were taken for each sample during the durability tests.

Appendix B Mineralogical Studies

When contaminated soils are treated using quicklime, new minerals will be formed as the pozzolanic reaction products. At the same time, heavy metals can be immobilized through several reactions, such as precipitation at high pH, enclusion of the heavy metals in the pozzolanic reaction products, and adsorption of heavy metals on the solid surface. The minerals formed in the treated solids also have significant effect on the physical properties of the solid, such as strength and swell. A thorough understanding of the mineralogical properties of quicklime treated soil will help us to undersign mechanisms for immobilization of heavy metals and to predict the long-term chemical and physical behaviors of the treated soils. In this work, the mineralogical compositions of the treated samples were investigated using X-ray diffraction. The effect of quicklime contents, clay type and curing time on the formation of minerals in the solid was studied.

The mineralogical changes with respect to curing time for representative samples are compared in Tables 11 and 12 for kaolinite and montmorillonite mixes, respectively. The results in Table 11 and 12 indicate that ettringite, a very important mineral because of its contribution to strength development of the treated solid and because of its ability to incorporate heavy metal species within its molecule leading to pozzolanic fixation, was formed in all lime-sulfate treated mixes after a short time of curing and remain stable thereafter. However, X-ray analyses of samples taken from the same K30L15S specimen and tested under air-dried and non air-dried conditions suggest that the monosulfate ettringite formation may proceed to the ettringite (trisulfate) formation at early stage of curing. This observation was based on the fact that monosulfate is not stable under air-dried conditions while trisulfate is not affected by them.

The formation of monosulfate or trisulfate ettringite is determined by the ratio between Al_2O_3 and SO_4. When this ratio is higher than 1.0, the monosulfate formation is favored. In the case of K30L15S specimen, it is suggested that the high pH caused dissolution of kaolinite which releases excess amount of alumina, leading to monosulfate ettringite formation rather than to trisulfate (Table 11). However, when barium hydroxide was added to the quicklime treated sample, neither trisulfate nor monosulfate ettringite was formed (Table 11). Instead, barium sulfate precipitate was formed.

Hydrated lime was detected in the quicklime treated samples since the first day of the treatment (Tables 11 and 12). The hydrated lime still existed after the treated samples were cured for half a year. However, quick lime crystals were also detected even after K30L10 and K30L15S specimens were cured for 6 months. In most of the cases, the presence of free quicklime and hydrated lime is associated with calcite formation, a reaction product of calcium carbonation.

As mentioned above, when a significant quantity of lime is added to a soil, the pH of the soil-lime mixture is elevated to the pH value of saturated lime water (pH=12.4). At such a high pH, the solubilities of silica and alumina are increased. Under these conditions, the lime, water, soil silica, and alumina coming from the clay mineral dissolution and to some extend from the quartz

dissolution, react to form various cementecious (pozzolanic) compounds, such as calcium silica hydrate (CSH), calcium alumina hydrate (CAH), calcium alumina silicate hydrate (CASH-Gismondine), etc. The amount and presence of pozzolanic reaction products is of great concern, mostly because of their contribution to heavy metal immobilization, also because of their ability to increase the soil mixture strength and to resist volumetric changes(expansion).

The results as reported in Tables 18 and 19, indicate the formation of pozzolanic reaction products in all the lime treated mixes. However, ettringite was formed only when (in this study with sodium sulfate decahydrate) sulfate was added to the lime stabilized mixes. In contrast to the treated mixes, the untreated mixes did not undergo any significant chemical reaction. No mineralogical changes were observed with respect to time for any untreated mix. Only quartz and clay minerals were detected for the untreated mixes.

It is known that the pozzolanic reactions are time dependent. That explains the absence of any cementecious compound at the early stage of curing, with the exception of ettringite which formed from the first day of curing for both kinds of clay-systems. Besides ettringite, the most dominant pozzolanic phase is CSH compound. Moreover, the X-ray analyses postulates the formation of some other pozzolanic products, such as CAH, CASH, and for some specimens $NaCaAl_3Si_3O_{12}$. The degree of crystallization and the quantity of these compounds seems to be proportional to the curing time, based on the intensity and the broadness of their X-rays scans.

The mineralogies of the treated kaolinite-sand and montmorillonite-sand specimens that cured for 28 days are presented in Tables 20 and 21. The results indicate 15% clay was usually enough to provide the treated mix with alumina and silica for pozzolanic reactions. When clay contents were higher, more free alumina and silica were available for the reactions. As the results, more pozzolanic reaction products were formed within a short period of curing time. Moreover, x-ray analyses suggest that under conditions where free alumina was in excess in specimens, such as high amount of clay (30%), the CASH formation was favored. Since kaolinite clay contains more alumina than montmorillonite, it seems that 15% kaolinite was enough for CASH formation.

The amount of quicklime as the stabilizing agent in the treated mixes is a critical factor for the heavy metal immobilization, since it controls the pozzolanic fixation process. The comparison between the mineralogy of specimens treated with various amount of quicklime (Tables 20 and 21) suggests that a treatment of 10% of quicklime by total weight was the optimum quicklime content, since it provided the soil mix with all the necessary amount of calcium cations for the chemical reactions leading to soil stabilization and heavy metal immobilization. An increase in quicklime content to 15% did not provide better fixation. Instead, the presence of excess lime usually led to calcite formation, which was an undesirable mineral in the lime stabilized soil.

The treated samples had experienced different experimental tests, including normal curing, water soaking during swell, and aggressive weathering (wet/dry and freeze/thaw). The mineralogical changes of the specimens were also

assessed using x-ray diffraction. The mineralogical properties of these specimens are summarized in Tables 22 and 23. According to the x-ray analyses, ettringite was not affected by the freeze and thaw, even at temperatures as low as -15°C. Thus, the presence of ettringite did not adversely affect the freeze-thaw durability. On the other hand, ettringite decomposed when the samples were heated to 110°C. Further experiments were conducted to investigate if ettringite could be formed again after oven drying. An oven-dried specimen was soaked in water for 12 hours, then examined using x-ray. The results indicated ettringite was formed again upon rehydration.(Figures 153 and 154).

Other pozollanic reaction products, such as CAH and CSH were also affected by wetting/drying or freezing/thawing weathering. On the other hand, CASH was not affected by wetting/drying and freezing/thawing weathering. The x-ray analyses indicate that the hydrated lime was converted to calcite during wetting/drying or freezing/thawing weathering. This process seems to be more pronounced during the wet/dry cycles.

X -ray scans for representative specimens are presented in Figures 147 to 155. The x - ray scans for specimens containing 30% montmorillonite and treated with 10% of quicklime are presented because they represent the optimum treatment conditions. The x - ray scans for untreated and the treated kaolinite specimens were already reported in the results section (Figures 22 to 24). Therefore, x - ray scans for kaolinite-sand specimens treated with quicklime/fly ash are presented in Figures 150 to 152. The x -ray scans for untreated specimens provide information on the basic minerals that present in the mixtures of clay and sand used in the study.

Table 18. X-Ray Analyses of Kaolinite Specimens Cured for Different Period of Time

Sample identification	K30L0						K30L10					K30L10S						K30L15S				K30L10S+Ba 1:1					
Phases / Curing time (days)	1	7	14	28	60	180	1	7	14	60	180	1	7	14	28	60	180	1	7	14	60	1	7	14	28	60	180
Montmorillonite	---	---	---	---	---	---	---	---	---	---	---	---	---	---	---	---	---	---	---	---	---	---	---	---	---	---	---
Kaolinite	✓	✓	✓	✓	✓	✓	✓	✓	✓	✓	✓	✓	✓	✓	✓	✓	✓	✓	✓	✓	✓	✓	✓	✓	✓	✓	✓
Sand	✓	✓	✓	✓	✓	✓	✓	✓	✓	✓	✓	✓	✓	✓	✓	✓	✓	✓	✓	✓	✓	✓	✓	✓	✓	✓	✓
Ettringite	---	---	---	---	---	---	---	---	---	---	---	---	✓	✓	✓	✓	✓	---	---	✓	✓	---	---	---	---	---	---
Monosulfate	---	---	---	---	---	---	---	---	---	---	---	---	---	---	---	---	---	✓	✓	---	---	---	---	---	---	---	---
Quicklime (CaO)	---	---	---	---	---	---	✓	✓	✓	✓	✓	---	---	---	---	---	---	✓	✓	✓	✓	---	---	---	---	---	---
Lime ($Ca(OH)_2$)	---	---	---	---	---	---	✓	✓	✓	✓	✓	✓	✓	✓	✓	✓	✓	✓	✓	✓	✓	✓	✓	✓	✓	✓	✓
Calcite($CaCO_3$)	---	---	---	---	---	---	---	---	---	✓	✓	---	---	---	---	---	---	---	---	---	---	---	---	---	---	---	---
Al_2O_3	---	---	---	---	✓	---	---	✓	✓	✓	---	---	---	---	✓	✓	✓	---	---	✓	✓	✓	✓	✓	✓	✓	✓
CSH	---	---	---	---	---	---	---	✓	✓	✓	✓	---	✓	✓	✓	✓	✓	---	---	✓	✓	---	---	---	---	✓	---
CAH	---	---	---	---	---	---	---	---	---	---	---	---	---	---	✓	✓	---	---	---	---	---	---	---	---	---	✓	✓
Gypsum ($CaSO_4.2H_20$)	---	---	---	---	---	---	---	---	---	---	---	---	---	---	---	---	---	---	---	---	---	---	---	---	---	---	---
$NaCaAl_3Si_3O_{12}$	---	---	---	---	---	---	---	---	---	---	---	---	---	---	---	---	---	---	---	---	---	---	---	---	✓	✓	---
Gismondine	---	---	---	---	---	---	---	---	---	✓	---	---	---	---	---	✓	✓	---	---	---	✓	---	---	---	---	---	---
Barium Sulfate ($BaSO_4$)	---	---	---	---	---	---	---	---	---	---	---	---	---	---	---	---	---	---	---	---	---	✓	✓	✓	✓	✓	✓
Barium Hydroxide ($Ba(OH)_2$)	---	---	---	---	---	---	---	---	---	---	---	---	---	---	---	---	---	---	---	---	---	✓	✓	✓	✓	✓	✓

ABBREVIATIONS USED:

This phase excists in the system for this corresponding time

---: This phase does not excist in the system for this corresponding time

Table 19. X-Ray Analyses Montmorillonite Specimens Cured for Different Period of Time

Sample identification	M30L0					M30L10						M30L10S						M30L15S				
Phases / Curing time in days	1	7	14	60	180	1	7	14	28	60	180	1	7	14	28	60	180	1	7	14	28	60
Montmorillonite	✓	✓	✓	✓	✓	✓	✓	✓	✓	✓	✓	✓	✓	✓	✓	✓	✓	✓	✓	✓	✓	✓
Kaolinite	---	---	---	---	---	---	---	---	---	---	---	---	---	---	---	---	---	---	---	---	---	---
Sand	✓	✓	✓	✓	✓	✓	✓	✓	✓	✓	✓	✓	✓	✓	✓	✓	✓	✓	✓	✓	✓	✓
Ettringite	---	---	---	---	---	---	---	---	---	---	---	✓	✓	✓	✓	✓	✓	✓	✓	✓	✓	✓
Monosulfate	---	---	---	---	---	---	---	---	---	---	---	---	---	---	---	---	---	---	---	---	---	---
Qlime (CaO)	---	---	---	---	---	---	---	---	---	---	---	---	---	---	---	---	---			---	---	---
Lime ($Ca(OH)_2$)	---	---	---	---	---	✓	✓	✓	✓	✓	✓	✓	✓	✓	✓	✓	✓	✓	✓	✓	✓	✓
Calcite($CaCO_3$)	---	---	---	---	---	✓	✓	✓	✓	✓	✓	✓	✓	✓	✓	✓	✓	---	---	✓	✓	✓
Al_2O_3	---	---	---	---	---	---	✓	✓	✓	✓	✓	✓	✓	✓	✓	✓	✓	---	---	✓	✓	✓
CSH	---	---	---	---	---	✓	✓	✓	✓	✓	✓	✓	✓	✓	✓	✓	✓	---	✓	✓	✓	✓
CAH	---	---	---	---	---	---	---	---	---	---	---	---	---	---	---	✓	---	---	---	✓	✓	✓
Gypsum ($CaSO_4.2H_20$)	---	---	---	---	---	---	---	---	---	---	---	---	---	---	---	---	---	---	---	---	---	---
$NaCaAl_3Si_3O_{12}$	---	---	---	---	---	---	---	---	---	---	---	---	---	---	---	---	---	---	---	---	✓	✓
Gismondine	---	---	---	---	---	---	---	---	---	---	---	---	---	---	---	---	---	---	✓	✓	✓	✓
Barium Sulfate ($BaSO_4$)	---	---	---	---	---	---	---	---	---	---	---	---	---	---	---	---	---	---	---	---	---	---
Barium Hydroxide ($Ba(OH)_2$)	---	---	---	---	---	---	---	---	---	---	---	---	---	---	---	---	---	---	---	---	---	---

ABBREVIATIONS USED:

✓: This phase exists in the system for this corresponding time; ---: This phase does not exist in the system for this corresponding time

Table 20. X-Ray Diffraction Analyses of Kaolinite-sand Specimens, 28 Days Curing

PHASES	SAMPLE IDENTIFICATION											
----------	K15L0	K15L10	K15L10S	K15L10S*	K15L10S +Ba 1:1	K30L10	K30L15	K30L10S	K30L10S+Ba 0.2:1	K30L10S+Ba 0.5:1	K30L10S+Ba 1:1	K30L15S
Montmorillonite	---	---	---	---	---	---	---	---	---	---	---	---
Kaolinite	✓	✓	✓	✓	✓	✓	✓	✓	✓	✓	✓	✓
Sand	✓	✓	✓	✓	✓	✓	✓	✓	✓	✓	✓	✓
Ettringite	---	---	✓	✓	✓	✓	✓	✓	✓	---	---	✓
Monosulfate	---	---	---	---	---	---	---	---	---	---	---	---
Quicklime (CaO)	---	---	---	---	---	---	---	---	---	---	---	✓
Lime ($Ca(OH)_2$)	---	✓	✓	✓	✓	✓	✓	✓	✓	✓	✓	✓
Calcite($CaCO_3$)	---	---	---	---	✓	✓	✓	✓	✓	✓	✓	---
Al_2O_3	---	✓	✓	✓	✓	✓	✓	✓	✓	✓	✓	---
CSH	---	✓	✓	✓	✓	✓	✓	✓	---	---	---	✓
CAH	---	---	---	---	---	---	---	---	---	✓	✓	---
Gypsum ($CaSO_4.2H_20$)	---	---	---	---	---	---	---	---	---	✓	✓	---
$NaCaAl_3Si_3O_{12}$	---	✓	✓	✓	---	---	---	---	---	---	---	---
Gismondine	---	✓	✓	✓	---	---	---	---	✓	---	---	✓
Barium Sulfate ($BaSO_4$)	---	---	---	---	✓	---	---	---	✓	✓	✓	---
Barium Hydroxide ($Ba(OH)_2$)	---	---	---	---	---	---	---	---	---	---	---	---

ABBREVIATIONS USED:

✓: This phase exists in the system for this corresponding time

---: This phase does not exist in the system for this corresponding time

Table 21. X-Ray Diffraction Analyses of Montmorillonite-sand Specimens, 28 Days Curing

PHASES	SAMPLE IDENTIFICATION															
----------	M5 L0	M5 L5	M5 L5S	M5 L10S	M15 L0	M15 L10	M15 L15	M15 L15S	M30 L0	M30 L5	M30 L5S	M30 L10	M30 L10S	M30 L10S*	M30 L15	M30 L15S
Montmorillonite	✓	✓	✓	✓	✓	✓	✓	✓	✓	✓	✓	✓	✓	✓	✓	✓
Kaolinite	---	---	---	---	---	---	---	---	---	---	---	---	---	---	---	---
Sand	✓	✓	✓	✓	✓	✓	✓	✓	✓	✓	✓	✓	✓	✓	✓	✓
Ettringite	---	✓	✓	✓	---	---	---	✓	---	---	✓	✓	✓	✓	---	✓
Monosulfate	---	---	---	---	---	---	---	---	---	---	---	---	---	---	---	---
Quicklime (CaO)	---	✓	✓	✓	---	---	---	---	---	---	---	---	---	---	---	---
Lime ($Ca(OH)_2$)	---	✓	✓	✓	---	✓	✓	✓	---	✓	✓	✓	✓	✓	✓	✓
Calcite($CaCO_3$)	---	✓	---	---	---	---	---	---	---	---	---	---	---	✓	✓	✓
Al_2O_3	---	✓	✓	✓	---	✓	✓	✓	---	---	---	✓	✓	✓	✓	✓
CSH	---	---	---	✓	---	✓	✓	✓	---	---	✓	✓	✓	✓	✓	✓
CAH	---	---	---	---	---	---	---	---	---	---	---	---	---	---	---	---
Gypsum ($CaSO_4.2H_20$)	---	---	---	---	---	---	---	---	---	---	---	---	---	---	---	---
$NaCaAl_3Si_3O_{12}$	---	---	---	---	---	---	---	---	---	---	---	---	---	---	---	✓
Gismondine	---	---	---	---	---	---	---	✓	---	---	✓	---	✓	✓	✓	✓

ABBREVIATIONS USED:

:This phase exists in the system for this corresponding time

--- :This phase does not exist in the system for this corresponding time

Table 22. X-Ray Analyses of Kaolinite-sand Specimens Tested under Different Conditions

Identification	2 theta	d-space	UNTREATED				LIME (10%) TREATED				LIME (10%) AND SULFATE TREATED			
			K30L0 Freeze& Thaw	K30L0 Wet&Dry	K30L0 Swell	K30L0 Strength	K30L10 Freeze& Thaw	K30L10 Wet&Dry	K30L10 Swell	K30L10 Strength	K30L10S Freeze& Thaw	K30L10S Wet&Dry	K30L10S Swell	K30L10S Strength
Ettringite	9.1	9.7	-	-	-	-	-	-	-	-	15	24	13	11
Kaolinite, CASH	12.15	7.27	100	100	100	100	100	100	100	100	98	88	100	100
Ettringite	15.8	5.6	-	-	-	-	-	-	-	-	7	13	8	8
CAH	17.17		-	-	-	-	-	-	6	7	-	-	-	-
Ettringite, Lime, CASH	17.8	4.98	-	-	-	-	16	-	16	22	20	17	17	19
Kaolinite	19.75	4.49	35	35	19	37	18	26	22	22	25	27	25	21
Sand, CASH	20.65	4.29	29	29	19	23	23	30	15	15	25	32	15	16
Ettringite	22.9	3.87	11	11	9	10	-	-	-	-	14.07	12	20	8
Kaolinite	24.75	3.59	83	85	87	77	71	77	90	55	100	100	89	66
Sand, CASH	26.45	3.36	31	78	35	37	10	34	15	15	20	18	51	21
Lime, CASH	28.65	3.11	-	-	-	-	-	-	-	10	16	22	9	26
CSH	29.3		-	-	-	-	-	-	12	-	-	-	-	-
Calcite	29.65	3.009	-	-	-	-	22	86	32	18	20	88	44	22
CSH	31.5		-	-	-	-	-	-	7	-	-	-	-	-
Aluminum oxide	32.15	2.78	10	16	6	10	-	-	-	-	-	-	-	-
CSH	33.15		-	-	-	-	-	-	7	-	-	-	-	-
Lime	33.95	2.63	-	-	-	-	23	-	26	32	31	24	24	39
Kaolinite, Ettringite, Aluminum oxide	34.85	2.57	22	17	14	17	20	14	15	15	22	25	20	21
Kaolinite, Sand	36.3	2.47	-	9	-	-	13	29	21	-	20	-	-	10
Kaolinite,Quicklime, Alum. oxide	37.6	2.39	10	28	-	23	10	-	15	10	13	18	15	8
Kaolinite, Aluminum oxide	38.2	2.353	28	18	16	22	19	25	20	16	20	33	27	18
Sand, Calcite, CAH	39.25	2.29	10	13	8	11	14	27	18	12	20	18	20	10
Sand, Aluminum oxide	42.25	2.13	-	6	-	-	-	13	-	-	-	17	-	-
Calcite	43.13		-	-	-	-	8	25	7	12	-	17	15	10
Kaolinite, CAH	45.8	1.979	12	10	8	10	8	10	-	8	16	13	10	10
Lime	46.95	1.93	-	-	-	-	14	-	8	16	15	31	16	20
Sand	49.95	1.82	11	10	-	6	-	20	10	-	-	16	-	-
Kaolinite, Lime, CSH	50.75	1.79	11	10	6	6	11	-	8	12	20	16	10	13
Lime	54.2	1.69	10	6	6	7	-	15	12	12	10	12	9	12
Sand	59.9	1.54	-	7	-	5	-	-	-	-	-	18	7	-
Kaolinite	62.3	1.468	19	13	16	16	13	16	15	17	24	25	17	15
Sand, Aluminum oxide	67.85	1.38	-	-	-	-	-	10	-	-	-	-	-	-
Sand	68.15	1.373	-	12	-	-	-	-	-	-	-	-	-	-

Table 23. X-Ray Analysis of Montmorillonite-sand Specimens Tested under Different Conditions

Identification	2 &	Spacing	NO LIME				LIME TREATED (10%)				LIME (10%) AND SULFATE			
			M30L0 Freeze&Thaw	M30L0 Wet&Dry	M30L0 Swell	M30L0 Strength	M30L10 Freeze&Thaw	M30L10 Wet&Dry	M30L10 Swell	M30L10 Strength	M30L10S Freeze&Thaw	M30L10S Wet&Dry	M30L10S Swell	M30L10S Strength.
Montmorillonite	6.95	12.71	62	100	80	74	35	33	80	80	84	55	48	65
Ettringite	9.1	9.7	-	-	-	-	14	16	38	30	88	25	16	39
Montmorillonite	11.7	7.55	15	-	-	-	-	-	-	-	-	-	-	-
CASH	12.15	7.27	-	-	-	-	8	10	30	12.2	-	-	-	-
Ettringite	15.8	5.6	-	-	-	-	-	12	24	20	50	27	11	18
CAH	17.17		-	-	-	-	10	-	16	26	10	-	5	10
Ettringite, Lime, CASH	17.8	4.98	-	-	-	-	6	-	-	-	45	-	-	15
Montmorillonite	19.55	4.53	43	50	55	60	17	17	36	65	58	16	19	43
Montmorillonite, Sand, CASH	20.65	4.29	60	46	50	51	16	35	100	52	42	28	45	26
Montmorillonite	21.7		-	86	100	100	14	20	-	45	-	-	-	-
Ettringite	22.9	3.87	-	-	-	-	-	20	37	33	25	22	11	22
Montmorillonite, Sand, CASH	26.45	3.36	100	80	98	75	45	24	55	100	100	41	54	52
Montmorillonite, Ettringite	27.2		65	-	-	95	17	27	-	35	-	-	-	-
Montmorillonite, Lime, CASH	28.65	3.11	-	-	-	-	-	-	-	-	50	15	17	35
CSH	29.3		-	-	-	-	15	-	26	45	-	-	-	-
Calcite	29.5	3.009	25	-	-	-	100	100	85	75	48	100	12	100
CSH	31.5		-	-	-	-	-	-	23	44	25	-	5	5
ettringite., Qlime, CASH, Alum. oxide	32.15	2.78	16	-	17	-	-	-	23	42	46	-	13	21
CSH	33.15		-	-	-	-	-	-	17	30	15	-	8	10
Lime	33.95	2.63	-	-	-	-	-	-	17	30	34	-	-	16
Montmorill., Ettringite, Alum. oxide	34.8	2.596	19	24	23	30	14	12	-	35	51	12	11	17
Montmorillonite, Sand	36.3	2.47	26	33	22	29	17	15	32	32	35	14	9	22
Quick lime	37.6	2.39	-	-	-	-	10	-	-	-	25	-	-	-
Sand, Calcite	39.25	2.29	22	-	-	20	12	20	30	31	-	24	16	16
Aluminum oxide	42.25	2.13	18	16	16	-	-	10	-	-	-	13	17	10
Calcite	43.3		-	-	-	-	14	18	32	-	-	-	-	-
Aluminum oxide	45.8	1.979	-	-	-	-	-	-	-	18	-	-	12	-
Lime	47.2	1.93	-	-	-	-	36	18	34	26	15	21	9	16
Aluminum oxide	48.5		-	-	-	-	11	20	30	-	-	-	18	-
Sand	49.95	1.82	13	12	17	13	7	13	90	30	20	12	13	20
Montmorillonite, Lime, CSH	50.6	1.802	10	10	-	13	6	10			18	-	-	-
Lime, Quicklime	54.2	1.69	12	10	14	17	5	12	26	20	10	10	8	15
Aluminum oxide	57	1.614	-	10	-	-	6	-	-	-	-	11	7	10
Sand	59.9	1.54	12	13	16	-	7	14	16	15	-	-	8	10
	62.3	1.468	17	19	26	22	9	-	-	25	20	-	8	-
Sand, Quicklime, Aluminum oxide	67.85	1.38	23	-	17	16	8	9	12	16	-	-	-	11
Sand	68.15	1.373	15	15	-	-	8	10	12	14	-	-	6	-

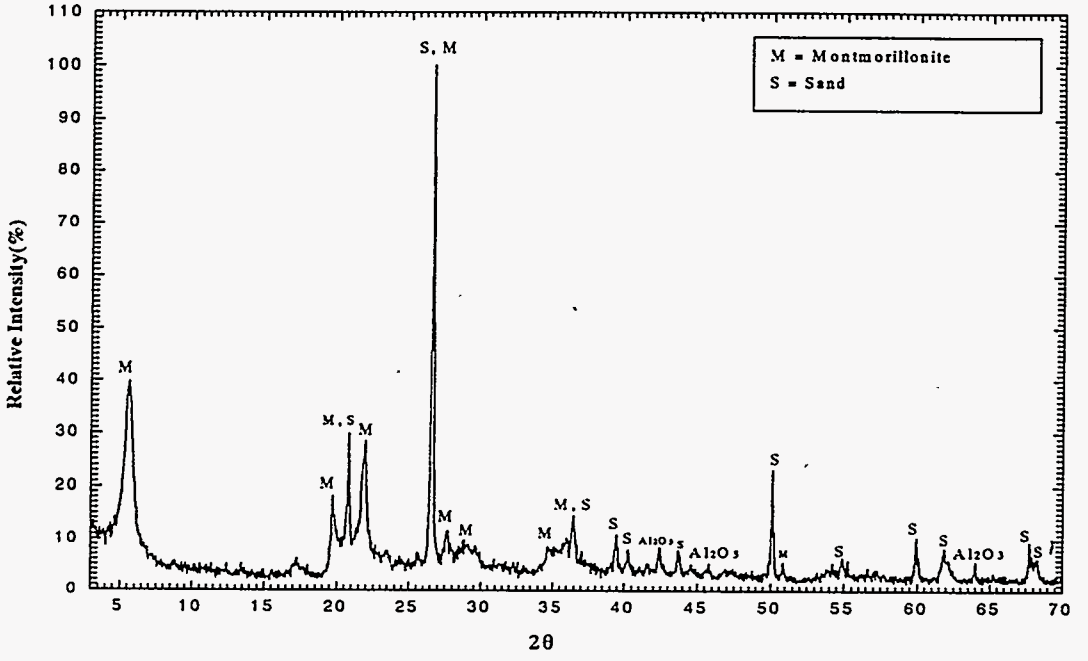

Figure 147. X-ray Scans for M30L0 Sample, 28 Days of Curing.

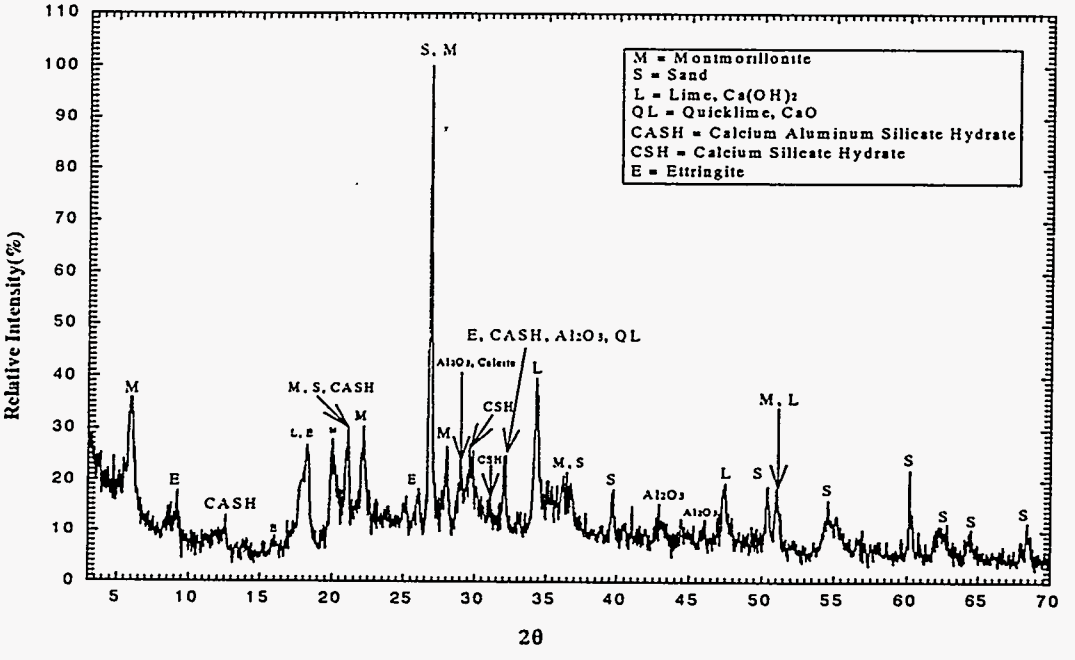

Figure 148. X-ray Scans for M30L10 Sample, 28 Days of Curing.

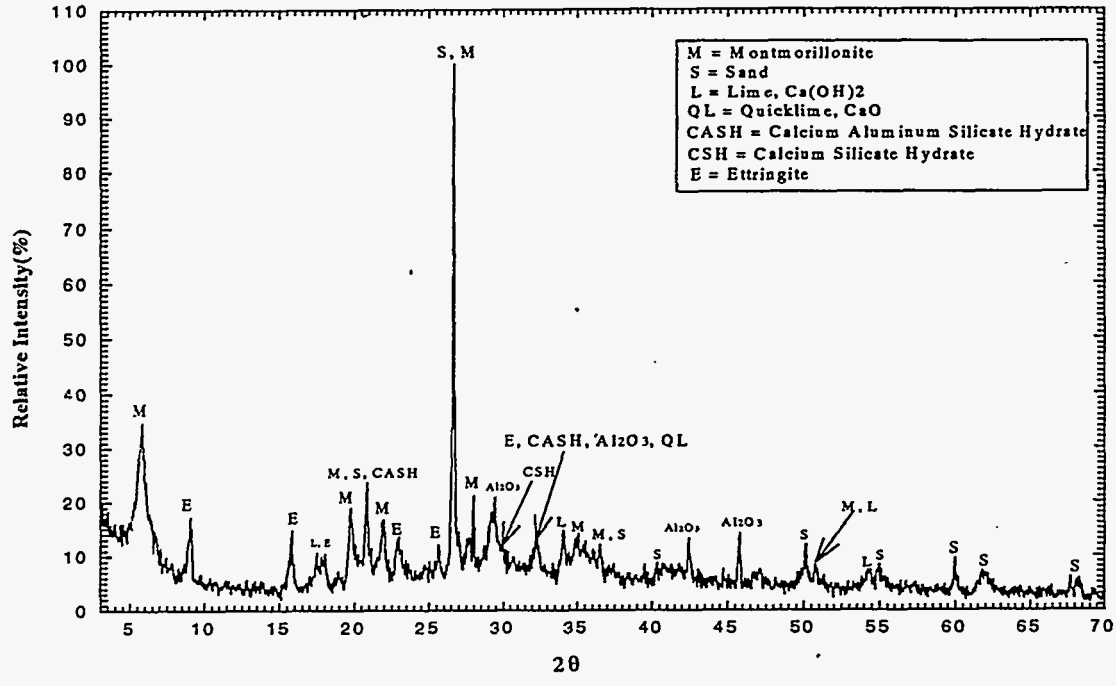

Figure 149. X-ray Scans for M30L10S Sample, 28 Days of Curing.

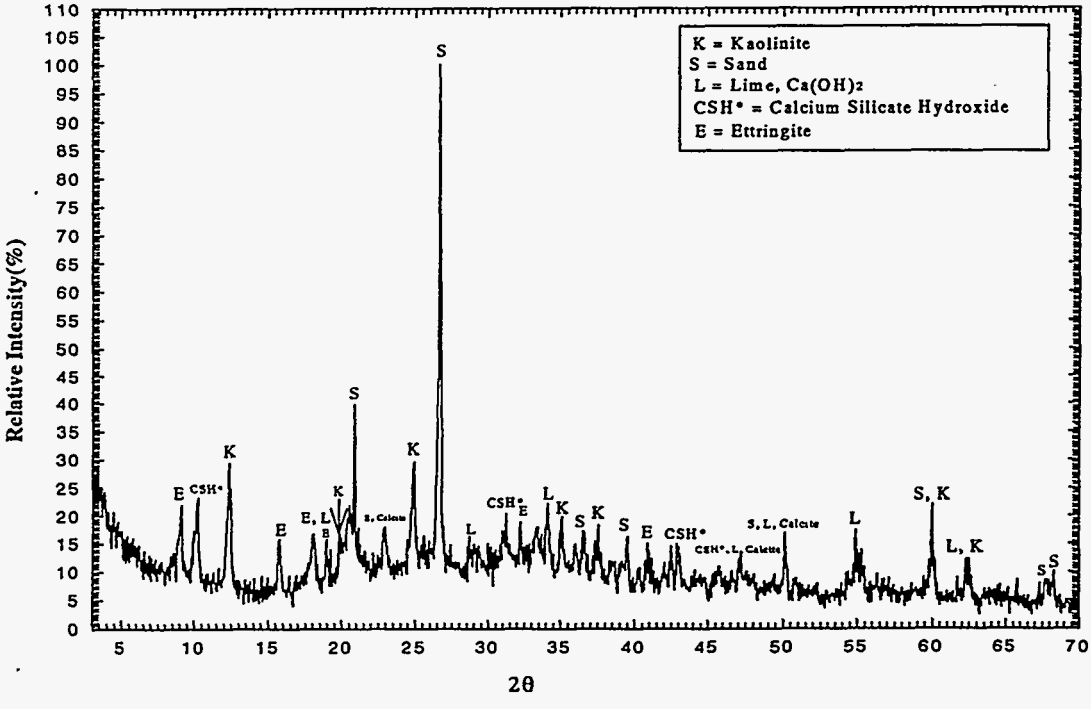

Figure 150. X-ray Scans for K5C25L0 Sample, 28 Days of Curing.

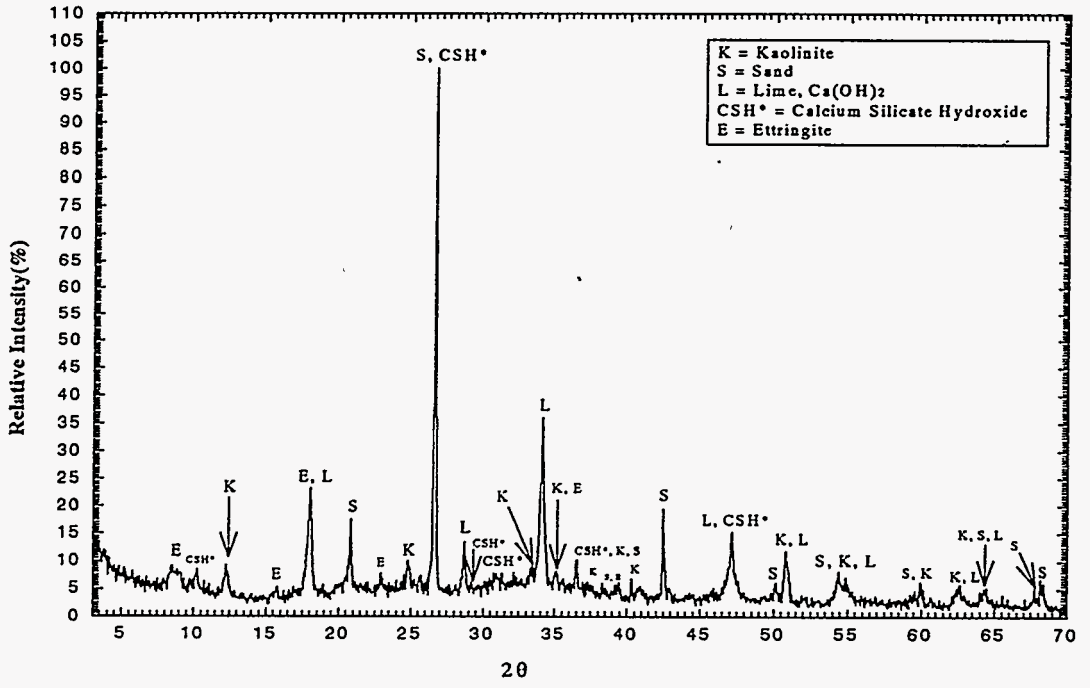

Figure 151. X-ray Scans for K5C25L10 Sample, 28 Days of Curing.

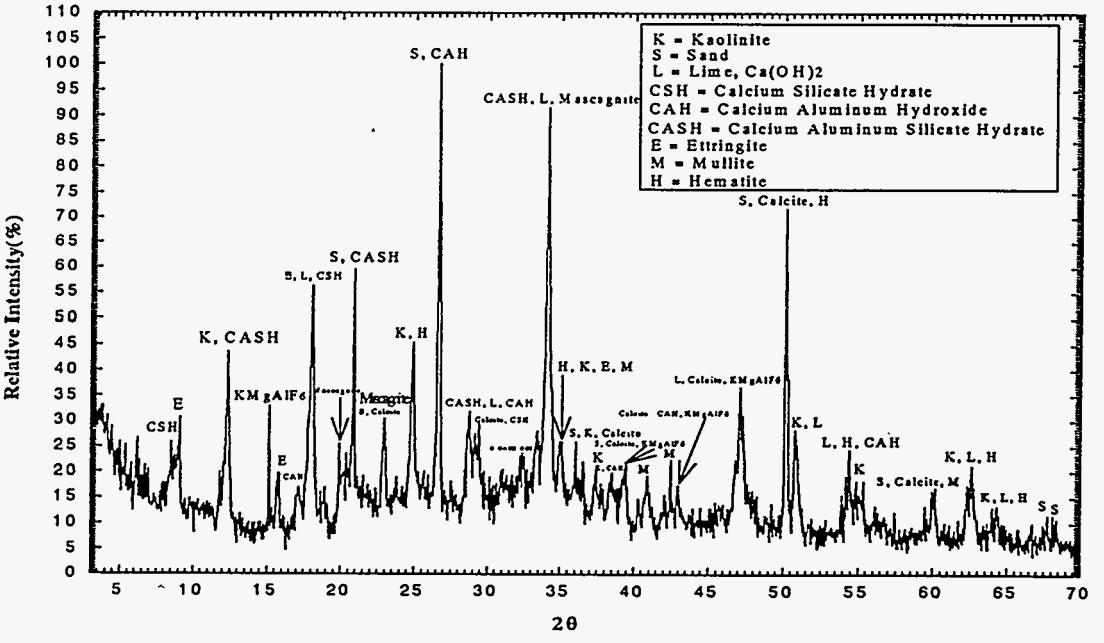

Figure 152. X-ray Scans for K5C25L10S Sample, 28 Days of Curing.

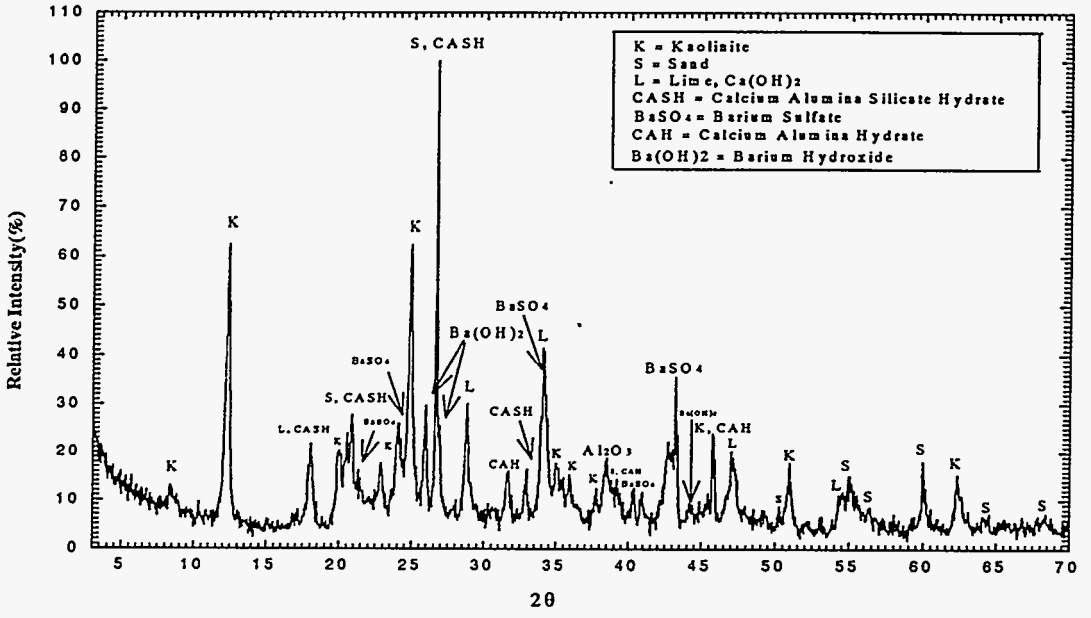

Figure 153. X-ray Scans for K30L10S+Ba 1:1 (Ba/SO_4 Molar Ratio = 1), 28 Days of Curing.

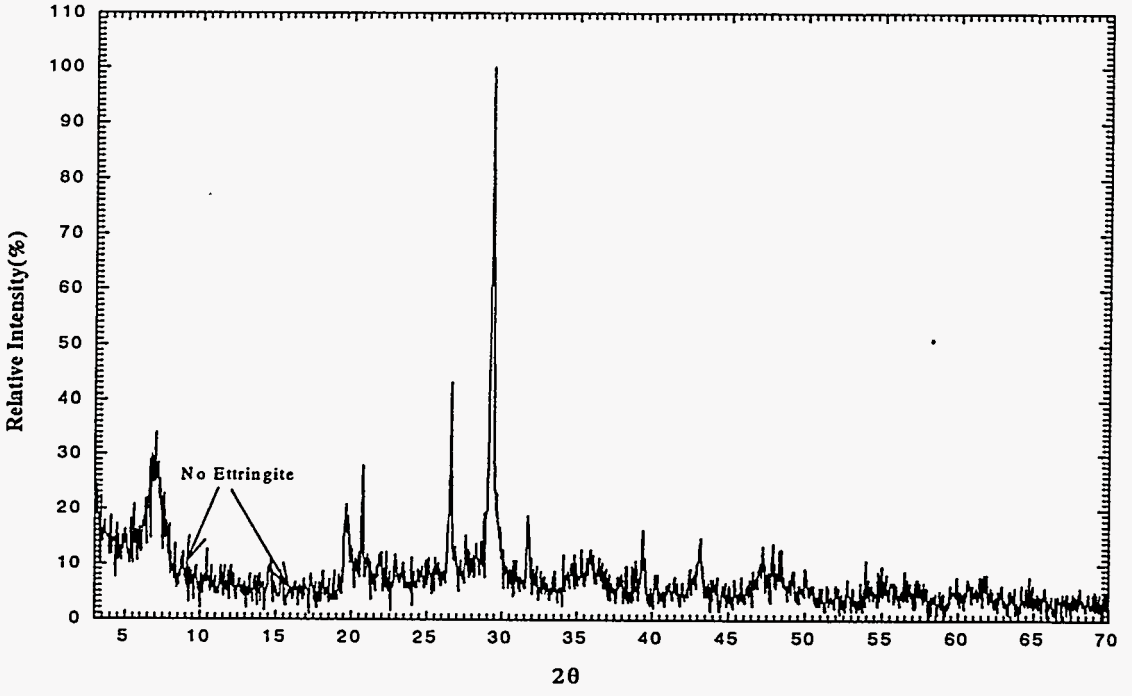

Figure 154. X-ray Scans for M30L10S (Wet and Dry) Sample----- before wetting

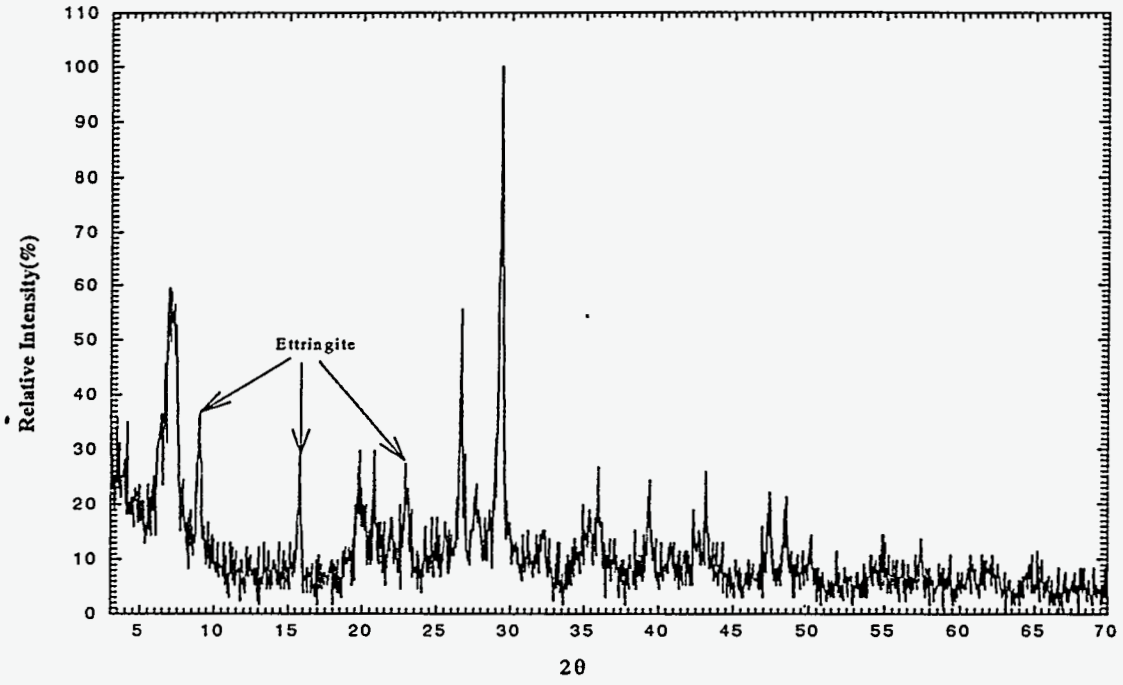

Figure 155. X-ray Scans for M30L10S (Wet and Dry) Sample

Appendix C Micromorphological Studies

Quicklime treatment of the contaminated soils will result in the formation of mineral crystals and amorphous materials. The chemical compositions of soil particle surface will also be changed as the results of quicklime treatment. The particle micromorphology and the surface chemical compositions of the quicklime treated soils were studied using a scanning electron microscope (SEM) and energy despersive x-ray (EDX), respectively.

Figures 156 to 157 are the SEM micrographs of quicklime treated and untreated kaolinite samples that were cured for 1 day. The SEM micrographs of the montmorillonite samples cured for 1 day are presented in Figures 160 to 162. Both treated and untreated samples contained aggregates of nondescript particles. No obvious difference in the particle morphologies were observed for the samples. However, the surface compositions of the treated samples were quite different from the untreated samples (Table 24). The untreated samples (K30L0 and M30L0) contained mainly Si and Al. No Ca was detected on the K30L0 sample, and only 5.4% Ca was detected for M30L0 sample. When the samples were treated with 10% of quicklime, approximately 50% Ca was detected. The results indicated Ca was enriched on the particle surface. This was mainly due to relatively high solubility of $Ca(OH)_2$, and Ca^{2+} adsorption or precipitation on clay and sand surfaces.

After the samples were cured for 28 days, needle-shaped crystals were observed for the quicklime/sulfate treated kaolinite (K30L10S) samples (Figure 165). Further analyses of the surface compositions using spot mode EDX revealed the chemical composition of the needles was different from the overall chemical composition of K30L10S samples (Table 24). The needle surface consisted of 63.1% Ca, 20.3% S, and 5.6% Al. This chemical composition was similar to needle-shaped ettringite. Based on the chemical formula of ettringite, $[Ca_3Al(OH)_6]_2(SO_4)_2 \cdot 26H_2O$, it was calculated that ettringite contained 62% Ca, 25% S, and 14% Al. In the calculation, oxygen and hydrogen were not considered because they were not detected by EDX. The results proved ettringite was formed in K30L10S sample. These results agreed with the X-ray diffraction results, which also indicated the formation of ettringite. Ettringite was not evidenced for K30L0 and K30L10 samples (Figures 163 and 164) because the presence of sulfate and quicklime was necessary for the formation of ettringite. When barium hydroxide was added to the quicklime/sulfate treated sample, small particles were formed (Figure 165). The EDX results (Table 24) indicated the small particles in K30L10S+Ba sample were mainly composed of Ba and Ca. It was obvious that the presence of Ba inhibited the formation of ettringite. In contrast to kaolinite samples, only a small amount of ettringite was observed in the quicklime/sulfate treated montmorillonite sample cured for 28 days (Figure 169). After 75 days of curing, a large amount of ettringite was formed in the montmorillonite sample (Figure 170). The EDX analyses detected

high Si content on the needle-shaped crystals in the montmorillonite specimens (Table 24).

Several authors have suggested that heavy metals can be immobilized by ettringite through isomorphous substitution of the ions in the mineral structure (Kamon and Nontananandh, 1991; Kumarathasan et al., 1990). However, no obvious differences in the leachability of the heavy metals were observed for the quicklime treated mixes with and without sulfate addition, although x-ray and SEM analyses indicated ettringite was formed in the treated specimens containing sulfates. To further elucidate the ettringite - heavy metal association, ettringite was precipitated in laboratory conditions in the presence of each of the four heavy metals under study. More specifically, ettringite was formed in a 1 g CaO/L and 5 mM of $Al_2(SO_4)_3$ solution (pH =11.3) in the presence of As, Cr, Hg or Pb ions.

The SEM micrographs (Figures 171 to 173) showed that both needle-shaped ettringite crystals and nondescript particles were formed in the presence of the heavy metals. Similar results were obtained for Hg. Chemical compositions of needle-shaped particles and nondescript shaped particles were determined using the EDX and results were summarized in Table 25. Compositions of needle-shaped particles formed in presence of heavy metals were similar to ettringite. The nondescript particles contained mainly aluminum and calcium. Chemical composition results together with x-ray diffraction patterns suggested the nondescript particles were mixtures of aluminum and calcium hydroxides, close to the composition of regular pozzolanic calcium-aluminate-hydrate products (CAH's).

X-ray results suggested that both ettringite and chromium (III) substituted ettringite (i. e. bentorite, $[Ca_3Cr(OH)_6]_2(SO_4)_26H_2O$) formed in the suspension. However, energy-dispersive x-ray analyses suggested the chromium content in the nondescript particles was more than twice as much as that detected in ettringite crystals (Table 25). Lead was also enriched in the nondescript particles, rather than ettringite. No As was detected in both ettringite and metal hydroxide surfaces. Overall, our results suggest the immobilization of heavy metals is not only controlled by ettringite formation in the lime treated specimens. In fact, it is CAH pozzolanic product formation (nondescript particles) that mostly controlled heavy metal immobilization.

Table 24. Chemical Composition Determined using EDX

Specimens	%								
	Al	Si	Ca	Ti	Cr	S	Ba	Fe	K
1 Day Curing									
K30L0	21.9	62.8	0	5.0	10.4	0	0	4.3	0
K30L10	12.0	26.8	61.2	0	0	0	0	0	0
K30L10S	12.1	25.5	53.5	2.18	1.8	4.9	0	0	0
K30L10S+Ba(1:1)	0	17.3	39.3	0	0	0	43.4	0	0
M30L0	6	88.6	5.4	0	0	0	0	0	0
M30L10	2.1	33.8	59.6	0	4.5	0	0	0	0
M30L10S	3.4	39.5	45.5	0	5.9	5.8	0	0	0
28 Days Curing									
K30L0	24.0	62.1	0	4.9	9.0	0	0	0	0
K30L10	12.0	38.9	49.1	0	0	0	0	0	0
K30L10S	13.1	33.7	46.4	2.4	0	4.4	0	0	0
Needles	5.6	9.4	63.1	0	1.6	20.3	0	0	0
K30L10S+Ba(1:1)	0	16.9	29.1	0	0	0	54.0	0	0
Small Particles	0	0	25.2	0	0	0	74.8	0	0
M30L0	6.1	78.6	3.6	0	3.8	0	0	8.0	0
M30L10	0	37.6	62.4	0	0	0	0	0	0
M30L10S	2.7	39.9	52.1	0	0	5.3	0	0	0
75 Days Curing									
M30L10S	0.6	42.3	49.3	0	1.9	4.9	0	0	0
Needles	4.6	33.7	52.6	0	0	9.1	0	0	0

TABLE 25. Chemical Composition of Particles in Synthesized Ettringite Suspension

Particles							
	Al	Ca	S	As	Cr	Pb	K
$As+CaO+Al_2(SO_4)_2$							
Needle	9.1	71.8	19.1	0	0	0	0
Nondescript	39.8	46.0	13.3	0	0	0	1.7
$Cr+CaO+Al_2(SO_4)_2$							
Needle	11.8	69.5	17	0	1.8	0	0
Nondescript	62.0	29.0	5.0	0	3.9	0	0
$Pb+CaO+Al_2(SO_4)_2$							
Needle	5.2	74.6	20.3	0	0	0	0
Nondescript	1.3	95.2	3.7	0	0	0	0

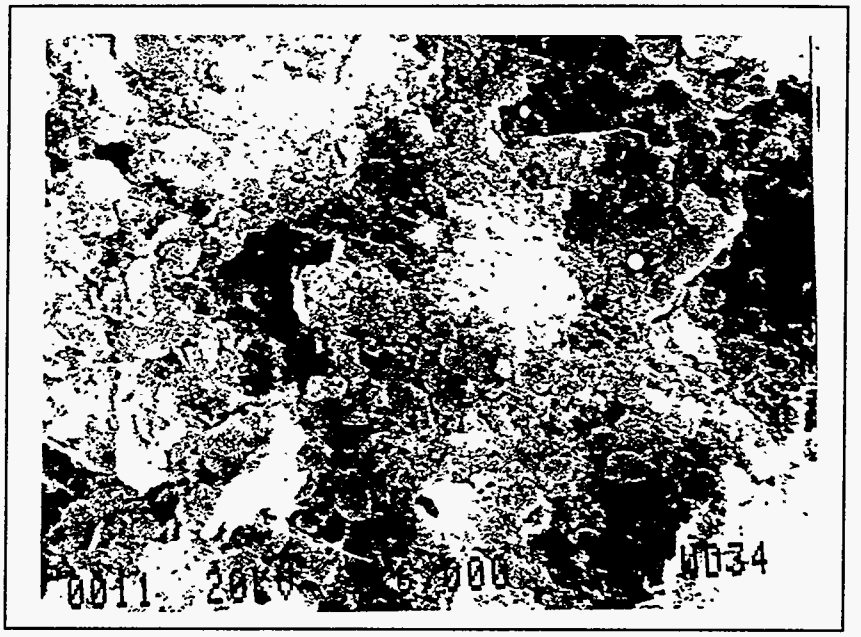

Figure 156. SEM Micrograph of K30L0 Specimen after Curing Period of 1 Day.

Figure 157. SEM Micrograph of K30L10 Specimen after Curing Period of 1 Day.

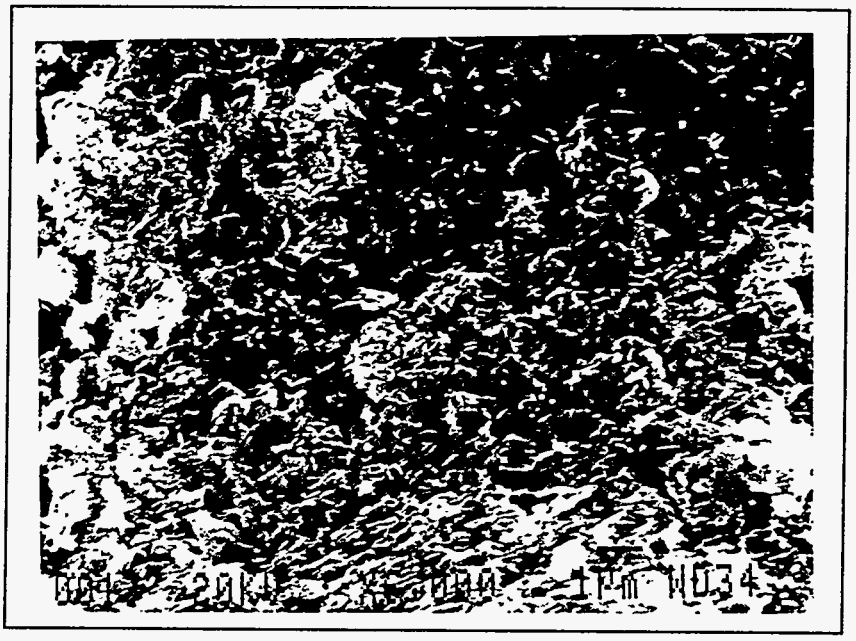

Figure 158. SEM Micrograph of K30L10S Specimen after Curing Period of 1 Day.

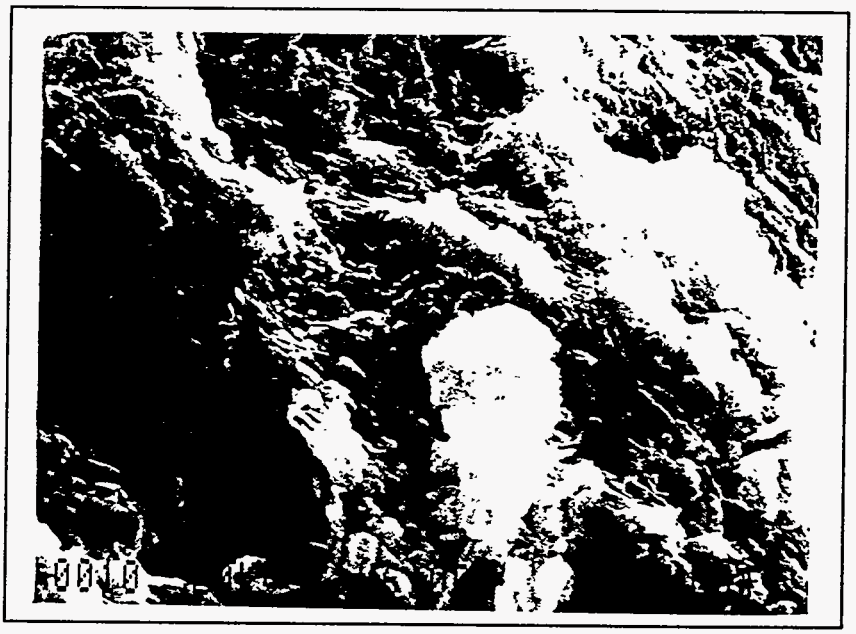

Figure 159. SEM Micrograph of K30L10S $Ba(OH)_2$ 1:1 Specimen after Curing Period of 1 Day.

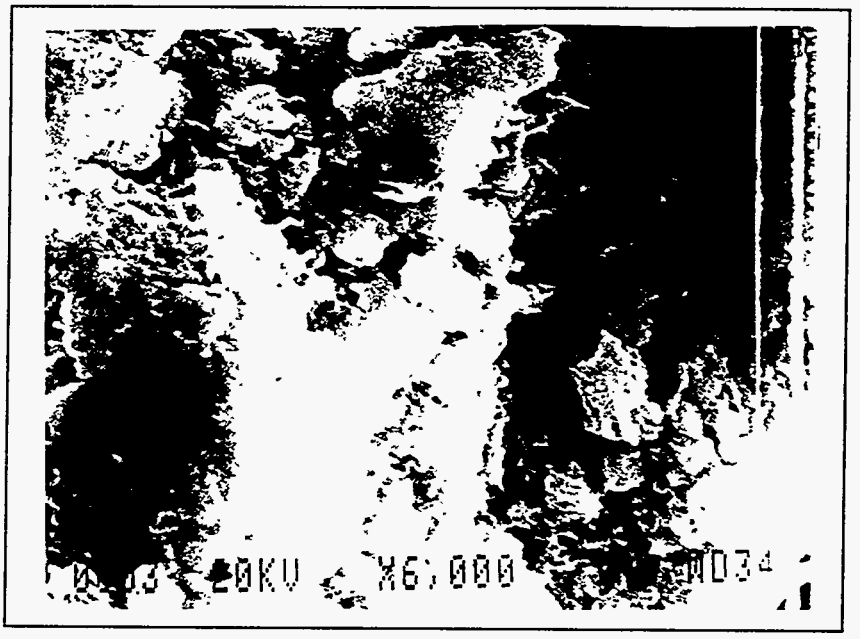

Figure 160. SEM Micrograph of M30L0 Specimen after Curing Period of 1 Day.

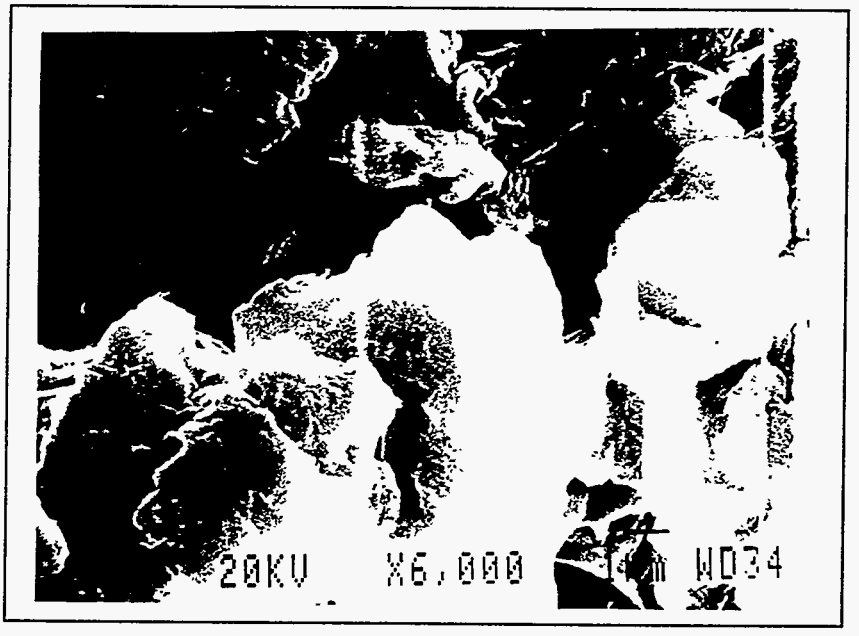

Figure 161. SEM Micrograph of M30L10 Specimen after Curing Period of 1 Day.

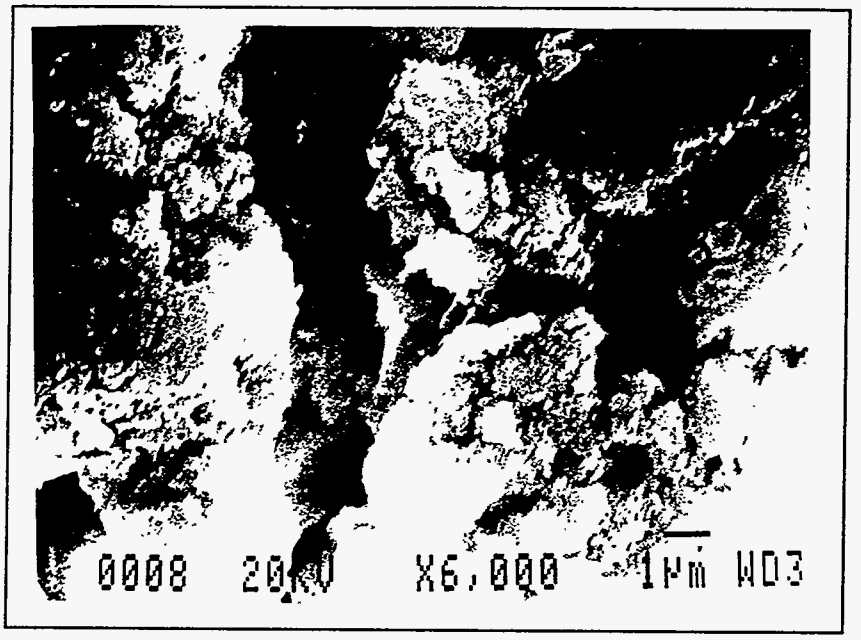

Figure 162. SEM Micrograph of M30L10S Specimen after Curing Period of 1 Day.

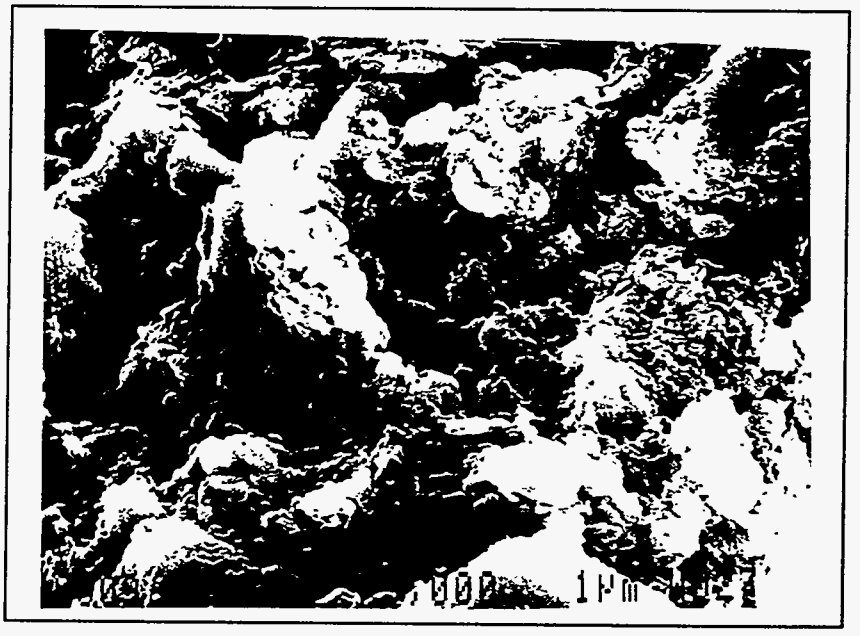

Figure 163. SEM Micrograph of K30L0 Specimen after Curing Period of 28 Days.

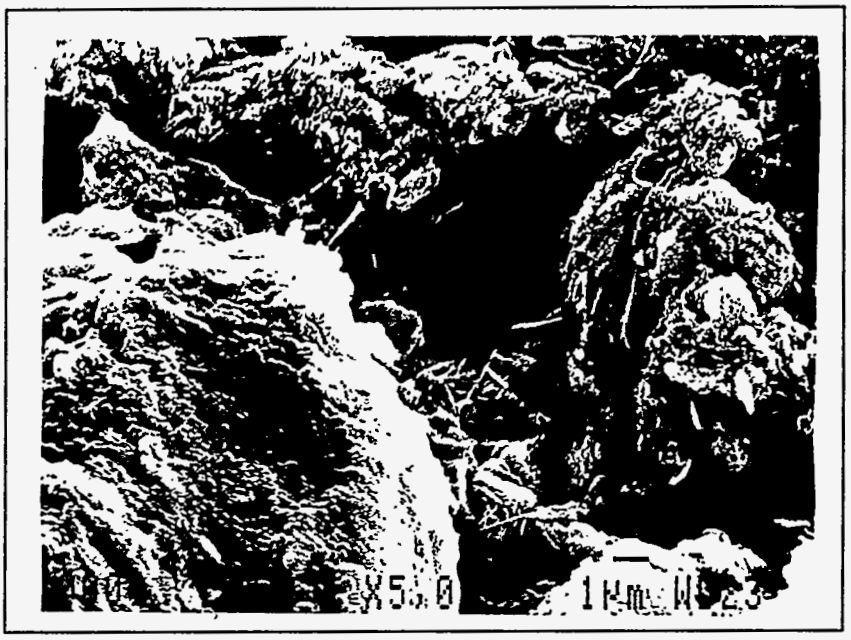

Figure 164. SEM Micrograph of K30L10 Specimen after Curing Period of 28 Days.

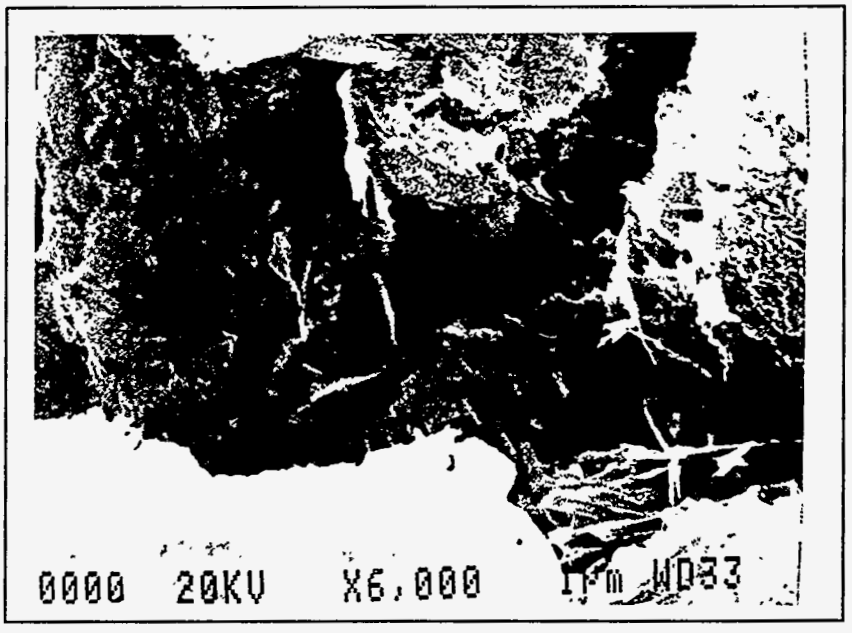

Figure 165. SEM Micrograph of K30L10S Specimen after Curing Period of 28 Days.

Figure 166. SEM Micrograph of K30L10S $Ba(OH)_2$ 1:1 Specimen after Curing Period of 28 Days.

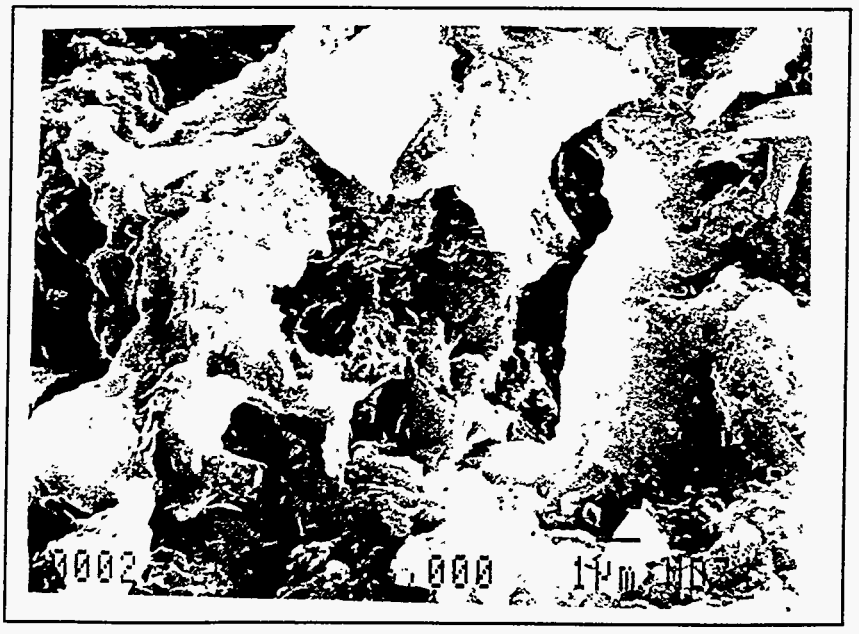

Figure 167. SEM Micrograph of M30L0 Specimen after Curing Period of 28 Days.

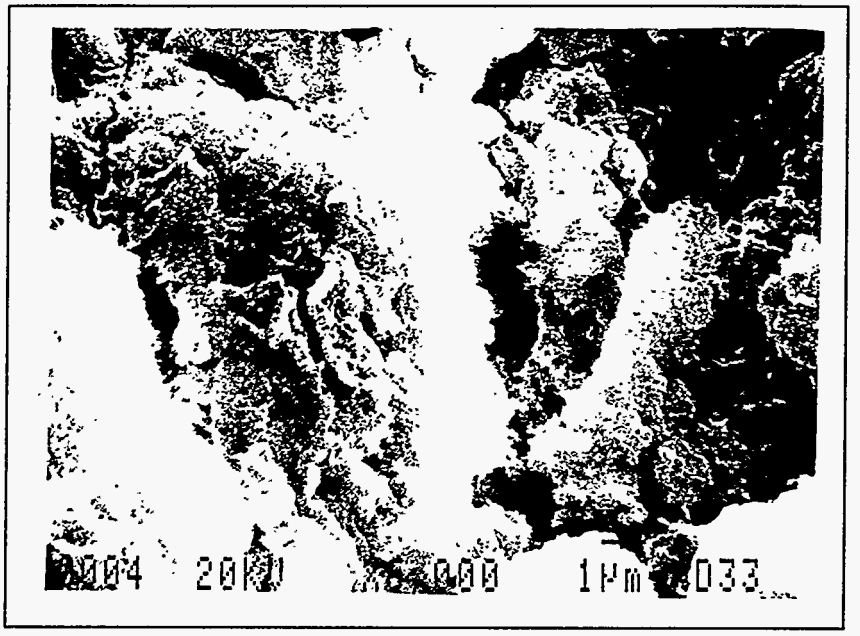

Figure 168. SEM Micrograph of M30L10 Specimen after Curing Period of 28 Days.

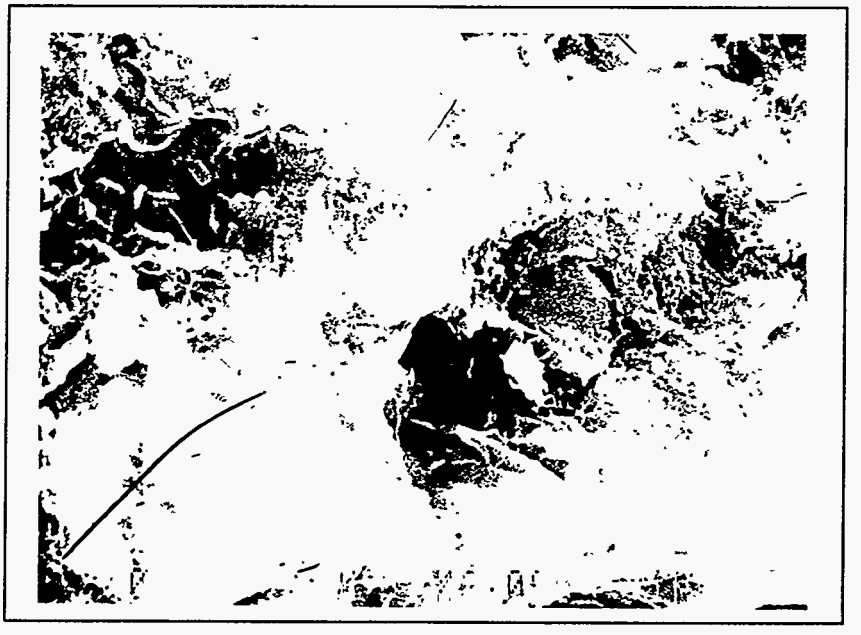

Figure 169. SEM Micrograph of M30L10S Specimen after Curing Period of 28 Days.

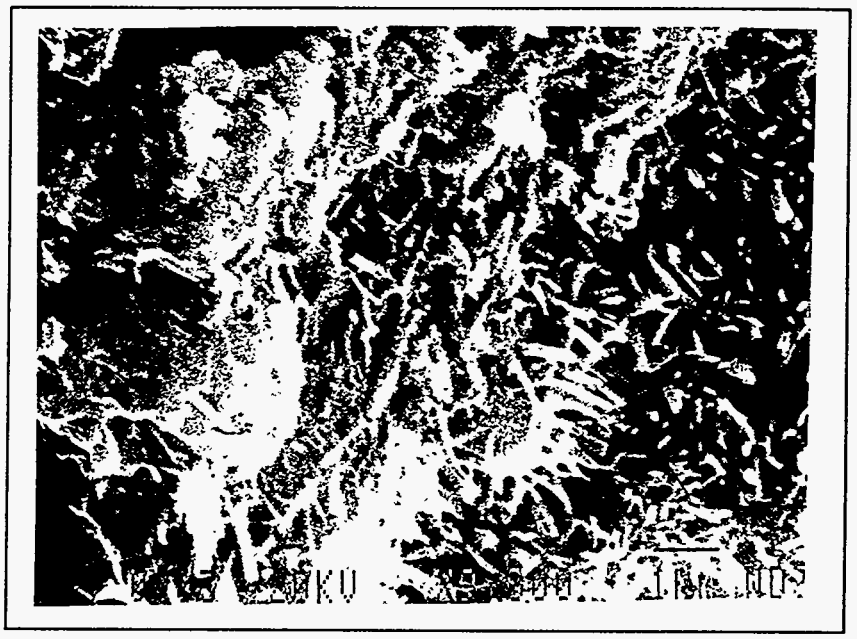

Figure 170. SEM Micrographof M30L10S Specimen after Curing Period of 75 Days.

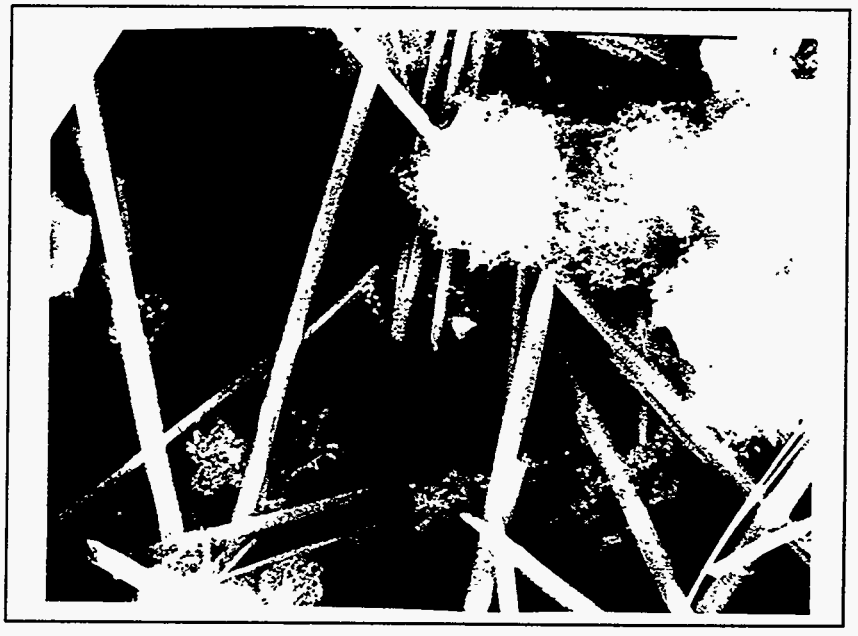

Figure 171. SEM Micrograph of Precipitates from As(III) + $CaO+Al_2(SO_4)_3$ Solution.

Figure 172. SEM Micrograph of Precipitates from Cr(III) + CaO+ $Al_2(SO_4)_3$ Solution.

Figure 173. SEM Micrograph of Precipitates from Pb(II) + CaO+ $Al_2(SO_4)_3$ Solution.

Appendix D Statistic Analysis of the Experimental Data

This project involved a variety of chemical measurements of muilt-component solid (artificial soils) samples. To ensue the accuracy and reproducibility of the experimental data, duplicates were prepared for each sample. For important tests, such as TCLP, strength, and swell, the experiments were repeated at least once to confirm the experimental results. The experimental data were summarized and analyzed using a statistical program (RS1 statistical software) to evaluate the contribution of the independent variables to the effectiveness of the quicklime. The mathematical correlation between the leachability of heavy metals of the quicklime-treated soil mixes and the independent variables was established.

The magnitude of TCLP leachability was affected to some extent by independent variables, such as quicklime, clay and sulfate contents, and curing time. To depict the contribution of each independent variable to the quicklime-treatment, a multilinear regression analysis was attempted on the experimental data obtained. By setting the probability of prediction to 0.95, multilinear regression equations 15 to 24 were derived to represent the relationship between heavy metal concentrations in the TCLP extracts and experimental conditions of the quicklime treatment.

Equation 15 represents the correlation between the lead concentration and independent variables for the kaolinite-sand mixes prepared using heavy metal oxides as the contamination source. This equation was derived based on 48 measurements under different treatment conditions. Equation 15 indicates that when stepwise linear regression model was employed to fit the experimental data, only lime and kaolinite contents had obvious effects on the lead concentration in the TCLP leachate. The curing time (between 28 and 85 days) had negligible effect on the leachability of the lead. The negative coefficients for percent lime and percent kaolinite terms in Equation 15 suggest the lead concentration is negatively correlated to lime and kaolinite contents. Because the absolute value for the lime term was larger than the absolute value of the kaolinite term, the contribution of lime content to the fit is larger than that of kaolinite content. Overall, Equations 15 to 24 indicate when quicklime content was between 0 and 10%, the concentration of lead, chromium, arsenic, and mercury in the leachate decreases with increasing lime content in all the clay-sand mixes. In a few cases, longer curing time seems to increase the leachability of the metals in the kaolinite-sand mixes contaminated with metal nitrates.

Lead

Oxides-Kaolinite: Concentration(ppm) = -23.0*(%lime) -1.9*(%kaol) +323.4 (15)

Oxides-Montmorillonite: Concentration(ppm) = -22.2*(%lime) +250.0 (16)

Nitrates-Kaolinite: Concentration(ppm) = -24.8*(%lime) +242.5 (17)

Arsenic

Oxides-Kaolinite: Concentration(ppm) = -0.14*(%lime) +1.34 (18)

Oxides-Montmorillonite: Concentration(ppm) = -0.06*(%lime) +0.78 (19)

Nitrates-Kaolinite: Concentration(ppm) = -0.25*(%lime) +0.02*(days) +1.92 (20)

Chromium

Nitrates-Kaolinite: Concentration(ppm) = -12.2*(%lime) +0.6*(days) +93.5 (20)

Mercury

Oxides-Kaolinite: Concentration(ppm) = -8.5*(%lime) +0.3*(days) +83.6 (21)

Oxides-Montmorillonite: Concentration(ppm) = -6.8*(%lime) +89.24 (22)

Nitrates-Kaolinite: Concentration(ppm) = -18.5*(%lime) +1.3*(days) +122.2 (23)

The statistical information about variance for Equations 15 to 24 is summarized in Table 26. The parameters in Table 26 indicate whether the equations explain a significant portion of the total variation in the data. R-squared is the multiple correlation coefficient and is used to measure the goodness-of-fit of the model. It ranges from 0.0 to 1.0, with values near zero implying little or no correlation in the samples and values near 1.0 implying strong correlation. The F value is the ratio of the regression mean square to the residual mean square and is a measure of the significance of the fit as a whole. The significance level of the F value is the probability of observing an F value as large, or larger than the one observed assuming that all the true coefficients are zero. A low F value (e.g., less than 0.05) for the significance level means the corresponding coefficient contributes significantly to the fit. An examination of Table 26 suggests that high R-squared values and low significance level are generally obtained, which implies that Equations 15 to 24 provide reasonable fit to the experimental data.

Table 26. Coefficients Table for Multilinear Regression with Respect to Leachate Concentration

Equation (17) $F=61.6, R^2=0.74$	%Lime	Curing Time (days)	%Clay
Fitted Coefficient	-23.008		-1.916
Standard Deviation	1.949		0.786
Significance Level	0.0001		0.024
Equation (18) $F=114.5, R^2=0.84$	%Lime	Curing Time (days)	%Clay
Fitted Coefficient	-22.245		
Standard Deviation	2.079		
Significance Level	0.0001		
Equation (19) $F=117.5, R^2=0.85$	%Lime	Curing Time (days)	%Clay
Fitted Coefficient	-24.827		
Standard Deviation	2.290		
Significance Level	0.0001		
Equation (20) $F=61.6, R^2=0.74$	%Lime	Curing Time (days)	%Clay
Fitted Coefficient	-0.144		
Standard Deviation	0.018		
Significance Level	0.0001		
Equation (21) $F=16.6, R^2=0.43$	%Lime	Curing Time (days)	%Clay
Fitted Coefficient	-0.061		
Standard Deviation	0.015		
Significance Level	0.0005		
Equation (22) $F=21.0, R^2=0.69$	%Lime	Curing Time (days)	%Clay
Fitted Coefficient	-0.251	0.015	
Standard Deviation	0.041	0.007	
Significance Level	0.0001	0.048	
Equation (23) $F=66.5, R^2=0.88$	%Lime	Curing Time (days)	%Clay
Fitted Coefficient	-12.156	0.613	
Standard Deviation	1.096	0.194	
Significance Level	0.0001	0.005	
Equation (24) $F=58.7, R^2=0.85$	%Lime	Curing Time (days)	%Clay
Fitted Coefficient	-8.470	0.268	
Standard Deviation	0.800	0.116	
Significance Level	0.0001	0.032	
Equation (25) $F=38.9, R^2=0.64$	%Lime	Curing Time (days)	%Clay
Fitted Coefficient	-6.812		
Standard Deviation	1.093		
Significance Level	0.0001		
Equation (26) $F=27.4, R^2=0.74$	%Lime	Curing Time (days)	%Clay
Fitted Coefficient	-18.471	1.303	
Standard Deviation	2.686	0.476	
Significance Level	0.0001	0.013	

Appendix E Specimen Visual Observation during Durability Testing

The swell results of the specimens under aggressive physical weathering in the form of wet/dry and freeze/thaw processes have been reported in Section 4.3.2. Because the swell value could not fully represent the physical disintegration of the samples, photographs were taken for each sample during the durability tests. The photographs of representative specimens are presented below.

E.1 Freeze/Thaw Tests

Before freeze/thaw and wet/dry tests, samples were soaked in a water saturated sand bath for 3 months to evaluate their swell under room temperature. Untreated kaolinite-sand (K30L0) and montmorillonite-sand (M30L0) specimens disintegrated after 3 months of soaking (Figures 174 and 175). The kaolinite specimen treated with 10% quicklime (K30L10) remained intact after the soaking (Figure 176). The first 12-cycles of freeze/thaw, including 24 hours freeze at 0°, and 24 hours thaw at 22°C, did not cause obvious damage to the specimen (Figure 177). For the samples which withstood the first 12 freeze/thaw cycles, more severe temperature changes (-15°C to 22°C) were used in the tests. The K30L10 specimen disintegrated after the second cycle of freeze/thaw under the more severe temperature changes (Figure 178). The specimen experienced a total of 14 cycles for the freeze/thaw tests before it failed. In contrast to the K30L10 specimen, the presence of sulfate in the treated kaolinite specimen (K30L10S) had an obvious crack in it after 3 months of soaking (Figure 179). After 4 cycles of freeze/thaw, the specimen was further disintegrated (Figure 180). A comparison of the physical behaviors of K30L10 and K30L10S specimens indicates that the formation of ettringite caused the crack in the K30L10S specimens. When kaolinite-sand mix was treated with quicklime/sulfate/barium hydroxide (K30L10S+Ba), the physical properties of the specimen were significantly improved (Figures 181 and 182). This was caused by the formation of barium sulfate, which depleted soluble sulfate for the formation of enttringite. The K30L10S+Ba specimen disintegrated after 15 cycles of freeze/thaw (Figure 183). The addition of fly ash into the treated kaolinite mix also improved the physical property of the specimen (Figure 184).

Significant coherent force was developed for the quicklime treated montmorillonite-sand specimens. The K30L10 specimen did have obvious damage after 3 months of soaking (Figure 185) and 13 cycles of freeze/thaw tests (Figure 186). The coherent force developed in the treated montmorillonite specimens could also overcome the swelling force caused by the formation and hydration of ettringite in the presence of sulfate (K30L10S, Figures 187 and 188). Both K30L10 and K30L10S specimens withstood 36 cycles of freeze/thaw without failure. The results suggest the coherent force developed in the treated montmorillonite specimens was much higher than that in the treated koalinite specimens. However, the montmorillonite specimen treated with 15% quicklime

and sulfate had disintegration after the second cycle of freeze/thaw (Figure 190). This was mainly caused by the excess amount of free lime in the specimen. The results suggest that the optimum quicklime content for the treatment of 30% montmorillonite/70% sand mix was 10%.

E.2 Wet/Dry Test

During the wet/dry tests, the samples were dried at 70°C for 24 hours and then soaked in water for 24 hours. Overall, 12 wet/dry cycles were conducted for each sample. For the samples which withstood the first 12 wet/dry cycles, a higher temperature (110°C) was used for the dry step of wet/dry tests. The quicklime treated kaolinite specimen (K30L10) had disintegration on the surface after 3 cycles of wet/dry tests (Figure 191). The kaolinite specimen treated with quicklime and sulfate also failed after the third cycle of wet/dry tests (Figure 192). The addition of barium hydroxide into the treated specimen (K30L10S+Ba) significantly improved the coherent force of the specimen (Figure 193). The specimen treated with fly ash and quicklime could also withstand more wet/dry cycles (Figure 194) than the quicklime treated specimen.

The quicklime treated montmorillonite specimen (M30L10) did not show disintegration after 12 cycles of wet/dry tests (Figure 195). After 36 cycles of tests it was still intact. However, K30L10S specimen failed after 12 cycles of tests(Figure 196). Overall, it seems the wet/dry cycles had more severe damage than the freeze/thaw cycles did.

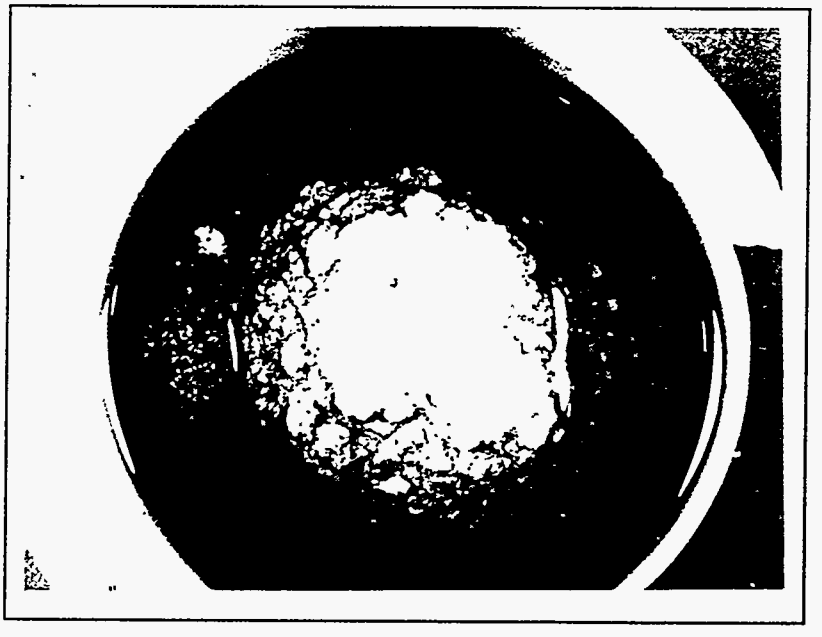

Figure 174. Disintegrated K30L0 Specimen after 3 Months of Soaking in Water Saturated Sand Bath under Room Temperature.

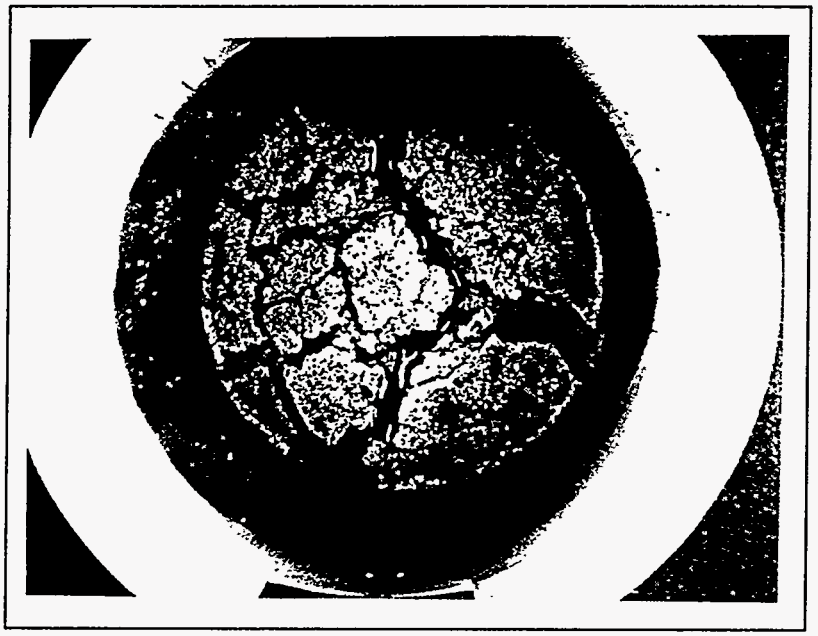

Figure 175. Disintegrated M30L0 Specimen after 3 Months of Soaking in Water Saturated Sand Bath under Room Temperature.

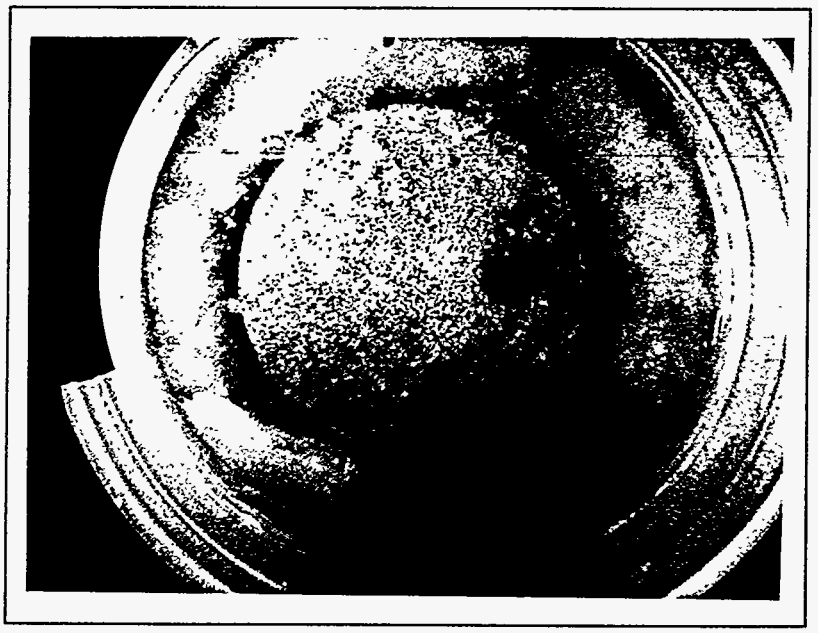

Figure 176. Intact K30L10 Specimen after 3 Months of Soaking in Water Saturated Sand Bath under Room Temperature.

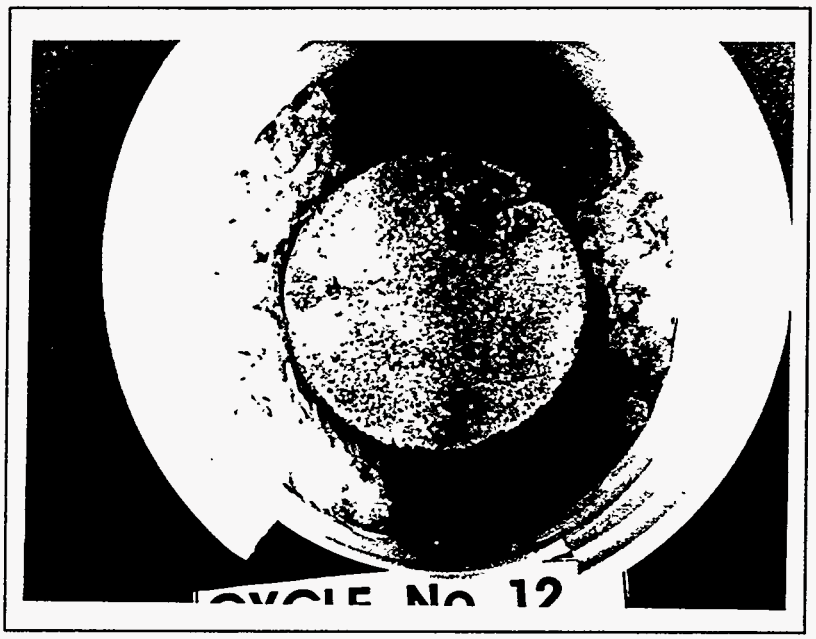

Figure 177. Intact K30L10 Specimen after 12 Cycles of Freeze/Thaw Weathering.

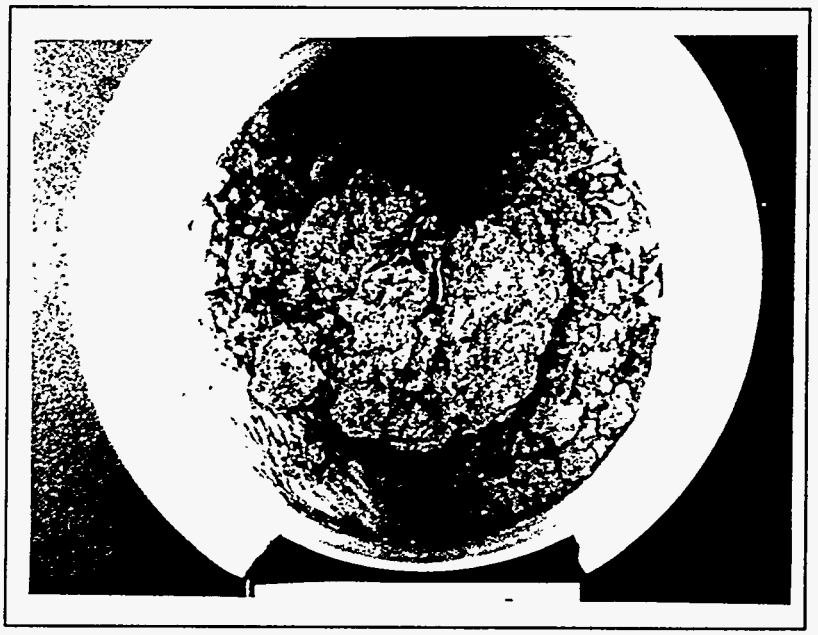

Figure 178. Damaged K30L10 Specimen after 14 Cycles of Freeze/Thaw Weathering.

Figure 179. Cracked K30L10S Specimen after 3 Months of Soaking in Water Saturated Sand Bath under Room Temperature.

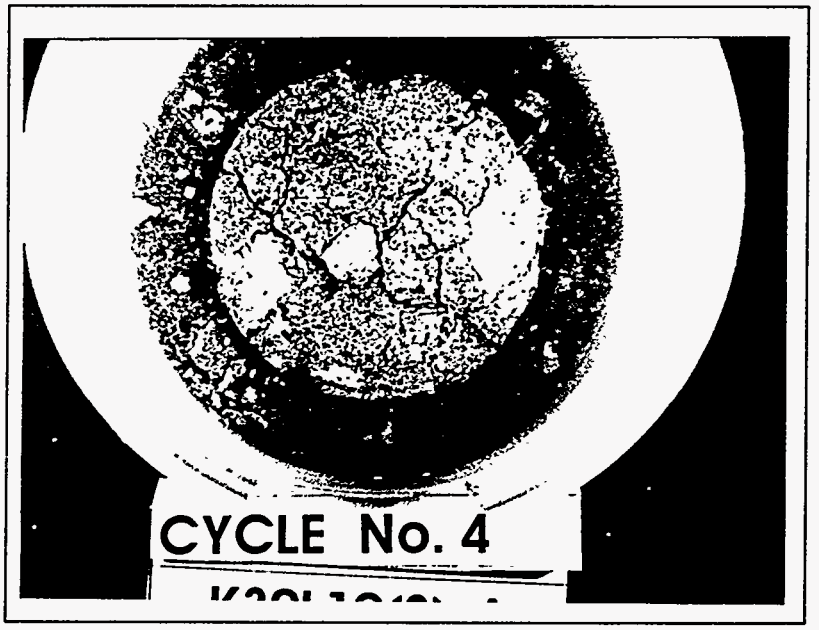

Figure 180. Damaged K30L10S Specimen after 4 Cycles of Freeze/Thaw Weathering.

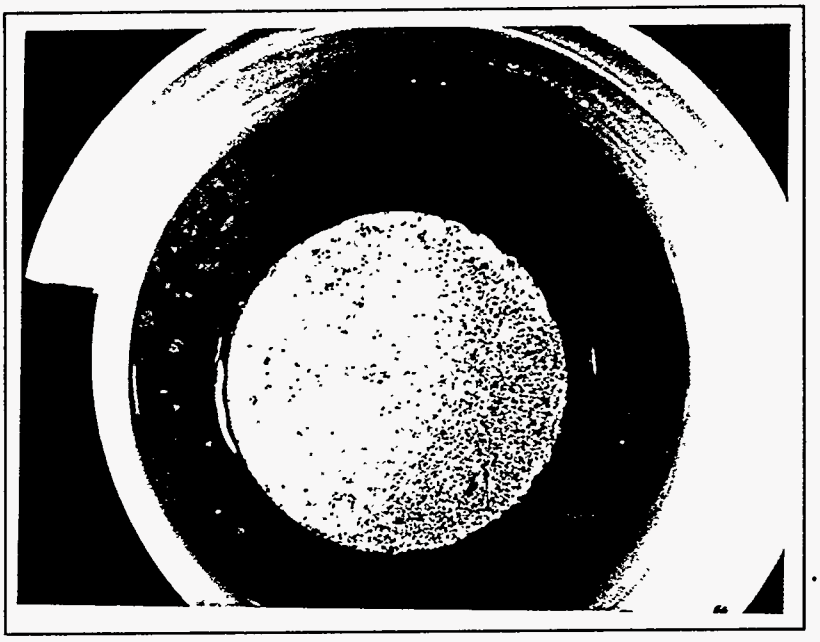

Figure 181. Intact K30L10S + Ba (1:1) Specimen after 3 Months of Soaking in Water Saturated Sand Bath under Room Temperature.

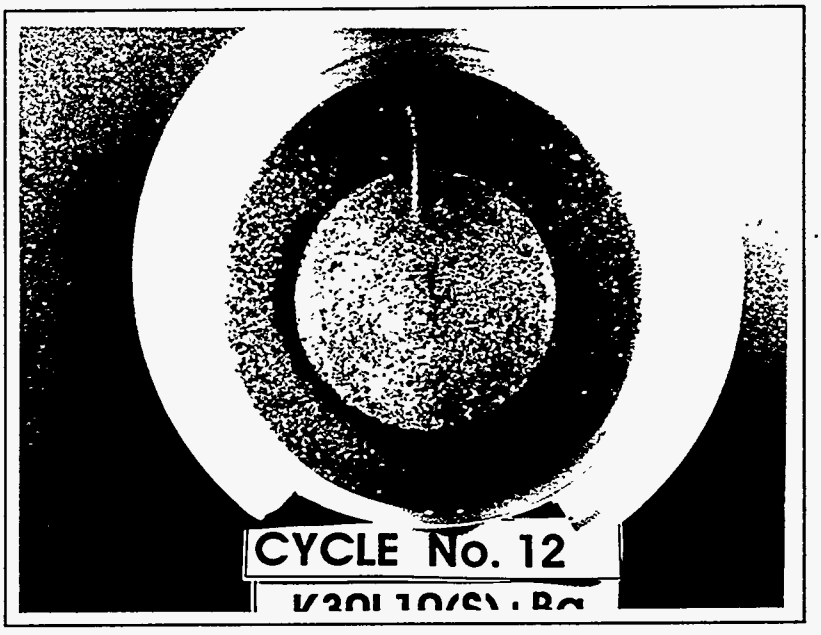

Figure 182. Intact K30L10S + Ba (1:1) Specimen after 12 Cycles of Freeze/Thaw Weathering.

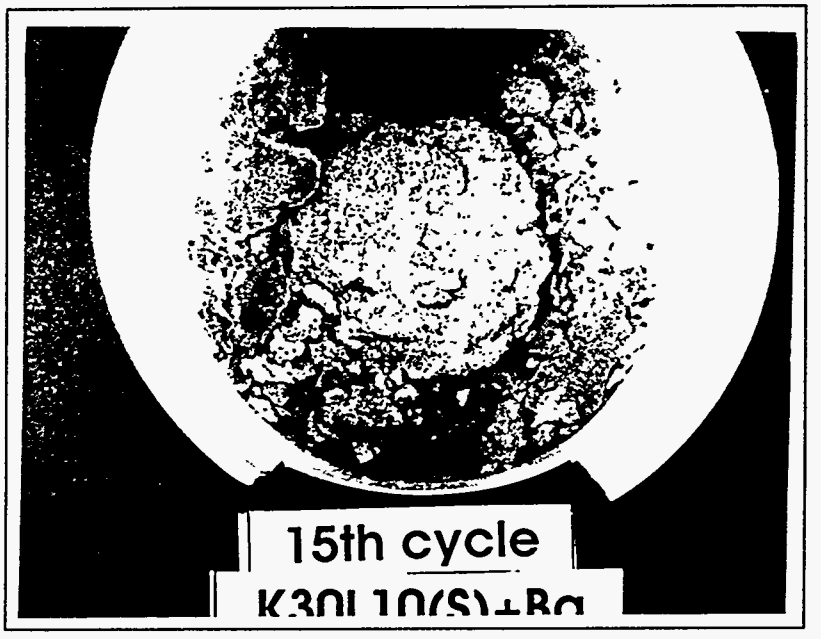

Figure 183. Disintegrated K30L10S + Ba (1:1) Specimen 15 Cycles of Freeze/Thaw Weathering.

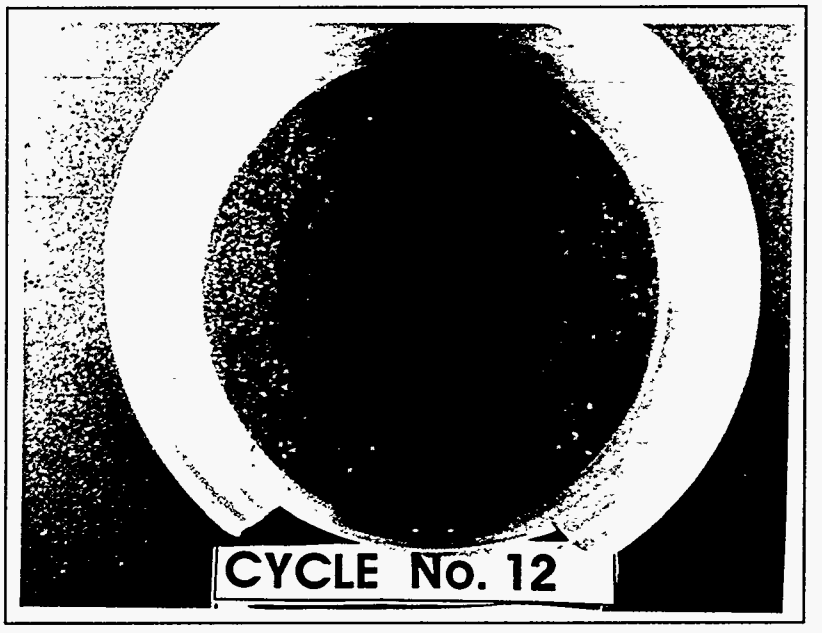

Figure 184. Intact K5C25L10S Specimen after 12 Cycles of Freeze/Thaw Weathering.

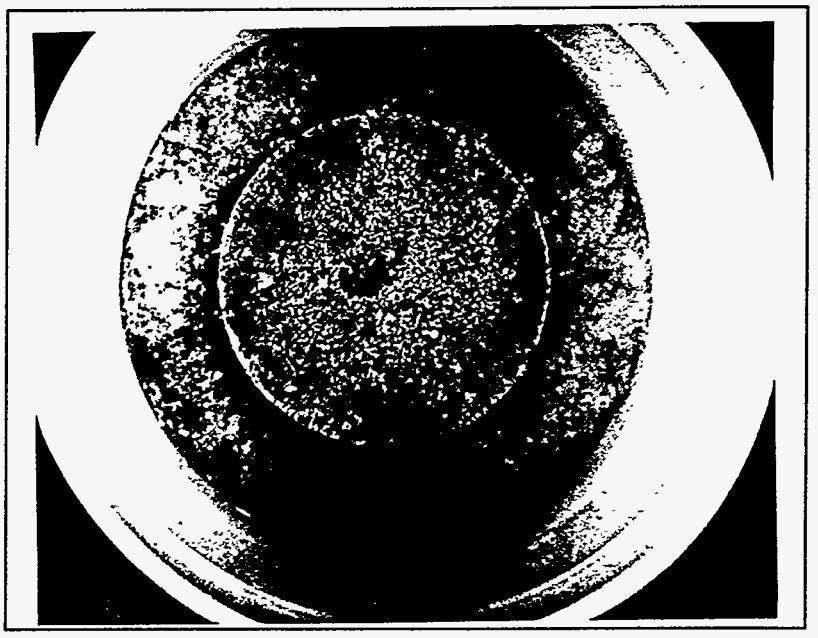

Figure 185. Intact M30L10 Specimen after 3 Months of Soaking in Water Saturated Sand Bath under Room Temperature.

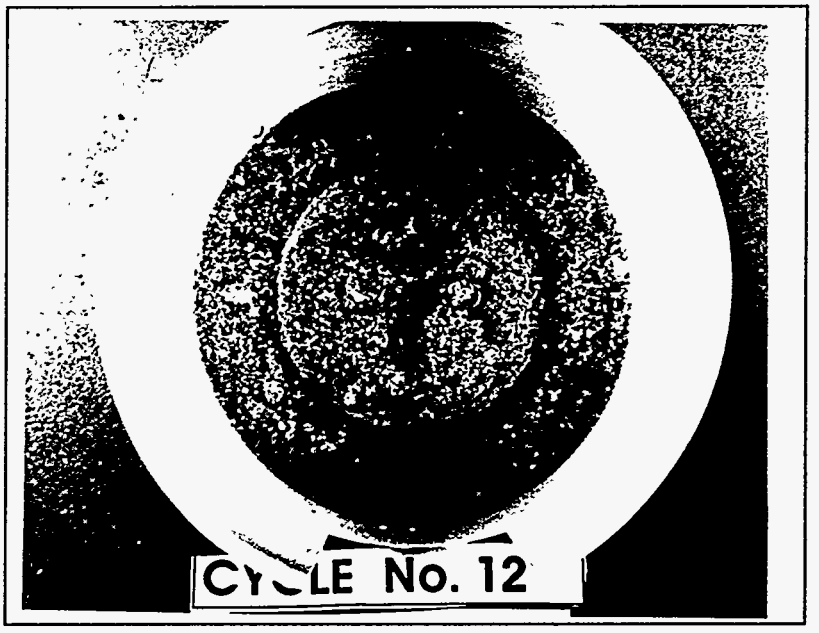

Figure 186. Intact M30L10 Specimen after 12 Cycles of Freeze/Thaw Weathering.

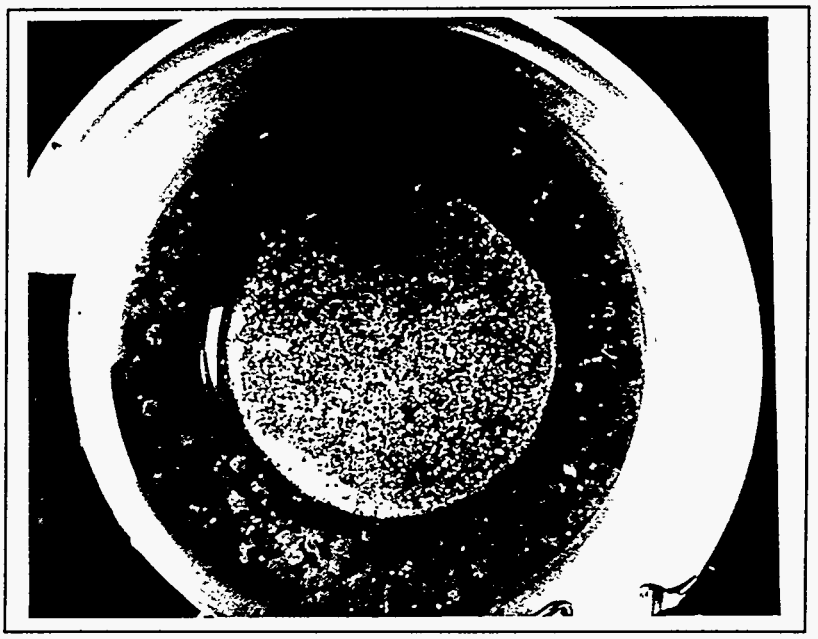

Figure 187. Intact M30L10S Specimen after 3 Months of Soaking in Water Saturated Sand Bath under Room Temperature.

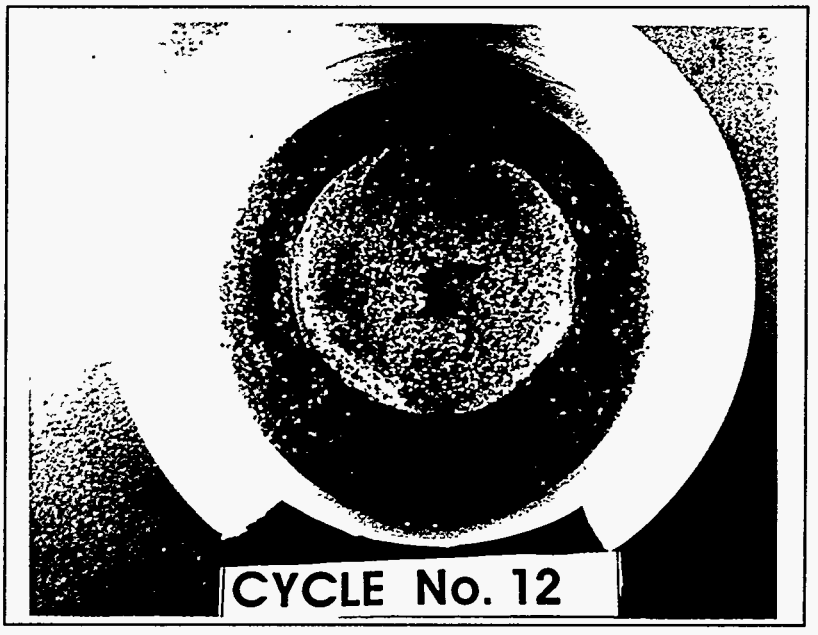

Figure 188. Intact M30L10S Specimen after 12 Cycles of Freeze/Thaw Weathering.

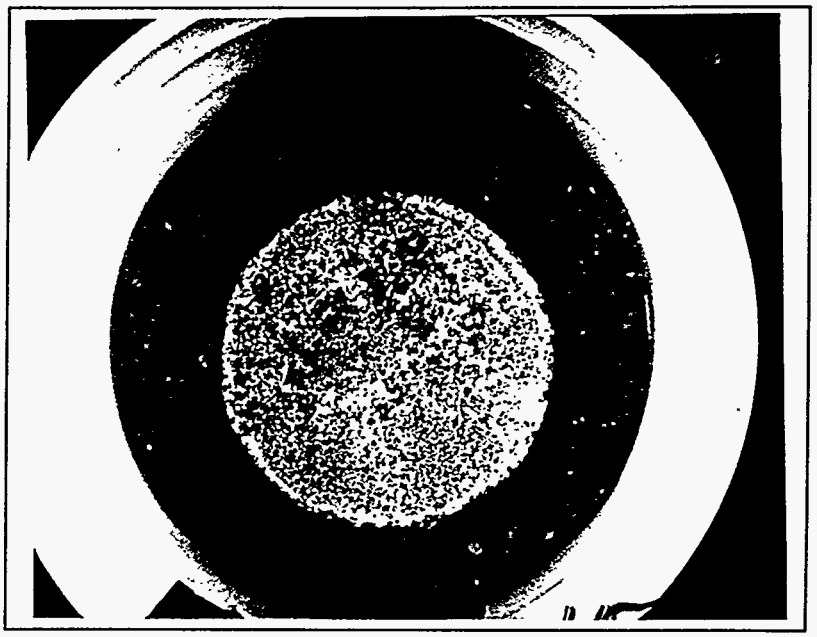

Figure 189. Intact M30L15S Specimen after 3 Months of Soaking in Water Saturated Sand Bath under Room Temperature.

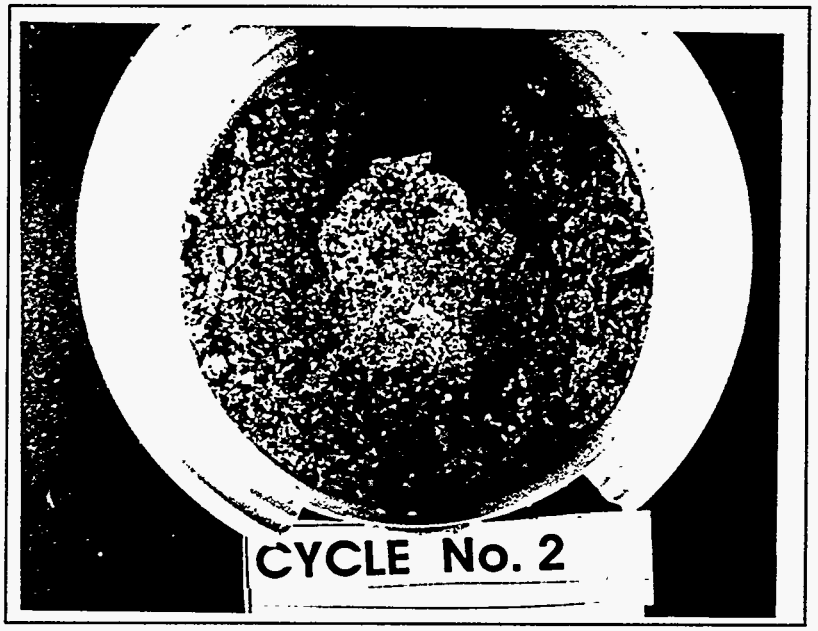

Figure 190. Damaged M30L15S Specimen after 2 Cycles of Freeze/Thaw Weathering.

Figure 191. Damaged K30L10 Specimen after 3 Cycles of Wet/Dry Weathering.

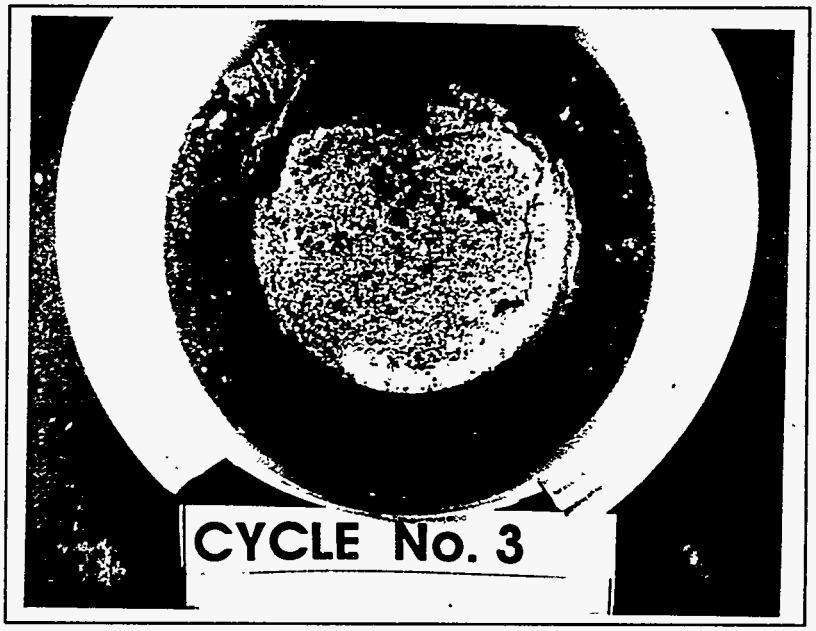

Figure 192. Damaged K30L10S Specimen after 3 Cycles of Wet/Dry Weathering.

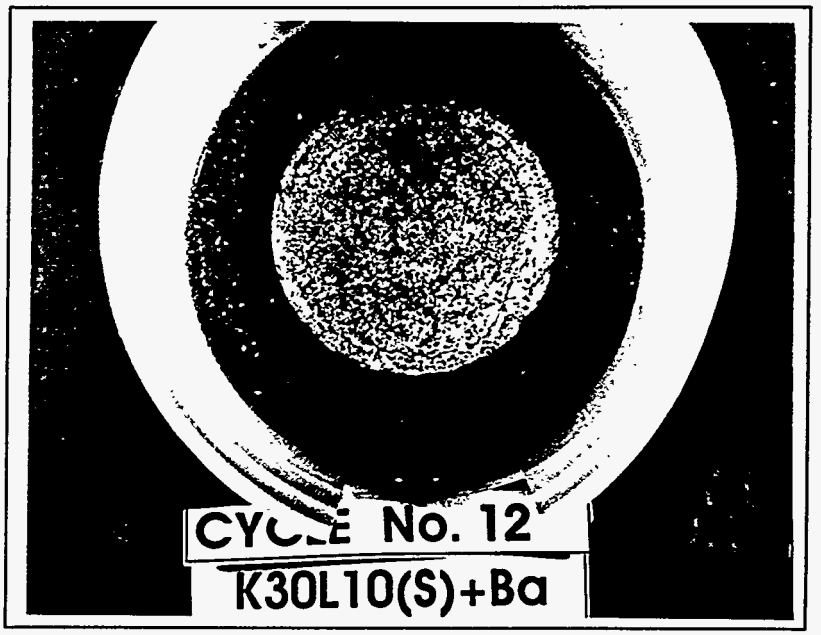

Figure 193. Intact K30L10s + Ba(1:1) after 12 Cycles of Wet/Dry Weathering.

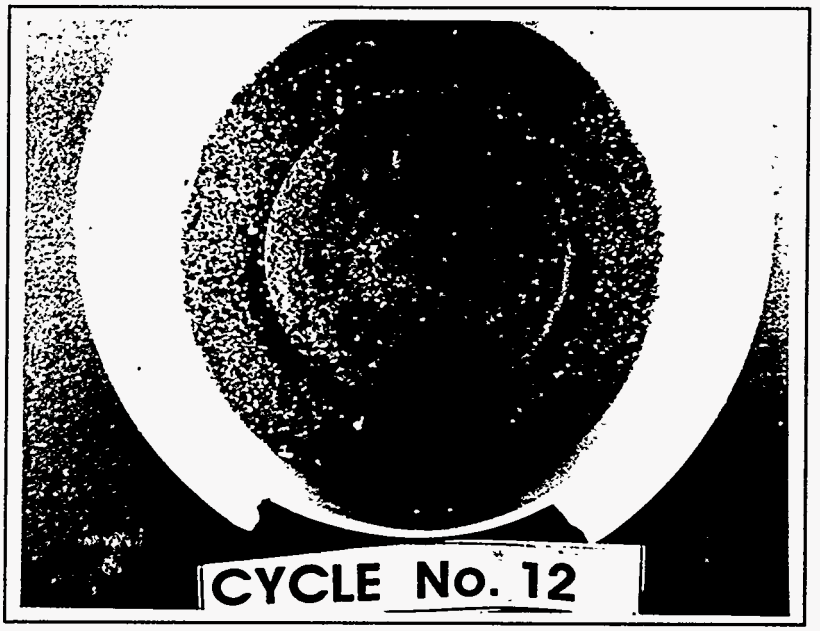

Figure 194. Intact K5C25L10S Specimen after 12 Cycles of Wet/Dry Weathering.

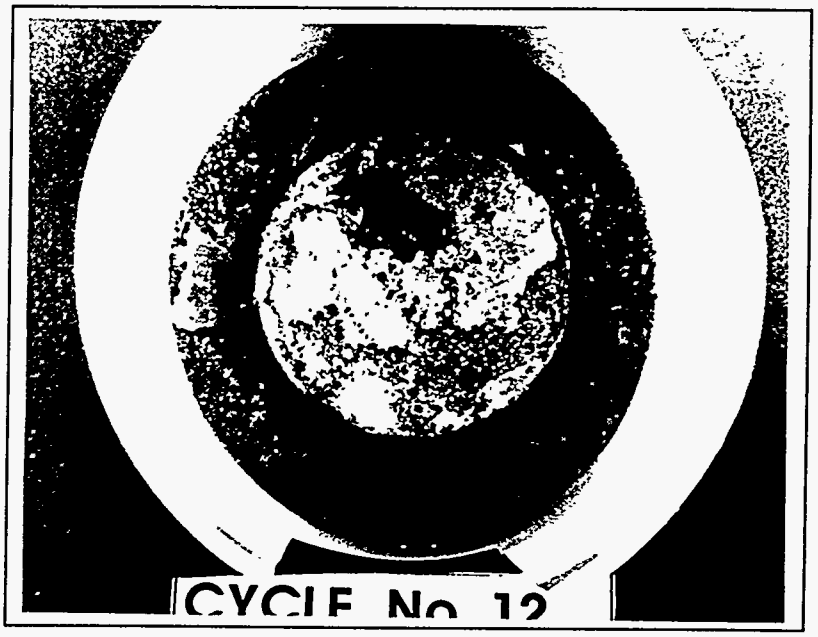

Figure 195. Intact M30L10 Specimen after 12 Cycles of Wet/Dry Weathering.

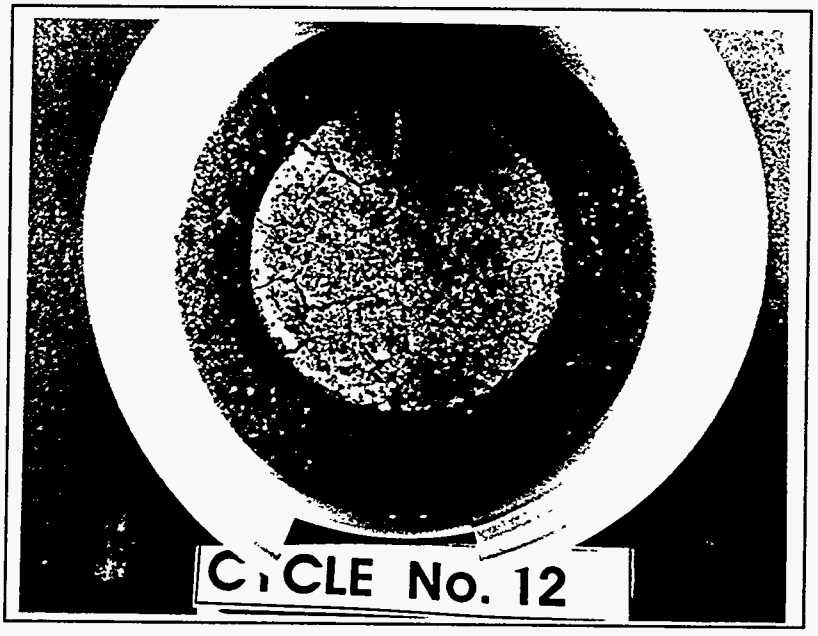

Figure 196. Damaged M30L10S Specimen after 12 Cycles of Wet/Dry Weathering.